Mechanisms and effects of the heterogeneous response of CAIX to hypoxia



Thesis submitted by

Katharina Feldinger

Keble College

For the degree of

Doctor of Philosophy

Trinity Term 2016

Abstract

Breast cancer is the most common cancer in females and several molecular subtypes have been described. However, intra-tumour heterogeneity exists and is associated with evolution of cancer metastasis and therapy resistance. The presence of regions of low oxygen (hypoxia) is associated with poor prognosis and the hypoxic microenvironment is also associated with resistance to current therapeutic strategies. Moreover, hypoxia and metabolite deficiency can alter the tumour microenvironment and drive heterogeneity.

The pH regulating enzyme carbonic anhydrase IX (CAIX) is strongly induced under hypoxic conditions and its overexpression is likewise associated with poor therapeutic outcome. In a previous study, taking advantage of the membranous localization of CAIX, it was shown that under hypoxia a CAIX positive and CAIX negative population is present in MCF7 cells. RNA sequencing suggested an enrichment of stem cell markers in the CAIX positive population as well as a potential symbiotic relationship between these two subpopulations.

In this study MCF7CAIX positive and negative populations were further investigated. Additionally, CAIX positive and negative populations were also found in HCT116 cells and subsequently established as stable cell populations. Both population show similar levels of induction of the hypoxia induced transcription factor HIF-1. The underlying mechanism of CAIX regulation was confirmed to rely on epigenetic modifications, as it could be shown that HIF-1 binding to the CAIX promoter is decreased in the CAIX negative population.

To investigate the interaction of CAIX positive and negative cells in 3D models, stably labelled cells using either mCherry of GFP were generated. Upon mixing the two populations in a 1:1 ratio an initially even mix of the cells was observed in the spheroid.

However, at a 72 h time point CAIX positive cells moved more towards the centre of the spheroid. This was inhibited by knockdown or pharmacological inhibition of CAIX. A key factor in migration and invasion are metalloproteinases/peptidases (MMPs). We found that MMP14 was upregulated in CAIX positive cells in 2D and 3D models, indicating an underlying mechanism for the re-localisation seen.

Analysis of co-culture experiments using 2D a trans-well system revealed that under hypoxia the number of the CAIX positive population was increased in the presence of CAIX negative cells but not *vice versa*. A similar effect was seen using conditioned media, pointing to a secreted factor. Using a FRET based intracellular sensor to measure lactate levels it could be shown that lactate was higher in the CAIX negative cells. After spiking of the media during live imaging the CAIX positive cells quickly absorbed and retained lactate. In comparison, the CAIX negative cells initially showed an uptake of the metabolite, which was followed by a much quicker release. During co-culture, lactate levels in the conditioned media of CAIX negative cells were higher. Incubation of CAIX positive cells with this conditioned media decreased lactate levels, indicating lactate uptake by the cells. Moreover, knockdown of LDHA and/or B decreased the survival benefit CAIX positive cells had from CAIX negative cells.

Another metabolic pathway showing marked differences between the two populations was lipid droplet formation. Under hypoxia CAIX positive cells showed an increased production of lipid droplet in comparison to CAIX negative cells and this was partly due to fatty acid uptake. In line with this, mRNA levels of the fatty acid transporter CD36 as well as some members of the FAB proteins were higher in the CAIX positive cells. Following a previous report showing that lipid droplets formed under hypoxia provide a survival benefit upon re-oxygenation, it was confirmed that CAIX positive cells grew indeed better in this set-up. Therefore, the results suggest a metabolic symbiosis

between the CAIX positive and negative populations based on a lactate shuttle and differential uptake of fatty acids.

Of wider significance, these findings show that tumours are heterogeneous in the response to hypoxia and that cell populations interact with each other in a symbiotic manner. This highlights the need for a better utilisation and combination of biomarkers to assess metabolic pathways and a better stratification of tumours. Moreover, this work highlights a potential effect of therapeutics addressing metabolic symbiosis.

Acknowledgment

At the end of my DPhil I am looking back to thank all the people who have helped, guided, and on occasions, challenged me. I would like to thank Dr Anthony Kong for first giving me the opportunity to come to Oxford.

I am very grateful to Professor Adrian Harris for giving me the opportunity to work in his laboratory. His support, guidance and drive were invaluable for my progression as a student and I very much enjoyed our discussions.

I would also like to thank all my previous colleagues from the Kong lab, Amalina, Ashwag, Fenix, Kenji, Merel, Sedigeh, and Siti for their support and friendship, and the supply with chocolate and waffles. Furthermore, I am grateful for all the advice and the kindness extended to me by members of the Harris lab: Helen Sheldon, Christos Zois, Karim Bensaad, Masahiro Kawashima, Alessandro Valli, Valentinos Kounnis, Fiona Larner. Shijie Cai, Ana Miar Cuervo, Helen Turley, Matteo Morotti, Hugh Wright and Anand Sharma.

A big thank you to Alan McIntyre, Simon Wigfield, and Ioanna Ledaki for the support and guidance throughout the project, to Syed Haider for helping me with bioinformatics and more, and to Chris Lagerholm and Esther Garcia for their patience explaining the FRET microscope to me. I am grateful to Sam Oats and Penny Berry for all your help and to Pete, Linda, and Rose who made my life so much easier.

I will always have fond memories of early morning teas and biscuits with Esther Bridges and Koon Hwee Ang and late night pizza with David Favara. Thank you for your smiles – keep smiling!

I am very grateful to have received funding from the Clarendon Fund, Keble College, and the MCR.

Last but not least, I would like to thank my parents and my partner for their support and their open ears through the highs and lows of my DPhil. Thank you for always being there for me.

List of contents

CHAPTER 1 INTRODUCTION 1

1.1. HALLMARKS OF CANCER 2

1.2. BREAST CANCER 4

1.2.1. Classification by staging 4

1.2.2. Histopathological classification 5

1.2.3. Immunohistochemical (HC) subtyping 8

1.2.4. Molecular subtypes 9

1.3. COLON CANCER 12

1.4. SHORTFALLS WITH SUBTYPING ATTEMPTS 14

1.5. IHC STAINING 14

1.6. COMPARISON BETWEEN SUBTYPING APPROACHES 15

1.7. CANCER HETEROGENEITY 16

1.7.1. Models for cancer heterogeneity 17

1.8. HYPOXIA 21

1.8.1. The HIF-1 pathways 22

1.8.2. Main pathways regulated by hypoxia 24

1.9. TUMOUR CELL METABOLISM 26

1.9.1. Cell metabolism 26

1.9.2. Metabolism and hypoxia 29

1.9.1. The Warburg effect and tumour metabolism 30

1.9.2. Metabolic symbiosis 33

1.9.3. Autophagy 35

1.10. CARBONIC ANHYDRASE IX (CAIX) 35

1.10.1. Structure of CAIX 35

1.10.2. The expression of CAIX 39

1.10.3. Regulation of CAIX 39

1.10.4. Role of CAIX *42*

1.10.5. Inhibition of CAIX *46*

1.11. AIMS AND OBJECTIVES 50

CHAPTER TWO MATERIALS AND METHODS 51

2.1. CELL LINES AND MAINTENANCE 52

2.2. MAINTENANCE OF CELL STOCKS 52

2.3. HYPOXIA 52

2.4. IMMUNOBLOTTING 52

2.4.1. Protein extraction and measurement of protein content *52*

2.4.2. Polyacrylamide gel electrophoresis and transfer *53*

2.4.3. Probing *53*

2.5. QPCR 54

2.5.1. RNA extraction *54*

2.5.2. Generation of cDNA *55*

2.5.3. qPCR *55*

2.6. FLOW CYTOMETRY 57

2.6.1. Staining for CAIX *57*

2.6.1. Cell sorting *57*

2.6.2. Staining for apoptosis marker Annexin V *57*

2.6.3. Staining for cell cycle analysis *58*

2.7. GENE SILENCING USING RNA INTERFERENCE 58

2.8. LENTIVIRAL TRANSDUCTION OF MCHERRY AND GFP 59

2.9. PLASMID TRANSFECTION 59

2.9.1. Laconic/pcDNA3.1(-) *60*

2.10. SPHEROID FORMATION 60

2.11. DETERMINATION OF PH LEVELS WITH PHLIP PEPTIDE (PRELIMINARY DATA IN FUTURE WORK SECTION) 61

2.12. MICROSCOPY 62

2.12.1. Fluorescence microscopy 62

2.12.2. FRET/FLIM 62

2.13. CO-CULTURE EXPERIMENTS 65

2.14. MEASUREMENT OF OXYGEN CONSUMPTION RATES USING THE MITOEXPRESS PROBE 65

2.15. LACTATE MEASUREMENTS IN THE MEDIA 66

2.16. STAINING FOR LIPID DROPLETS 67

2.17. IMMUNOHISTOCHEMISTRY (IHC) 67

2.18. CHROMATIN IMMUNOPRECIPITATION ASSAY FOR HIF-1 B 68

2.19. ANALYSIS OF THE METABRIC DATASET 70

2.20. STATISTICAL ANALYSIS 70

2.21. BUFFERS AND SOLUTIONS 71

CHAPTER THREE HYPOXIA INDUCED CAIX EXPRESSION DEFINES CELL LINE SUBPOPULATIONS WITH DIFFERENT PROPERTIES 73

3.1. INTRODUCTION 74

3.1.1. Epigenetic regulation of gene expression 74

3.1.2. Epigenetic regulation in tumours 76

3.1.3. CAIX as a biomarkers for tumour heterogeneity 77

3.2. RESULTS 78

3.2.1. Expression of CAIX 78

3.2.2. Mechanism of CAIX regulation 85

3.2.3. Evaluation of CAIX expression in a panel of breast cancer cell lines 88

3.2.4. Confirmation of model – HCT116 colon cancer cell line 92

3.3. DISCUSSION 97

CHAPTER 4 INTERACTION OF CAIX POSITIVE AND NEGATIVE CELLS IN SPHEROID MODELS 102

4.1. INTRODUCTION 103

4.1.1. Studying cell-cell interaction in 3D 103

4.1.2. Imaging approaches 103

4.2. RESULTS 107

4.2.1. MCF7 CAIX positive cells adopt a central localization in 3D culture 107

4.2.2. CAIX positive cells can invade CAIX negative spheroids 111

4.2.3. Central localisation of CAIX positive cells is dependent on CAIX 113

4.2.4. Imaging lactate in 3D models 115

4.2.5. The role for CAIX and MMP-14 during invasion/migration 119

4.3. DISCUSSION 122

CHAPTER 5 CO-OPERATION OF CAIX POSITIVE AND NEGATIVE POPULATIONS 125

5.1. INTRODUCTION 126

5.2. RESULTS 129

5.2.1. Co-culture of CAIX positive and negative populations in 2D 129

5.2.2. CAIX negative cells support growth of CAIX positive cells 131

5.2.3. Co-culture using conditioned media 136

5.2.4. Co-culture experiments are replicable using the HCT116 cell line 142

5.2.5. Mechanisms underlying the co-culture effects 144

5.2.6. CAIX positive cells produce more lipid droplets under hypoxia 158

5.3. DISCUSSION 171

6. FINAL DISCUSSION 176

6.1. CAIX EXPRESSION AND HYPOXIC HETEROGENEITY 177

6.2. TUMOUR CELL REORGANIZATION AND THE HYPOXIC STEM CELL NICHE 179

6.3. A SYMBIOTIC RELATIONSHIP BETWEEN CAIX+VE AND CAIX-VE CELLS 182

6.4. CONCLUDING REMARKS AND FUTURE PROSPECTS 186

6.5. FUTURE EXPERIMENTAL WORK 189

PUBLICATIONS AND CONFERENCE ABSTRACTS PUBLICATIONS AND CONFERENCE ABSTRACTS 194

REFERENCES 195

APPENDIX – PERMISSIONS FOR REPRINT 230

List of Tables

TABLE 1.1 TNM STAGING. TAKEN FROM CANCER RESEARCH UK (CANCERRESEARCHUK, 2014) 5

TABLE 1.2 COLON CANCER TNM ASSESSMENT TAKEN FROM CANCER RESEARCH UK (CANCERRESEARCHUK) 12

TABLE 1.3 COLON CANCER STAGES. TAKEN FROM CANCER RESEARCH UK (CANCERRESEARCHUK) 13

TABLE 1.4 COLON CANCER GRADING. TAKEN FROM CANCER RESEARCH UK (CANCERRESEARCHUK) 13

TABLE 2.1 TABLE OF PRIMARY AND SECONDARY ANTIBODIES 54

TABLE 2.2 PRIMER SEQUENCES FOR QPCR 56

TABLE 2.3 LIST OF SIRNAS 59

TABLE 2.4 ANTIBODIES USED FOR IHC 68

TABLE 2.5 PRIMERS FOR CHIP EXPERIMENT 70

TABLE 2.6 BUFFERS AND SOLUTIONS 71

TABLE 2.7 ANTIBIOTICS AND DRUGS 72

TABLE 5.1 INGENUITY CANONICAL PATHWAY ANALYSIS OF CAIX POSITIVE MCF7 CELLS (EXPERIMENT AND DATA FROM DR IOANNA LEDAKI) 131

TABLE 5.2 INGENUITY CANONICAL PATHWAY ANALYSIS OF CAIX NEGATIVE MCF7 CELLS (EXPERIMENT AND DATA FROM DR IOANNA LEDAKI) 133

List of Figures

FIGURE 1.1 HALLMARKS OF CANCER.. 3

FIGURE 1.2 HISTOLOGICAL CLASSIFICATION OF BREAST CANCER. 7

FIGURE 1.3 CLINICAL CLASSIFICATION OF BREAST CANCER 8

FIGURE 1.4 NEXT GENERATION SEQUENCING BASED CLUSTERING OF 2000 BREAST CANCERS. 11

FIGURE 1.5 REGULATION OF HIF-1 AND ITS TRANSCRIPTIONAL ACTIVITY 26

FIGURE 1.6 METABOLIC PATHWAYS IN PROLIFERATING CELLS. 29

FIGURE 1.7 SCHEMATIC STRUCTURE OF CAIX 38

FIGURE 2.1 REPRESENTATIVE LIFETIME MEASUREMENT ANALYSIS 64

FIGURE 2.2 REPRESENTATIVE LACTATE STANDARD CURVE – ENZYMATIC METHOD 67

FIGURE 3.1 CAIX EXPRESSION IN BREAST CANCER SUBTYPES 80

FIGURE 3.2 MCF7 CELLS WERE SORTED INTO CAIX POSITIVE AND NEGATIVE POPULATIONS 82

FIGURE 3.3 MCF7 CAIX POSITIVE AND NEGATIVE POPULATIONS KEEP CHARACTERISTICS 84

FIGURE 3.4 CAIX IS THE MOST DIFFERENTIALLY EXPRESSED HIF-1 TARGET GENE 85

FIGURE 3.5 MCF7 CAIX EXPRESSION IS REGULATED BY DIFFERENTIAL BINDING OF HIF-1 87

FIGURE 3.6 CAIX EXPRESSION IN A PANEL OF BREAST CANCER CELL LINES 89

FIGURE 3.7 SORTING OF CAIX HIGH AND LOW ZR 75-1 AND MDA-MB-453 BREAST CANCER CELLS 91

FIGURE 3.8 HCT116 CELLS WERE SORTED ACCORDING TO THEIR CAIX LEVEL 92

FIGURE 3.9 CAIX EXPRESSION IN HCT116 CELLS OVER TIME 94

FIGURE 3.10 LONG TERM LEVEL OF CAIX IN HCT116 SORTED POPULATIONS 96

FIGURE 4.1 PRINCIPLE OF MEASURING INTRACELLULAR LACTATE LEVELS USING A FRET BASED PLASMID 106

FIGURE 4.2 REPRESENTATIVE FACS BLOTS SORTING CAIX POSITIVE AND NEGATIVE POPULATIONS FROM LABELLED MCF7 CELLS 107

FIGURE 4.3 MCF7 CONTROL SPHEROIDS CONFIRM SPECIFICITY OF FLUORESCENCE MICROSCOPY 108

FIGURE 4.4 MCF7 CAIX POSITIVE CELLS LOCALISE TOWARDS THE CENTRE OF A SPHEROID TUMOUR MODEL 110

FIGURE 4.5 MCF7 CAIX POSITIVE CELLS INVADE CAIX NEGATIVE SPHEROIDS 112

FIGURE 4.6 CENTRAL LOCALISATION OF THE MCF7 CAIX POSITIVE POPULATION IS DEPENDENT ON CAIX 114

FIGURE 4.7 TESTING OF THE LACONIC PLASMID IN MCF7 CELLS 118

FIGURE 4.8 MMPS MAY INTERACT WITH CAIX TO FACILITATE LOCALISATION IN MCF7 CELLS 120

FIGURE 5.1 CO-CULTURE OF LABELLED MCF7 CAIX POSITIVE AND NEGATIVE POPULATIONS IN 2D 130

FIGURE 5.2 MCF7 CAIX NEGATIVE CELLS SUPPORT GROWTH OF THE CAIX POSITIVE POPULATION 135

FIGURE 5.3 OPTIMISATION OF MCF7 CAIX POSITIVE AND NEGATIVE CELL CO-CULTURE USING CONDITIONED MEDIA OVER A PERIOD OF 5 DAYS 137

FIGURE 5.4 MEDIA FROM MCF7 CAIX NEGATIVE CELLS ENHANCES CELL NUMBER OF THE MCF7 CAIX POSITIVE POPULATION 139

FIGURE 5.5 EFFECT OF MCF7 CAIX POSITIVE AND NEGATIVE CELLS CO-CULTURE ON CELL VIABILITY AND PI BINDING 141

FIGURE 5.6 CO-CULTURE EXPERIMENTS IN HCT116 CELLS 143

FIGURE 5.7 FILTERED CONDITIONED MEDIA STILL CONFERS AN ADVANTAGE 145

FIGURE 5.8 OXYGEN CONSUMPTION IS HIGHER IN THE MCF7 CAIX POSITIVE CELLS AND IS POSITIVELY AFFECTED BY CO-CULTURE WITH CONDITIONED MEDIA FROM THE CAIX NEGATIVE CELLS 148

FIGURE 5.9 LACTATE LEVELS IN MCF7 CAIX POSITIVE AND NEGATIVE POPULATIONS 150

FIGURE 5.10 THE MCF7 CAIX POSITIVE POPULATION CAN TAKE UP AND USE LACTATE... 153

FIGURE 5.11 FATTY ACID UPTAKE IS ENHANCED IN THE MCF7 CAIX POSITIVE CELLS 161

FIGURE 5.12 COMPARISON OF GENES ASSOCIATED WITH FATTY ACID TRANSPORT AND LIPID DROPLET FORMATION IN MCF7 CAIX POSITIVE AND NEGATIVE CELLS 163

FIGURE 5.13 MCF7 CAIX POSITIVE CELLS GROW BETTER DURING RE-OXYGENATION LINKED TO FATTY ACID UPTAKE DURING HYPOXIA 165

FIGURE 5.14 LIPID DROPLET FORMATION IN MCF7 CAIX POSITIVE CELLS IS ENHANCED IN CO-CULTURE WITH CONDITIONED MEDIA FROM CAIX NEGATIVE CELLS 168

FIGURE 5.15 AUTOPHAGY IS HIGHER IN THE MCF7 CAIX NEGATIVE POPULATION..... 170

FIGURE 6.1 PROPOSED MODEL OF CAIX POSITIVE AND CAIX NEGATIVE CELL INTERACTION 183

FIGURE 6.2 THE CENTRES OF MCF7 SPHEROIDS ARE MORE ACIDIC 190

List of Abbreviations

ABC transporters	ATP binding cassette transporters
ACC	Acetyl-CoA carboxylase
ACLY	ATP citrate lyase
ADCC	Antibody dependent cell cytotoxicity
AP1	Activator Protein 1
ASCO / CAP	American Society of Clinical Oncology / College of American
BC	Breast cancer
bHLH	Basic helix-loop-helix
CA	Catalytic
CA9	Carbonic Anhydrase 9
CAF	Cancer associated fibroblast
CAN	Copy Number Aberrations
CBP	CREB-binding protein
CIS	Carcinoma in situ
CSC	Cancer stem cell
DCIS	Ductal carcinoma in situ
ECM	Extracellular matrix
EGF	Epidermal growth factor
EGFR	Epidermal Growth Factor Receptor
EMT	Epithelial to mesenchymal transition
ER	Oestrogen Receptor
ET	Endocrine Therapy
FABP	Fatty acid binding proteins
FASN	Fatty acid synthase
FHIF	Factor inhibiting HIF
FISH	Fluorescence in situ hybridization
GLS	Glutaminase

HDAC	Histone deacetylase
HIF	Hypoxia inducible factor
HRE	HIF Response Element
IC	Intracellular
IDH	Isocytrate dehydrogenase
IFN	Interferon
IGF	Insulin growth factor
IHC	Immunohistochemistry
IL-6	Interleukin 6
iPS	Induced Pluripotent Stem cell
LCIS	Lobular carcinoma in situ
LDH A/B	Lactate dehydrogenase A/B
MAPK	Mitogen activated protein kinase
MCT	Monocarboxylate transporter
MDR	Multi drug resistance
MMP	Matrix metalloproteinase
NO	Nitric Oxide
ODDD	**O**xygen **d**ependent **d**egradation **d**omains
OxPhos	Oxidative phosphorylation
PAS	PER-ARNT-SIM domain
PBS	Phosphate Buffered Saline
PDH	Pyruvate dehydrogenase
PDK-1	Pyruvate dehydrogenase kinase-1
PFA	Paraformaldehyde
PG	Proteoglycan
PHD	Prolyl hydroxylase
PI3K / mTOR	Phosphoinositide 3-kinase/ mammalian target of rapamyc
PKM	Pyruvate kinase
PLIN	Perilipin

pO_2	Oxygen pressure
PR	Progesterone Receptor
PR	Protected region
PTEN	Phosphatase and tensin homolog deleted on chromosome 10
RCC	Renal cell carcinoma
ROS	Reactive Oxygen Species
RT	Room temperature
SCO2	Cytochrome c oxidase 2
SP	Specificity protein
SP domain	Single Peptide
TCA	Tricarboxylic acid
TIGAR	TP53-induced glycolysis and apoptosis regulator
TM	Transmembrane
TMA	Tissue Microarray
TNM	Tumour, Node, Metastasis
VEGF / VEGFR	Vascular endothelial growth factor / receptor
VHL	Von Hippel Lindau

Chapter One

Introduction

1.1. Hallmarks of cancer

Neoplastic disease is highly complex and more than 200 different cancer types have been recognised. Thousands of publications report various mechanisms of tumour initiation, progression, and general biology in a range of cancers.

In an attempt to organise these mechanisms, Hanahan and Weinberg first proposed six hallmarks of cancer in 2000. These biological capabilities are acquired during a multistep development of human cancers. As outlined in Figure 1.1 A these more generalised tumour characteristics include:

- sustained proliferative signalling;
- evading growth suppressors;
- activating invasion and metastasis;
- enabling replicative immortality;
- inducing angiogenesis, and
- resisting cell death.

In an updated review a decade later two emerging hallmarks were added to this list:

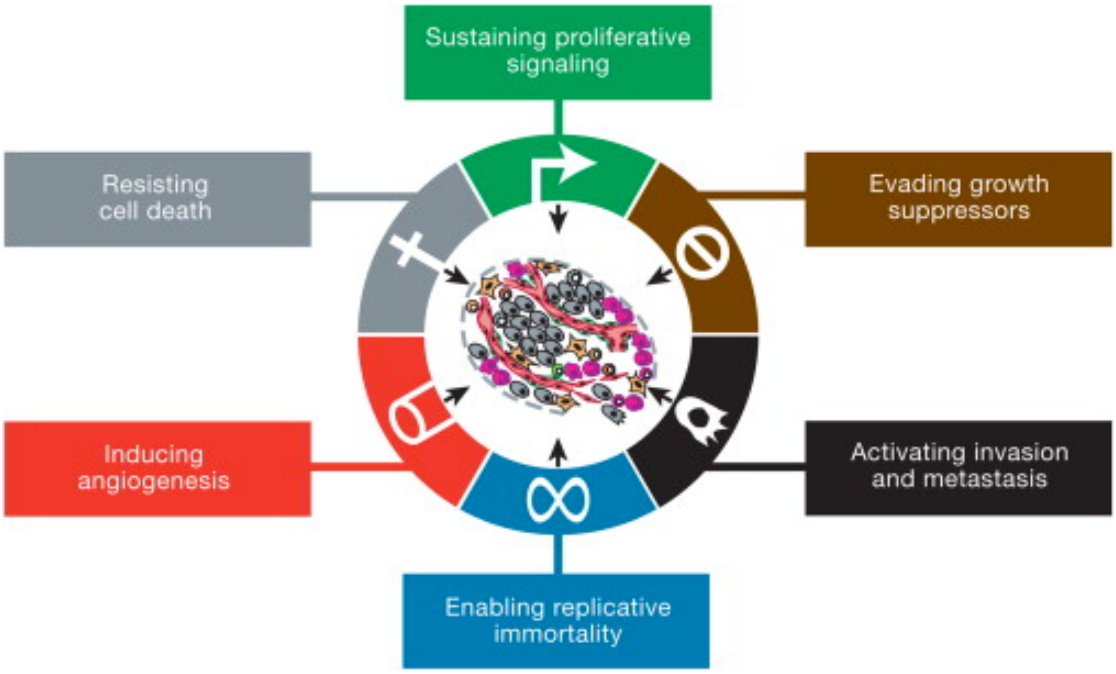
- reprogramming of energy metabolism, and
- evading immune destruction.

Moreover, they described two “enabling characteristics”, which are the main factors underlying many of the hallmarks leading to tumour formation, diversity, and growth. The enabling characteristics are

- genome instability and mutation
- tumour promoting inflammation

However, as with any tissue in the human body, tumours were found to interact with other cells. This adds yet another level of complexity, namely the tumour microenvironment; non-tumour cells that are influenced at site or recruited to the tumour contribute to the acquisition and/or maintenance of certain tumour characteristics [Figure 1.1 B, (Hanahan and Weinberg, 2011)].

A



B

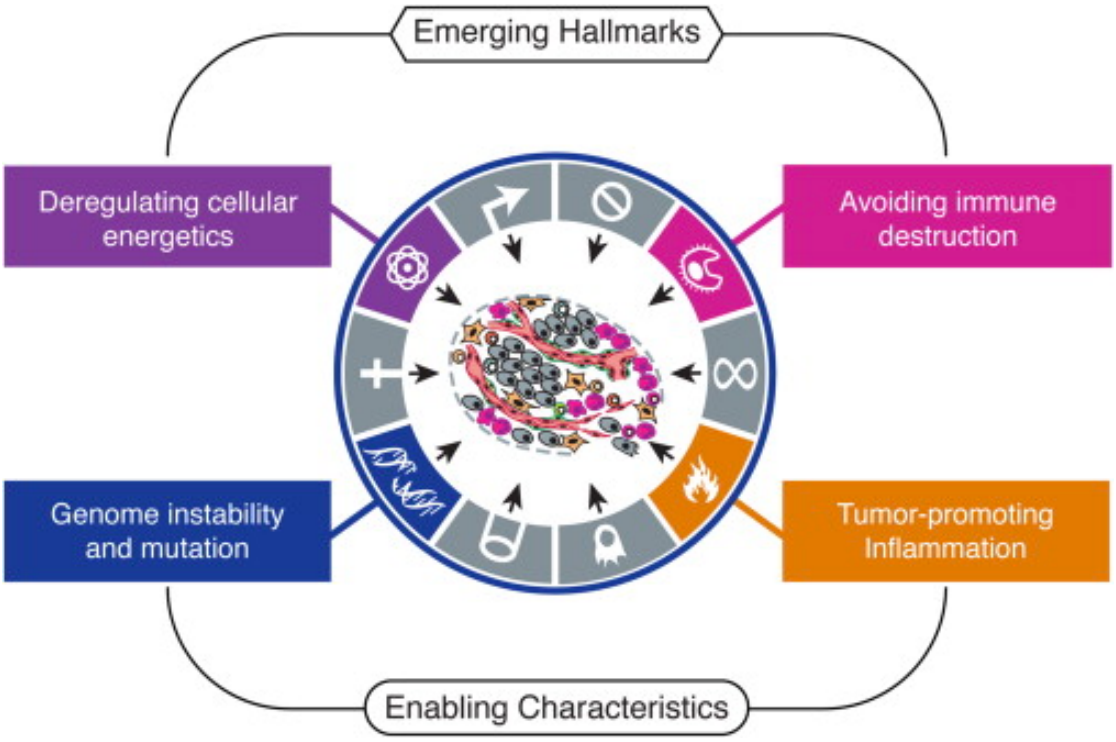


Figure 1.1 Hallmarks of cancer. Taken from Hanahan and Weinberg (Hanahan and Weinberg, 2000, Hanahan and Weinberg, 2011), permission for reprint obtained.

1.2. Breast cancer

Breast cancer is the most common cancer in females. In 2013 around 50,000 women were newly diagnosed with invasive breast cancer in the UK. Breast cancer was the third most common cause of cancer death in the UK in 2014, accounting for over 11,000 cases (CancerResearchUK, 2016).

The notion that breast cancer is not a homogenous disease evolved early on and attempts to classify tumours in order to stratify patients have since been ongoing. Indications of prognostic factors being present in breast cancer were already published mid 20th century (Culter et al., 1963). Several models for breast cancer classification are now available.

1.2.1. Classification by staging

In the clinical setting breast cancers have traditionally been classified by clinicopathological features such as **t**umour size, involvement of lymph **n**odes, and presence of **m**etastases (=TNM, see Table 1.1) (CancerResearchUK, 2014). Although nowadays molecular biomarkers are also assessed, the traditional TNM staging tool has recently been shown to still reliably predict overall survival (Orucevic et al., 2015).

Table 1.1 TNM staging. Taken from Cancer Research UK (CancerResearchUK, 2014)

Tumour	
TX	tumour size cannot be assessed
Tis	DCIS
T1	≤ 2cm across
T2	> 2 cm, ≤ 5 cm across
T3	> 5cm across
T4	T4a – The tumour has spread into the chest wall T4b –The tumour has spread into the skin and the breast may be swollen T4c – The tumour has spread to both the skin and the chest wall T4d – Inflammatory carcinoma – this is a cancer in which the overlying skin is red, swollen and painful to the touch
Nodes	
NX	Lymph nodes cannot be assessed
N0	Lymph nodes are negative
N1	Positive lymph nodes in the armpit, but nodes are not attached to surrounding tissue
N2	N2a – positive lymph nodes in the armpit, which are associated with each other and with other structures N2b – positive lymph nodes behind the breast bone but no evidence of cancer in lymph nodes in the armpit
N3	N3a – positive lymph nodes below the collarbone N3b – positive lymph nodes in the armpit and behind the breast bone N3c – positive lymph nodes above the collarbone
Metastasis	
M0	No detectable metastasis
cMo(i+)	Cancer cells detectable in blood, bone marrow, or distant lymph nodes
M1	Metastases present

1.2.2. Histopathological classification

Breast cancer is characterised as either carcinoma in situ (CIS) or invasive carcinoma. A CIS is then further classified as lobular (LCIS) or the more common ductal (DCIS) (Figure 1.2) (Malhotra et al., 2010). About 25% of all new breast cancers are diagnosed as DCIS in the US. Although it is difficult to define the

progression of breast cancer due to a lack of markers (Stingl and Caldas, 2007), it is thought that breast cancer starts with a hyperplasia and then develops to DCIS, which can then develop into invasive breast cancer (Wellings and Jensen, 1973). Although a DCIS is by definition non-invasive, grading can vary and, if untreated, a DCIS is thought likely to give rise to invasive disease (Rivenbark et al., 2013). Consistent with this, a DCIS is a risk factor for invasive breast cancer, and often both are present at the time of diagnosis (Allred, 2010).

Invasive carcinomas are also regularly classified into histological subtypes, as shown in Figure 1.2 (Malhotra et al., 2010).

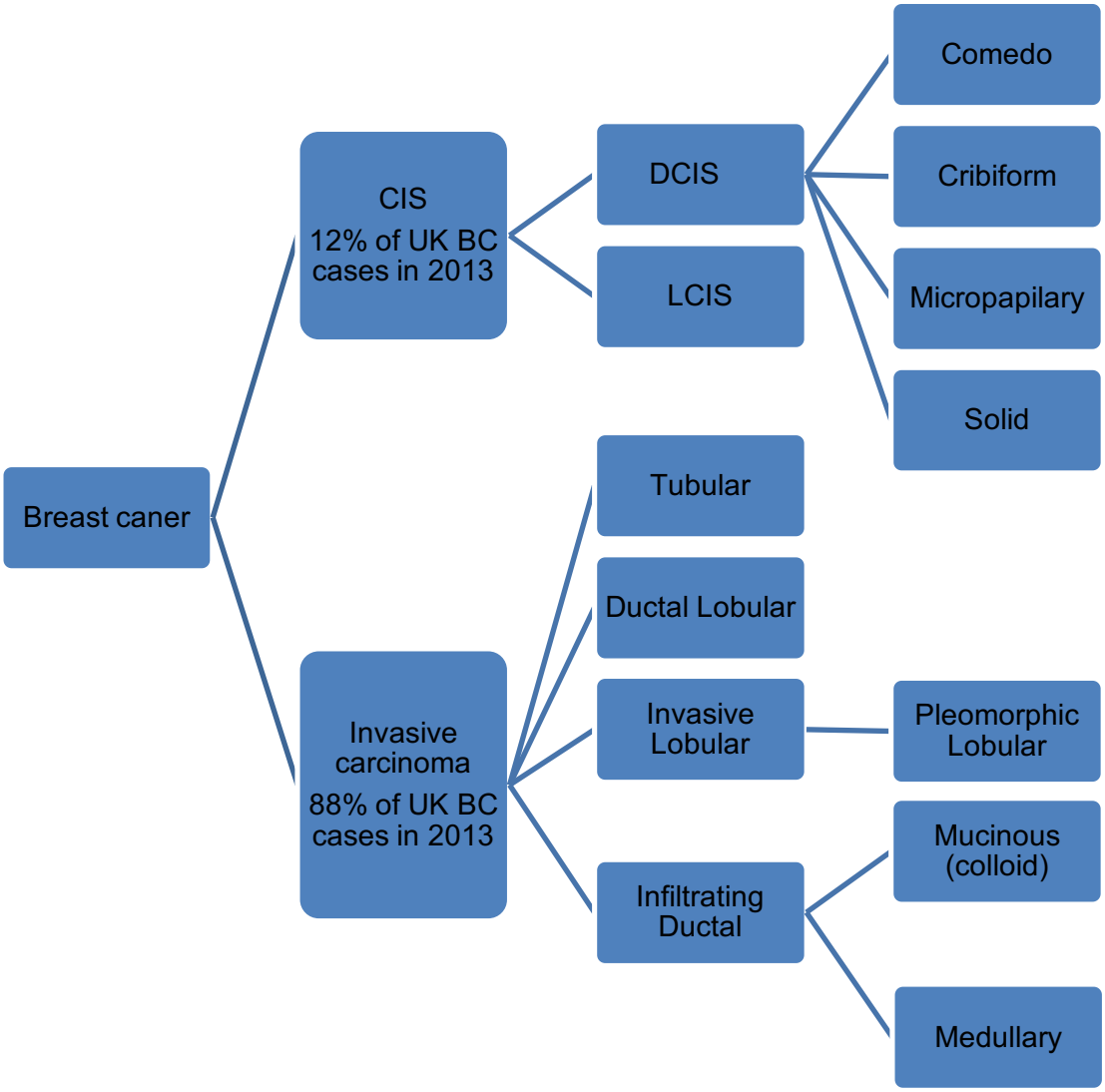


Figure 1.2 Histological classification of breast cancer. Modified from Malhotra et al. (2010) and Cancer Research UK, BC- breast cancer, CIS – Carcinoma in situ, DCIS – Ductal carcinoma in situ, LCIS – lobular carcinoma in situ

Infiltrating ductal carcinoma accounts for 70-80% of all invasive breast cancers (Li et al., 2005a) and is further classified according to the grade of differentiation (grade 1 being well differentiated to grade 3 being poorly differentiated) based on histological features (Lester et al., 2009).

1.2.3. Immunohistochemical (IHC) subtyping

The status of the hormone receptors for estrogen (ER) and progesterone (PR) as well as the level of HER2/neu is also regularly tested by IHC for invasive carcinomas (Malhotra et al., 2010, Harris et al., 2007). Further markers are cytokeratin 5/6 and EGFR. Positive staining for one or more of these markers leads to a certain sub-classification as outlined (Figure 1.3) (Rivenbark et al., 2013). However, sub-classification is problematic when the expression pattern does not fall into one of those categories or if neither of the markers is expressed.

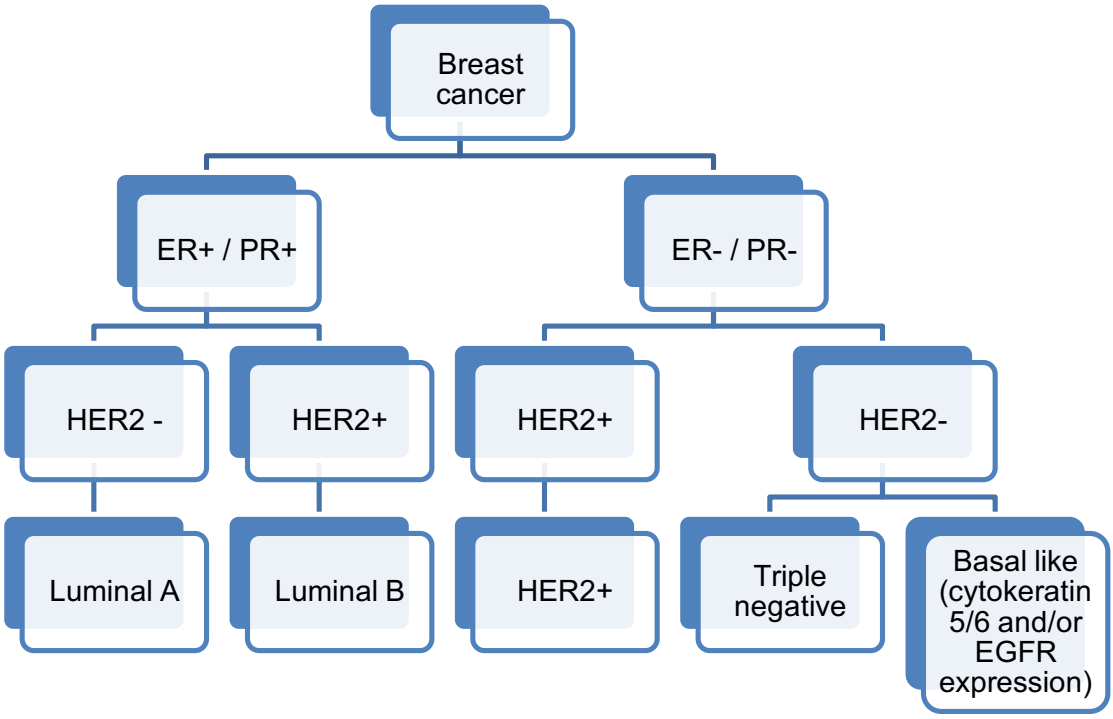


Figure 1.3 Clinical classification of breast cancer according to immunohistochemistry staining. Adapted from (Rivenbark et al., 2013)

This categorisation of breast cancer has a major impact on the decision for a particular treatment option. Targeted treatments such as endocrine therapy (ET) and trastuzumab are options for ER+ and HER2+ patients respectively in conjunction with

chemotherapy after studies showed improved response in those patient groups (Joensuu et al., 2009, Lumachi et al., 2013). More and more targeted therapies are in pre-clinical or clinical studies with a steady focus on the identification of biomarkers to better stratify patients.

1.2.4. Molecular subtypes

Over the last decade, molecular approaches for breast cancer subtyping have attempted to generate an improved stratification model for patients with regard to overall prognosis and treatment strategies.

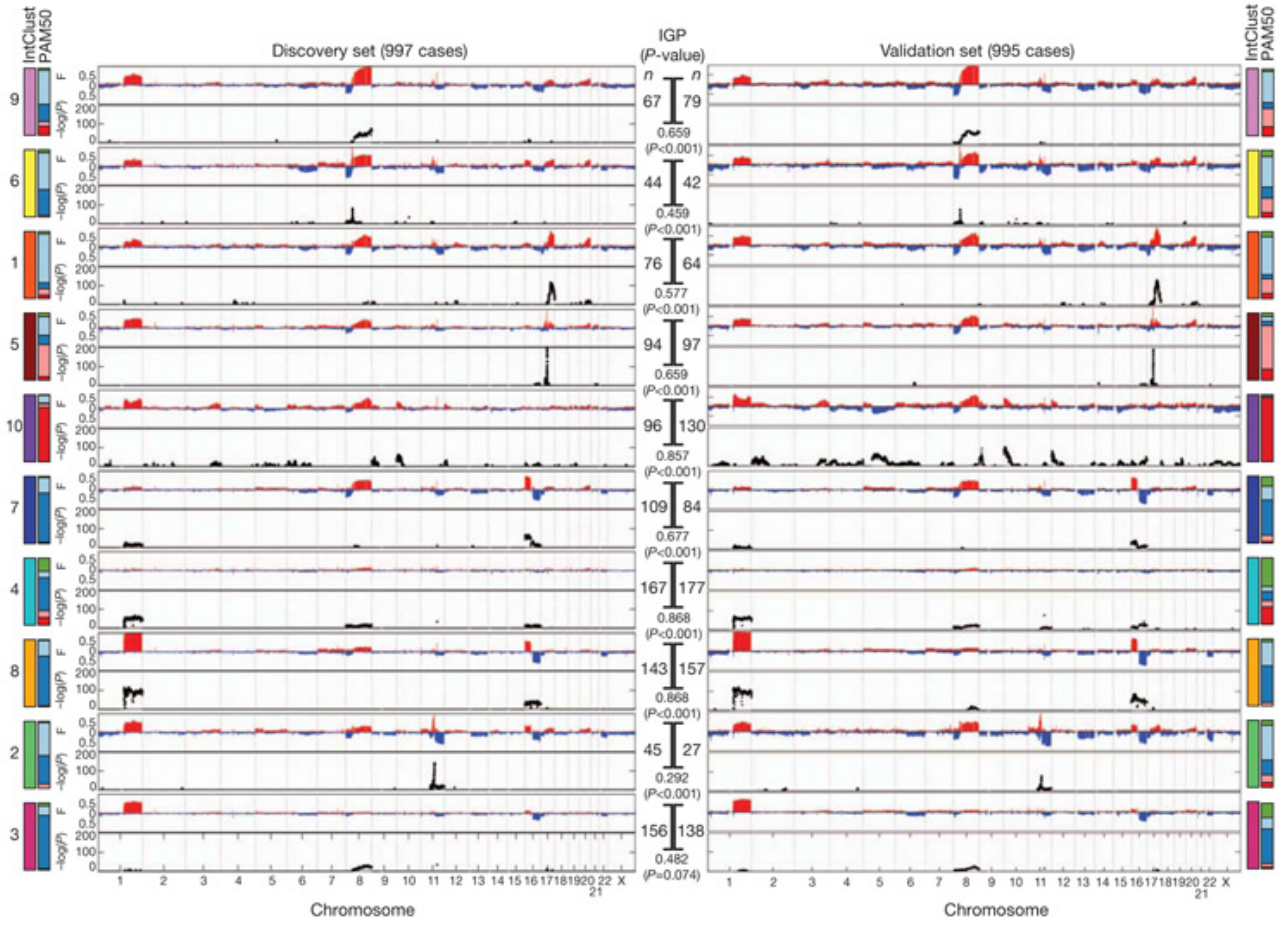
This new era started with the profiling of expression patterns of 65 breast tumours from 42 individuals using a cDNA microarray. This led to the identification of four distinct molecular breast cancer subtypes: luminal, basal-like, HER2+ve, and normal-like (Perou et al., 2000). The luminal (ER+ve) subtype was further divided into luminal A and luminal B breast cancers, which were shown to have a different prognosis. These intrinsic subtypes were each significantly correlated with a distinctive overall and relapse-free survival, and basal-like as well as HER2 overexpressing breast cancer are now associated with poorer outcome in comparison with luminal breast cancers (Sorlie et al., 2001, Sorlie et al., 2003).

In order to make this type of molecular subtyping more affordable and therefore more accessible in clinical practice, a limited gene signature of 50 genes has been developed. This signature, named PAM50, was shown to be able to efficiently classify tumours into one of the subtypes. The PAM50 signature was also better in predicting risk of relapse in comparison to the clinical markers (size, node status, and grade); however, a combination of all variables (clinical and molecular) had the best chance of predicting outcome (Parker et al., 2009).

With the wider availability of next generation sequencing technologies, the question of breast cancer subtyping was addressed with genomic as well as transcriptomic analysis. In a milestone paper, Curtis et al (2012) reported a study that included

samples from 2000 breast tumours as part of the Molecular Taxonomy of Breast Cancer International Consortium (METABRIC) (Curtis et al., 2012). Using this approach, the breast tumours were separated into 10 molecular subgroups associated with distinct copy number aberrations (CNAs), gene expression profiles and clinical outcomes (Figure 1.4 A and B).

A



B

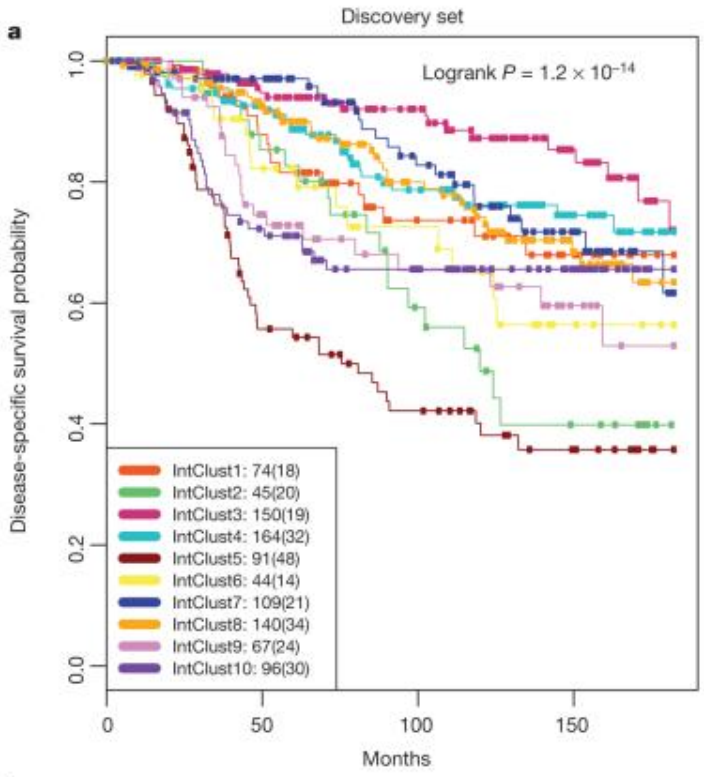


Figure 1.4 Next generation sequencing based clustering of 2000 breast cancers. Taken from (Curtis et al., 2012), permission for reprint obtained. (A) Genomic and transcriptomic landscape of 10 integrative subgroups from the METABRIC data set. Accordance with the PAM50 subgroups is shown in the bars on either side. Each of the 10 integrative subgroups contain cases that would have fallen in different groups if classified by the PAM50 signature (as indicated by the different colours in the PAM50 bar). (B) Kaplan–Meier plot of disease-specific survival for these subgroups.

1.3. Colon cancer

Bowel (Colon / colorectal) cancer is the fourth most common cancer and is the second most common cancer related cause of death in the UK (CancerResearchUK, 2014).

Similar to breast cancer, there have been attempts to characterise the tumours in order to stratify patients. Clinically, the most common methods include TNM staging (Table 1.2) as well as grading and this is used to select patients for adjuvant treatment.

Table 1.2 Colon Cancer TNM Assessment Taken from Cancer Research UK (CancerResearchUK, 2014)

Tumour	
T1	Tumour only affects the inner layer of the bowel
T2	Tumour has invaded the muscle layer of the bowel wall
T3	Tumour has infiltrated the outer lining of the bowel wall
T4	Tumour has grown through the bowel wall
Nodes	
N0	Lymph nodes are negative
N1	1-3 lymph nodes adjacent the bowel are positive
N2	≥ 4 lymph nodes are positive
Metastasis	
M0	No metastasis detected
M1	Metastasis detected

According to the classification from the TNM system, colon cancer is then grouped in 4 stages as outlined in table 1.3.

Table 1.3 Colon Cancer Stages. Taken from Cancer Research UK (CancerResearchUK, 2014)

Stage 0 / CIS	T1, N0, M0
Stage 1	T1 or T2, N0, M0
Stage 2	2a: T3, N0, M0 2b: T4, N0, M0
Stage 3	3a: T1 or T2, N1, M0 3b: T3 or T4, N1, M0 3c: any T, N2, M0
Stage 4	Any T, any N, M1

Another factor that determines treatment decisions is the grading, which assesses the level of differentiation of the cancer cells (Table 1.4).

Table 1.4 Colon Cancer Grading. Taken from Cancer Research UK (CancerResearchUK, 2014)

Grade 1 (low grade)	Well differentiated
Grade 2 (moderate grade)	Moderately differentiated
Grade 3 (high grade)	Poorly differentiated

Additionally, molecular markers that were investigated with relation to subtyping and prognosis include microsatellite instability, which was associated with a better prognosis (Popat et al., 2005) as well as CpG island methylator phenotype [CIMP], chromosomal instability [CIN], and BRAF and KRAS mutations (Hutchins et al., 2011, Jass, 2007, Shen et al., 2007, Kang, 2011).

Attempts to achieve a clearer subtyping system using microarray technology have been reported by several groups (Salazar et al., 2011, O'Connell et al., 2010). More recently, an approach that integrated unsupervised hierarchical clustering with genetic and epigenetic data including methylome data (Hinoue et al., 2012), identified

three (Shen et al., 2007) or four (Kang, 2011) distinct subtypes in colon cancer and gave rise to the ColoPrint subtyping signature.

Marisa et al (2013) reported six distinct molecular subtypes based on the gene expression of 443 samples. The subtypes reported were: a subtype with deficient mismatch repair; KRAS mutation; a cancer stem cell (CSC) subtype, and three subtypes with chromosomal instabilities (downregulation of immune pathways, Wnt upregulation, and a normal-like subtype). Two out of those six subtypes, the CSC and the normal-like clusters, were correlated with a poorer progress free survival in the stage II and III subset which was independent of factors like stage and the Oncotype DX Colon Cancer Assay recurrence score (HR 1.5, 95% CI 1.1–2.1, p = 0.0097) (Marisa et al., 2013).

1.4. Shortfalls with subtyping attempts

Despite the common practice of cancer subtyping at the time of diagnosis, this stratification of patients still invites much discussion.

For example, in colon cancer, staging fails to accurately predict the likelihood of recurrence and 10-20% and 30-40% of patients initially diagnosed with stage II or stage III disease respectively relapse after “curative” surgery (Marisa et al., 2013).

Some of the possible shortfalls include observer-subjectivity, lack of concordance between approaches, and intratumour heterogeneity.

1.5. IHC staining

For breast cancer cases ER, PR, and HER2 status are commonly determined by IHC staining. However, staining intensity is very much dependent on the staining method. Moreover, pathologists evaluate the slides. This makes it prone to subjective scoring, which is also dependent on the experience and exposure of the pathologist. Therefore, different pathologists may score the same slides differently. Moreover, the scoring cut-off points to define for example HER2 positivity have been changed over

the years. This affects which and how many patients are eligible for targeted treatment.

The recommendation by the American Society of Clinical Oncology / College of American Pathologists (ASCO/CAP) from 2013 considers dark IHC staining intensity (3+) of >10% of the tumour as a marker for HER2 positivity. For borderline cases, HER2 status is also determined by fluorescence in situ hybridisation (FISH), where a copy number of ≥6 or a HER2/Chromosome 17 ratio > 2.0 is considered HER2 positive (Wolff et al., 2013).

1.6. Comparison between subtyping approaches

Despite the fast progress in molecular subtyping, the main clinical approach to classify a cancer sample consists of staging, histopathology and immunohistochemistry as outlined above as a proxy.

However, Rivenbark et al. (2013) showed that the correlation between IHC and molecular classification in breast cancer is poor. The group did a comparison of subtypes in a set of 381 breast cancers for which molecular (Harrell et al., 2012) and IHC classifications were known (Rivenbark et al., 2013).

They found that only 49% of samples that were classified as Luminal A by IHC were subtyped as the same class of breast cancer by the molecular testing strategy. This means that 51% of samples could be expected to behave like breast cancers with a much less favourable prognosis. Considering that the treatment decision is made depending on the immunohistochemical data, this may account for adverse outcomes in patient groups that are expected to do well.

However, molecular approaches may also produce variable results. In the analysis of 2000 breast cancer patients using next generation sequencing an overlay of the 10 subtypes with the PAM50 signature is also shown (Figure 1.4 A). Comparing how the samples were classified using the 10 subgroups with how the cases would have been classified using the PAM50 signature (bars on either side), it is obvious that there is

not a full concordance between the 10 subgroups and the distribution of the PAM50 subgroups within them in either the discovery or the validation set.

In colon cancer, several groups have suggested signatures for subtyping. So far, 3, 4 or 6 subtypes have been reported (Kang, 2011, Marisa et al., 2013, Salazar et al., 2011, Kopetz et al., 2015, You et al., 2015). However, the concordance between those signatures is also variable (Marisa et al., 2013).

1.7. Cancer heterogeneity

As described above, several models to classify breast and colon cancer subtypes have been established and/or are currently under development. However, establishing a distinct tumour subtype between different approaches seems to be poor in a significant number of cases. This indicates that the disease is much more complex and that heterogeneity exists both between tumours and also within tumours.

At the same time many advanced cancers are still associated with poor outcome, often failing to respond adequately to chemotherapeutics and/or targeted therapies. Intratumour heterogeneity may contribute to this problem by inducing different phenotypes within the tumour, potentially leading to a bias in the initial classification during diagnosis. A recent study showed that trastuzumab response was poorer in breast cancer patients who had tumours that were heterogeneous in HER2 expression as measured by the HER2/CEP17 ratio, or had a HER2/CEP17 ratio of 2.2 in less than 80% of tumour cells (a IHC staining of 3+ in less than 75%). This was also correlated with a shorter time to relapse and overall survival (Lee et al., 2014).

Therefore, there is a need to better understand tumour heterogeneity as many treatment options currently struggle to address this aspect.

Several studies have now shown considerable intratumour heterogeneity, finding heterogeneous cell types within and between biopsies of the primary tumour as well as between the primary tumour and associated metastases. This has led to the

notion that these cellular phenotypes may interact and are caused by genetic and non-genetic/microenvironmental factors (Marusyk et al., 2012).

1.7.1. Models for cancer heterogeneity

Yap et al. (2012) proposed that, according to molecular evidence, intratumour heterogeneity follows a branched (polytypic) rather than a linear pattern. According to this, tumour growth resembles a tree like structure with different levels of complexity. The first level or "trunk" would consist of cells with ubiquitous driver mutations. On level two are the "branches", representing different areas of a tumour that may harbour different heterogeneous mutations. All these mutations are subject to changing environmental conditions and the biological behaviour of these cells is liable to distinct selection pressures (complexity level 3). This means that different clones may become more/less important for tumour growth throughout different the stages of disease development or even during treatment, as resistance may result from a small number of cells carrying a specific mutation (Yap et al., 2012).

For example, EGFR tyrosine kinase inhibitors erlotinib and gefitinib have been shown to be a good treatment option for non-small cell lung cancer (NSCLC) patients with activating EGFR mutations including L858R (Pao et al., 2004). However, resistance is conferred by an alternative T790M mutation (Yun et al., 2008).

Three main models to explain the establishment and maintenance of intratumour heterogeneity have been proposed: the cancer stem cell (CSC) hypothesis, clonal evolution, and tumour plasticity (Campbell and Polyak, 2007, Merlo et al., 2006, Hill, 2006, Michor and Polyak, 2010).

The cancer stem cell (CSC) hypothesis

The cancer stem cell (CSC) theory is a controversial area. The hypothesis proposes that a tumour consists of cells with similar underlying genetic make-up, but with

varying degrees of stemness / differentiation. CSCs are thought to develop from adult stem cells that acquire a mutation. As stem cells are long-lived, they would have more time to be hit by mutational load. Similar to physiological stem cells, CSCs are thought to undergo symmetric division to maintain the CSC pool. Likewise, differentiated (and heterogeneous) cells are generated during asymmetric division. The CSCs are considered highly tumourigenic and thought to drive tumour initiation, progression and recurrence whereas the differentiated cells bear a lower tumourigenic potential (Ichim and Wells, 2006, Al-Hajj and Clarke, 2004, Michor and Polyak, 2010).

Tumour cells with stem cell-like features were first identified in 1994 in human acute myeloid leukaemia (AML). These tumour cells shared surface markers normally associated with haematopoietic stem cells and were further able to induce leukemia in NOD/SCID mice, while other cells missing these markers could not (Lapidot et al., 1994). CSCs have since been reported in various malignancies including lung (Kim et al., 2005), brain (Singh et al., 2003), colon (Ricci-Vitiani et al., 2007), and breast cancer (Al-Hajj et al., 2003).

Clonal evolution

The clonal evolution hypothesis can be seen as a Darwinian survival of the fittest theory. First proposed in 1976 (Nowell, 1976), the underlying mechanism of heterogeneity stems from normal cells that have acquired several genetic mutations and epigenetic changes over time to form new populations. If the acquired changes are beneficial for tumour growth, these populations will be evolutionary favoured and will drive tumour progression. Further mutations enhance tumour heterogeneity and resistance to therapy (Michor and Polyak, 2010).

In support of this notion, cancer cells genomes are notably unstable and this is actually considered as one of the hallmarks of cancer (Hanahan and Weinberg, 2011).

Previously, Aubele et al. in 1999 had reported that cells from the same invasive breast tumour tissue had differential chromosomal gains and losses (Aubele et al., 1999) and similar reports have since followed.

The recognition of somatic driver mutations aids the development of targeted treatments. Testing of HER2 status is now standard in the clinics and patients who are diagnosed with HER2 positive breast cancer have access to targeted treatment options such as the monoclonal antibody trastuzumab (Herceptin) in combination with chemotherapy (Wolff et al., 2014). However, although HER2 is now considered a reliable clinical marker, HER2 copy numbers have also been shown to vary considerably within the tumour tissue (Szollosi et al., 1995) and improvements in testing methods and cut-off points are ongoing.

Tumour plasticity

The third model to explain tumour heterogeneity is tumour plasticity. Cells acquire stem cell-like properties as a result of tumour-microenvironmental influences and/or intrinsic cell variability. Factors implicated in this setting are microenvironmental

changes such as the onset of hypoxia and nutrient deprivation as the tumour grows. Moreover, autocrine or paracrine signalling via cytokines and chemokines, the infiltration of other cell types such as macrophages, the interaction between the tumour cells and the surrounding stroma, and epithelial to mesenchymal transition (EMT) may all influence the fate of tumour cells (Tang, 2012). Furthermore, microenvironmental conditions may vary within the tumour, therefore promoting the development of different populations.

In conclusion, all three models may have an impact on treatment options and success. With regard to this, one characteristic of putative stem cells is the upregulation of ATP binding cassette (ABC)-transporters, a system involved in multi-drug resistance (MDR) (Zhou et al., 2001, Hiraga et al., 2011, Hegedus et al., 2012). Targeting these receptors together with the anti-apoptotic mechanisms associated with cancer stem cells increased response to chemotherapy *in vitro* (Sun et al., 2015). Moreover, while the recognition of driver mutations such as HER2 has led to the development of targeted treatment options, it is now well reported that drug treatment can drive the development of resistant clones (Yun et al., 2008, Oxnard, 2016).

Following the first model (the CSC theory), targeting the putative stem cells, which are deemed to be the driving force behind tumour development, would be pivotal in cancer treatment. However, the tumour plasticity theory suggests that this could be difficult as differentiated cells may acquire stem cell-like features. Additionally, there is now evidence suggesting that clonal evolution and CSC-driven tumour development mechanisms may interact, furthering heterogeneity (Anderson et al., 2011, Notta et al., 2011).

Therefore, a better understanding of tumour heterogeneity, its underlying causes and the resulting interaction of the different populations with each other and their microenvironment are of pivotal importance.

Changes in the microenvironment can lead to the activation / shut down of cell pathways and may even select for cells more equipped to survive certain conditions. A common change in tumours is the onset of hypoxia, which has been shown to drive tumour heterogeneity through a change in cellular pathways.

1.8. Hypoxia

Hypoxia is defined as regions that are supplied with low or insufficient oxygen. Oxygen levels vary considerably between different body tissues but also between tumours. The partial pressure of oxygen (pO_2) can vary between around 24 mmHg in liver and brain to about 66 mmHg in the spleen. In tumours pO_2 levels of < 20 mmHg are often measured. Therefore, most tumours have a lower mean pO_2 in comparison to surrounding tissues, indicating the onset of hypoxia (Vaupel et al., 1989).

Onset of hypoxia in most solid tumours is due to insufficient vascularisation leading to a decrease in the number of functional vessels as well as severe structural abnormalities. Consequently, this leads to a heterogeneous oxygenation of the tumour and areas of the tumour mass with inadequate supply of oxygen as well as nutrients (Harris, 2002).

This can happen in two ways. Thomlinson and Gray first showed in 1955 that cells residing > 180 µm from vascularisation become hypoxic/necrotic due to the limited diffusion of oxygen (Thomlinson and Gray, 1955). It is now established that as a tumour grows, the oxygen supply will be inadequate if cells are > 70 µm away from a blood vessel (Harris, 2002). This is termed chronic (diffusion-related) hypoxia (Harris, 2002). Acute (perfusion-related) hypoxia on the other hand occurs when blood flow fluctuates or stops transiently because of defective blood vessels. This concept has been proven in murine but also human tumour models (Hill et al., 1996). However, blood flow can be restored leading to re-oxygenation (Harris, 2002, Hill et al., 1996) within minutes or hours.

1.8.1. The HIF-1 pathways

A main factor mediating the response to hypoxia is the hypoxia inducible transcription factor 1 (HIF-1). An overview of HIF-1 regulation and activity is shown in Figure 1.5. HIF-1 is a heterodimer, which needs two subunits to become functionally active: the HIF1-α and the HIF-1β subunit (or aryl hydrocarbon receptor nuclear translocator, ARNT). Both, HIF-1α and HIF-1β are classified as PER-ARNT-SIM (PAS) basic helix-loop-helix (bHLH) transcription factors (Jiang et al., 1996). Structurally both subunits consist of the following domains: a N-terminus bHLH domain for DNA binding, a PAS domain needed for heterodimerisation and a C-terminal domain that recruits co-regulatory proteins for transcription (Zhulin et al., 1997) (Yang et al., 2005).

Lesser focus has been given to two other members of the HIF family, namely HIF-2 and HIF-3. The former is structurally similar to HIF-1 but is only expressed in certain tissues including endothelium, kidney, and liver (Wiesener et al., 2003). HIF-3 may act as a dominant–negative regulator of HIF (Makino et al., 2001).

Hypoxia dependent HIF-1 activation

The activation of the HIF-1 pathway is tightly regulated (Figure 1.5). Both subunits are expressed constitutively. Under normoxic conditions, HIF-1α is marked for degradation by prolyl hydroxylases (PHDs) that hydroxylate two proline residues, P402 and P564, present in the **o**xygen **d**ependent **d**egradation **d**omains (ODDDs) of the protein (Yee Koh et al., 2008). This targets HIF-1α for ubiquination by the von Hippel Lindau (VHL) protein and proteosomal degradation.

Moreover, HIF-1α is also regulated by the factor inhibiting HIF-1 (FIH1). This factor hydroxylates the asparagine 803 residue in the C-terminal domain; thereby preventing binding to the co-transcriptional factor p300 and inhibiting HIF mediated transcription (Hewitson et al., 2002).

In hypoxic conditions the “oxygen sensing” PHDs do not bind HIF-1α and the protein is therefore stabilised. HIF-1α translocates to the nucleus to dimerise with HIF-1β. The heterodimer then binds co-activators such as CREB-binding protein (CBP)/p300 (Yamashita et al., 2001). The complex binds to hypoxia response elements (HRE) in the promoters of hypoxia response genes involved in various cellular processes such as pH regulation, angiogenesis and metabolism (Forsythe et al., 1996).

Hypoxia independent HIF-1 activation

Under certain circumstances, HIF-1α can also be activated in normoxia. Loss of function of the VHL leads to increased stabilisation of HIF-1α and also HIF-2α (Semenza, 2003). Clear cell carcinomas and cerebral haemangiomas often display this phenotype (Maxwell et al., 1999, Zhong et al., 1999).

Moreover, the loss of other tumour suppressor genes such as p53 and phosphatase and tensin homolog deleted on chromosome 10 (PTEN) have been shown to be linked to increased HIF-1α expression. Regulation of HIF-1α by p53 has been demonstrated to occur via MDM-2 mediated ubiquination and loss of p53 enhanced HIF-1α levels (Ravi et al., 2000).

Growth factor signalling such as from insulin growth factor (IGF) or epidermal growth factor (EGF) can enhance HIF-1α expression; this has been shown to be mediated via the downstream activation of the mitogen activated protein kinase (MAPK) pathway (Semenza, 2003), or via the phosphoinositide 3-kinase/ mammalian target of rapamycin (PI3K/mTOR) pathways (Zundel et al., 2000). Likewise, loss of PTEN – a negative regulator of the PI3K/mTOR pathway - led to an increase of HIF-1α in non-hypoxic conditions (Zundel et al., 2000).

1.8.2. Main pathways regulated by hypoxia

Hypoxia has been implicated to influence a number of pathways (Figure 1.5).

Angiogenesis

As described earlier, inadequate blood supply and therefore low levels of oxygen and nutrients are stress factors for cells. In turn, hypoxia has been shown to be a key regulator of angiogenesis – the formation of new blood vessels via the sprouting of endothelial cells.

This is achieved by the upregulation of growth factors that regulate endothelial cell growth and vessel formation. A main upregulated pathway in this response is the vascular endothelial growth factor (VEGF) pathway. The growth factor as well as its corresponding receptors (VEGFR) are targets of HIF-1α transcription. The circulating VEGF binds to the VEGFR1 and VEGFR2 on endothelial cells and promotes angiogenesis. Other angiogenesis-related proteins upregulated by hypoxia include angiopoietin-2 and transforming growth factor β (TGF β) (Pugh and Ratcliffe, 2003).

pH regulation

Hypoxia has been associated with a more acidic microenvironment with pH_e values around 6.2-6.3 in comparison to normoxic tissues (7.2-7.4) (Gillies et al., 2002). This was attributed to the high proliferation activity of tumour cells, coupled with the production of lactic acid as the end product of glycolysis (Gillies et al., 2002, Gatenby and Gillies, 2004, McDonald et al., 2012). Moreover, HIF-1α upregulates several proteins essential for the glycolytic pathway. Maintenance of a physiological intracellular pH confers a survival benefit and hypoxia has been shown to upregulate carbonic anhydrases (CA) 9 and 12, which regulate pH levels by the reversible conversion of water and carbon dioxide to carbonic acid (Harris, 2002).

Invasion and Metastasis

Acidic conditions are also associated with invasion and metastasis (McGillen et al., 2014), via several mechanisms including the remodelling of extracellular matrix (Estrella et al., 2013).

Hypoxia and re-oxygenation have also been shown to increase the invasive potential of pancreatic cancer cells via the induction of reactive oxygen species (ROS) and subsequent upregulation of the collagenase matrix metalloproteinase-2 (MMP-2) (Binker et al., 2010).

Stem Cell Maintenance

Hypoxia has been shown to promote the expansion of CSCs (Paranjape et al., 2012, Mathieu et al., 2011). Additionally, it was shown that differentiated cells become pluripotent progenitor stem cells (iPS) by the induction of only a few transcription factors such as OCT4, SOX2, Nanog (Jeter et al., 2011, Paranjape et al., 2012, Scaffidi and Misteli, 2011, Yamanaka and Blau, 2010). Hence the finding that hypoxia enhances the activity of OCT4, c-Myc and Nanog (Gordan et al., 2007, Covello et al., 2006) gave further insight into how hypoxia supports stem cell maintenance.

Proliferation and Survival

Hypoxia is a stress factor for cell growth. In order to maintain proliferation, the hypoxic response includes upregulation of growth factors including transforming growth factor β (TGFβ), and platelet-derived growth factor (PDGF) (Harris, 2002). Moreover, it has been shown that there is increased activity of the PI3K pathway, which is associated with survival and proliferation (Zundel et al., 2000, Harris, 2002). Hypoxia is also thought to push the “survival of the fittest”, for example by selecting cells with defects in apoptotic mechanisms (eg p53 mutation/deficiency) (Graeber et al., 1996) and also to be driving a more resistant and invasive phenotype (Maxwell et al., 2001, Harris, 2002).

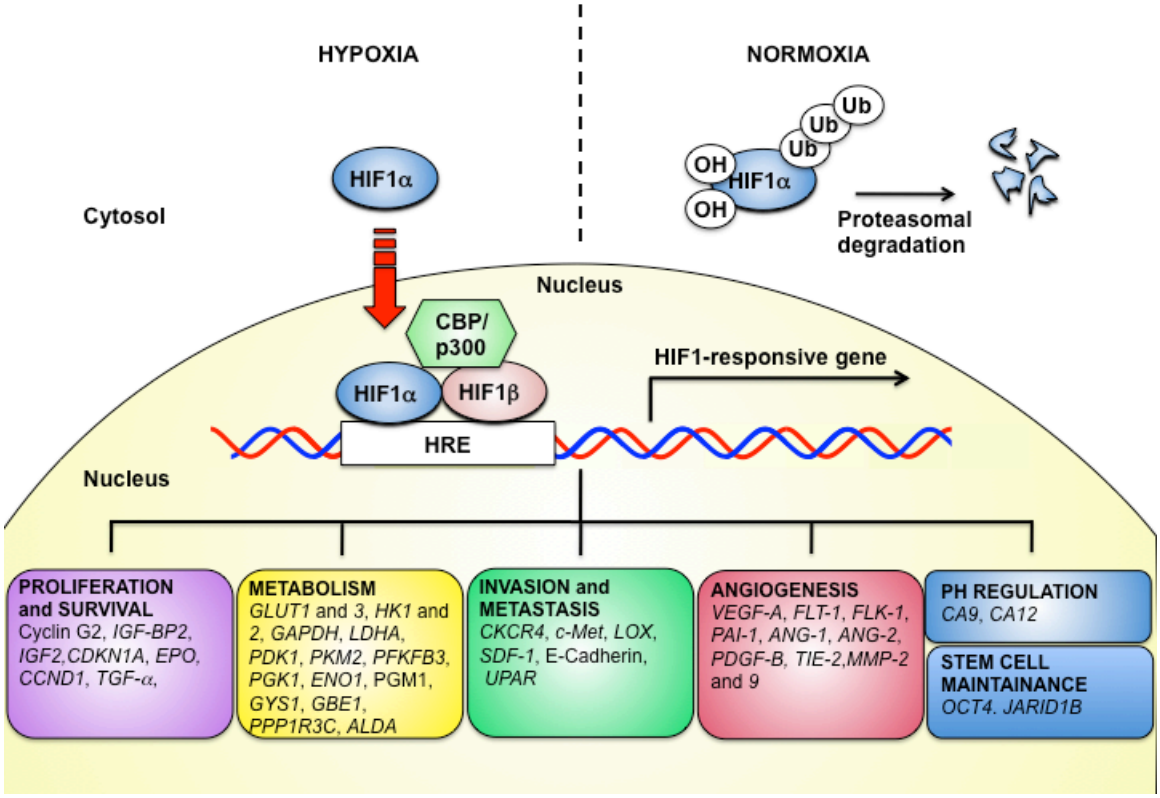


Figure 1.5 Regulation of HIF-1 and its transcriptional activity. Taken from (Favaro et al., 2011), permission for reprint obtained.

1.9. Tumour cell metabolism

The development of cancer is also intimately connected with changes in the cells' metabolism, which is now recognised as a hallmark of cancer. Moreover, hypoxia has been shown to play a major role in regulating genes that are associated with changes in metabolic pathways.

1.9.1. Cell metabolism

Cell metabolism is required to produce the energy as well as the metabolic precursors needed for cell function. Generally, metabolism describes two processes, catabolism and anabolism. Catabolism describes the metabolic pathways that break down molecules into smaller units used for cellular respiration. Anabolism, in contrast, is the set of pathways for the synthesis of complex molecules.

Depending on the cell state – proliferating or quiescent – the metabolic machinery has a different focus. Proliferating cells, for example, need more anabolic processes in order to duplicate. Cells can utilise different starting molecules in both catabolic and anabolic processes (Vander Heiden et al., 2009).

The most well studied pathway in the production of ATP in aerobic conditions is probably the usage of glucose, fats and proteins through the citric acid cycle (also known as tricarboxylic acid – TCA – cycle). As depicted in Figure 1.6, a glucose molecule is broken down through various steps to generate pyruvate (glycolysis). Pyruvate is then actively transported into the mitochondria, where it can either be carboxylated to form oxaloacetate or oxidised by pyruvate dehydrogenase (PDH) and combined with coenzyme A to form CO_2, acetyl-CoA and NADH (Voet et al., 2006). The acetyl group from acetyl-CoA is linked with oxaloacetate to form citrate. This is then oxidised in 8 steps by various enzymes, and the energy made available by this is transferred as electrons to nicotinamide adenine dinucleotide (NAD^+) to form NADH. Other products of the cycle are two molecules of water and carbon dioxide, flavin adenine dinucleotide ($FADH_2$) as well as amino acid precursors (Stryer, 1995).

The NADH and FADH2 generated in this process can donate the gained electrons in the oxidative phosphorylation to facilitate the production of ATP. The theoretical net yield of one glucose molecule through glycolysis, TCA cycle and oxidative phosphorylation is 36 ATP (Stryer, 1995).

Moreover, some amino acids are derived from TCA cycle intermediates, for example aspartate and asparagine can be formed from oxaloacetate and glutamine, proline and arginine can be formed from α-ketoglutarate. From these, purines and pyridines can be formed which are the bases for many essential cell molecules including DNA and RNA as well as ATP and NAD (Stryer, 1995).

Likewise, amino acids such as leucine, isoleucine, lysine, phenylalanine, tryptophan, and tyrosine can be converted into acetyl-CoA. TCA cycle intermediates can also be

formed by amino acids; it has been shown that glutamine can be converted into α-ketoglutarate via glutamate (Stryer, 1995).

Another main metabolite is fatty acids. Citrate can be transported out of the mitochondrion and converted to acetyl-CoA and oxaloacetate by ATP citrate lyase (ACLY). Acetyl-CoA is then converted into malonyl-CoA by acetyl-CoA carboxylase (ACC). Fatty acid synthase (FASN) catalyses the formation of fatty acids such as palmitate from malonyl-CoA and acetyl-CoA (Harjes et al., 2016).

The de novo synthesis of fatty acids has been associated with rapid cell proliferation and decreased drug sensitivity (Mashima et al., 2009, Rysman et al., 2010).

Other than de novo synthesis, tumour cells can also upregulate fatty acid uptake. A main transporter involved is FAT/CD36 (Abumrad et al., 1993). Fatty acids are then transported within the cell by fatty acid binding proteins (FABP). Several members of the FAB protein family such as FABP5 (Liu et al., 2011, Levi et al., 2013) and FABP7 (Liu et al., 2012) have been associated with tumour aggressiveness.

Lipids are dynamically stored in lipid droplets, consisting of a core of neutral lipids, triglycerides and sterol esters, a monolayer of polar lipids and a protein coat including perilipin (PLIN) proteins. Fatty acids in turn are a substrate for oxidation, a cyclical series of reactions that shorten the fatty acids by 2 carbons/cycle, generating NADH, FADH2, and acetyl-CoA. NADH and FADH2 are in turn used for ATP production (Carracedo et al., 2013) and ROS scavenging.

Cell metabolism is highly regulated including by genes and pathways that are known tumour suppressors or oncogenes such p53 and PI3K/AKT respectively.

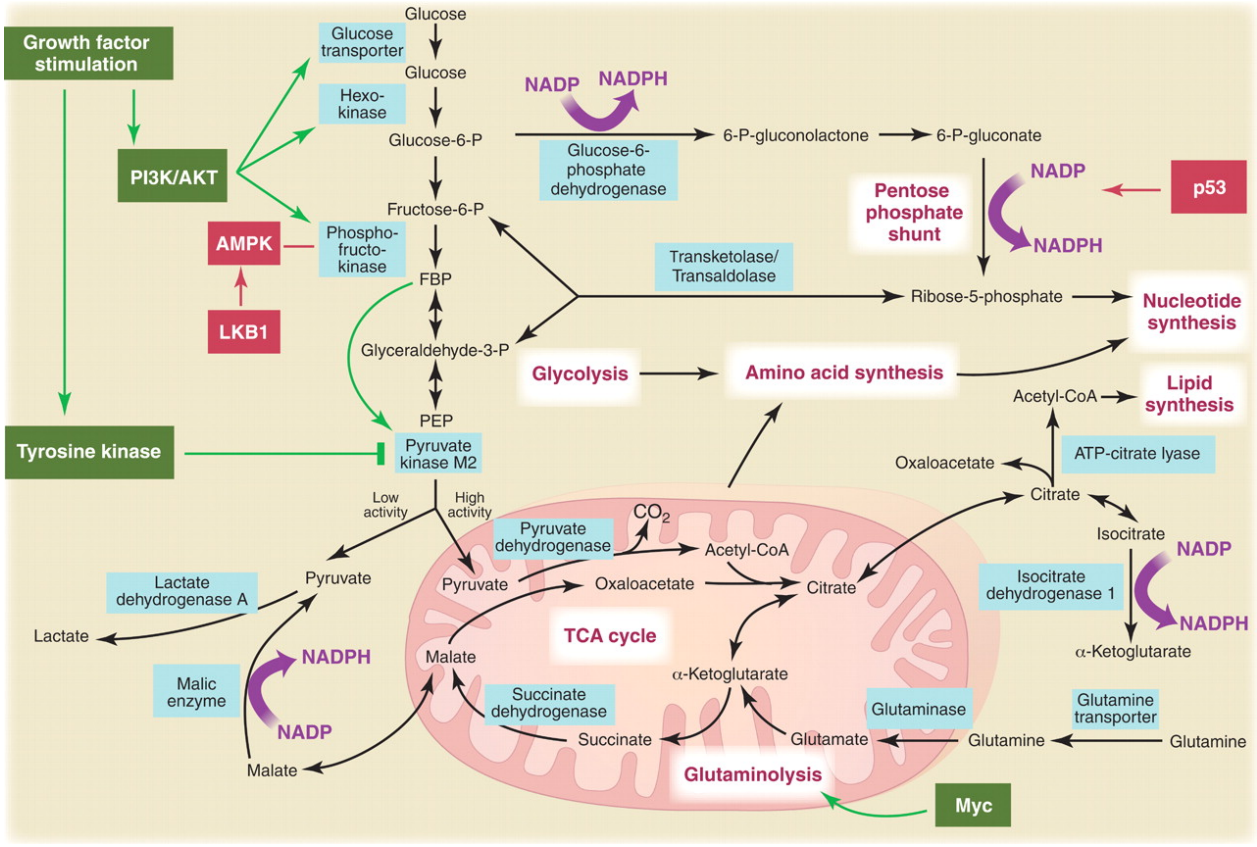


Figure 1.6 Metabolic pathways in proliferating cells. Taken from (Vander Heiden et al., 2009), permission for reprint obtained.

1.9.2. Metabolism and hypoxia

In normoxic conditions, cells utilise glucose to produce energy via glycolysis and oxidative phosphorylation. This yields 36 molecules of ATP per molecule of glucose. However, in hypoxia, when low oxygen will not support oxidative phosphorylation at the mitochondria, cells increase the glycolytic flux for glucose metabolism (Warburg effect), which generates 2 molecules of ATP per molecule of glucose, as pyruvate is then converted to lactate rather than used in the mitochondria (Dang and Semenza, 1999, Seagroves et al., 2001).

Lower oxygen tensions have been shown to decrease the respiratory rate, decrease ATP production and concomitantly increase ADP and AMP levels (Wilson et al., 1977).

To compensate for the fewer molecules of ATP produced, the glycolytic rate of tumours in hypoxia is increased. This is facilitated by the HIF1 mediated upregulation of enzymes involved in glycolysis. It has been shown that HIF-1 directly affects the expression of the glucose transporters GLUT1 and GLUT3 (Chen et al., 2001). Additionally, levels of glycolytic players such as lactate dehydrogenase A (LDHA), which is responsible for the conversion of pyruvate to lactate, are also upregulated by HIF-1 (Cantor and Sabatini, 2012). Moreover, it induces the expression of pyruvate dehydrogenase kinase-1 (PDK-1), which blocks the utilisation of pyruvate in the TCA cycle by inactivating PDH (Wigfield et al., 2008, Kim et al., 2006). Interestingly, this helps to maintain ATP production as PDK-1 induction in hypoxic HIF1-negative cells increased ATP levels in comparison to control and decreased hypoxic ROS generation by the mitochondria. Moreover, blocking the mitochondrial TCA cycle leads to a decrease in mitochondrial oxygen consumption and therefore an increase in intracellular pO_2 and decreased cell death in relation to limiting oxygen levels (Kim et al., 2006, Papandreou et al., 2006)

On the other hand, it has been shown that the TCA cycle intermediates fumarate and to a lesser extent succinate and oxaloacetate, can inhibit HIF-1α hydroxylation, thereby stabilising HIF-1 levels and transcriptional activity even in normoxic conditions. In the same study citrate was shown to be able to inhibit FIH1 (Koivunen et al., 2007). Independently, pyruvate was also shown to inhibit HIF-1α degradation (Lu et al., 2005)

1.9.1. The Warburg effect and tumour metabolism

A high rate of cell proliferation is a hallmark of cancer. This requires energy as well as sufficient biomass to sustain cellular growth. It was first found in yeast that proliferating cells convert a significant amount of glucose-derived carbon through fermentation. Otto Warburg described in the beginning of the 20th century that tumour cells differ from non-tumour cells. He found that in these cells a majority of glucose

was used in glycolysis but that pyruvate was then converted into lactate instead of being used in the TCA cycle and oxidative phosphorylation. Interestingly, this was independent of oxygen levels (Warburg, 1956). Cancer cells have an up to 200 times increased level of glycolysis (Warburg, 1956) and up to 90% of the glucose is converted to lactate (DeBerardinis et al., 2007). The fact that tumour cells display a higher uptake of glucose is now clinically used for [18F]-deoxyglucose positron emission tomography (FDG-PET) to diagnose and monitor treatment response in cancer.

Warburg initially hypothesised that this effect was due to defective mitochondria in cancer cells and indeed it has been shown that dysfunctional mitochondria can cause cancer (Koppenol et al., 2011), yet tumour cells can also harbour functional mitochondria (Weinhouse, 1976).

However, more recent results show that tumour suppressor and oncogenes also have regulatory roles in cell metabolism (also see Figure 1.6). To this end it has been shown that growth factor abundance (and the related signalling) influences cell metabolism. In an environment where cells have to compete for growth factors, the focus lies on efficient ATP production through catabolic metabolism (Deberardinis et al., 2006; Lum et al., 2005; Vander Heiden et al., 2009). On the other hand, if growth signalling is increasing, cells adopt an anabolic metabolism, preparing for cell division (Bauer et al., 2004).

The idea can be interpreted in two ways. Initially, it was thought that changes in cell metabolism are a secondary response to a decrease in the ATP:ADP ratio due to transcriptional and translational activity. However, it also emerges that changes in metabolic fluxes can be independent of ATP levels, but are rather driven by the need for synthesis of macromolecules such as nucleotides (Ward and Thompson, 2012).

Pathways that enhance anabolic metabolism

Activating changes in the PI3K/AKT pathways is one of the most common features of cancers and can lead to enhanced glycolysis (Elstrom et al., 2004). Another major role of AKT is the phosphorylation and activation of ACLY, the enzyme that facilitates the re-conversion of citrate into oxaloacetate and acetyl-CoA in the cytoplasm, the latter being an important precursor especially for fatty acids (Berwick et al., 2002, Bauer et al., 2005). In turn, ACL knockdown in AKT dependent tumours leads to a decrease of tumour growth *in vitro* and *in vivo* (Hatzivassiliou et al., 2005). Moreover, the downstream target of AKT, mTOR, has been shown to drive proliferation via the generation of lipids (Duvel et al., 2010).

Another oncogene involved in metabolism is the Myc transcription factor. Most importantly, Myc enhances mitochondrial gene expression and biogenesis (Li et al., 2005b). It also promotes the expression of glutaminase (GLS), needed to deaminate glutamine to glutamate, and it has been shown *in vitro* that Myc dependent tumour cells are also glutamine dependent (Wise et al., 2008).

Likewise, the tumour suppressor gene p53 has been shown to regulate aspects of cell metabolism (Gottlieb and Vousden, 2010), including stimulation of oxidative phosphorylation (OxPhos) through enhancing expression of the cytochrome oxidase chaperone cytochrome c oxidase 2 (SCO2) (Matoba et al., 2006). Wt p53 decreases glycolysis by downregulation of glucose transporters and controls the expression of the TP53-induced glycolysis and apoptosis regulator (TIGAR), which negatively affects fructose-2,6 bisphosphate (Bensaad et al., 2006). Loss of p53 can enhance glycolysis (Matoba et al., 2006) and anabolic metabolism from glycolytic intermediates (Bensaad et al., 2006, Kondoh et al., 2005, Matoba et al., 2006).

Some pathways are also influenced by alternative splice variants of metabolic enzymes. The isoform 2 of pyruvate kinase (PKM2) is the major isoform of this enzyme found in tumours, whereas isoform 1 (PKM1) is predominant in most

differentiated tissues (Mazurek, 2011). It was also shown that PKM2-expressing tumour cells form bigger tumours in xenograft models than PKM1-expressing cells (Christofk et al., 2008). PKM2 has also been shown to be a HIF-1 target. PKM2 in turn interacts with HIF-1α and promotes HIF-1 transcriptional activity. This was shown to be dependent on its interaction with prolyl hydroxylase 3 (PHD3). Knockdown of PHD3 reduced glucose uptake and lactate production and increased oxygen consumption (Luo et al., 2011).

Mutations are also involved in metabolism regulation. For example, it has been shown that a K-RAS mutation led to increased glycolysis, but a decreased use of glucose in the TCA cycle. This was accompanied by an increased utilization of glutamine for anabolic metabolism (Gaglio et al., 2011).

Mutations in isocytrate dehydrogenase (IDH) resulted in the loss of the enzyme's ability to catalyse the conversion of isocitrate to α-ketoglutarate; rather it enhanced the reduction of α-ketoglutarate to R(-)-2-hydroxyglutarate (2HG) (Dang et al., 2009). 2HG was shown to prevent the binding of α-ketoglutarate to histone demethylases (Xu et al., 2011), suggesting a role in epigenetic regulation.

Moreover, copy number gains have been reported for fatty acid synthase in prostate cancer (Shah et al., 2006) and for phosphoglycerate dehydrogenase in breast cancer and melanoma, leading to an increased flux through the serine/glycine synthesis pathway (Locasale et al., 2011, Possemato et al., 2011).

1.9.2. Metabolic symbiosis

Despite a main focus in metabolism research being on glucose, it is now clear that glucose is not the only carbon source for cancer cell metabolism. This is also emphasised by the variability of PET-FDG imaging results (Westerterp et al., 2008, Avril et al., 2001). To this end it has been shown that HeLa cells are able to generate ATP almost entirely from glutamine and pyruvate (Rossignol et al., 2004). Prostate cancers on the other hand preferably rely on the beta-oxidation of fatty acids for the

production of ATP, despite the presence of abundant glucose (Liu et al., 2010, Liu, 2006).

Further to the above-mentioned factors influencing tumour cell metabolism, it has also been proposed that tumour cells may acquire essential metabolites and/or signalling from a symbiosis with other tumour cells or the tumour stroma.

To this end it is noteworthy that co-operation between cells is vital in many tissues. It has for example been shown that only astrocytes produce and store glycogen in the adult brain (Cataldo and Broadwell, 1986). Astrocytes can then access this store, use glycogen for glycolysis and supply neurons with lactate (and possibly pyruvate) in order to maintain axonal and synaptic functions (Magistretti and Pellerin, 1999, Wender et al., 2000).

More recently, it also became apparent that tumours interact with their microenvironment (stroma, adipocytes, fibroblasts, muscle cells, and endothelial cells) as well as other tumour cells. Valencia et al (2014) reported that p62, a stress-response protein, modulates the metabolism of stromal fibroblasts, which led to an upregulation of stromal interleukin 6 (IL-6) production. Interestingly, IL-6 was required for the tumour promotion of prostate cancer cells (Valencia et al., 2014). Moreover, cancer cells can drive autophagy and mitophagy in their microenvironment, which produces high-energy metabolites (Capparelli et al., 2012b). These metabolites can be taken up by tumour cells and used for energy production (Salem et al., 2012).

Interaction with fibroblasts has also been shown to include “the reverse Warburg effect”, in which cancer-associated fibroblasts (CAF) were found to have an increased level of glycolysis. Subsequently, adjacent tumour cells could use the metabolites for oxidative phosphorylation (Migneco et al., 2010, Bonuccelli et al., 2010, Martinez-Outschoorn et al., 2011a). A main “waste” product of glycolysis is lactate. However, lactate metabolism is used in normal tissues, including the brain (Hashimoto et al., 2008) and the myocardium (Gertz et al., 1988). Lactate dehydrogenase is the key enzyme that interconverts pyruvate and lactate. Elevated

LDH levels are correlated with a poor prognosis in several cancers including prostate (Yamada et al., 2011) and colorectal tumours (Koukourakis et al., 2006). LDH-A is also a HIF-1 target gene (Semenza et al., 1994).

1.9.3. Autophagy

Autophagy is a physiological process, whereby cells under metabolic or other stresses remove unwanted or dysfunctional proteins and cell organelles by shuttling them in autophagosomes to lysosomes for degradation. However, this pathway also enhances the recycling of metabolites and structural building blocks. For example, amino acids and other nutrients are recycled or can be oxidised to fuel bioenergetics (Yang and Klionsky, 2010).

One form of autophagy is mitophagy, whereby mitochondria are degraded via autophagolysosomes. Mitochondria are tightly regulated as they play an important role not only in ATP synthesis, but also in ROS production as well as apoptosis (Kubli and Gustafsson, 2012). Mitophagy is mainly regulated by BNIP3, a mitochondrial protein belonging to the BH3-only sub-group of the Bcl-2 family. BNIP3 interacts with OPA-1 and LC-3 to facilitate mitochondrial fragmentation and mitophagy respectively (Landes et al., 2010, Rikka et al., 2011). BNIP3 was also shown to promote mitophagy by negatively affecting oxidative phosphorylation (Thomas et al., 2011).

It has been shown that cancer cells induce autophagy in response to stress factors such as hypoxia, nutrient starvation, as well as treatments such as radiotherapy (Rouschop et al., 2010, Rzymski and Harris, 2007, Rzymski et al., 2010).

1.10. Carbonic Anhydrase IX (CAIX)

1.10.1. Structure of CAIX

The transmembrane protein CAIX was initially named MN and was discovered *in vitro* in HeLa cells (cervical carcinoma) (Opavsky et al., 1996). The protein was found to be expressed in confluent cultures and in cells that were infected with the MaTu

quasi-viral agent, derived from a breast cancer. MN was shown to produce two bands in western blotting, one of 54 and one of 58 kilo Daltons (kDa) (Reiserova et al., 1999). Subsequent sequence analysis revealed a carbonic anhydrase domain in the MN cDNA (257 AA), which made it the ninth CA to be identified (Opavsky et al., 1996, Pastorek et al., 1994).

The schematic domain composition of CAIX is shown in Figure 1.7 A. It comprises an extracellular domain with a single peptide (SP), a proteoglycan (PG)-like domain and a catalytic (CA) domain. The catalytic domain is important for the CO_2 hydration reaction, and with regard to this CAIX has been shown to be one of the most active CAs. The reaction is pH dependent. It was also shown that the presence of the PG domain enhances the catalytic function at lower pH values; the optimal activity of the whole construct was measured to be at pH 6.49 (vs. 7.01 for the catalytic domain alone) (De Simone and Supuran, 2010, Alterio et al., 2009, Innocenti et al., 2009).

The extracellular domain is linked to a transmembrane region (TM). The structure also includes a C-terminal intracellular domain (IC), which has been shown to be involved in the enzymatic activity of CAIX (Ditte et al., 2011).

Although the crystal structure of the full-length protein is not yet available, the catalytic domain has been resolved (Alterio et al., 2009). The crystallographic data implies that CAIX is a dimer, which is linked by a disulphide bond and stabilised by hydrogen bonds and van der Waals interactions. The PG domains are predicted both to be located near the active site, again suggesting a supporting role for the catalytic activity (De Simone and Supuran, 2010, Alterio et al., 2009, Innocenti et al., 2009) (Figure 1.7 B).

A soluble form of CAIX, s-CAIX, has been identified and is characterised by a shorter extracellular domain (Zavada et al., 2003). The shedding of CAIX is thought to be mediated by a disintegrin and metalloproteinase 17 (ADAM17/TACE) (Zatovicova et al., 2005).

Soluble CAIX was detected in the media of *in vitro* experiments as well as patients' serum and urine (Zavada et al., 2003, Schutze et al., 2013). A study involving 169 patients with primary breast cancer found an association of membranous CAIX expression with shorter disease-free survival. However, s-CAIX levels did not correlate with CAIX mRNA levels or with clinicopathological characteristics and outcome (Schutze et al., 2013).

A



B

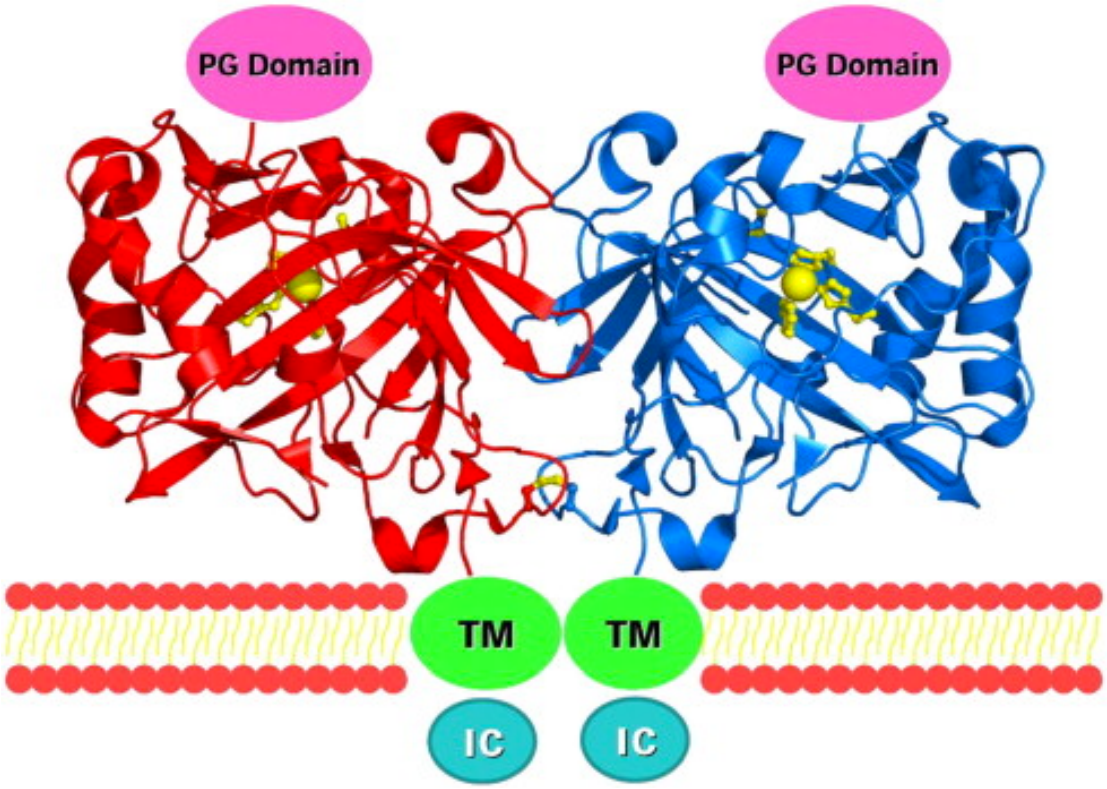


Figure 1.7 Schematic structure of CAIX. (A) Linear structure, SP, signal peptide; PG, proteoglycan-like domain; CA, carbonic anhydrase domain; TM, transmembrane domain; IC, intracellular domain; Numbers indicate associate AA positions. Adapted from Hulikova et al. (2009) (Hulikova et al., 2009), permission for reprint obtained. (B) Crystal structure of the catalytic domain and proposed model for the arrangement of the full-length CAIX. Taken from De Simone G. et al (2010). (De Simone and Supuran, 2010)

1.10.2. The expression of CAIX

Under normoxic conditions and in normal tissues, the expression of CAIX is low and restricted to a few tissues including the mucosa of the stomach and gallbladder (Pastorekova et al., 1997) and to a lesser extent the cryptal areas of the intestinal epithelium (Saarnio et al., 1998), the epithelia of pancreatic ducts (Kivela et al., 2000b) and male reproductive organs (Karhumaa et al., 2001).

In contrast, CAIX is expressed in most solid tumours including cervix (Liao et al., 1994), and renal clear cell carcinomas (Liao et al., 1997), breast (Chia et al., 2001), head and neck (Beasley et al., 2001), and lung cancers (Giatromanolaki et al., 2001) as well as tumours of the brain (Proescholdt et al., 2005). In breast cancer, CAIX was associated with the basal-like / triple negative subtype (Lou et al., 2011b, Tan et al., 2009) but also with the HER2 positive subtype (Kajo et al., 2013, Kaya et al., 2012) and in lung cancer with the squamous cell carcinoma subtype (Ilie et al., 2010).
CAIX expression has been associated with enhanced lymph node metastasis (Lee et al., 2007, Woelber et al., 2011) and with poor prognosis in several cancers including breast cancer (Chia et al., 2001), non-small cell lung (Giatromanolaki et al., 2001) and head and neck (Jonathan et al., 2006).

1.10.3. Regulation of CAIX

CAIX expression is strongly induced in hypoxic conditions. The promoter features a HRE immediately upstream of the transcription start site (-3-10) which has been shown to be critical. The fact that the promoter is so close to the transcription start site is crucial for the tight, yet strong regulation of *CA9*. Mutations within the *CA9* HRE inactivate the promoter and suppress CAIX expression. Likewise, knockdown of HIF-1 has been shown to decrease CAIX expression (Kaluz et al., 2009).

The expression of CAIX is furthermore regulated by five so-called protected regions (PR1-5) located within the *CA9* promoter. Of these, PR1 and PR2 were shown to be most critical (Kaluz et al., 1999).

PR1 and PR5 attract binding of specificity proteins (SP) SP1/SP3 transcription factors and this binding has been associated with the induction of CAIX in dense cultures (mild hypoxia) as well as by incubation in a hypoxic chamber. Inhibition of the binding of SP1/SP3 by mithramycin A reduces CAIX expression in dense cultures (Kaluzova et al., 2001, Kaluz et al., 2003).

PR2 was shown to bind activator protein (AP) 1, and stimulation of AP1 activity with PMA increased CAIX promoter activity, but the relation to HIF-1 induced CAIX expression was not investigated in that study (Kaluzova et al., 2001). Nevertheless, AP1 is hypoxia inducible and is further regulated by PI3K and MAPK signalling (Laderoute, 2005). This may help to integrate signals from these pathways into *CA9* transcription.

The function of PR3 is not well understood; however, it is thought that this region has a minor but positive effect on CAIX expression (Kaluz et al., 1999).

PR4 has been shown to repress CAIX transcription and deletion/mutation of the region increased the activity of the *CA9* promoter (Kaluz et al., 1999).

In glioblastoma cells, acidification of the culture media in normoxic conditions increases the activity of the *CA9* promoter and upregulates CAIX expression due to the stabilisation of HIF-1 and ERK signalling (Ihnatko et al., 2006). However, similar experiments in HeLa cells did not show the same result, indicating cell line specific mechanisms (Rafajova et al., 2004).

PI3K and MAPK regulation of CAIX

In line with the notion that the protected regions in the *CA9* promoter region may be activated in dense cultures and by signalling pathways, it has been shown that mild hypoxia (as induced by dense cultures) can activate PI3K signalling (Zavada et al., 1993, Kaluz et al., 2002), suggesting further cross-talk between the different control mechanisms.

CAIX was shown to be upregulated in dense cultures of HeLa cells during reduced oxygen tension; and using PI3K inhibitors could reduce the expression. The lower oxygen tension was not enough to trigger stabilisation of HIF-1α, but HIF-1 activity was shown to be needed for *CA9* transcription as the effects were not seen in HIF-1α deficient cells. These experiments indicate that CAIX induction in high-density cultures is dependent on PI3K signalling as well as a low-level activity of HIF-1 (Kaluz et al., 2002, Kopacek et al., 2005a).

The MAPK signalling pathway has also been implicated in dense cell cultures. Sheta et al (2001) showed that pericellular hypoxia as induced by high cell density increased nuclear HIF-1α in LNCaP cells but not in PC3 cells. In the former, HRE activity was also induced which was dependent on the oxygen tension, as shaking or incubation in 95% O_2 abolished HRE activation. Subsequently, HRE activation was shown to be dependent on a nitiric oxide (NO) - RAS – HIF-1α dependent pathway (Sheta et al., 2001). Moreover, several groups have shown that inhibition of the MAPK pathway inhibited HRE activation and CAIX expression in dense cultures as well as conditions of hypoxic incubation (Sheta et al., 2001, Kaluz et al., 2006, Kopacek et al., 2005b). The effect of MAPK pathway inhibition was additive to PI3K inhibition in decreasing CAIX levels (Kopacek et al., 2005b). The MEK1/2 inhibitor U0126 exerted its effects by targeting the HRE and SP1 sites as well as the HIF-1 transcriptional co-regulator p300 (Kaluz et al., 2006). However, in the same paper the authors showed that there was no direct quantitative correlation between levels of

phosphorylated (activated) ERK and CAIX expression in high/low density culture experiments in HeLa cells (Kaluz et al., 2006). This is in contrast to findings in LNCaP cells and may again indicate cell line / tumour specific regulation (Sheta et al., 2001).

Furthermore, we previously found that CAIX is heterogeneously induced under severe hypoxia *in vitro*, with CAIX positive and negative populations present. This could be shown to be due to an epigenetic difference between the two populations, where the promoter region of CAIX is more condensed in the CAIX negative population (Ledaki et al., 2015).

1.10.4. Role of CAIX

pH regulation

Cells need a physiological internal pH for cellular processes and a moderately alkaline pH is needed for cell proliferation (Pouyssegur et al., 1984). Cells able to cope with harsh pH conditions are thought to gain a selective advantage over cells that cannot (eg non-cancer cells) (McDonald et al., 2012). The acidification of the extracellular matrix (ECM) enhances its degradation, promoting cancer cell invasion.

pH regulation in normal cells

Cellular functions and related pathways are often dependent on a physiological cell internal pH (pH_i). Proteins' tertiary structure and therefore functionality can be pH dependent. The response to pH is related to H+ affinity (KH), which for many proteins is close to physiological pH and even small changes can affect functionality. Therefore, the pH is tightly regulated (Swietach et al., 2010). The physiological H+ ion concentration lies between 50 and 100 nM; however, cellular processes can induce acid/base changes in the mM range (Swietach et al., 2010). A considerable impact on pH comes from cellular metabolism, which produces lactic acid and CO_2 via glycolysis and mitochondrial respiration. Cancer cells have a higher metabolic

rate (Gatenby and Gillies, 2004); however, experiments using nuclear magnetic resonance showed an alkaline pH, suggesting a good buffering system (Gillies et al., 2004).

Many molecules are either weak acids or bases that can release or bind protons (H+ ions) respectively, aiding in buffering pH internally (Boron, 2004).

Moreover, H^+ ions can be shuttled outside the cells by primary (eg H^+ ATPase) or secondary (eg Na^+/H^+ exchanger (NHE) active transporters (Martinez-Zaguilan et al., 1993, McLean et al., 2000). Likewise, cells can also import H^+ ions if required (eg Cl^-/H^+-equivalent transport) (Niederer et al., 2008).

An alternative intracellular buffer system relies on CO_2/HCO_3^- (Alper, 2006, Boron, 2004). CO_2 (the proton acceptor) can diffuse through the membrane (independently of transporters). This flux, however, must be equalised by a counter flux of HCO_3^-, which is transporter-dependent. Moreover, the conversion of CO_2 and HCO_3^- is slow, but can be catalysed by carbonic anhydrase (CA) enzymes. This family of 16 distinct zinc metalloenzymes catalyses the following reaction: $CO_2 + H_2O \leftrightarrow H^+ + HCO_3^-$. Moreover, the enzymes were associated with the regulation of respiration, and biosynthetic processes (Supuran, 2008).

pH regulation in tumour cells

As described earlier, the higher rate of glycolysis in tumour cells (the “Warburg effect”) as well as pathways upregulated in hypoxia lead to an extensive generation of acidic metabolites such as lactic and carbonic acids (McDonald et al., 2012).. These products are largely excreted, promoting an acidification of the extracellular microenvironment. Furthermore, in normal tissues the cellular efforts of pH regulation are aided by blood perfusion, which allows diffusion of buffer components between the compartments and a pH of the latter at 7.4. However, tumours are often characterised by poor vascularisation (Swietach et al., 2010). As a consequence of these increased diffusion distances gradients of extracellular pH (pHe) develop.

Role of CAIX in pH regulation

CAIX has been shown play a major role in the acidification of extracellular and maintenance of intracellular pH (Swietach et al., 2010, Parks et al., 2011). As a member of the carbonic anhydrase family it facilitates the conversion of CO_2 (a weak base acid), to H+ and HCO3-. In this the catalytic domain of CAIX is crucial and CAIX was shown to contribute to the acidification of the extracellular environment under hypoxic conditions (Hilvo et al., 2008). CAIX overexpression in kidney epithelial cells decreased the pH in the culture medium under hypoxic conditions. This could be reversed by addition of a CAIX inhibitor (Svastova et al., 2004).

At the same time, the proteoglygan domain of CAIX ensures continued high activity in this low pH milieu (Innocenti et al., 2009).

The bicarbonate generated may subsequently be taken up by bicarbonate transporters to help the maintenance of intracellular pH. In support of this hypothesis it has been shown that in transfected HEK293 cells CAIX bound the Cl^-/HCO_3^- exchanger AE2 and the interaction was dependent on the catalytic domain. Additionally, CAIX expression increased the activity of the bicarbonate transporter by 28% (+/- 7%) (Morgan et al., 2007). Subsequent reports indicated the importance of other bicarbonate transporter such as sodium bicarbonate co-transporters (Chiche et al., 2010).

Adherence, invasion and metastasis

It was shown that cells are able to adhere to purified and immobilised CAIX. This could be abrogated by pre-treatment with the M75 antibody, which binds to CAIX. This proved that the site of interaction is located in the proteoglycan domain (Zavada et al., 2000).

Moreover, it was shown that in CAIX overexpressing MDCK cells, the protein was located in cell-cell contacts together with E-cadherin. In hypoxic conditions both

proteins adopted a cytoplasmic localisation, but this was reverted upon re-oxygenation. In CAIX high cells CAIX could be co-precipitated with α- and β-catenin but to a lesser extent with E-cadherin, suggesting that CAIX expression decreases the association of E-cadherin with the cytoskeleton. In line with this, CAIX high cells displayed a reduced cell-cell adhesion (Svastova et al., 2003).

In a separate study, high CAIX cervical carcinoma cells expressed a gene signature enriched for genes associated with cell growth, cell adhesion and cytoskeletal organization pathways. Again these cells were found to harbour a weakened cell-cell adhesion and an enhanced level of cell motility (Shin et al., 2011).

Additionally, CAIX's role in the acidification of the microenvironment has been associated with increased invasion (Martinez-Zaguilan et al., 1996) and patients with high CAIX expression have a higher risk to develop metastasis (van Kuijk et al., 2016, Yang et al., 2015). In line with this, broad inhibition of CAs (Kivela et al., 2000a) and specifically CAIX (Ward et al., 2015) decreased the migratory, invasive and metastatic potential of tumour cells.

Proliferation

A number of publications elucidate the role of CAIX in cell proliferation. Expression of the protein increases tumour growth, whereas inhibition using small molecule inhibitors decreases it (Cianchi et al., 2010, Dubois et al., 2011, Morris et al., 2011).

Similarly, hypoxia induced CAIX expression was shown to be critical for tumour growth in breast and colon cancer xenografts (Chiche et al., 2009a, Lou et al., 2011a). Induction of CAIX in HCT116 colon cells increased tumour growth, whereas CAIX knockdown in high expressing HT29 cells decreased tumour burden *in vivo.* Expression of CAIX correlated with higher levels of the proliferation marker KI67 (McIntyre et al., 2012).

Furthermore, CAIX expression has been associated with stemness and subsequently an increased ability to form mammospheres as well as tumour formation in xenograft experiments when low numbers of cells were injected (Ledaki et al., 2015).

1.10.5. Inhibition of CAIX

As the low expression of CAIX in normal tissues and its various roles in tumour biology have been established, its inhibition became a focus for the development of targeted treatments. The two major approaches in this field are monoclonal antibodies and small molecules.

Small molecules

The binding of small molecules depends on how complementary they are in shape and charge to the target. In order to shed more light on this, in silico experiments using programmes such as three-dimensional quantitative structure-activity relationship (3D-QSAR) and Glide XP software (to assess docking of inhibitors to active sites) tried to define guidelines for the development of CAIX inhibitors (Sethi and Verma, 2013, Singh and Supuran, 2014).

Initially, CAIX inhibitors were based on acetazolamide conjugated with albumin binding domains or charged fluorophores. These compounds were designed to bind the Zn(II) ion in the active site of CAs and decreased growth rate *in vitro* (Ahlskog et al., 2009a).

A promising group of compounds are those containing (benzene-sulfonamides/sulfamates. Several reports detailed the synthesis of such compounds, which were shown to have anti-proliferative activity *in vitro* with IC50 values of 20-30 μM (Bashandy et al., 2014) or even in the nM-range (Supuran et al., 2001). Considerable activity against other carbonic anhydrase family members such as isozymes II and IV was observed and the exact mechanism of tumour growth

inhibition was unclear (Supuran et al., 2001, Supuran and Scozzafava, 2000a, Supuran and Scozzafava, 2000b).

Subsequently, more specific compounds for inhibiting CAIX were also reported to have a significant anti-proliferative effect with an IC50 in the nM-range in several breast cancer cell lines (Winum et al., 2012) as well as in colon, lung-derived cell lines *in vitro* (Morsy et al., 2009).

Rogez-Florent et al (2013) reported a compound shown in silico to have a higher selectivity for CAIX over CAII due to the meta-position of the sulphonamide group. Although the compound itself had limited cytotoxicity, it was additive to doxorubicin in hypoxic conditions (Rogez-Florent et al., 2013). TR1 and GA15, two aromatic sulphonamides, were shown to inhibit CAIX in a number of human cancer cell lines *in vitro*. Treatment with the inhibitors resulted in lower intracellular pH, induction of apoptosis and decrease in proliferation in CAIX positive but not CAIX negative cells (Cianchi et al., 2010).

In vivo work with sulphonamide/sulphamate-based compounds showed anti-metastatic activity in breast cancer models, with limiting effects on the primary tumour burden (Pacchiano et al., 2011, Gieling et al., 2012). In contrast, treatment with the indanesulphonamide (11c) decreased acidification of the extracellular space *in vitro* and reduced tumour growth *in vitro* and *in vivo*. The inhibitor also showed a synergistic effect when combined with 10Gy radiotherapy *in vivo* (Dubois et al., 2011).

Additionally, Touisni et al (2011) showed that a coumarin based compound could attenuate primary tumour growth (Touisni et al., 2011).

Monoclonal antibodies

Taking advantage of the fact that CAIX is a membrane protein with a structure that is largely located in the extracellular space, the development of specific monoclonal antibodies (mAb) to target the protein is encouraging.

Antibodies targeting CAIX potentially have four main underlying working principles. Firstly, reliable CAIX staining is an indicator for hypoxic regions in the tumour and is a good biomarker for prognosis and treatment decisions. Secondly, antibodies binding the active site of CAIX can block its function. Thirdly, the binding of an antibody to its target may trigger the activation of effector cells of the host immune system and induce antibody dependent cell cytotoxicity (ADCC). In fact it has been shown that Trastuzumab (Herceptin, Roche), a mAb targeting the HER2 receptor, exerts its effect partly via ADCC (Clynes et al., 2000, Gennari et al., 2004).

Lastly, a specific CAIX antibody may be linked with a cytotoxin or radionucleotide. This would enhance drug specificity to the tumour site, as CAIX expression in normal tissues is low.

Antibodies against the catalytic domain are being developed with the aim of inhibiting CAIX activity in pH regulation. Using phage display libraries CAIX targeting antibodies have been identified, some of which were mapped to the CAIX's catalytic site. Two of the identified antibodies were shown to stain CAIX in colon cancer xenograft models (Ahlskog et al., 2009b).

Another approach was to use hybridoma technology. The resulting antibody targets the catalytic domain. Upon binding, the antibody was shown to undergo receptor-mediated internalisation, which may be a good way to deliver additional agents. The antibody was tested *in vitro* and *in vivo*. However, in the latter the antibody was only effective if mice had been treated before the tumour was established (Zatovicova et al., 2010).

Petrul et al (2012), developed CAIX specific antibodies by using the ectodomain of CAIX and the MorphoSys HUCAL Gold library of human Fabs. Antibodies were further characterised by their ability to undergo internalization upon binding. The lead compound was further linked to monomethyl auristatin E (MMAE), an antimitotic agent. The resulting coupled antibody showed potent antitumour effects in several *in*

vivo models, which was linked to CAIX expression and the effects of the linked antitubulin agent (Petrul et al., 2012).

Two antibodies that have progressed further are M75 (Zavada et al., 1993) and G250 (Oosterwijk et al., 1986).

The antibody M75 has been shown to target the PG domain of the extracellular structure of CAIX (Zavada et al., 2000). It is commonly used for detection of CAIX in tissue samples and cell lines. Moreover, another antibody based on M75 was developed for preclinical imaging of CAIX (Chrastina et al., 2003b, Chrastina et al., 2003a).

The mAb G250 targets CAIX and a humanised version has been used for immunotherapy, in which has been shown to induce antibody dependent cell cytotoxicity (ADCC) (Surfus et al., 1996).

Combination with cytokine therapy enhanced the antibody treatment. Safety together with low toxicity and survival benefit of the cG250 treatment alone or in combination with interferon therapy (IFN-α) were demonstrated in phase I and II clinical trials (Siebels et al., 2011, Davis et al., 2007). The ARISER phase III clinical trial has set out to assess the efficacy of the antibody in combination with interleukin-2 or IFN-α in the adjuvant setting in renal cell carcinoma (RCC).

1.11. Aims and objectives

Over recent years, it has become more and more obvious that cancer is a heterogeneous disease, and a tumour may harbour different genetic, epigenetic, and molecular properties. It is also known that hypoxia as a stress factor can alter the tumour microenvironment as well as tumour cell behaviour. In this context previous work in the laboratory showed that CAIX expression is heterogeneous during hypoxia (Ledaki et al., 2015). In MCF7 cells, a CAIX positive and a CAIX negative population were present.

This thesis investigates the hypothesis that hypoxia induces subpopulations, which can be marked by presence/absence of CAIX expression, to benefit tumour growth by enabling metabolic symbiosis.

Therefore, this work aimed to investigate how hypoxic conditions can drive heterogeneity in hypoxia and what the biological significance of the presence of two populations defined by CAIX expression was. Specifically, the objectives were as follows:

- To further investigate the heterogeneity in CAIX expression in response to hypoxia in a panel of cell lines.
    - To establish and monitor populations defined by CAIX expression
    - To assess the biological mechanism underlying the differential expression.
    - To assess differences in molecular biology between the populations
- To investigate the biological significance of the presence of the CAIX populations in 2D and 3D models
- To assess the metabolic differences of populations and the effect of co-culturing

Chapter Two

Materials and Methods

2.1. Cell lines and maintenance

Cell lines were obtained from ATCC. All cell lines were grown in DMEM media (Gibco) supplemented with 10% FCS (Gibco) and 1% Penicillin/Streptomycin (PAA laboratories) unless otherwise stated. Cell cultures were maintained in a humidified incubator, at 5% CO_2, and 37°C.

When confluent, cells were washed once with Phosphate Buffered Saline (PBS) before addition of trypsin-EDTA (PAA laboratories). Cells were sub-cultured in a 1:9 ratio every 5-6 days. A stringent schedule for mycoplasma testing was maintained.

2.2. Maintenance of cell stocks

To maintain a cell stock, cell pellets of mycoplasma tested cells were re-suspended in FCS / 10% DMSO, frozen at -80°C in an isopropanol-containing freezing container (Nalgene Mr. Frosty), and stored in liquid nitrogen. For recovery, vials were quickly thawed at 37°C and cells transferred to pre-warmed medium.

2.3. Hypoxia

For induction of hypoxia, cells were plated and left to settle overnight. The cells were then placed in an INVIVO$_2$ 400 hypoxic (0.1% O_2, 5% CO_2,) workstation (Pro-Lab Diagnostics) for indicated time points.

2.4. Immunoblotting

2.4.1. Protein extraction and measurement of protein content

Cells were washed once with ice-cold PBS before being scraped down in RIPA buffer (Sigma). Subsequently, samples were centrifuged at 12,000 g, 4°C for 10 min. Supernatants were transferred to fresh vials and protein contents measured using a Bradford assay (BioRad). In brief, the protein assay stock solution was diluted 1:5 in deionized water. To this 1 µL of a BSA standard (0, 2, 4, 6, 8, 10 mg / mL) or sample was added and absorbance at 595nm was measured with a µQuant microplate

reader (Bio-tek Instruments). Sample concentrations were interpolated from the generated standard curve.

2.4.2. Polyacrylamide gel electrophoresis and transfer

Normalised samples were mixed with appropriate amounts of loading buffer (4x LDS loading buffer [Invitrogen], 10% β-mercaptoethanol [Sigma]) and heated to 70°C for 10 min. Equal amounts of protein were loaded on 4-12% Bis Tris gels (Invitrogen) and proteins were separated at 130 V for 1.5 h. This was followed by a semi-dry transfer onto a polyvinylidene difluoride membranes (Millipore), or a wet transfer onto hybond C membranes (Amersham Biosciences).

2.4.3. Probing

After the transfer, membranes were incubated in 5% milk in PBS / 0.1% Tween 20 (PBS-T) for 1 h at room temperature or overnight at 4°C. Primary antibodies (see Table 2.1) were diluted in the blocking solution and incubated overnight at 4°C. This was followed by three washes with PBS-T and incubation with the appropriate secondary antibody for 1 h at room temperature (RT).

After another washing step, membranes were incubated with an ECL system (Amersham Biosciences) and visualised using the Fusion system (Vilber Lourmat).

Table 2.1 Table of primary and secondary antibodies

Antigen	Company	Concentration
Primary antibodies		
AK4 (goat)	Santa Cruz	1:1000
CAIX (M75) (mouse)	Gift from J. Pastrorek, Institute of Virology, Slovak Republic	1:1000
HIF-1α (mouse)	BD Transduction Laboratories, USA	1:500
HIF-2α (rabbit)	BD Transduction Laboratories USA	1:500
Lamp1 (goat)	Santa Cruz	1:500
LC3β (mouse)	Cell Signalling	1:1000
LDH-A (goat)	Santa Cruz	1:500
MCT1 (mouse)	Novus Biologicals	1:1000
MCT4 (mouse)	Novus Biologicals	1:1000
MMP14 (mouse)	Novus Biologicals	1:500
β-actin (HRP conjugated)	Sigma	1:5000
Secondary antibodies		
Anti-mouse	Dako	1:2500
Anti-rabbit	Dako	1:2500
Anti-goat	Dako	1:2500

2.5. qPCR

2.5.1. RNA extraction

RNA was extracted using the RNeasy Mini Kit (Qiagen) according to the manufacturer's instructions. Cells were placed on ice and the media and two washes with PBS were discarded. Cells were then lysed using 350 µL of the provided RNA complete lysis buffer. This was mixed with the same volume of 70% ethanol and applied to a RNA binding column. Columns were centrifuged, washed and incubated

with DNAse for 15 min at RT. Columns were washed twice before RNA was eluted in RNAse free water. RNA samples were stored at -80°C.

2.5.2. Generation of cDNA

After RNA extraction, the amount of nucleic acid was quantified using nanodrop software. An absolute amount of 2000 ng of RNA was diluted in 10 µL of nuclease-free water and the High Capacity cDNA Reverse Transcription Kit (Applied Biosystems) was used for cDNA synthesis according to manufacturer's instructions. The Thermal Cycler (GeneAmp, PCR System 9700, Applied Biosystems) was set to 10 min at 25°C followed by 2 h at 37°C. Samples were then kept at 4°C or stored at -20°C.

2.5.3. qPCR

Primers for qPCR were taken up in RNAse-free water in a final concentration of 100 µM. Working dilutions had a concentration of 10 µM of forward and reverse primer. Sensimix SYBR Mastermix was used according to manufacturer's instructions and actin was used as a housekeeping gene and control. The PCR was carried out using Rotor Gene RG 3000 thermal cycler (Corbett Research) which was set at the following profile for all reactions: hold phase at 95°C for 15 min, 40 cycling runs (95°C for 10 s and 60°C for 1 min) and a melt phase (from 50-99°C).

Relative quantification of gene expression was performed using the method described by Pfaffl (Pfaffl, 2001). In brief, comparisons were made between the number of cycles required for the fluorescence of a sample to reach a predetermined threshold that lay within the exponential phase and above the non-specific background.

The relative ration of gene expression was calculated as follows

$$\text{Relative ratio} = \frac{(Etarget)^{\Delta Ct\ TARGET(mean\ comparator - mean\ sample)}}{(Eref)^{\Delta Ct\ REF(mean\ comparator - mean\ sample)}}$$

Etarget=reaction efficiency of the gene of interest, Eref=reaction efficiency of the reference gene, ∆Ct=the cycle difference between the comparator and the sample. All calculations are based on the mean value of PCRs performed in triplicate.

Table 2.2 Primer sequences for qPCR

Gene Name	Forward Primer	Reverse Primer
CA9	CTTGGAAGAAATCGCTGAGG;	TGGAAGTAGCGGCTGAAGTC
LDHA	CAGAAGGCTCGAGAAGGTATATTGCT GTTGACAGTGAGCG	CCTAAAGTAGCCCCTTGAATTCCGAGG CAGTAGGCA
LDHB	AACACCTGCCACATTCACAC	GATGGATTTTGGGGGAACAT
FABP1	TGATCCAAACGAATTCACG	CACCTTCCAACTGAACCACTG
FABP2	CAATCTAGCAGACGGAACTGAA	CCGTTTGAATTTTCCAATAAGTTT
FABP3	CTGGGCACCTGGAAGCTA	TGGTAGCAAAACCCACACC
FABP4	CCACCATAAAGAGAAAACGAGAG	GTGGAAGTGACGCCTTTCAT
FABP5	GCAGACCCCTCTCTGCAC	TCGCAAAGCTATTCCCACTC
FABP7	AGGATGGCAAAATGGTTATGA	TCATAGTGGCGAACAGCAAC
FABP8	TTGACGATTACATGAAAGCTCTG	GCTGATGATCACAGTGGGTTT
FABP9	GTTGAGCCCTTCTTGGGAAC	TTTCACTAACCCTGCCATGTT
PLIN1	GCGGAATTTGCTGCCAACACTC	AGACTTCTGGGCTTGCTGGTGT
PLIN2	GATGGCAGAGAACGGTGTGAAG	CAGGCATAGGTATTGGCAACTGC
CD36	CCTCCTTGGCCTGATAGAAA	GTTTGTGCTTGAGCCAGGTT
β-Actin	CCCAGCACAATGAAGATCAA	CGATCCACACGGAGTACTTG

2.6. Flow cytometry

Expression of cell surface proteins or stably transfected GFP / mCherry was evaluated using flow cytometry. Samples were analysed using a Dako Cytomation Cyan machine, or sorted using a Fusion cell sorter (Beckman Coulter). Data was analysed by Summit 4.3 software. In each experiment, unstained and single stained samples determined the voltage-settings and compensation was adjusted manually as necessary.

2.6.1. Staining for CAIX

For analysis of surface CAIX, cells were detached and washed once with PBS. After a centrifugation step at 1100 g /4°C/4 min, 2 x 10^6 cells were re-suspended in 100 uL PBS / 10% FCS and stained using a PE or FITC conjugated antibody against CAIX (1:10 dilution, Sigma) or isotype IgG control. Cells were incubated for 1 h at 4°C, washed and re-suspended in in PBS / 10% FCS for analysis.

2.6.1. Cell sorting

For cell sorts, cells were stained as described above. The sort was performed using a Fusion sorter and gating is shown in the respective result section. Sorted cells were plated in media / 20% FCS which was replaced when cells were settled.

CAIX positive and negative populations were periodically re-sorted to ensure the respective phenotype. After sorting, cells were incubated in normoxia until settled (approximately 5-6 days). Afterwards cells were plated and used for experiments as described (and re-subjected to hypoxia as indicated). Cell stocks of sorted CAIX positive and negative populations were also generated and used for experiments.

2.6.2. Staining for apoptosis marker Annexin V

Staining cells for Annexin V assessed the degree of apoptosis. For analysis, the media, as well as the PBS used for washing the cells, were collected and used to take up trypsinised cells. Subsequently, cells were washed twice with ice cold PBS.

An absolute number of 10^6 cells was taken up in 1 mL of 1X Annexin V binding buffer (Applied Biosystems) and 150 µL of each sample were transferred to FACS tubes. Samples were stained with 5 µL of Annexin V antibody (Applied Biosystems) and 2 µL of propidium iodide (Applied Biosystems) for 20 min at RT in the dark. 500 µL of Annexin V binding buffer were added before for analysis.

2.6.3. Staining for cell cycle analysis

In order to analyse cell cycle distribution, cells were harvested and washed twice with ice-cold PBS. Cells were then fixed in ice-cold methanol overnight at -20°C. After another wash with PBS, 100 µg / mL of RNAse (Sigma) was added and cells incubated for 30 min at 37°C to reduce background noise.

Cells were then stained with 10µg / mL of propidium iodide (Sigma) overnight at 4°C.

2.7. Gene silencing using RNA interference

Cells were transfected with siRNA (see table 2.3) using oligofectamine. For a 6-well plate, 3 µL of oligofectamine (Life technologies) were mixed with 12 µL of Optimem (Gibco) and incubated for 5 min at RT. Meanwhile, 20 uM of siRNA was diluted in Optimem in a final volume of 185 µL. The oligofectamine mix was added and incubated for 20 min at RT before adding it to 0.8 mL of cell suspension (containing 250000 cells).

This set-up was scaled up as necessary.

Table 2.3 List of siRNAs

siRNA – target	Sequence
CAIX	GCGCUCAUCUUGAUAAUA UGAACCUACUACCUUCUUU UGUGAAUCUUGCUAUGAUA
HIF1-α	CAAGCAACUGUCAUAUAUA UGCCACCACUGAUGAAUUA UGACUCAGCUAUUCACCAA
LDHA	GGGUCUUUACGGAAUAAAG GGCUACACAUCCUGGGCUA
LDHB	GCUAAAAGGAUAUACCAAC GGAUUCAUCCCGUGUCAAC GGAUAUACCAACUGGGCUA

2.8. Lentiviral transduction of mCherry and GFP

For the expression of GFP or mCherry, 3 x 10^5 cells were transduced with 100 uL of lentiviral particles (Gene Copoeia, LP-MCHR-LV105-0200, titer ~1 x 10^{10} copies/ mL), which was added to 100 uL of full medium and 8 μL / mL of polybrene.

The medium was changed 48 h post transduction and positive cells selected by co-culture with 1 ug / mL puromycin. The selective antibiotic was renewed every 72 h.

Expression of mCherry and GFP was confirmed by fluorescence microscopy and flow cytometry.

2.9. Plasmid transfection

Plasmids expressing E. coli were plated onto agarose plates containing the appropriate selective antibiotic and left to grow overnight at 37°C. The next day single colonies were suspended in LB media containing 50 μg / mL of the selection antibiotic and left to grow overnight at 37°C and 220 rpm. A glycerol stock was

generated by mixing 500 µL of the culture with an equal amount of 50% glycerol and stored at -80°C.

The Qiagen plasmid extraction kit was used to extract DNA. Briefly, bacteria were lysed and DNA purified in a column before it was precipitated using isopropanol. After a wash with 70% ethanol, DNA was taken up in TE buffer, content and purity measured using nanodrop technology, and stored at -20°C.

Lipofectamine LTX (Life technologies) was used for transfection. 2.5 x 10^5 cells were seeded in 6-well plates and left to settle overnight. The next day 2000 ng of plasmid or empty vector were mixed with 8 µL of LTX reagent in 500 µL Optimem (Gibco) and incubated for 30 min at RT before it was added to the cells. After 24 h the media was replaced.

2.9.1. Laconic/pcDNA3.1(-)

Laconic/pcDNA3.1(-) was a gift from Luis Felipe Barros (Addgene plasmid # 44238) (San Martin et al., 2013).

Control plasmids to assess states of no FRET (mTFP donor only) and maximal FRET (mTFP and Venus pair) were kindly provided by Dr. Christoffer Lagerholm from Dr. Eggeling's group (Weatherall Institute of Molecular Medicine, University of Oxford). Control plasmids were first transfected into chemically competent Top10 E.coli (Invitrogen) according to the manufacturer's instructions and bacteria selected using ampicillin and kanamycin respectively.

All plasmids were transfected into MCF7 CAIX positive and negative populations and lactate levels assessed using FLIM, see 2.12.2

2.10. Spheroid formation

For MCF7 3D spheroid studies, a total of 1x10^4 cells/well were seeded in a low attachment, round-bottom 96-well plate (Costar) with the addition of 2.5% matrigel (BD Biosciences) Plates were then centrifuged for 10 min at 1500 g. Pictures of

spheroids were taken regularly using a brightfield microscope and the size assessed using ImageJ. At the end of the experiment, spheroids were fixed in formalin for 24 h, embedded in 2% agarose, and processed. Then samples were embedded in paraffin and sections were cut.

2.11. Determination of pH levels with pHLIP peptide (preliminary data in future work section)

Assessment of pH within spheroids was done using a pHLIP peptide in collaboration with Dr. Tapmeier (Tapmeier et al., 2015).

The peptide was made using solid-phase peptide synthesis with 9-fluorenylmethyloxycarbonyl (Fmoc) chemistry. Reverse phase chromatography was used to purify the peptide. This was done by Dr. James I. Elliott at the W.M. Keck Foundation Biotechnology Resources Laboratory at Yale University (New Haven, CT).

The peptide was then incubated with Alexa 546-maleimide (Life Technologies) in dimethylformamide (DMF) at a ratio of 1:1 for 8 h at RT, followed by incubation at 4°C to facilitate conjugation at the N-terminal side of the peptide.

Reverse phase HPLC (semi-prep Zorbax SB-C18 columns, 9.4 x 250 mm 5 microns, Agilent Technology) using gradients of 10-65% acetonitrile and water containing 0.05% of trifluoroacetic acid was used to purify the peptide. Afterwards the peptide was lyophilised and tested by SELDI-TOF mass spectrometry.

For a stock solution, 40 µM of the pHLIP peptide was then dissolved in PBS.

In order to visualise and measure the pHLIP peptide/pH level in 3D models, spheroids were grown for 5 days. 400 nM of the peptide were added overnight before the spheroids were washed twice with PBS. Images were acquired with a confocal microscope (Zeiss 710 LSM) using an excitation wavelength of 516 nm, 512x512 pixels and 10 µm z-stacks.

2.12. Microscopy

2.12.1. Fluorescence microscopy

Fluorescence microscopy was carried out using a Zeiss microscope in conjunction with Zen software. GFP and mCherry were measured at excitation wavelengths of 400 nm and 590 nm respectively.

2.12.2. FRET/FLIM

Intracellular lactate levels were measured using the Laconic plasmid (San Martin et al., 2013) or control plasmids, which were transfected into the cells (as described in 2.9.1,). After transfection cells were seeded into Ibidi cell culture dishes for subsequent imaging. The plasmid encodes a Foerster resonance energy transfer (FRET/FLIM) based system, where two fluorophores are linked by a lactate binding sequence.

FLIM measures fluorescence lifetime, which is inversely correlated to FRET. FLIM measurements were carried out using an inverted Leica SP8 laser-scanning microscope equipped with an incubator and fitted with a TCSPC upgrade from PicoQuant. The TCSPC included a 440-nm pulsed laser excitation source set to 40 MHz, a laser driver, and two external single-photon avalanche diodes (SPADs).

To measure the lifetime of the mTFP donor part of the plasmid, a 440-nm laser was used for excitation, together with a 483/32 filter. Images were taken at 20x magnification using a water-immersion objective with the following settings: pixel and image size 512x512. Laser intensity was adjusted relative to signal intensity to avoid signal overlap. Each measurement consisted of at least 25 repetitions. Measurements of the donor fluorescence were taken using a bandpass filter and a 50/50 beamsplitter.

Quantitative analysis was carried out using the Picoquant SymPhoTime software. For the lifetime analysis, the TCSPC histogram [N(t)] was fitted with a curve over a time range of with stable signal after the laser pulse as in this period the signal to noise ratio was best (Figure 2.1)., whereas noise increased with the length of time after the pulse. For the control experiments, where only the donor fluorophore (mTFP) was transfected, the curve fit was calculated taking into account a single exponential decay [$N(t)=A\ exp^{-t/\tau}$. For the actual experiment using the Laconic sensor, a double exponential decay model [$N(t)= A_1\ exp^{-t/\tau}+ A_2\ exp^{-t/\tau}$ was used.

Moreover, applying a colour scheme, ranging from blue to red - with lower lifetimes being indicated in blue - generated a visual output of FLIM lifetime measurements.

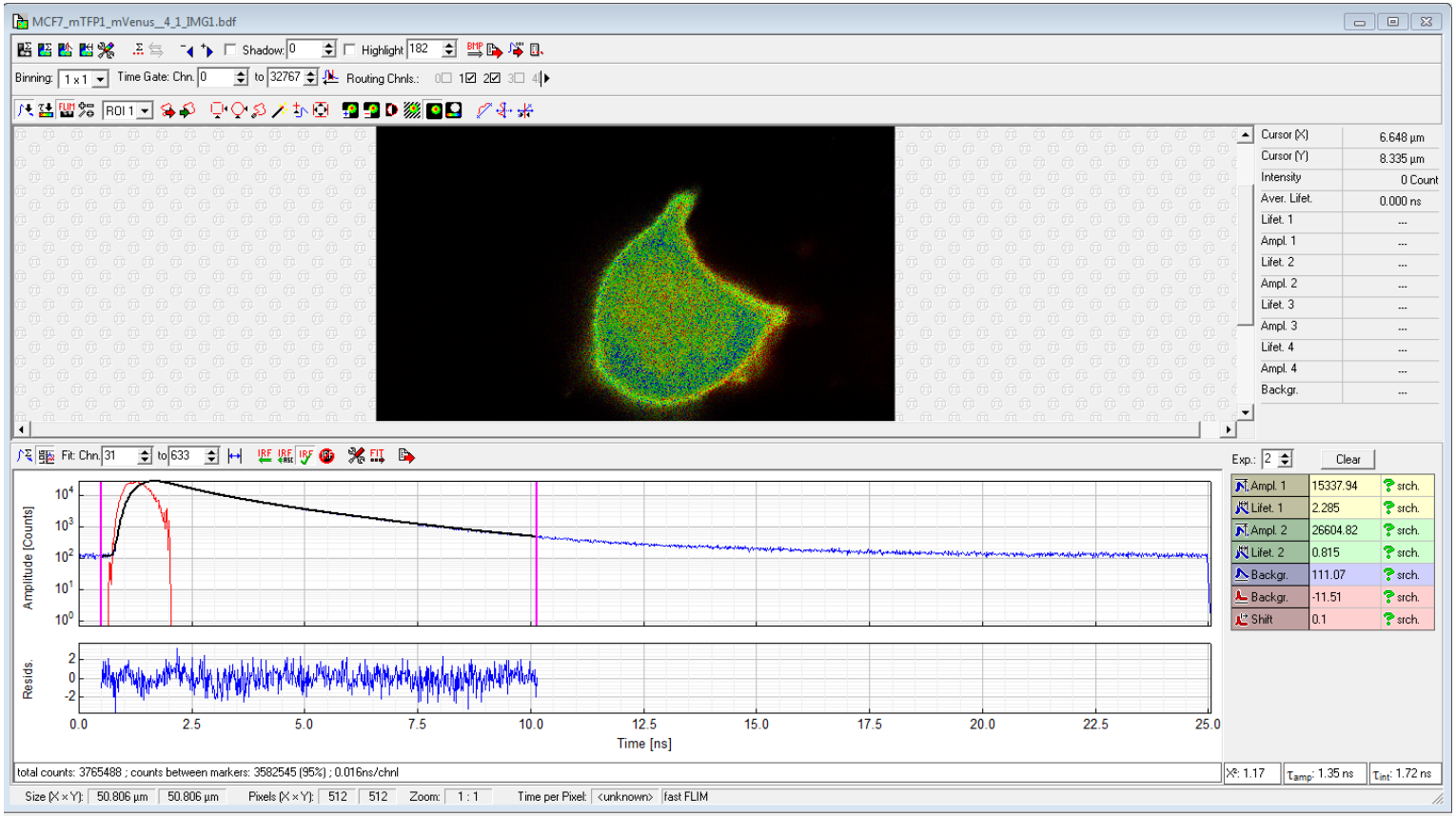


Figure 2.1 Representative lifetime measurement analysis. The analysis shows the pulse (red line) and the photon count over time. A stable region of the curve (between the two pink lines) is used for fitting / lifetime calculations.

The range of potential measurements was tested using either a donor only (mTFP) or a full-FRET (mTFP-Venus) plasmid.

The sensitivity to changing lactate levels by the plasmid was tested by pre-incubating cells with 500 µM iodoacetic acid to block glycolysis, after which cells were washed and cultured with a glucose-free buffer consisting of 10 mM NaCl, 130 mM KCl, 1.25 mM $MgSO_4$, 10 mM HEPES pH 7.2, supplemented with 10 µM of the proton ionophore nigericine (for stable pH) and 2 µM rotenone (to block mitochondrial metabolism). To this lactate was added and cells imaged over time in a time-lapse experiment, where an image was taken every 2.5 min over the course of 1 h. Each image consisted of at least 25 scanning repetitions. Time lapse image sequences were stitched together using Fiji by ImageJ (http://fiji.sc/Fiji).

This generated a standard curve as well as an overall idea of lactate uptake/release in the populations.

2.13. Co-culture experiments

Co-culture experiments were carried out using the 12-well, 0.4 µm translucent thincert trans-well system by Greiner Bio-One. $3x10^4$ cells were seeded in triplicate in the compartments and left to settle overnight. The next day cells were exposed to hypoxia or stayed in normoxia for 5 days in total before cell numbers were assessed.

For co-culture with conditioned media, cells were seeded in 10 cm dishes and left to settle overnight. According to the time point, media was changed and cells subjected to hypoxia or normoxia. Afterwards, the media was, collected, centrifuged, and transferred to cells seeded in 12-well or 6 cm plates. These plates were then again subjected to hypoxia or normoxia for 5 days before cell numbers were assessed.

2.14. Measurement of oxygen consumption rates using the MitoExpress probe

For measurement of oxygen consumption rates, 40,000 cells were seeded in black 96-well plates and left to settle overnight. Approximately 6 h before the reading, the

medium was changed to 1 mM glucose as initial experiments indicated that 5 mM glucose was too high (ie the rate of change in the oxygen consumption was very weak). Before the actual measurement, the MitoExpress probe was taken up in 1 mL of water. 140 μL of media were mixed with 10 μL of reconstituted probe and added to the wells. The different media are indicated in the respective figures. For media from co-culture conditions, conditioned media was centrifuged at 2000 g for 5 min before usage. Wells were covered with two drops of oil to reduce oxygen diffusion and wells were read several times at equal intervals overnight. Readings were normalised to a negative control containing no probe and a positive control containing probe, but no oil.

2.15. Lactate measurements in the media

Lactate levels in the media were measured using a kit by Instruchemie, which is based on an enzymatic reaction. In principle the reaction involves lactate dehydrogenase which catalyses the reaction lactate + NAD <-> pyruvate + NADH. The reagents provide an excess of NAD and hydrazine and the enzyme, driving the conversion of all lactate present to pyruvate. This leads to a relative increase in the reduction of NAD to NADH and this shift is measured as an increase of absorbance at 340 nm. A lactate standard curve was used to relate absorbance measurements to lactate levels (Figure 2.2).

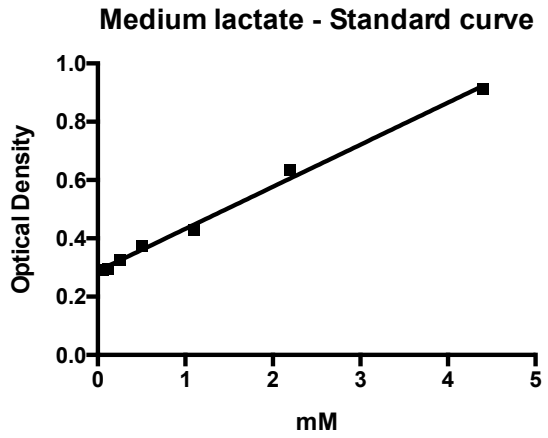


Figure 2.2 Representative lactate standard curve – enzymatic method

2.16. Staining for Lipid droplets

To assess intracellular lipid droplet formation $1x10^4$ cells were seeded on coverslips. After incubation at the conditions indicated in the respective figures, cells were washed three times in PBS before being fixed in 4% paraformaldehyde (PFA) for 20 min at RT. After another three washes with PBS, cells were stained for lipid droplets using LD540 (Spandl et al., 2009) for 15 min at RT in the dark. Cells were again washed three times with PBS and once with water. Cover slips were mounted on slides using DAPI mounting medium (Vectashield) and were imaged at steady excitation times with a ZEISS fluorescence microscope.

Alternatively, lipid droplet formation was assessed by flow cytometry using a cyan flow cytometer.

2.17. Immunohistochemistry (IHC)

Slides for immunohistochemistry were incubated for 10 min at 60°C. The slides were then immersed twice in histo-clear solution (National Diagnostics) for 5 min, twice in 100% ethanol for 5 min and then once each in 70% and 50% ethanol for 5 min and finally tap water for 5 min.

After rehydration, slides were placed in antigen retrieval buffer (see Table 2.4) and heated to 125°C for 2 min in a pressure cooker. Slides were then washed in water and blocked with normal horse serum (ImmPRESS kit, Vector Laboratories) for 30

min at RT. Following a washing step, the primary antibody was diluted in PBS/3% BSA and added onto the slides overnight at 4°C. The slides were washed again and incubated with 0.3% hydrogen peroxide in PBS for 15 min to decrease background signal. The appropriate secondary antibodies (ImmPRESS kit, Vector Laboratories) were applied for 1 h at RT. Following another wash, the signal was visualised by adding ImmPACT DAB peroxidase substrate (Vector Laboratories) for 30-60 s. Slides were then counterstained using haematoxylin solution (Vector Laboratories) and cover glasses were mounted with Aquatex mounting agent (Merck).

Table 2.4 Antibodies used for IHC

Antibody	Concentration	Antigen retrieval solution
CAIX M75	1:100	DAKO, low pH
MMP-14	1:100	DAKO, low pH

2.18. Chromatin immunoprecipitation assay for HIF-1β

Immunoprecipitation assays for HIF-1β were performed using the Millipore ChIP Kit Reagents and chromatin immunoprecipitation (ChIP) assay. Briefly, 10 x 10^6 CAIX+ve and CAIX-ve cells were incubated in hypoxia or normoxia for 24 h. Cells were then cross-linked with formaldehyde (final concentration of 1%) for 10 min on ice and the reaction was quenched by adding glycine (final concentration of 125 mM) and incubating the cells for 5 min on ice. After five washes with PBS, the cells were lysed in 1 mL of 1% SDS lysis buffer with added protease inhibitor cocktail. The cells were sonicated in 30 s on/off pulses for a total of 13 min using a Diagenode Bioruptor water bath sonicator and the supernatant was collected.

To avoid unspecific binding, supernatants were incubated with 60 μL of protein G agarose beads for 1 h at 4°C on a rotator. This was followed by a centrifugation step and 10 μL of the supernatant were kept as input control.

The remaining supernatant was collected into fresh tubes and the Hif-1β (Novus NB-100-110) antibody for immunoprecipitation was added in a 1:100 ratio and incubated at 4°C overnight on a rotator. Normal mouse IgG was used as a negative control.

The next day, 60 µL of protein G agarose beads were added to each sample and incubated for 1 h at 4°C on a rotator to bind the antibody/antigen/DNA complex. This was followed by a centrifugation step for 1 min at 5000 g. The beads were then washed by adding 800 µL of ice cold buffers as listed, incubated for 5 min at 4°C on a rotator and subsequent centrifugation (1 min, 5000 g).

1) Low Salt Immune Complex Wash Buffer
2) High Salt Immune Complex Wash Buffer
3) LiCl Immune Complex Wash Buffer
4) TE Buffer

After the washes, 100 µL of Elution Buffer was added to each sample and incubated for 15 min at room temperature. The tubes were then again centrifuged at 5000 g for 1 min and the supernatant was collected in to new tubes. This process was repeated twice, combining the resulting supernatants. In order to free the DNA from the crosslinking, 8 µL of 5 M NaCl was added to each samples and tubes were incubated overnight at 65°C.

The next day 1 µL of RNase A was added to all tubes and incubated at 37°C for 30 min to remove RNA contamination. Afterwards 4 µL 0.5 M EDTA, 8 µL of 1 M Tris-HCl, and 1 µl Proteinase K was added to each tube and tubes were incubated for 2 h. In the next step, the DNA was purified using spin columns. For this 1 mL of bind reagent A was added to each sample as well as the input from day 1. The resulting samples were transferred to the filter columns and spun for 30 s at 10,000 g. Samples were washed twice with the supplied wash reagent and spun again.

Afterwards the filter columns were placed into new collection tubes and 30 μL of Elution Buffer was added. The isolated DNA was assessed using qPCR for the amount of *CA9* promoter binding. VEGFR was used as a control. The data was normalised to the input.

Table 2.5 Primers for ChIP experiment

Gene	Forward Primer	Reverse Primer
CA9 HREs	GTCCATGGCCCCGATAACCTTCTG	GGGGCAACCTCTGGGGATGGAC
VEGF	TGCCCGCTGCTGTCTAAT	TCTCCGCTCTGAGCAAGG

2.19. Analysis of the METABRIC dataset

The analysis of the METABRIC data set was kindly perfromed by Dr. Syed Haider (postdoctoral fellow in Dr. Francesca Buffa's group, Department of Oncology, University of Oxford). The METABRIC breast cancer dataset was preprocessed, summarised and quantile-normalised from the raw expression files generated by Illumina BeadStudio (R packages: beadarray v2.4.2 and illuminaHuman v3.db_1.12.2). The raw METABRIC files were downloaded from the European genome-phenome archive (EGA) (Study ID: EGAS00000000083).

The METABRIC analysis and the graphs were carried out using R statistical environment (v3.0.1). The hazard ratio (HR) was calculated by fitting the cox proportional hazards model and the Wald test was used to test the significance of the outcome difference between the lower and higher than median expression groups.

2.20. Statistical analysis

Statistical analysis was done using GraphPad Prism Version 6.0 software. For comparison of two groups, t-tests were used, whereas for more groups ANOVA with Bonferrroni post-test was chosen. Significance is denoted as: * $p \leq 0.05$, ** $p \leq 0.01$, *** $p \leq 0.001$.

2.21. Buffers and solutions

Table 2.6 Buffers and solutions

Cell culture	
PBS	137 mM NaCl 2.7 mM KCl 4.3 mM NA_2HPO_4 CA^{2+} and Mg^{2+} free pH 7.3
Trypsin / EDTA	PAA
DMEM media	Gibco (Invitrogen) 10% FCS (Gibco) 100 IU / mL Penicillin (PAA) 100 mg / mL Streptomycin (PAA)
Optimem	Gibco
Protein extraction and Western blot	
RIPA buffer	Sigma
Complete protease inhibitor tablets	Roche
Sample buffer	Invitrogen
1x Running buffer	Invitrogen
1x Transfer buffer – semi-dry transfer	2x transfer buffer (Invitrogen), 10% Methanol in dH_2O
1x Transfer buffer – wet transfer	25 mM TrisBase, 192 mM Glycine, 20%

	Methanol in dH_2O
PBS-T	0.2% Tween [Sgima] in PBS
Stripping buffer	Sigma

Table 2.7 Antibiotics and drugs

Compound name	**Compound action**	**Company**	**Concentration**
Ampicillin	Antibiotics/selection marker	Sigma Aldrich	50 µg/ mL
Kanamycin	Antibiotics/selection marker	Sigma Aldrich	50 µg/ mL
Puromycin	Antibiotics/selection marker	Sigma Aldrich	0.75 µg/ mL
Neomycin	Antibiotics/selection marker	Sigma Aldrich	1000 µg/ mL
Sodium Butyrate (NaBu)	HDAC inhibitor	Sigma Aldrich	5 mM

Chapter Three

Hypoxia induced CAIX expression defines cell line subpopulations

3.1. Introduction

Inter- but also intra-tumour heterogeneity has been identified as a major challenge in cancer diagnosis and the subsequent selection of treatment options.

The fast growth of aggressive tumours leads to regions of inadequate vascularisation, characterised by hypoxia and an inefficient level of nutrients (Heddleston et al., 2010a).

The onset of hypoxia in parts of the tumour contributes to heterogeneity, as the hypoxic microenvironment influences various pathways mainly by the direct regulation of gene expression via hypoxia inducible transcriptional factors (HIFs) (see section 1.8.2,). A main target of HIF-1 transcriptional activation is carbonic anhydrase IX (CAIX) and CAIX expression has been successfully used as a reliable marker for regions of hypoxia.

Furthermore, the survival advantage of genes activated during hypoxia leads to a selection of populations, also contributing to the establishment tumour heterogeneity (Harris, 2002, Diaz-Cano, 2012). Indeed, it was reported that hypoxic conditions select for cells that are insensitive to p53 mediated apoptosis (Sermeus et al., 2008).

3.1.1. Epigenetic regulation of gene expression

The expression of genes, RNAs and proteins is tightly regulated. On gene level, a major aspect of regulation involves epigenetics, or the accessibility of DNA regions for transcriptional activity.

Commonly, chromatin organisation is classified by describing the “openness” of the chromatin structure, broadly differentiating euchromatin and heterochromatin.

Euchromatin describes genomic regions that are “relaxed” or “open”, allowing a greater exposure to transcription factors. These regions often contain active genes. In contrast, heterochromatin describes regions that are more “compact” or “closed”, containing mostly inactive genes.

DNA modification can occur via methylation, meaning the addition of a methyl group to the 5-position of cytosine. These modifications are mostly reported in the context of CpG dinucleotides. Some of these 5-methylcytosines have been shown to be convertible to hydroxymethylated, formylated, or carboxylated forms via ten eleven translocation (TET) proteins, adding another layer of complexity (Tahiliani et al., 2009, He et al., 2011, Ito et al., 2011).

CpG dinucleotides occur symmetrically on both DNA strands, ensuring the inheritance of this feature to the daughter strands during replication. DNA methylation is broadly associated with heterochromatin, whereas regions with non-methylated CpGs – CpG islands – often feature gene promoters (Illingworth et al., 2010).

Another layer of regulation is comprised of histones. Histones H2A, H2B, H3 and H4 form an octamer, which is wrapped by 147bp of DNA for form a nucleosome. These proteins can undergo several modifications, including acetylation, methylation, ubiquitylation, and phosphorylation. Histone acetyltransferases (HATs) or deacetylases (HDACs) specifically acetylate or deacetylate lysine residues on histones (Kurdistani, 2007, Peng et al., 2008). In this context heterochromatin is characterised by H3K9 (di- and tri-) methylation, trimethylation at H3K36, dimethylation at H3K79, global histone hypoacetylation and the recruitment of heterochromatin protein 1 (HP1) (Portela and Esteller, 2010, Berger, 2007).

By contrast euchromatin is associated with increased acetylation, di- and trimethylation at H3K4, H3K27, and H4K20 (Strahl et al., 1999).

The borders of such regions are, moreover, regulated by specific factors such as CTCF, or a specific histone variant (H2A.Z) (Barski et al., 2007), ensuring the distinction between specific chromatin regions (Ong and Corces, 2009).

Analysing the binding pattern of a number of chromatin proteins in *D. melanogaster* led Filion et al (2010) to propose five individual genomic domains of chromatin structure (Filion et al., 2010).

3.1.2. Epigenetic regulation in tumours

The current understanding of an epigenetic role in tumour formation and progression is mainly focussed on two mechanisms:

1. Epigenetics can alter the gene expression, leading to upregulation of oncogenes and/or downregulation of tumour suppressors
2. Histone modifications may affect genome integrity

Several studies have investigated the methylation status of DNA of tumour cells. Initially, much focus was given to the idea that cancer-DNA is hypomethylated. Already in the early 1980s, Feinberg et al. showed that genes (Feinberg and Vogelstein, 1983a), including ras oncogenes (Feinberg and Vogelstein, 1983b), in cancer DNA were hypomethylated in comparison to DNA from adjacent healthy tissue, although numbers were small. Moreover, studies looking at the general 5-methylcytosine content found a decrease in global DNA methylation in tumour tissues (Gama-Sosa et al., 1983), including in Wilms (Ehrlich et al., 2002), liver (Lin et al., 2001), and breast (Bernardino et al., 1997, Soares et al., 1999) tumours.

Despite this notion that cancers are globally hypomethylated, defined regions of hypermethylation have also been found. Abnormal hypermethylation in tumours was mostly associated with CpG islands (Costello et al., 2000), with some overlap between different tumour types (Costello et al., 2000, Esteller et al., 2001).

Esteller et al (2000) showed that hypermethylation of the DNA region encoding for MGMT (O6-methylguanine DNA methyltransferase), a DNA repair gene, was linked to K-ras mutation in colorectral cancer (Esteller et al., 2000). Likewise, silencing of BRCA1 (Chiang et al., 2006) by promoter methylation was associated with poor prognosis in ovarian cancer. RASSF1A was found to be a tumour suppressor as it is a regulator of BRCA2 and hence involved in genome stability (Pefani and O'Neill, 2015). Accordingly RASSF1A hypermethylation was associated with tumorigenesis in various models (Grawenda and O'Neill, 2015)

The onset of hypoxia in tumours has also been associated with global changes in histone modifications, although the exact mechanism of regulation is likely to be complicated, as modifications typically associated with both repression and activation of genes could be found in hypoxia-regulated promoters (Johnson et al., 2008).
Moreover, several members of the JmjC-containing family of histone demethylases were found to be direct targets of HIF-1 and 2 (Xia et al., 2009, Wellmann et al., 2008, Pollard et al., 2008), and a robust upregulation of these proteins was shown *in vitro* but also in patient samples (Xia et al., 2009). A potential explanation for this upregulation is that an increased level of enzyme would drive the maintenance of H3K4 methylation homeostasis despite the limiting molecular oxygen tension (Xia et al., 2009).

3.1.3. CAIX as a biomarker for tumour heterogeneity

Tumour heterogeneity is associated with differential gene expression profiles. The characterisation of these populations will be helpful in patient stratification.
CAIX as a biomarker for hypoxia has been mainly investigated by immunohistochemistry and/or immunofluorescence; however, this is highly dependent on the size and number of tissue samples (biopsy/TMA core) (Iakovlev et al., 2007).

Therefore, we developed an interest in assessing the tumour heterogeneity of CAIX expression using the stability and the transmembrane location of the protein to our advantage. Using flow-cytometry it had previously been shown that in MCF7 cells, CAIX induction during hypoxia is heterogeneous, with a CAIX positive and a CAIX negative population present. The CAIX positive population was furthermore shown to be more stem cell-like as indicated by a relative increase of putative stem cell markers and the ability of this population to form tumours in xenograft experiments when injected in low numbers (Ledaki et al., 2015).

3.2. Results

3.2.1. Expression of CAIX

CAIX expression in breast cancer subtypes

Firstly, the expression level of CAIX mRNA in the different breast cancer subtypes, thus the heterogeneity between subtypes was analysed. In this approach data from a large publicly available cohort of breast cancer patients (n=1988, METABRIC dataset) was used, from whom clinical outcome data was also available (Curtis et al., 2012).

The median expression of CAIX was assessed for all patients and the data was also stratified according to breast cancer subtypes including triple negative (ER, PR and HER2 negative), ER status (ER-positive versus ER-negative), HER2 status (HER2-positive versus HER2-negative) and using the PAM50 gene expression profiler (Parker et al., 2009). CAIX expression in nearly all of the subtypes is varied with a number of cases displaying a higher than median CAIX expression. The highest median CAIX expression in comparison to normal is visible in the triple negative / basal subtype, followed by the ER- and the HER2+/ER- and HER2 subtypes (Figure 3.1 A).

CAIX levels were also correlated with overall survival data (OS). In a cohort comprising all breast cancers, higher than median CAIX expression correlated significantly with poorer outcome (HR 1.19, 95% CI 1.03-1.37, p=0.017). High CAIX expression correlated most significantly with poorer outcome in the HER2/ER positive subtype (HR 1.72, 95%CI 1.03-2.87, p=0.039) and the triple negative breast cancer subtype (HR 1.71, 95%CI 1.2–2.45, p=0.003). This trend was also visible in the basal subgroup, the characterisation of which overlaps with the triple negative subtype. Interestingly, high CAIX levels were not always correlated with poorer outcome; in the Luminal A subtype it was even associated with better outcome (HR 0.81, 95% CI

0.63-1.05, p=0.113); however, this was not statistically significant (Figure 3.1 B). This shows that the role of CAIX in breast cancer may be dependent on different co-factors.

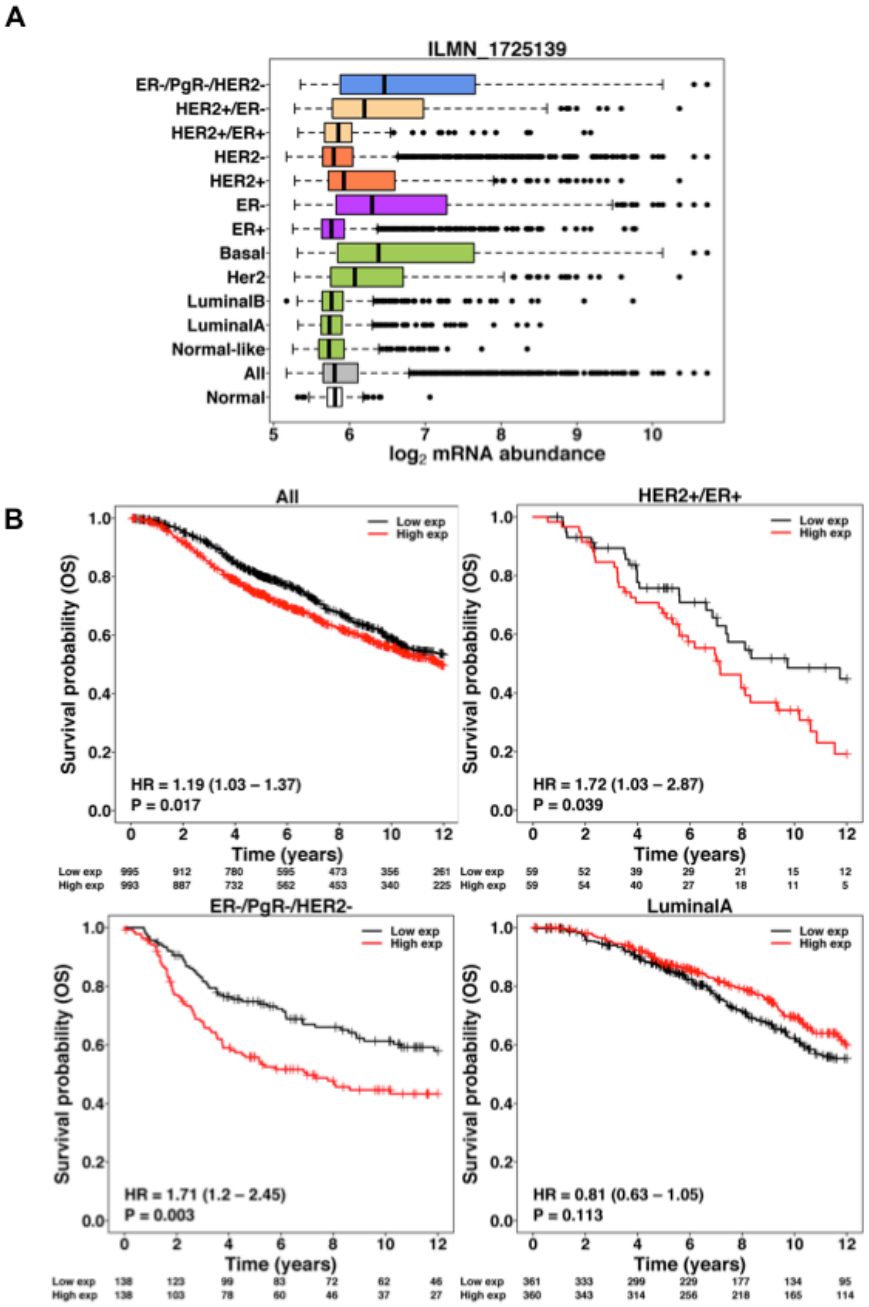


Figure 3.1 CAIX expression in breast cancer subtypes

CAIX mRNA levels were assessed in a large cohort of breast cancer patients (n=1988, METABRIC dataset) (Curtis et al., 2012). (A) The median CAIX mRNA is plotted. (B) Overall survival was plotted for patients with higher vs lower than median CAIX levels. The analysis was performed by **Dr. Syed Haider**.

Hypoxia-heterogeneous induced populations indicated by differential CAIX expression

Hypoxia has been shown to induce changes in the tumour microenvironment as well as in the tumour cells themselves through epigenetic and molecular changes. Previous work from our laboratory identified that in MCF7 cells hypoxia induces heterogeneous populations marked by CAIX expression (Ledaki et al., 2015). In comparison to the normoxic sample, it appeared that under hypoxia one population does express CAIX, whereas the other one does not (Figure 3.2 A). These HHIPs were sorted by collecting the top and bottom 10% of CAIX expressing cells. The two populations were cultured for more than six months and, whereas the CAIX negative population remained negative over time, the CAIX positive population was shown to mimic the initial cell line features with a positive and negative population present under hypoxia (Figure 3.2 B) (Ledaki et al., 2015).

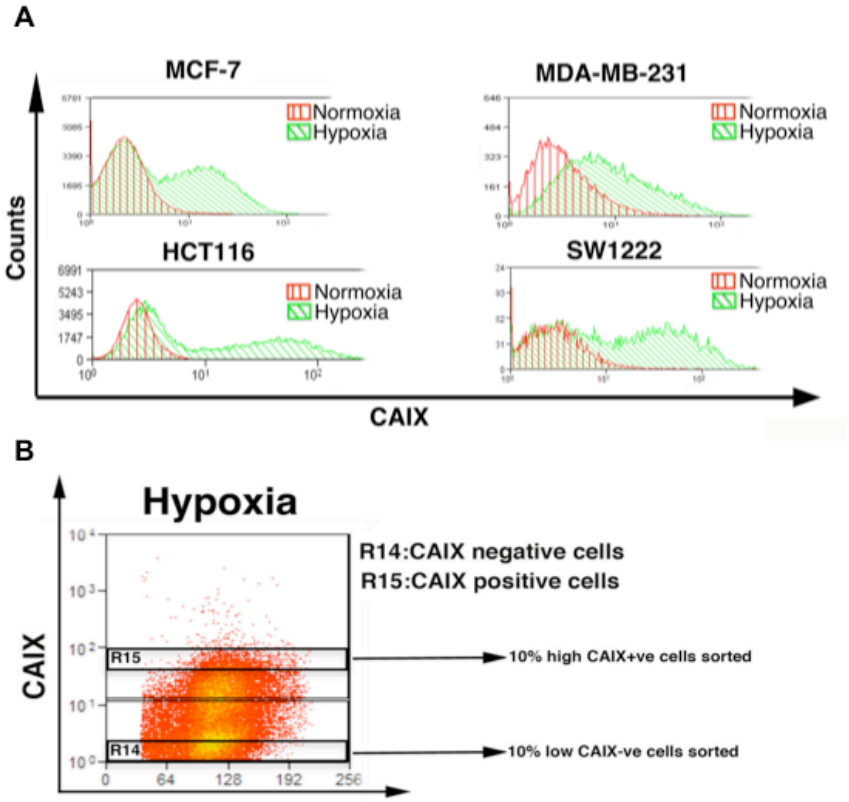


Figure 3.2 MCF7 cells were sorted into CAIX positive and negative populations

(A) Depicted cell lines were incubated at normoxia or 0.1% oxygen for 72 h, before samples were stained for CAIX and analysed using flow cytometry. (B) MCF7 cells were incubated at 0.1% oxygen for 72 h before being stained for CAIX. CAIX positive and negative cells (top and bottom 10% as indicated) were sorted. This work was done and published by **Dr Ioanna Ledaki** (Ledaki et al., 2015) Permission for reprint granted by Oncotarget, https://creativecommons.org/licenses/by/3.0/.

These results were replicable even after two years of culture as shown in Figure 3.3 A and throughout the results chapters, the populations will be referred to as CAIX positive and negative cells respectively.

Analysis of mRNA and protein levels by qPCR and Western blot respectively revealed a marked increase of CAIX in the sorted CAIX positive population in comparison to the CAIX negative population after re-exposure to severe hypoxia for 72 h. This indicates an intrinsic mechanism of CA9 regulation rather than just a difference in cell surface localisation (Figure 3.3 B)

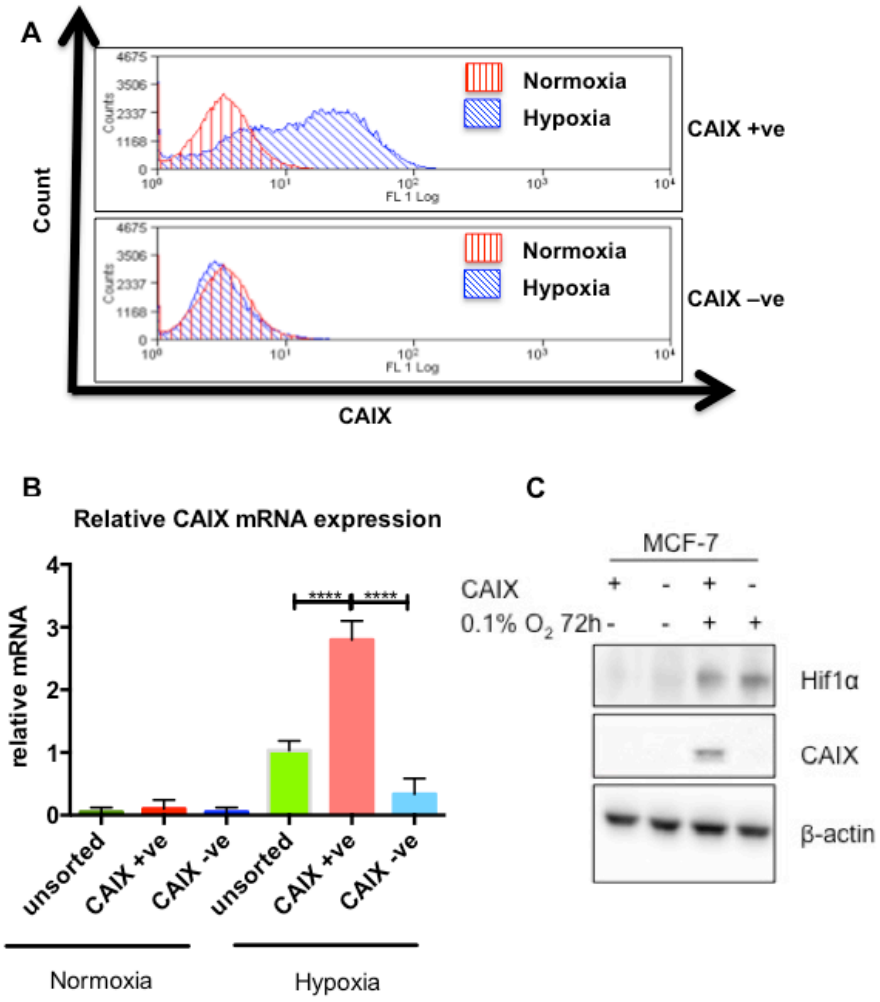


Figure 3.3 MCF7 CAIX positive and negative populations keep characteristics

MCF7 CAIX positive and negative populations have been cultured long-term (>2 years). Cells of both populations have been incubated at normoxia or 0.1% for 72h, after which CAIX expression was assessed by (A) flow cytometry, (B) qPCR, and (C) Western blot.

n=3, Graphs show mean ± SD, ****p<0.0001

3.2.2. Mechanism of CAIX regulation

CAIX expression is epigenetically regulated

CAIX is regulated by the hypoxia mediated transcription factor HIF-1. However, the level of HIF-1 was similar in the CAIX positive and negative populations. Moreover, the level of a number of other well-known HIF-1 target genes such as LDH-A, and AK4 were not differentially expressed (Figure 3.4) on protein levels in such a significant manner. This raised the question of how CAIX expression was regulated differentially in these populations.

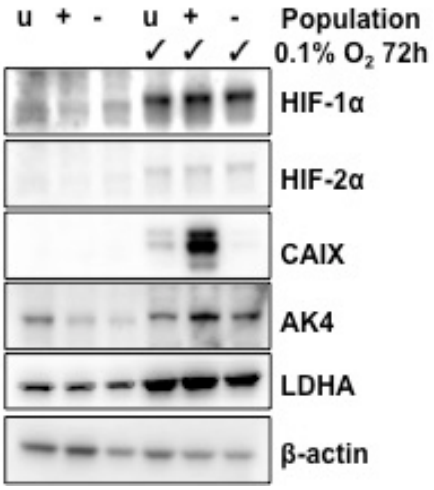


Figure 3.4 CAIX is the most differentially expressed HIF-1 target gene in the MCF7 CAIX positive in comparison to the CAIX negative population

Unsorted (u), CAIX +ve (+) or CAIX –ve (-) cells were incubated in normoxia or 0.1% hypoxia for 72 h before protein levels of indicated proteins were assessed.

To assess whether CAIX expression in the positive population was still HIF-1 dependent, a knockdown experiment was performed. Cells were either incubated with control or HIF-1 specific siRNA. In comparison to normoxic conditions, CAIX was expressed in the CAIX positive population treated with control siRNA under hypoxic conditions (0.1% O_2, 72h). However, knockdown of HIF-1 in this setting diminished

CAIX expression on mRNA and protein level, confirming that transcription of CAIX in these cells is still mainly driven by HIF-1 (Figure 3.5 A and B). It was next hypothesised that the difference in CAIX expression may be due to differential binding of HIF-1 to the CAIX promoter in the two populations. In order to investigate this, cells of both populations were incubated in normoxia and hypoxia, after which cells were subjected to chromatin immunoprecipitation (ChIP). Subsequent analysis of the DNA fragments revealed that HIF-1 binding to the CAIX promoter region was decreased in the CAIX negative population by five-fold in comparison to the CAIX positive population under hypoxic conditions (Figure 3.5 B). In contrast, the promoter region of VEGF – another HIF-1 target gene – showed similar binding affinities (Figure 3.5 C and D).

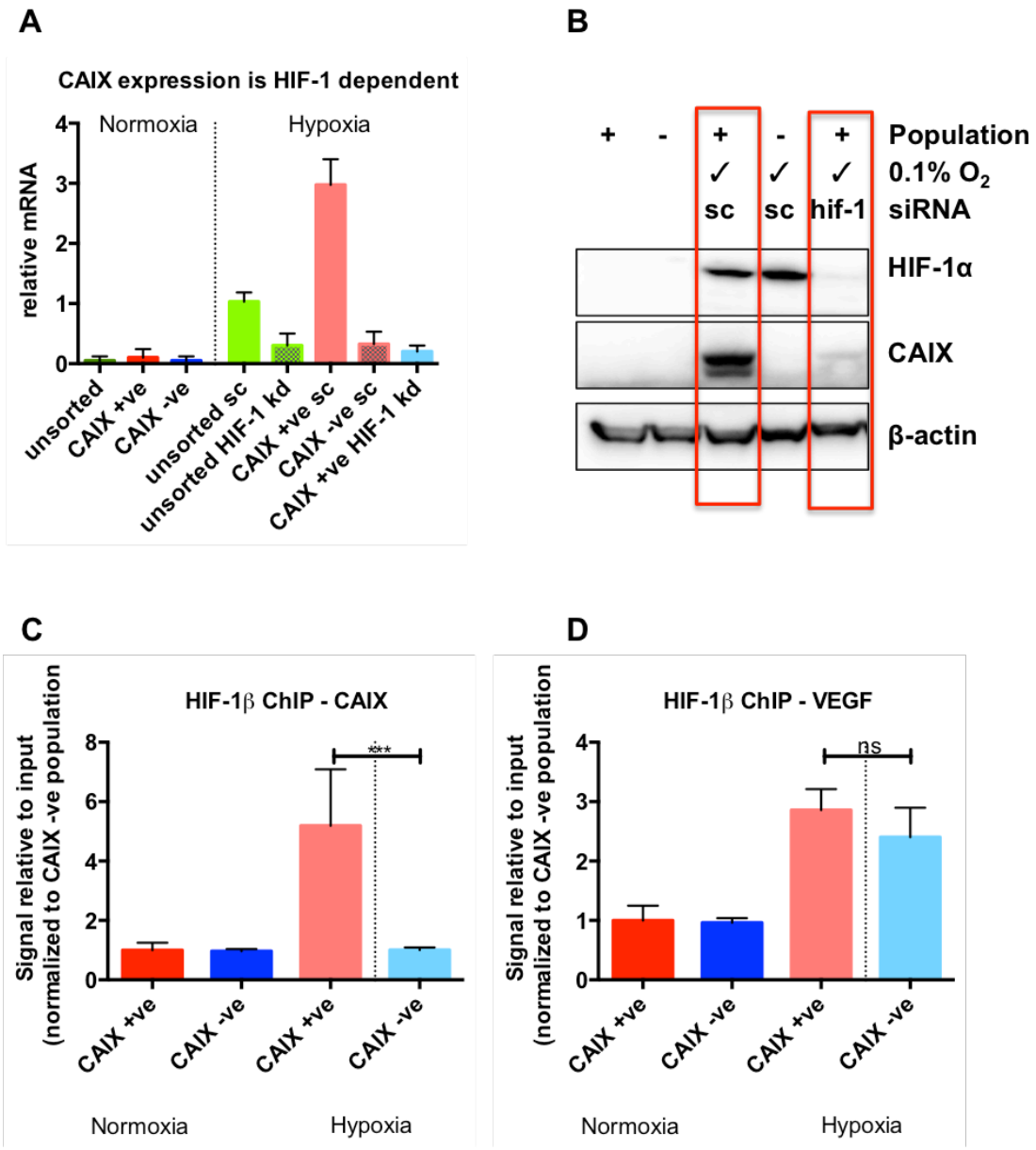


Figure 3.5 MCF7 CAIX expression is regulated by differential binding of HIF-1

(A) and (B) CAIX positive and negative MCF7 populations were treated with scramble control (sc) or HIF-1α specific siRNA (kd) as indicated and incubated in normoxia or at 0.1% oxygen for 72 h. CAIX expression was then assessed by qPCR and Western blot respectively. (C) and (D) ChIP was performed as described in the M&M section. Briefly, MCF7 CAIX positive and negative populations were incubated in normoxia or at 0.1% oxygen for 24 h before cells were fixed and DNA sheared using a sonicator. HIF-1 and bound DNA fragments were pulled down used for qPCR analysis. n=3, Graphs show mean ± SD, ns= not significant, * $p<0.05$, ** $p<0.01$, *** $p<0.001$

3.2.3. Evaluation of CAIX expression in a panel of breast cancer cell lines

A number of other cell lines were assessed with regard to CAIX expression induced by hypoxia (0.15 O_2) for 72 h. In three out of nine cell lines tested – BT474, SKBR3, MDA-MB-361 - no CAIX induction was observed in the chosen setup. The other six cell lines (MDA-MB-453, HCC1569, ZR 75-1, MDA-MB-468, HCC 70, and HCC 1806) showed a homogenous shift of the expression of CAIX after 72 h of hypoxia, in comparison to normoxic control (Figure 3.6).

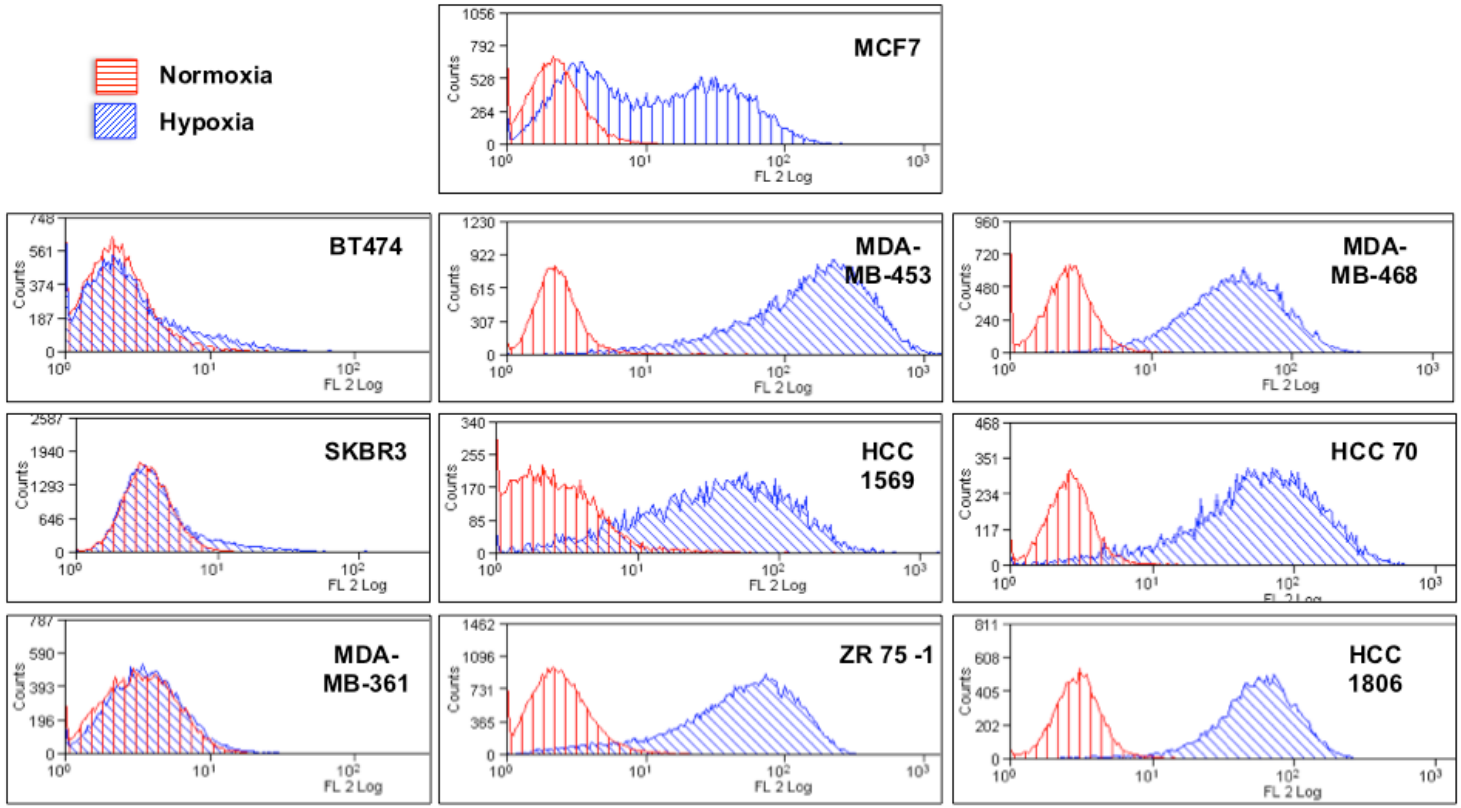


Figure 3.6 CAIX expression in a panel of breast cancer cell lines. Indicated cell lines were incubated in normoxia or at 0.1% oxygen for 72 h before cells were stained for CAIX and analysed using flow cytometry. n=3

It was then investigated whether cells with higher or lower levels of CAIX would have similar properties to the CAIX positive and negative populations respectively. Therefore, cells of two more cell lines with a homogeneous CAIX expression after hypoxia (ZR 75-1 and MDA-MB-453) were sorted into CAIX high and low cells (top and bottom 20%) (Figure 3.7 A). In the short-term, properties similar to those of CAIX positive/negative cells respectively was observed. CAIX high cells formed more and larger colonies after sorting (Figure 3.7 B and C). Moreover, initial CAIX high cells retained a higher level of CA9 upon re-exposure to severe hypoxia than CAIX low cells (Figure 3.7 D) even though HIF1-α levels were similar between the two populations.

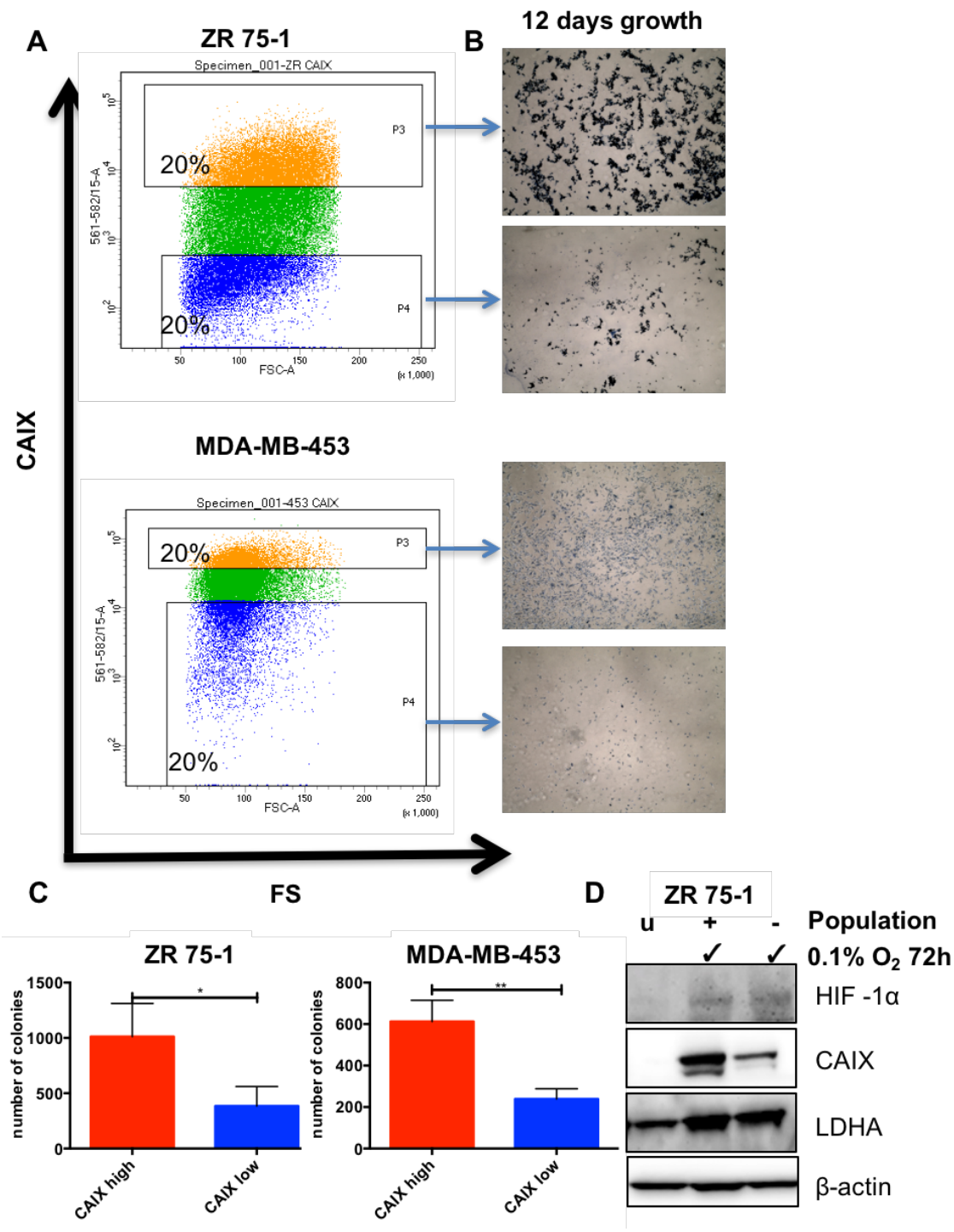


Figure 3.7 Sorting of CAIX high and low ZR 75-1 and MDA-MB-453 breast cancer cells

(A) Indicated cell lines were incubated at 0.1% oxygen for 72 h before cells were stained for CAIX. CAIX high and low expressing cells were sorted by FACS. (B) CAIX high and low expressing cells were seeded for clonogenic assays after sorting and clones were assessed after 12 days of growth in normoxia. Mean number of clones

are shown in (C). (D) ZR 75-1 CAIX high and low cells were re-exposed to 0.1% hypoxia for 72 h and indicated proteins were assessed using Western blot.

n=3, Graphs show mean ± SD, * p<0.05, **p<0.01, FS= Forward Scatter

3.2.4. Confirmation of model – HCT116 colon cancer cell line

In order to decrease the probability of cell line specific one-off effects, we sought to establish a second cell model to investigate the hypothesis of hypoxia induced subpopulation marked by presence/absence of CAIX expression. To this end the colon cell line and tumour model HCT116 were also tested. In comparison to normoxic conditions where cells were negative for CAIX expression, we found a CAIX positive and a CAIX negative population after incubation in hypoxia (0.1% O_2) for 72 h (Figure 3.8 A). Again, the top and bottom 10% of CAIX expressing cells were sorted (Figure 3.8 B) and subsequently cultured in normoxia.

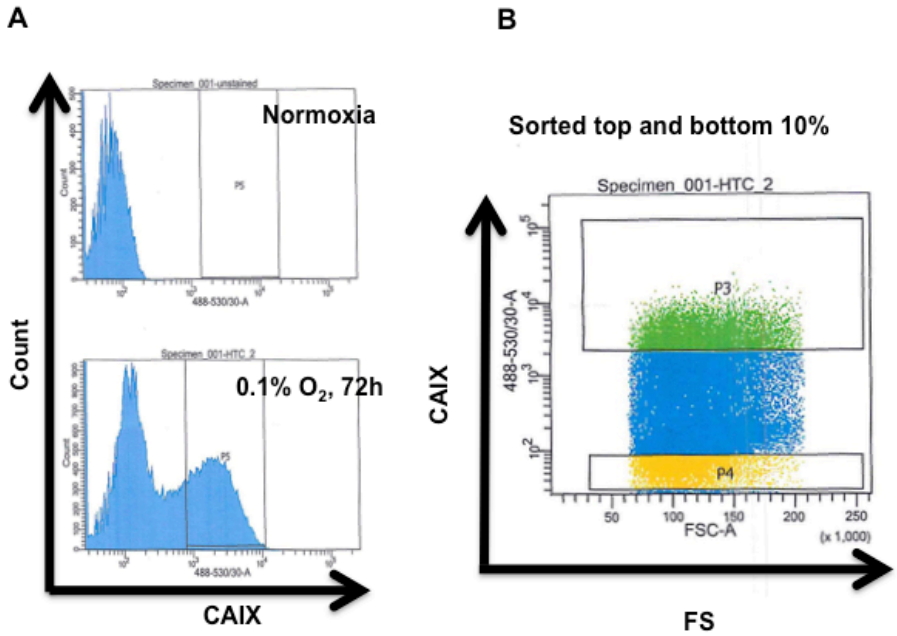


Figure 3.8 HCT116 cells were sorted according to their CAIX level

(A) HCT116 cells were incubated in normoxia or at 0.1% hypoxia for 72 h before cells were stained for CAIX and assessed by flow cytometry. (B) Top and bottom 10% of CAIX expressing cells were sorted. FS= Forward Scatter

After two weeks, an initial check showed that the population that had been sorted as CAIX positive contained CAIX positive and negative cells, whereas the CAIX negative sorted population remained largely negative upon re-exposure to 0.1% hypoxia for 72 h (Figure 3.9 A). This was also confirmed by mRNA and Western blot analysis (Figure 3.9 B and C). To reinforce this phenotype, the top and bottom 10% of CAIX positive and negative populations respectively were sorted again and cultures were regularly checked for the level of CAIX.

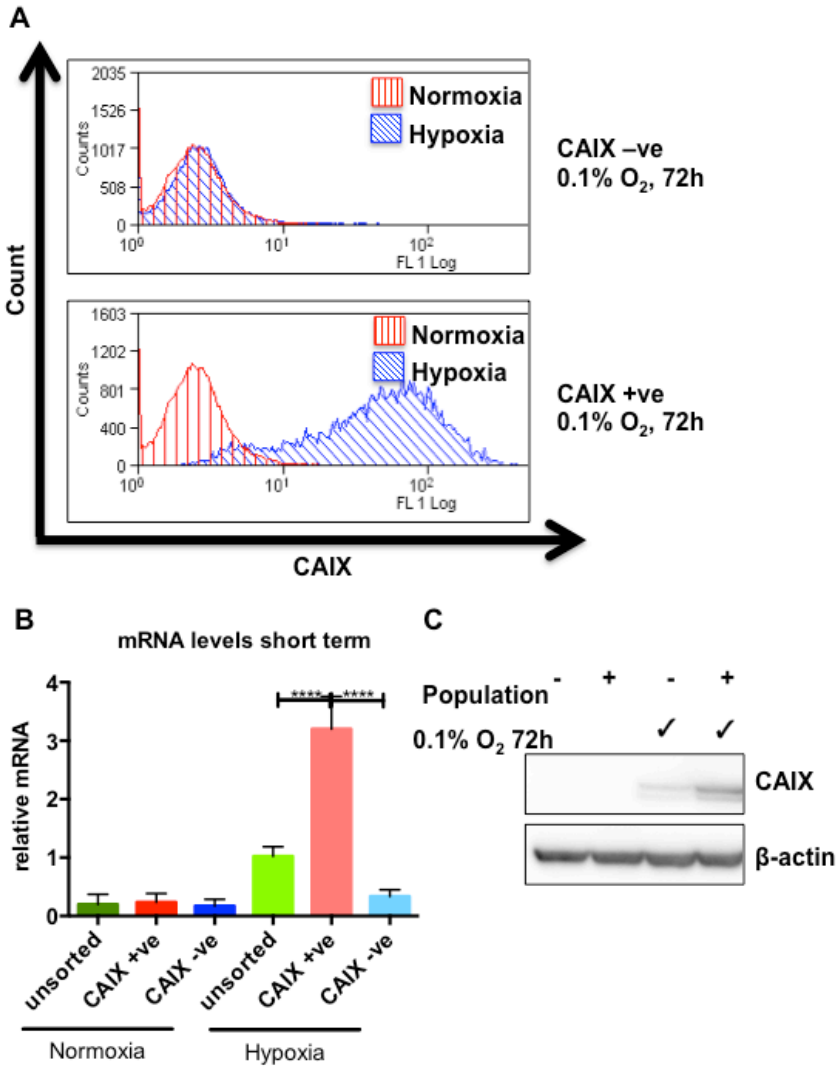


Figure 3.9 CAIX expression in HCT116 cells over time

HCT116 CAIX positive and negative populations were cultured for three weeks before cells were re-exposed to normoxia or 0.1% hypoxia for 72 h and CAIX levels were assessed by (A) flow cytometry, (B) qPCR, and (C) Western blot

n=3, Graphs show mean ± SD, ****p<0.0001

As shown by flow cytometry as well as on mRNA and protein level, the CAIX positive population had an increased number of CAIX positive cells upon re-exposure to severe hypoxia in comparison to the unsorted/parental. However, this population also contained CAIX negative cells. Conversely, the CAIX negative cells remained largely CAIX negative in comparison to normoxic control (Figure 3.10 A - C). Similar to CAIX positive and negative populations of other cell lines, higher clonogenic ability was found in the CAIX positive population of HCT116 sorted cells (Figure 3.10 D).

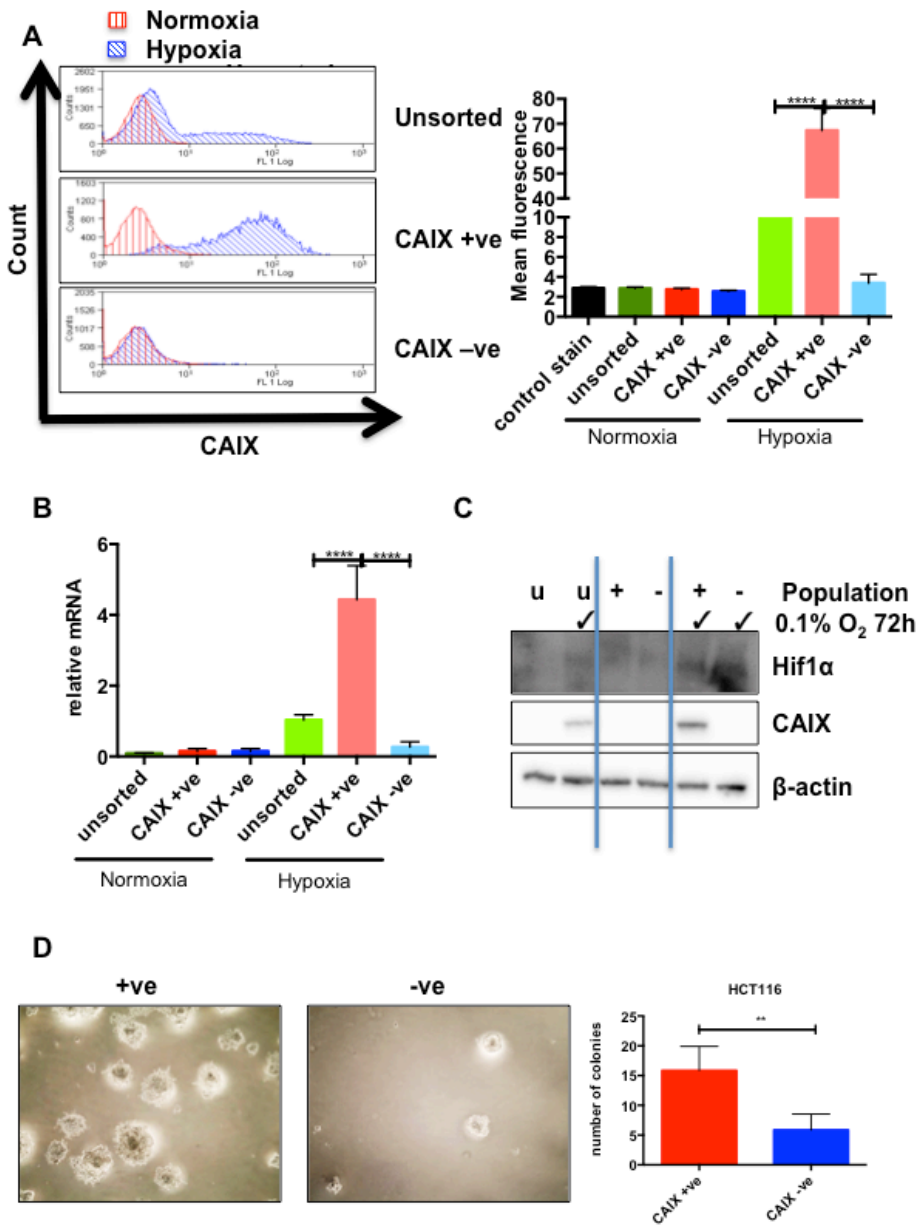


Figure 3.10 Long term level of CAIX in HCT116 sorted populations

HCT116 CAIX positive and negative populations cell stocks were maintained for six months before cells were re-exposed to normoxia or 0.1% hypoxia for 72 h and CAIX levels were assessed by (A) flow cytometry, (B) qPCR, and (C) Western blot. (D) Sorted cells were seeded and growth monitored. Colonies were counted after 12 days.

n=3, Graphs show mean ± SD, **p<0.01, ****p<0.0001

3.3. Discussion

The onset of hypoxia in tumours has clearly been associated with poor prognosis and decreased response to treatment. Therefore, reliable biomarkers of tissue hypoxia are important for diagnosis and treatment options. In this context, CAIX has been established as a promising proxy marker of hypoxia, as it is a direct target of HIF-1α transcription under conditions of low oxygen. In line with this, CAIX itself has been associated with poor prognosis in a global cohort of breast cancer as well as in some breast cancer subtypes.

This study is a continuation of another project by Ioanna Ledaki, who showed a heterogeneous expression of CAIX under hypoxia using flow cytometry (Ledaki et al., 2015). The current study confirms that stability of the generated cell populations – where the initial CAIX positive population is able to regenerate the parental MCF7 cell line (i.e. forming a CAIX positive and a CAIX negative population), whereas the initial CAIX negative population remained negative.

Moreover, a second model, using colon HCT116 cells, was established showing a similar pattern of CAIX heterogeneity under severe hypoxia.

Interestingly, none of the other cell lines tested showed distinct positive and negative populations with regard to CAIX expression. However, it was shown that the relative level of CAIX expression still matters. In cell lines that showed a homogenous induction of CAIX under hypoxia (rather than two populations), CAIX high expressing cells and CAIX low expressing cells behaved similarly to CAIX positive and negative populations respectively. CAIX high cells displayed a higher level of survival (clonogenic) and sorted cells of either category showed the same level of CAIX expression (i.e. high or low) upon re-exposure to severe hypoxia. This indicates that CAIX expression under hypoxia is tightly controlled. However, how this differential expression is regulated is not fully clear. In this work, some potential mechanisms were looked at.

The first discussion point is the technique used to prepare cell samples for flow cytometry/FACS. In general, cells were trypsinised for 5min at 37°C, washed with PBS, and stained for cell surface CAIX expression. Previous papers reported that trypsin treatment affected detection of CAIX expression (Vordermark et al., 2005, Tu et al., 2012). In the present set-up, this effect could not be observed because mRNA and Western blot analysis confirmed the respective level of CAIX expression in the putative CAIX positive and negative populations. Moreover, in the breast cancer cell panel experiment all cell lines were tested for CAIX expression at the same time using the same concentration and incubation time as trypsin.

The breast cancer cell panel experiment showed marked differences in hypoxic CAIX induction between different breast cancer subgroups. CAIX expression has previously been associated with the triple negative (Kajo et al., 2013, Neumeister et al., 2012) but also with the HER2 positive breast cancer subtype (Kajo et al., 2013, Kaya et al., 2012). In our hands two established HER2 positive cells lines (BT474 and SKBR3) showed the lowest induction of CAIX under hypoxia. We therefore also tested the hypothesis that HER2 and CAIX expression may be correlated *in vitro*.
However, knockdown of HER2 in HER2 positive cell lines or overexpression of HER2 in basal cell lines did not alter CAIX expression patterns, indicating no direct relationship between the two proteins (data not shown).
High CAIX expression was associated with poor prognosis in the HER2 positive (ER positive) subgroup, which would be represented by the BT474 cell line. One explanation of why CAIX could not be detected in this cell line after exposure to hypoxia may be found in figure 3.1 A. It can be seen that median CAIX expression level was not increased in the group in question; however, considerable spread towards high CAIX levels were detected. This may suggest that more HER2 positive cell lines would need to be tested.

Another mechanism implicated as a co-regulator of HIF-1 transcriptional activity and hence CAIX expression may be the Hippo-YAP pathway. YAP (Yes-associated protein) is a transcriptional co-activator and has been shown to undergo nuclear translocation during hypoxia (Dai et al., 2016) and has been shown to interact with HIF-1α *in vivo* (Ma et al., 2015). Collaborative unpublished data indicated a role for YAP in our system; however, YAP knockdown did not affect CAIX expression in the CAIX positive cells under hypoxia.

CAIX has been shown to be one of the most sensitive markers of HIF-1 activity (Grabmaier et al., 2004, Kaluz et al., 2009). In this context, the HRE/HIF-1 binding site located at -3/-10 position within the CA9 promoter seems to have an essential role (Kaluz et al., 2002). Further evidence that CAIX is a marker of HIF-1 activity rather than mere expression is a report of apparently discordant cases of *in vivo* staining showing CAIX positivity in the absence of HIF-1α staining and vice versa (Kaluz et al., 2009). In line with this, the difference in CAIX expression determined in this study does not seem to be related to differences in HIF-1 expression, as both populations stabilise HIF-1 and HIF-2 to similar extents, and other HIF-1 target genes did not show a similar difference in expression to CAIX (Ledaki et al., 2015).

One potential mechanism of the differential expression of CAIX in the two populations is the ability of HIF-1 to bind to the CAIX promoter. Indications for differential binding were drawn from an increased resistance to nuclease digestion in the CAIX negative population, combined with a higher level of tri-methyl H3K9 histone, indicating a more condensed chromatin structure in this population (Ledaki et al., 2015). In the parental cell line this mechanism would be similar to the regulation of cell-cycle-dependent cyclin E, which is repressed by retinoblastoma (RB) via the recruitment of HDACs and H3K9 methylation activity until the cell cycle progresses (Zhang et al., 2000, Nielsen et al., 2001).

Moreover, the binding of HIF-1 to the CAIX promoter region was reduced in the CAIX negative population at a 72 h time-point, although the absolute difference was small (Ledaki et al., 2015). As HIF-1α levels are highest at 24 h of severe hypoxia, the chromatin immunoprecipitation (ChIP) experiment was repeated showing a 4-fold difference in HIF-1 binding to the CAIX promoter region between the two populations. Interestingly, the promoter region of VEGF, which was used as a control as its mRNA levels were not significantly different between the two populations, showed similar binding to HIF-1 between the populations.

Overall these results suggest that one mechanism underlying the differential CAIX expression in the two populations is based on a differential binding of HIF-1, with an increased binding of HIF-1 to the promoter region of CAIX in the positive population.

To further characterise the differences in chromatin structure in the two populations, other markers such as H3K27me3 (repressing function) or H3K4me3, H3K4Ac, H3K9Ac (activating function) (Shi, 2007) could be tested. In this context, it would also be interesting to study whether other differentially expressed genes undergo a similar regulation and how this may be influenced by epigenetics.

CAIX expression in hypoxia is heterogeneous *in vivo* as well. This was demonstrated previously in the laboratory by staining consecutive sections for CAIX, HIF-1, pimonidazole, or GLUD1, which is another HIF-target. This experiment showed some but not complete overlap between these markers, indicating differential gene expression under hypoxia. However, whether these differences are also influenced by differential binding of HIF-1 to promoter regions, would need to be investigated using uncultured primary cells, as tissue culture conditions can induce changes in gene expression patterns by influencing epigenetics (Smiraglia et al., 2001).

Crucially, epigenetic modifications would be potentially reversible, opening the possibility for epigenetic drugs. Previously, the CAIX positive population has been

shown to harbour an increased level of stem cell markers (Nanog, OCT4) and features (mammosphere forming capacity) (Ledaki et al., 2015). Interestingly, CSC properties can also be regulated by epigenetic mechanisms (Hochedlinger and Plath, 2009). Epigenetic modifications are influenced by the opposing activity of histone acetyltransferases (HAT) and histone deacetylases (HDAC) (Zhou et al., 2011). Treatment with SAHA, a HDAC inhibitor, had a greater effect on the CAIX positive than the CAIX negative population, which was CAIX dependent (Ledaki et al., 2015).

So far, HDAC inhibitors have been found to be effective in inhibiting tumour growth and inducing apoptosis (Pandolfi, 2001). Hence, some treatments have gained FDA approval for haematological malignancies, namely Vorinostat, Romidepsin, and Belinostat (Mottamal et al., 2015). Clinical trials testing HDAC inhibitors in solid tumour are being conducted. Phase I/II trials so far have reported partly encouraging (Yardley et al., 2013, Witta et al., 2012) but also partly negative results (Hainsworth et al., 2015, Han et al., 2015), indicating a potential need for better patient stratification (Witta et al., 2012, Hainsworth et al., 2015, Han et al., 2015) and a need for treatment combinations due to the potential heterogeneous response of tumour cells.

Chapter Four

Interaction of CAIX positive and negative cells in spheroid models

4.1. Introduction

4.1.1. Studying cell-cell interaction in 3D

In physiological conditions, cells are always surrounded by other cells of either the same or a different type. Historically a lot of cell culture based experiments have been performed in two dimensions (2D) due to technical limitations but also practicality. However, the development of three-dimensional (3D) models has provided an increased insight into cell-cell interaction and also organisation.

Urich et al (2013) reported using primary brain endothelial cells, pericytes and astrocytes to experimentally mimic the blood brain barrier *in vitro*. In 3D, multicellular spheroids consisting of the three cell types in a 1:1:1 ratio, a spontaneous reorganisation was observed. This resembled the physiological blood brain barrier, with the astrocytes located in the core of the spheroid, followed by a pericyte middle layer and an outer layer formed by endothelial cells (Urich et al., 2013).

Similarly, when olfactory ensheathing cells (OECs) were cultured in a 1:1 ratio with astrocytes or Schwann cells in a 3D model, OECs mainly localised at the outside of the spheroid at a 48 h time point (Vadivelu et al., 2015).

4.1.2. Imaging approaches

Apart from trying to mimic the tumour cell environment more closely, another approach to gain more insight into cell behaviour is imaging.

Imaging using fluorescence microscopy based techniques has improved significantly over recent decades and is now regularly used to investigate molecular interactions on single cell level with high temporal and spatial resolution.

Fluorescence is visible as a result of initial quick absorption of light (excitation) and the subsequent emission that occurs within nanoseconds. As shown in the Jablonski diagram (Figure 4.1 A) the excitation pulse triggers the absorption of a photon and a transition to an electronic excited state. The subsequent relaxation to the base state

emits light at a different wavelength. The difference between the excitation and emission wavelengths is known as Stokes shift.

In this chapter, it will be seen how fluorescence imaging was used in several ways. First, cells were stably transduced with either GFP or mCherry to allow observation of cell movements in a 3D model.

Additionally, fluorescence imaging was used to assess intracellular lactate levels in 3D and 2D (see chapter 5.2.5, page 144 ff.) using the laconic plasmid (see method section 2.9.1, page 60). The laconic plasmid contains two fluorophores linked by a lactate binding sequence. Lactate binding changes the relative distance between the fluorophores, which was measured using a FRET/FLIM based system in collaboration with the Wolfson Imaging Centre. The basic underlying principle was described by German physicist Theodor Förster (Förster, 1948). His observations were subsequently used in the development of a system to monitor distances between two fluorescent chromophores that form a donor/acceptor pair – known as Förster-resonance energy transfer (FRET). This can be used to image live cell protein localisation and interaction (Sekar and Periasamy, 2003).

In a FRET system, the donor fluorophore is excited by a specific wavelength. If a matching acceptor fluorophore is in close range ($r \approx 1\text{-}10$ nm), the initial excitation energy can be transferred from the donor to the acceptor fluorophore by non-radiative energy transfer. When the acceptor fluorophore relaxes to its ground state it emits light at a wavelength specific to its emission spectrum. The resulting emission spectrum is highly dependent on the distance between the two fluorophores and is defined as:

$$E = \frac{1}{1 + (r/R_0)^6}$$

E = FRET efficiency

r = distance between donor and acceptor

R0 = Foerster distance, distance at which the energy transfer efficiency is 50% (depends on physical parameters of donor-acceptor pair)

The presence of lactate within the cells increases the distance between the two fluorophores and hence decreases the FRET efficiency of the laconic plasmid (Figure 4.1 B). Using FLIM, the donor lifetime was measured/calculated, which is inversely related to FRET efficiency. Therefore, the longer the measured donor lifetime, the more lactate is present (Figure 4.1 C).

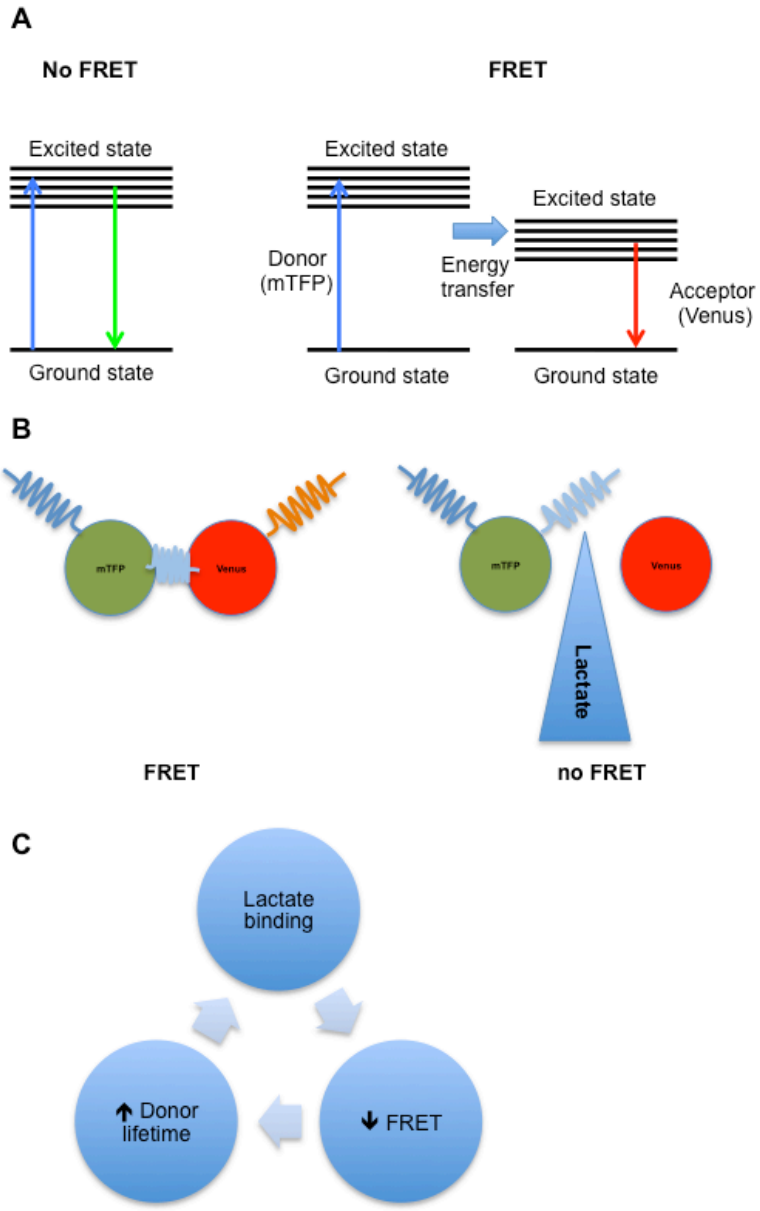


Figure 4.1 Principle of measuring intracellular lactate levels using a FRET based plasmid

(A) Jablonski diagram showing the principle of electron excitation and relaxation in non FRET and FRET setups. (B) Schematic representation of the laconic plasmid. A mTFP and a Venus fluorophore are linked by a lactate binding sequence. Presence of lactate determines the spacing between the fluorophores, which can be measured by the degree of FRET. (C) The relationship between FRET, donor lifetime and lactate levels when measuring signals from the laconic plasmid (see method section 2.9.1, page 60).

4.2. Results

4.2.1. MCF7 CAIX positive cells adopt a central localization in 3D culture

In order to assess the properties of CAIX positive and negative MCF7 cells in 3D culture, both populations were stably labelled with either GFP or mCherry as described in the methods section (section 2.8). Subsequently, cells were incubated in 0.1% O_2 for 72 h, stained for CAIX and sorted for high CAIX/high degree of labelling or low CAIX/high degree of labelling. Representative FACS blots are shown in Figure 4.2 A (mCherry labelled CAIX –ve cells) and B (GFP labelled CAIX +ve cells).

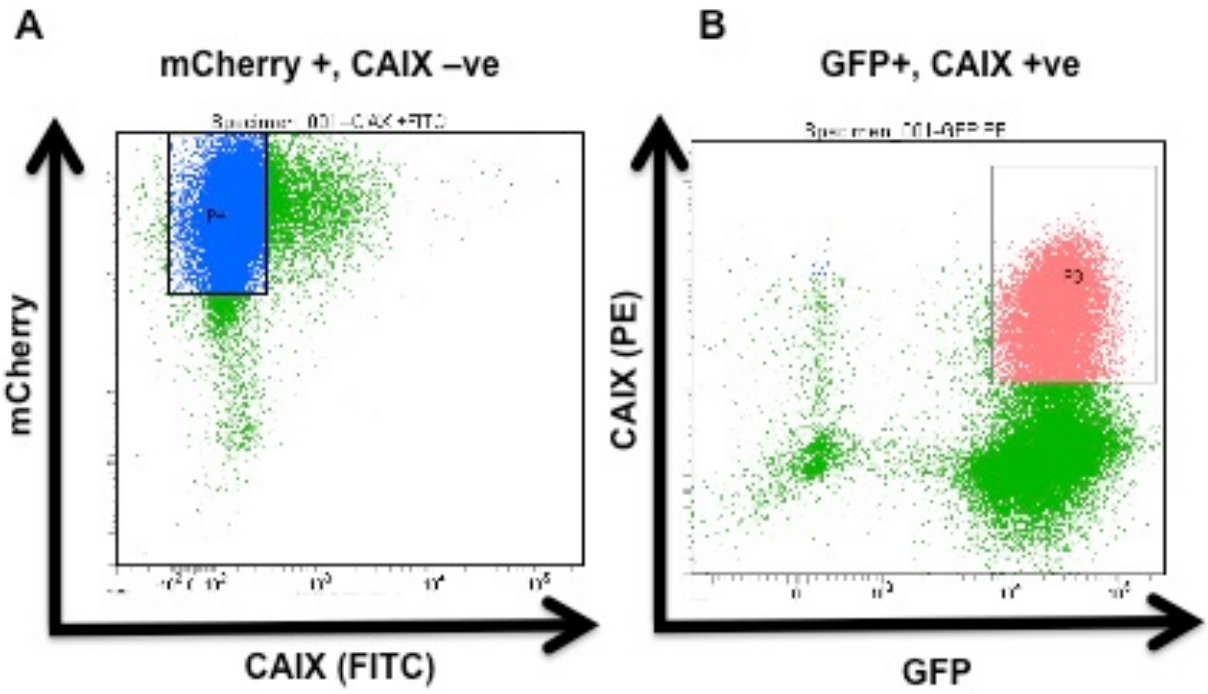


Figure 4.2 Representative FACS blots sorting CAIX positive and negative populations from labelled MCF7 cells

Stable GFP and mCherry labelled CAIX positive and negative populations were incubated in 0.1% hypoxia for 72 h before cells were stained with a CAIX antibody and FACS sorted.

(A) Representative FACS blot of mCherry CAIX negative cells. (B) Representative blot of GFP CAIX positive cells.

10,000 cells in total were then used to generate spheroid cultures. Spheroids containing only one population/colour were used as controls to determine possible bleeding when using fluorescence microscopy. As visible in Figure 4.3 excitation and imaging of GFP or mCherry, labelled cells did not lead to cross-detection of the other channel (Figure 4.3).

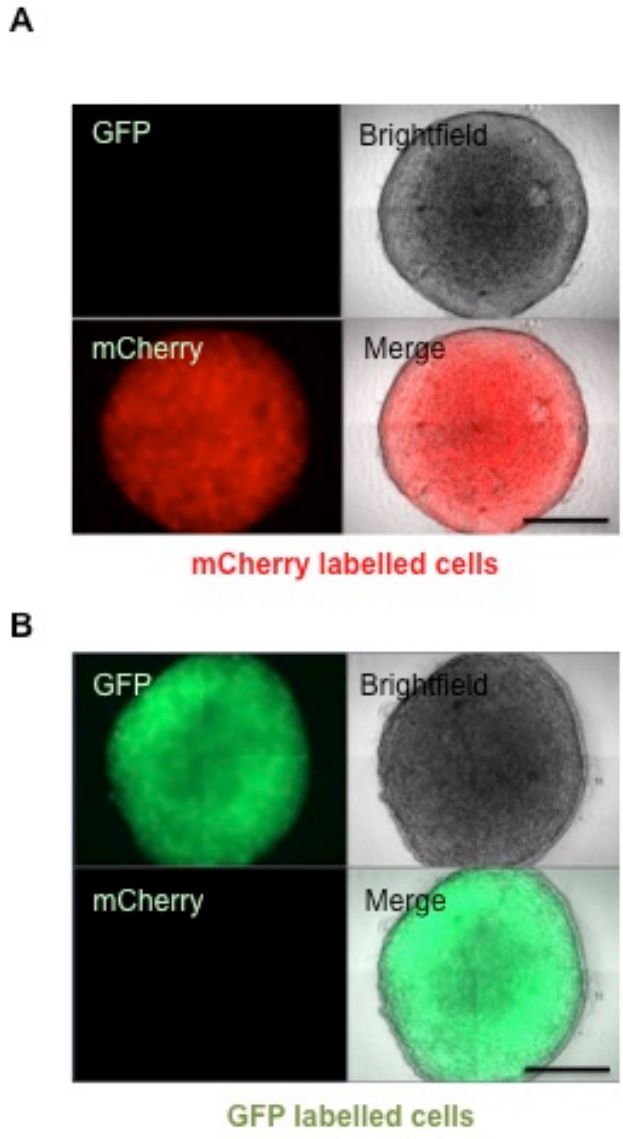


Figure 4.3 MCF7 control spheroids confirm specificity of fluorescence microscopy

10,000 stable GFP or mCherry labelled cells/well were seeded in low-adhesion round bottom 96-well plates with 2.5% matrigel. Images were taken after 72 h using a fluorescence microscope and representative results are shown. Scale bar: 250 μm

In mixed spheroids, the CAIX positive and negative populations labelled with either GFP or mCherry were co-cultured in a 1:1 ratio (a total of 10,000 cells). The spheroids and the movement of the populations in them (Figure 4.4) were evaluated using a fluorescence microscope at indicated time points. Spheroids tended to form within 24 h of seeding. Initially, a homogenous mixing of both populations was seen throughout the spheroids (Figure 4.4 i).

In spheroids with GFP and mCherry CAIX positive cells only, or with GFP and mCherry CAIX negative cells only, no specific localisation pattern emerged at 72 h (Figure 4.4 ii).

However, in spheroids consisting of both populations (1:1 ratio, 10,000 cells in total) the CAIX positive cells localised more towards the centre of the spheroid with the CAIX negative cells present on the rim after 72 h (Figure 4.4 iii). To ensure that this was not due to the labelling itself, dye swap experiments were carried out, which confirmed the initial observation (Figure 4.4).

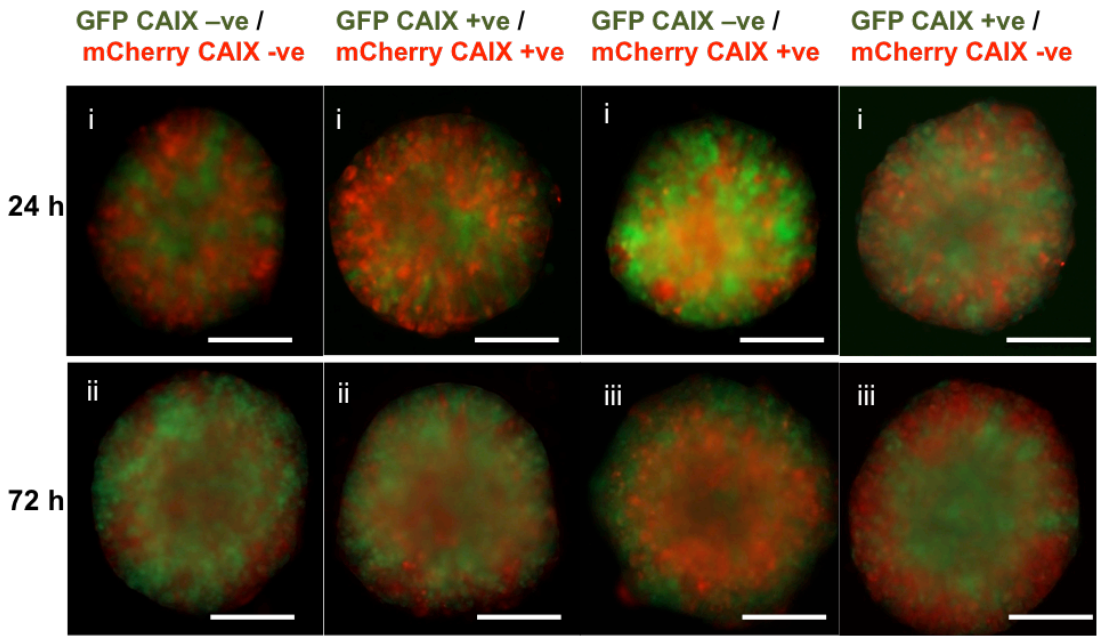


Figure 4.4 MCF7 CAIX positive cells localise towards the centre of a spheroid tumour model

Stable GFP or mCherry labelled CAIX positive and negative cells were used to generate spheroids. 10,000 cells in total (1:1 ratio of indicated populations) were seeded in a low-adhesion, round bottom 96-well plate with 2.5% matrigel. Spheroids were imaged 24 and 72 h as indicated using a fluorescence microscope. n=3, representative images shown Scale bar: 250 μm

4.2.2. CAIX positive cells can invade CAIX negative spheroids

Next it was investigated how CAIX positive and negative cells behave if added to an existing spheroid. GFP labelled CAIX negative spheroids and mCherry CAIX positive spheroids were generated and cultured for three days.

Subsequently, cells of the other population/labelling were added as cell suspension around the spheroids. Plates were incubated in normoxia and regularly imaged using a fluorescence microscope. Both the CAIX positive and negative cells that were added as cell suspension formed small cell clusters over time.

Some of the GFP CAIX negative cells clusters attached to the existing mCherry CAIX positive spheroids, but no infiltration could be observed (Figure 4.5 A).

In the reverse experiment, when mCherry CAIX positive cells were seeded on top of GFP CAIX negative spheroids, it was observed that some CAIX positive cells invaded the pre-existing spheroid (Figure 4.5 B).

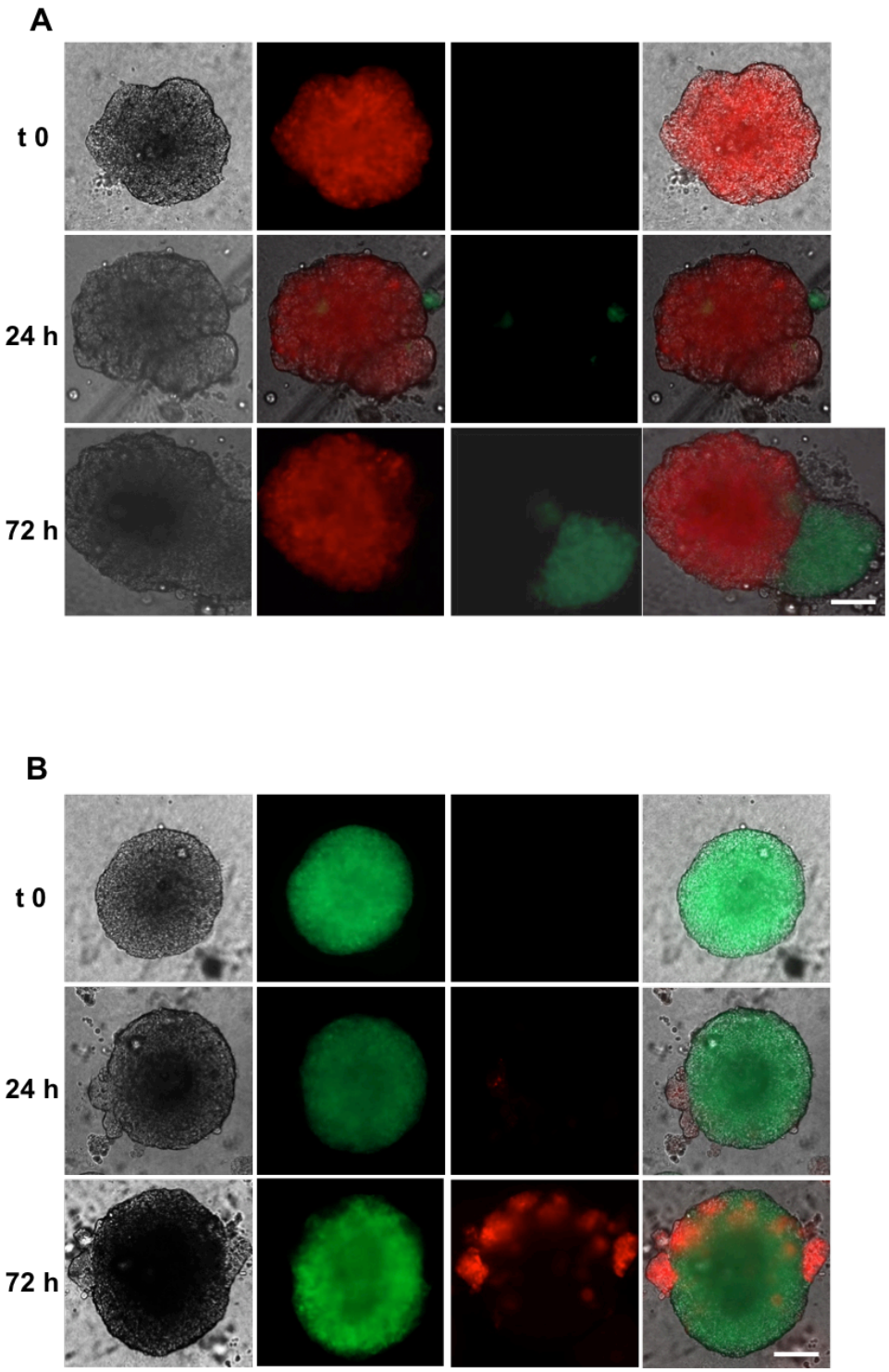


Figure 4.5 MCF7 CAIX positive cells invade CAIX negative spheroids

10,000 mCherry CAIX positive cells (A) or GFP CAIX negative cells (B) were seeded in low-adhesion, round bottom 96-well plates with 2.5% matrigel. Spheroids were left to grow for 72 h and were imaged (t0). Afterwards, 5,000 GFP CAIX negative cells (A) or mCherry CAIX positive cells (B) were added as cell suspension to each well

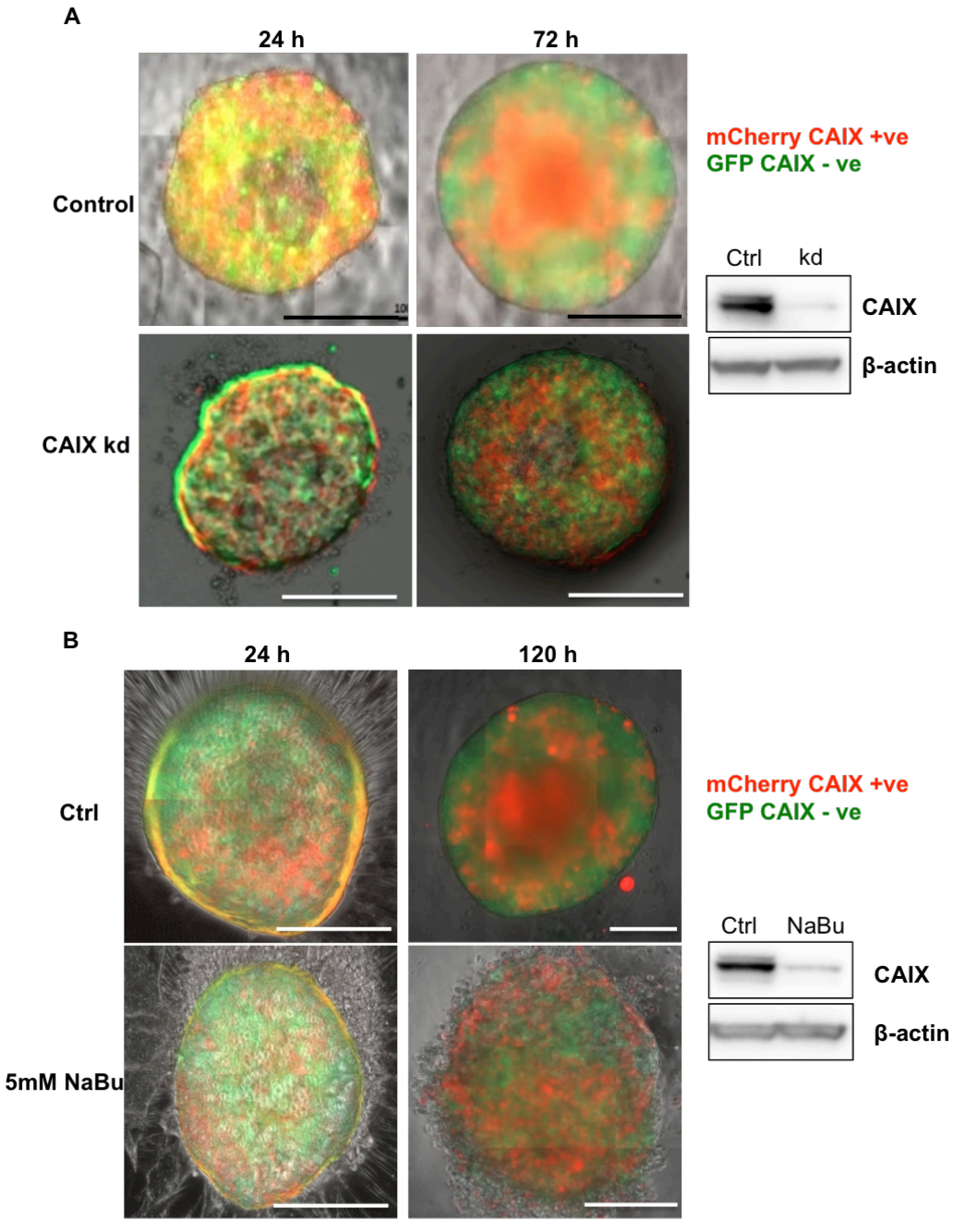
and spheroids were imaged at the indicated time points. n=3, representative images shown Scale bar: 250 μm

4.2.3. Central localisation of CAIX positive cells is dependent on CAIX

Figures 4.4 and 4.5 show a clear reorganisation of CAIX positive and negative populations in the 3D model, which seem to be dependent on the presence of both populations. To investigate the underlying mechanism, spheroids were generated in which CAIX expression in the CAIX positive cells was decreased either using siRNA or an inhibitor.

Knockdown of CAIX was confirmed using Western blot (Figure 4.6 A). Spheroids were also treated with 5 mM sodium butyrate (NaBu), a HDAC inhibitor that has been shown to inhibit CAIX expression. The effect of NaBu in decreasing CAIX is shown in a Western blot (Figure 4.6 B).

In comparison to control, at 72 h no specific spatial rearrangement was observed if CAIX expression had been decreased (Figure 4.6 A and B).



NaBu: Sodium butyrate (HDACi)

Figure 4.6 Central localisation of the MCF7 CAIX positive population is dependent on CAIX

(A) CAIX positive and negative cells were transfected with either scramble control or siCAIX before spheroids were generated using 10,000 cells (1:1 ratio between populations). CAIX positive cells were incubated in 0.1% hypoxia for 72 h and

subjected to Western blot analysis to assess knockdown efficiency. (B) Spheroids were formed using 10,000 cells (1:1 ratio between populations). After 24 h, spheroids were treated with 5mM NaBu or control and the effect of the treatment on CAIX is shown in the Western blot (CAIX positive cells, after 72 h of 0.1% hypoxia). n=3, representative images shown Scale bar: 250 μm

4.2.4. Imaging lactate in 3D models

In 2009, Swietach et al published a report on the role of CAIX expression in pH regulation in HCT116 spheroids. Spheroids with no CAIX expression developed very low intracellular pH (around 6.3) and an extracellular pH of around 6.9 at the core with a decreasing gradient towards the edges.

When CAIX was expressed, intracellular pH was less acidic, whereas extracellular pH was decreased (Swietach et al., 2009). The study further suggested that CAIX is involved in CO_2 excretion by converting vented CO_2 to extracellular H+ as well as lactic acid emission to regulate intra- and extracellular pH (Swietach et al., 2009). In this work, I also tried to assess pH and lactate levels in spheroids using pH low insertion peptides (pHLIPs). The work on pH is ongoing and preliminary data is shown in the future work section (page 189). Additionally, I tried to assess intracellular lactate levels in spheroids.

Lactate is a metabolite directly affected by hypoxia. HIF1-α stabilisation leads to upregulation of PDK1, which inhibits PDH, thereby reducing the conversion of pyruvate to acetyl-CoA. Concomitantly, LDH-A is induced, enhancing lactate production from pyruvate.

In order to measure intracellular lactate levels, cells were transfected with the laconic plasmid (San Martin et al., 2013). The plasmid is built up of an mTFP and a Venus fluorophore linked by a lactate binding sequence. The presence of lactate within the

cells increases the distance between the two fluorophores and hence decreases the FRET efficiency of the laconic plasmid (Figure 4.1 B, page 106). Using FLIM, the donor lifetime was measured/calculated, which is inversely related to FRET efficiency. Therefore, the longer the measured donor lifetime, the more lactate is present (Figure 4.1 C).

In order to determine the range of possible measurements, a donor only as well as a tandem plasmid were also transfected into cells and the lifetime was measured. This determined a working range between 1.7ns for full FRET (tandem plasmid) and 2.7ns for no FRET (donor only plasmid) (Figure 4.7 A).

In order to assess the response of the plasmid to lactate, cells were first incubated with the glycolysis inhibitor iodoacetic acid for one hour before the media was changed to a glucose-free, potassium-rich buffer supplemented with the proton ionophore nigericine, and rotenone to inhibit mitochondrial metabolism (see 2.12.2 FRET/FLIM, page 62). Cells were allowed to equilibrate in this buffer.

Next, cells were spiked with 0, 0.01, 0.1, 1, and 10mM lactate. Although the overall range of the laconic FRET sensor is quite narrow, increasing lactate concentrations yielded longer lifetimes (Pearson correlation R^2 = 0.7) (Figure 4.7 B). There was heterogeneity visible between the cells, leading to overlapping standard deviations (Figure 4.7 B).

In order to assess lactate levels in a 3D model, cells were transfected with the laconic plasmid prior to spheroid generation.

In a 2D model it was assessed whether the mCherry label would be compatible with the controls as well as the laconic plasmid; however, the cells did not express both labels at the same time.

Therefore, spheroids were generated as described in the materials and methods section using CAIX positive and negative unlabelled cells. Imaging depth turned out to be difficult to adjust and, overall, fewer photons were received from the centre of

the spheroids. Generally, it seemed that more intracellular lactate was present on the outer rim of the spheroid, which would indicate higher lactate level in CAIX negative cells which were located more towards the rim (Figure 4.7 C). However, to obtain a clearer image, a better microscopy set-up would be needed in combination with the generation of cell lines stably expressing the laconic plasmid (see future work).

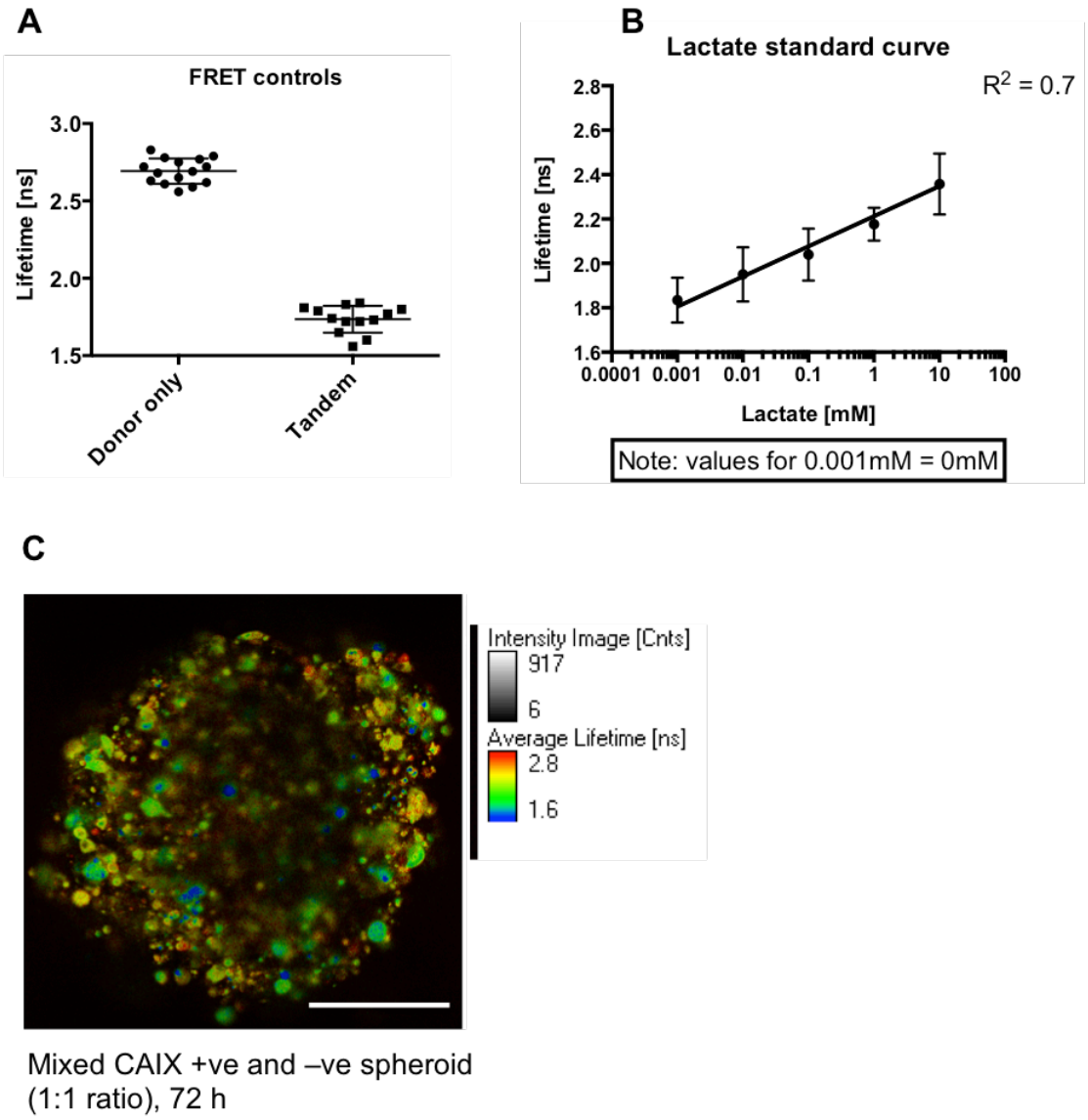


Figure 4.7 Testing of the laconic plasmid in MCF7 cells

(A) Donor only (mTFP / no FRET) or a tandem fluorophore (mTFP-Venus / full FRET) plasmids were transfected into MCF7 cells and FLIM signals were measured using a LEICA FRET microscope. (B) MCF CAIX positive cells were transfected with the laconic plasmid overnight. Cells were incubated with the glycolysis inhibitor iodoacetic acid for one hour, before the media was changed to a glucose-free, potassium-rich buffer supplemented with the proton ionophore nigericine, and rotenone to inhibit mitochondrial metabolism. Cells were spiked with the indicated levels of lactate and the response of the plasmid was measured. (C) CAIX positive and negative cells were transfected with the laconic plasmid overnight, before 10,000

cells in total (1:1 ratio) were used to form spheroids. Spheroids were imaged and a colour image reflecting FLIM states is shown. Low to high levels of lactate are indicated as a colour range from blue to red respectively.

n=3, representative images shown. Scale bar: 250 μm

4.2.5. The role for CAIX and MMP-14 during invasion/migration

Vallejo Epsi (2015) explored the role of CAIX in migration and invasion. It was shown that CAIX interacts with MMP-14 to promote invasion (Espi, 2015). Therefore the role of MMP-14 was also explored in this project.

First of all, levels of MMP-14 protein levels between the CAIX positive and negative population were compared in normoxic conditions or after incubation in 0.1% O_2 for 72 h. It appeared that levels of MMP-14 were higher in the CAIX positive cells (Figure 4.8 A). To further determine the localisation of MMP-14 in both populations, the membrane expression of the protein was assessed using flow cytometry. As the antibody recognises the extracellular domain, cells were not permealised, enabling the assessment of membranous MMP-14 only. A comparison of the flow cytometry blots show that MMP-14 surface expression was more prevalent in the CAIX positive fraction of unsorted, parental MCF7 cells (Figure 4.8 B).

Consecutive IHC sections of the spheroids shown in Figure 4.4 were stained for CAIX and MMP-14 expression. In spheroids made from the CAIX negative population only, no CAIX and only very light MMP-14 staining could be observed. In contrast, in spheroids made from the CAIX positive population only, CAIX staining was observed in the centre, whereas MMP-14 staining was seen in the whole section (Figure 4.8 C). Lastly, in mixed (1:1 ratio) spheroids at 72 h, CAIX expression was seen in the centre of the spheroid matching the fluorescence images. MMP-14 staining was also present in the centre with some degree of overlap with the CAIX staining as indicated by arrows (Figure 4.8 D).

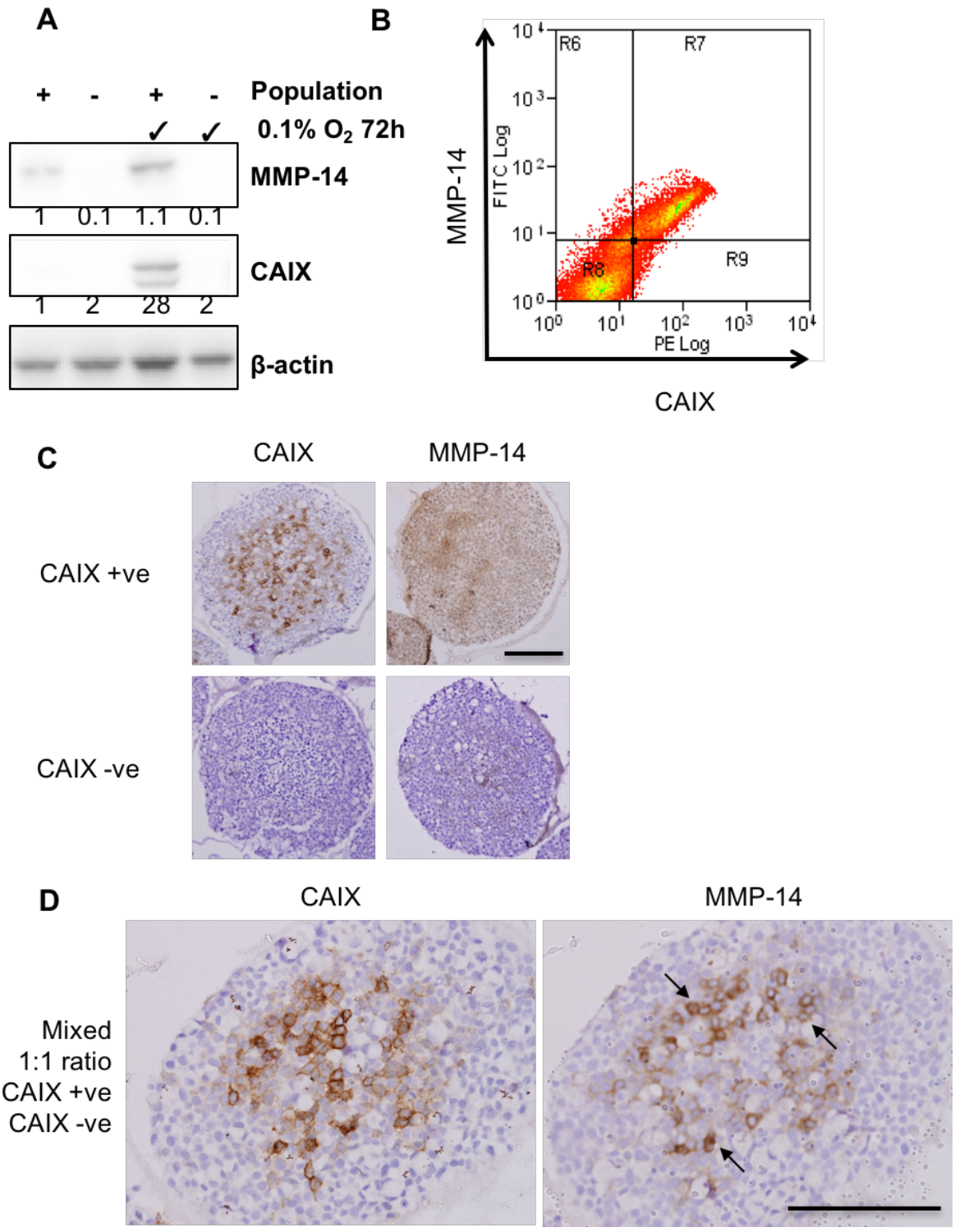


Figure 4.8 MMPs may interact with CAIX to facilitate localisation in MCF7 cells

(A) MCF7 CAIX positive and negative cells were incubated in normoxia or 0.1% hypoxia for 72 h before protein levels were assessed by Western blot. (B) Parental MCF7 cells were incubated in 0.1% hypoxia for 72 h before cells were stained for cell-surface CAIX and MMP-14 expression and assessed using flow cytometry. (C)

and (D) 10,000 cells in total of either population or a 1:1 ratio ('mixed') as indicated were used to form spheroids. After 72 h of growth, spheroids were fixed and immunohistochemistry slides were prepared. Consecutive sections were stained for CAIX and MMP-14 as indicated. n=3, representative images shown Scale bar: 250 μm

4.3. Discussion

3D cell models of tumour formation and growth is an interesting intermediary step in understanding the pathology *in vivo*, as it allows for cells to act and interact in their spatial environment. Moreover, in 3D models a gradient of oxygen and nutrient availability is generated.

Previous reports have shown that a mix of different cell types seeded in 3D *in vitro* can recapitulate the *in vivo* spatial arrangement (Urich et al., 2013, Vadivelu et al., 2015). In this report, it is shown that cell populations stemming from the same parental MCF7 cell line are also reorganising spatially in a 3D model over time.

The simplest explanation for this observation could be a technical one. Expression of CAIX during hypoxia has previously been shown to be important in the homeostasis of intracellular pH (Swietach et al., 2009). As hypoxia develops in the core of the spheroid, the CAIX negative cells may undergo apoptosis/necrosis, while CAIX positive cells have a survival benefit (Chiche et al., 2009b). However, CAIX negative cells can be cultured in 2D in hypoxic conditions and while there is decreased cell viability in comparison to CAIX positive cells at 72 h of about 15%, this would not fully account for the effect seen. Moreover, if the observation was based on CAIX -ve cells dying in the centre, one would expect an overall dimmer centre in spheroids made of these cells only. Moreover, dye swap experiments show that the labelling itself is not responsible for the effect.

Instead, relocation is only seen when both populations are present.

In trying to explain the underlying mechanism it was shown that knockdown or inhibition of CAIX abolished the spatial relocation. This is in concordance with previous reports linking CAIX to cell migration and invasion (Lou et al., 2011a).

Hypoxia leads to the induction of CAIX, which enhances extracellular tumour acidification (Gallagher et al., 2015). In line with this the decrease of extracellular pH

towards the centre in 3D models expressing CAIX has been well established (Swietach et al., 2009).

Low pH promotes tissue remodelling at the tumour-stroma interface (Gatenby and Gawlinski, 1996), and furthers invasion (Rofstad et al., 2006).

Cell migration and invasion have previously been linked with the expression of matrix metalloproteinases (MMP) and a dependency on pH (Gioia et al., 2010, Magalhaes et al., 2011, Estrella et al., 2013).

MMP-14 has been previously associated with CAIX expression and in this model it could be shown that CAIX co-localised with this metalloproteinase in mixed spheroids. Therefore, the data confirms data from Robertson et al. that CAIX positive cells have a higher potential for invasion and migration (Robertson et al., 2004) due to CAIX itself, the acidic environment it helps to create, as well as the upregulation of MMPs that need this environment to work.

Future work would include the inhibition of MMP-14 to observe its effect on 3D cell re-localisation and growth. Moreover, it has previously been reported that increased levels of MMP-14 are associated with decreased metastasis free survival (Lodillinsky et al., 2016). Therefore, it would be interesting to stain a cohort of CAIX positive TMAs for MMP-14 to assess the overlap with the CAIX staining and its effect on patient outcome.

The next step in characterising the behaviour of the CAIX positive and the CAIX negative populations *in vivo* would be a zebrafish model, taking advantage of the inherent fluorescent labelling of the cells in combination with the easy imaging of the zebrafish. For this experiment cells would be pre-incubated in normoxia or hypoxia for 72 h, sorted and injected. Over time the localisation patterns of both populations would be observed, giving insight into migration and cell co-localisation.

CAIX knockdown or treatment with an HDAC inhibitor slowed growth of mixed spheroids in line with previous papers (McIntyre et al., 2012), indicating that CAIX inhibition is a good treatment target *in vitro*. Nevertheless, clinical studies using CAIX inhibitors have not yet shown similarly good results. Another potential problem for treatment options is the extracellular acidification due to CAIX. This can lead to decreased uptake and efficiency of weak base drugs such as doxorubicin (Kleeberger and Rottinger, 1993, Raghunand and Gillies, 2001).

On the other hand, the fact that tumours have a lower extracellular pH is now being exploited for the design of molecular probes for imaging. Moreover, these probes could also be coupled with cytotoxic compounds, to ensure tumour specific delivery. The probe accumulates in tumour sites with high specificity as shown in mouse models. It also accumulates in sites of inflammation and in kidneys; however, the latter was counteracted by providing mice with bicarbonate containing drinking water (Andreev et al., 2007). The acidic environment of tumours is also an area of investigation for cancer drug delivery via prodrug nanoparticles. It was shown that a doxorubicin and curcumin drug combination could be linked to a prodrug and the resulting nanoparticles showed increased anti-tumour activity in comparison to free doxorubicin (Zhang et al., 2016).

The presence of different tumour cell types means that a multidrug approach will be needed to target the different populations. The emerging evidence that cells undergo reorganisation in a 3D environment implies that this improves survival for all or at least some populations.

A potential effect of cell reorganisation within a 3D network is the change in cell-cell interaction between cells of the same population and cells of another one. Subsequently, this potentially changes the induction/general availability of growth factors, metabolites, and other small molecules. The next chapter focuses more closely on the interaction between CAIX positive and CAIX negative cells.

Chapter Five

Co-operation of CAIX positive and negative populations

5.1. Introduction

The human body consists of many different cell types and its functionality depends on the interaction between them as and where necessary. This is true for many physiological processes, but this chapter will focus on metabolic symbiosis and regulation.

Metabolic interaction and regulation has been reported in various tissues and research models. Speder et al (2014) showed that in the *Drosophila* melanogaster central nervous system nutritional signals trigger insulin production by glial cells. Insulin subsequently leads to reactivation, growth and proliferation of previously quiescent neural stem cells (Speder and Brand, 2014).

Metabolic collaboration is also present in mammalian brains. The brain has a very high energy demand; some studies suggest that up to 20% of the available glucose and oxygen in the body are utilised by this organ alone (Magistretti et al., 1999). Moreover, the availability of energy is crucial to consistent neuronal function. Therefore, brain metabolism is tightly regulated. A main cellular glucose storage mechanism in mammals is glycogen and, in the brain, astrocytes are the main cells using a glycogen store (Phelps, 1972). In times of increased neuronal activity or glucose shortage, glycogen from astrocytes can be used to bridge energy supply (Brown et al., 2005). Glycogenolysis is furthermore important to meet the energy demand of another metabolic symbiosis mechanism between neurons and astrocytes: the glutamate-glutamine cycle or glutaminolysis.

In the brain, glutamate is an important neurotransmitter, needed for neuronal activity. However, early studies already showed compartmentalisation of glutamate in the brain. This and subsequent studies suggested that neurons lack enzymes for *de novo* synthesis of glutamate and instead convert this metabolite from astrocyte derived glutamine or α-ketoglutarate [reviewed in (Shank and Aprison, 1981)] (Yu et al., 1983, Shank et al., 1985).

Apart from its role in neuronal activity, neurons can also use glutamine as an energy substrate during glucose starvation or for the generation of TCA cycle intermediates (Peng et al., 2007, Shokati et al., 2005).

Further to glycogen and glutamate/glutamine, lactate has also been identified within this network of interdependent metabolites that are shuttled between astrocytes and neurons (Pellerin et al., 1998). In this system astrocyte derived lactate (from glycolysis) can be utilised for neuronal oxidative metabolism (Kasischke et al., 2004, Machler et al., 2016).

Interdependence of metabolites has also been shown in a study using the anti-anginal drug perhexiline. The drug was known to cause a switch from fatty acid to glucose metabolism. More recently it was shown to induce several metabolic changes including a decrease in creatine and taurine levels and an increased uptake of amino acids and lactate (Yin et al., 2013).

The proteins needed for this reversible conversion of lactate to pyruvate are LDHA and B. Lactate is then actively transported across the cell membrane by monocarboxylate transporters (MCT) 1 and 4 (Fujiwara et al., 2015, Hashimoto et al., 2008, Pellerin et al., 1998).

Metabolic interaction/symbiosis has also been a focus in cancer research for some years. The main focus has been on the interaction between tumours and the adjacent stroma, especially cancer associated fibroblasts (CAFs). In this context it has been shown that oncogenes in tumour cells can drive the CAF transformation of adjacent fibroblasts via paracrine oxidative stress. Specifically the activation of the oncogenes RAS, NFκB, and the tumour suppressor BRCA1 in tumour cells have been shown to lead to a loss of caveolin-1 (cav-1), increased glycolytic metabolism and an increase of lactate export transporter MCT4 in adjacent fibroblasts (Martinez-Outschoorn et al., 2013, Martinez-Outschoorn et al., 2012a, Fiaschi et al., 2012). On the stroma site, upregulation of migration stimulation factor (MSF) is enough to induce myofibroblastic

differentiation via TGF-β and NFκB signalling, induction of autophagy and glycolysis. In this model MSF fibroblasts enhanced adjacent tumour growth by up to 4-fold in comparison to control (Carito et al., 2012).

Increased autophagy in stroma cells, which subsequently leads to the support of tumour cells with ketones and lactate, has also been implicated in various other reports (Capparelli et al., 2012a, Castello-Cros et al., 2011, Martinez-Outschoorn et al., 2010, Capparelli et al., 2012b, Pavlides et al., 2012).

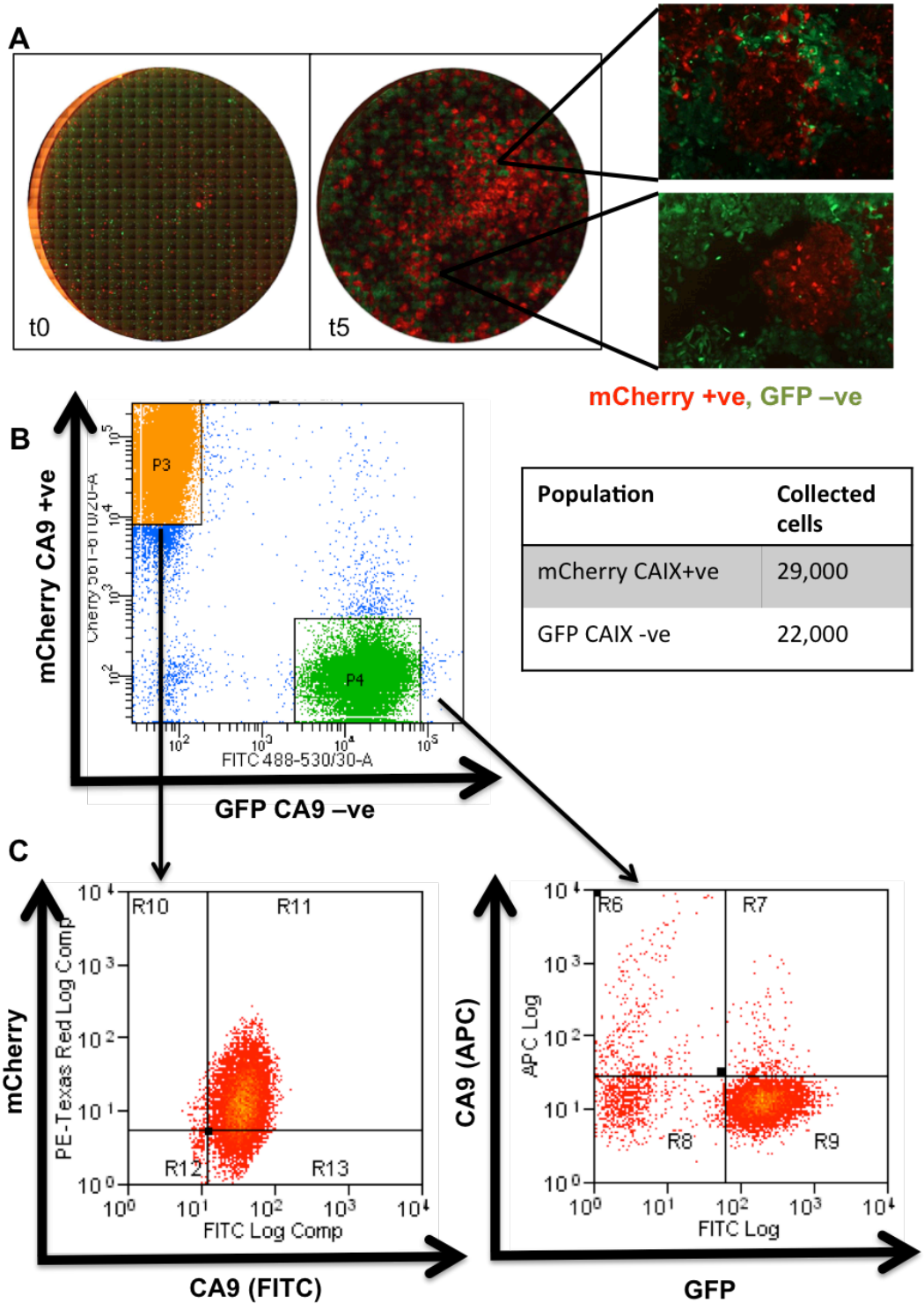
Similarly, adipocytes can promote tumour growth in breast, prostate, and ovarian tumour models (Manabe et al., 2003, Dirat et al., 2011, Tokuda et al., 2003, Nieman et al., 2011). Co-culture of adipocytes with ovarian cancer cells induced lipolysis in adipocyte, transfer of lipids to and concomitant upregulation of β-oxidation in the cancer cells, suggesting that adipocytes can act as energy provider. This was underlined by an upregulation of fatty acid binding protein 4 (FABP4) in the cancer cells at the tumour-adipocyte interface (Nieman et al., 2011).

While all these studies report the metabolic interaction between different cell types, this thesis is focussed on the collaboration of cancer cells stemming from the same parental tumour cell line. Using different co-culture models, our results suggest that different tumour cell populations also act in metabolic symbiosis to enhance tumour cell survival and proliferation.

5.2. Results

5.2.1. Co-culture of CAIX positive and negative populations in 2D

After observing the spatial re-localisation in 3D models, labelled CAIX positive and negative cells were also seeded in 2D in a clonogenic assay. In an image taken at t0, a fairly uniform distribution of cells of both populations can be seen (Figure 5.1 A, left panel). Cells were then incubated under hypoxic conditions (0.1% O_2) for 5 days. It was observed that some CAIX positive colonies (mCherry) were surrounded by CAIX negative cells (GFP) (Figure 5.1 A, middle and right panels). To further analyse this experiment, the two populations were sorted (Figure 5.1 B left panel). Overall, more mCherry (putative CAIX positive) cells were collected from the well, indicating that this population grew slightly better in hypoxic conditions (Figure 5.1 B right panel). To confirm that the cells still were CAIX positive or negative respectively, the sorted cells were stained for CAIX expression. Even after 5 days of hypoxia, the putative CAIX positive population was indeed CAIX positive (double positive for mCherry and FITC CAIX), whereas the putative CAIX negative population was negative for the protein (GFP positive but negative for APC CAIX staining) (Figure 5.1 C).



Population	Collected cells
mCherry CAIX+ve	29,000
GFP CAIX -ve	22,000

Figure 5.1 Co-culture of labelled MCF7 CAIX positive and negative populations in 2D

(A) 3,000 cells each of mCherry CAIX positive and GFP CAIX negative cells were seeded in a 6-well plate and left to settle overnight. The whole well was imaged (left panel) before the plate was incubated in 0.1% hypoxia for five days and was imaged

again (middle and right panels). (B) Cells were then FACS sorted to separate mCherry and GFP labelled cells. (C) Separated cells were stained for CAIX expression and analysed using flow cytometry. n=3, representative blots shown

5.2.2. CAIX negative cells support growth of CAIX positive cells

Analysis of the RNA microarray data from the MCF7 cells indicated differences in metabolic processes between the CAIX positive and negative populations (Ledaki et al., 2015).

The pathway analysis suggested a higher level of genes associated with citrate cycle, OxPhos and fatty acid metabolism in the CAIX positive cells (table 5.1), whereas CAIX negative cells had a higher level of genes related to pentose and glucuronate Interconversions amongst others (table 5.2).

Table 5.1 Ingenuity Canonical Pathway Analysis of CAIX positive MCF7 cells (Experiment and Data from Dr Ioanna Ledaki)

Ingenuity Canonical Pathways	-log(p-value)
Lysine Degradation	5.2E00
Butanoate Metabolism	4.89E00
Fatty Acid Metabolism	4.81E00
Mitochondrial Dysfunction	4.52E00
Valine, Leucine and Isoleucine Degradation	4.48E00
Propanoate Metabolism	4.18E00
Oxidative Phosphorylation	3.47E00
Glycolysis/Gluconeogenesis	3.35E00
Pyruvate Metabolism	3.16E00
Glyoxylate and Dicarboxylate Metabolism	3.11E00

Tryptophan Metabolism	3.11E00
Purine Metabolism	2.89E00
Phenylalanine, Tyrosine and Tryptophan Biosynthesis	2.86E00
Glycine, Serine and Threonine Metabolism	2.68E00
One Carbon Pool by Folate	2.61E00
Fatty Acid Elongation in Mitochondria	2.45E00
Citrate Cycle	2.2E00
ATM Signalling	2.18E00
Valine, Leucine and Isoleucine Biosynthesis	2.15E00
Pyrimidine Metabolism	2.11E00
Role of CHK Proteins in Cell Cycle Checkpoint Control	2.04E00
EIF2 Signalling	1.97E00
Ubiquinone Biosynthesis	1.89E00
Alanine and Aspartate Metabolism	1.85E00
Biosynthesis of Steroids	1.84E00
Protein Ubiquitination Pathway	1.82E00
Urea Cycle and Metabolism of Amino Groups	1.79E00
Fructose and Mannose Metabolism	1.21E00
mTOR Signalling	6.16E-01
Wnt/β-catenin Signalling	5.93E-01

Table 5.2 Ingenuity Canonical Pathway Analysis of CAIX negative MCF7 cells (Experiment and Data from Dr Ioanna Ledaki)

Ingenuity Canonical Pathways	-log(p-value)
Actin Cytoskeleton Signalling	2.62E00
Pentose and Glucuronate Interconversions	2.06E00
Nucleotide Sugars Metabolism	2.04E00
TNFR2 Signalling	1.82E00
TR/RXR Activation	1.76E00
Cardiomyocyte Differentiation via BMP Receptors	1.69E00
IL-1 Signalling	1.58E00
C21-Steroid Hormone Metabolism	1.56E00
RAR Activation	1.5E00
MIF Regulation of Innate Immunity	1.5E00
Hypoxia Signalling in the Cardiovascular System	1.49E00
IGF-1 Signalling	1.48E00
ILK Signalling	1.48E00
Renal Cell Carcinoma Signalling	1.47E00
April Mediated Signalling	1.47E00
Molecular Mechanisms of Cancer	1.44E00
B Cell Activating Factor Signalling	1.41E00
PDGF Signalling	1.39E00
Signalling by Rho Family GTPases	1.38E00
BMP signalling pathway	1.37E00
Glycosphingolipid Biosynthesis - Neolactoseries	1.31E00
Glucocorticoid Receptor Signalling	1.31E00
TNFR1 Signalling	1.28E00
EGF Signalling	1.28E00

On the basis of this observation, it was hypothesised that the two populations may metabolically support each other. Therefore, the objective of this chapter is to investigate the growth effects of the CAIX positive and negative populations when cultured together.

In order to test the basic hypothesis, cells of both populations were co-cultured in a trans-well system (Figure 5.2 A). For the insert, a pore diameter of 0.4 µm was chosen to decrease the possibility of cell migration through the insert.

The set-up is depicted in Figure 5.2 A. Equal numbers of cells were seeded in the well of a plate as well as in the trans-well insert and plates incubated in normoxia or 0.1% hypoxia for five days. At the end of the experiment, the cells in the well were counted. In this setup the cells of the two populations do not come into physical contact, but both populations share the same media.

In normoxic conditions, no statistically significant differences between co-culture of a population with the same population or the other population was seen (Figure 5.2 B).

When CAIX positive cells were co-cultured with the CAIX negative population in hypoxia, a significant increase in cell number was observed (Figure 5.2 C, fifth and sixth bar).

Conditions with trans-wells containing no cells (media only) were included as an overall control. Interestingly, these controls yielded cell counts that were not significantly different from those in which the same population was seeded in both layers, indicating that co-culture with the same population did not have a negative effect on cell numbers in the lower well (Figure 5.2 C).

The effect of co-culturing the two populations was also assessed in 3D models. The comparison of growth curves shows that CAIX positive spheroids grew better than CAIX negative ones; however, mixed spheroids were biggest, indicating a additive effect on growth between the two populations (Figure 5.2 D).

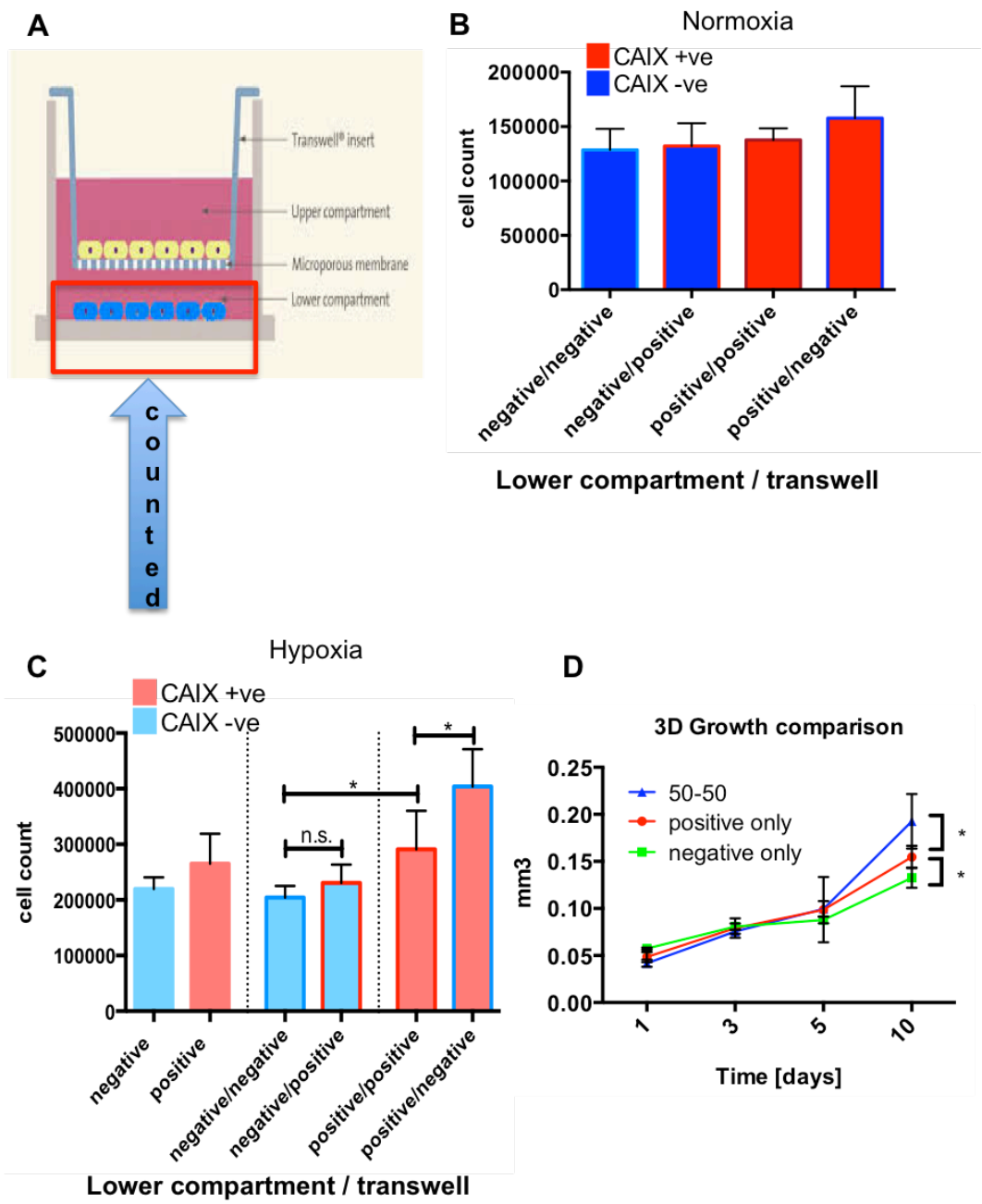


Figure 5.2 MCF7 CAIX negative cells support growth of the CAIX positive population

(A) Schematic representation of the co-culture setup. Cells of one population were seeded in the bottom of the well, whereas cells of the other population were seeded in the trans-well insert. At the end of the experiment, the lower compartment was counted. (B) and (C) Cells of both populations were seeded in the trans-well setup as indicated. Plates were incubated in normoxia (B) or hypoxia (C) for five days and cells in the lower compartment were counted. (D) Spheroids were formed using

10,000 cells of either CAIX positive or negative cells or of a 1:1 ratio of both and spheroid growth was monitored over time. n=3, Graphs show mean ± SD, *<p0.05

5.2.3. Co-culture using conditioned media

From the initial set up of the co-culture as a trans-well system, it seemed a reasonable hypothesis that the enhancing effect on cell number was conferred via the media. To further explore this hypothesis, the factors likely to affect the set up for experiments with conditioned media were optimised; those were initial cell number and duration of the pre-culture as well as media composition (FCS concentration) (Figure 5.3).

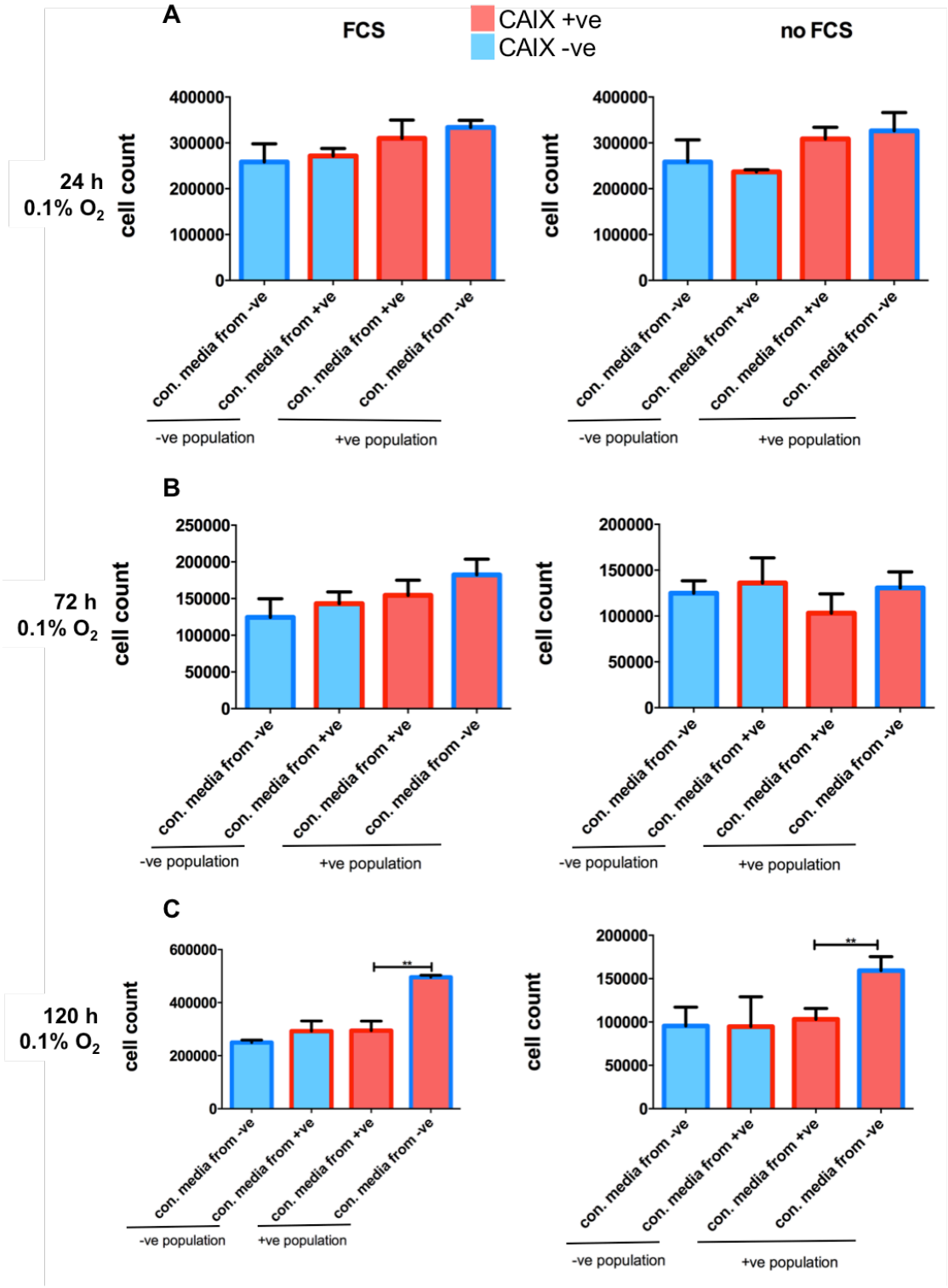


Figure 5.3 Optimisation of MCF7 CAIX positive and negative cell co-culture using conditioned media over a period of 5 days

500,000 cells of each population were seeded in a 10cm dish in either 10% FCS (left panels) or no FCS (right panels), left to settle overnight and incubated in 0.1% hypoxia for (A) 24 h, (B) 72 h, or (C) 120 h. Conditioned media was then added to

CAIX positive and negative cells in the combinations indicated and plates were incubated in 0.1% hypoxia for a further five days before final cell counting.

n=3, Graphs show mean ± SD, **p<0.01

After optimisation, the duration of the pre-culture was set to 96 h, after which conditioned media was transferred to new plates that were incubated for further 120 h before final cell counting.

The results showed that, similar to the cell co-culture, media from CAIX negative cells significantly enhanced the cell number of CAIX positive cells in comparison to conditioned media from the CAIX positive cells.

For subsequent experiments the experiment was up-scaled using 10 cm dishes instead of 12-well plates. As the results are similar, a plate effect could also be excluded (Figure 5.4).

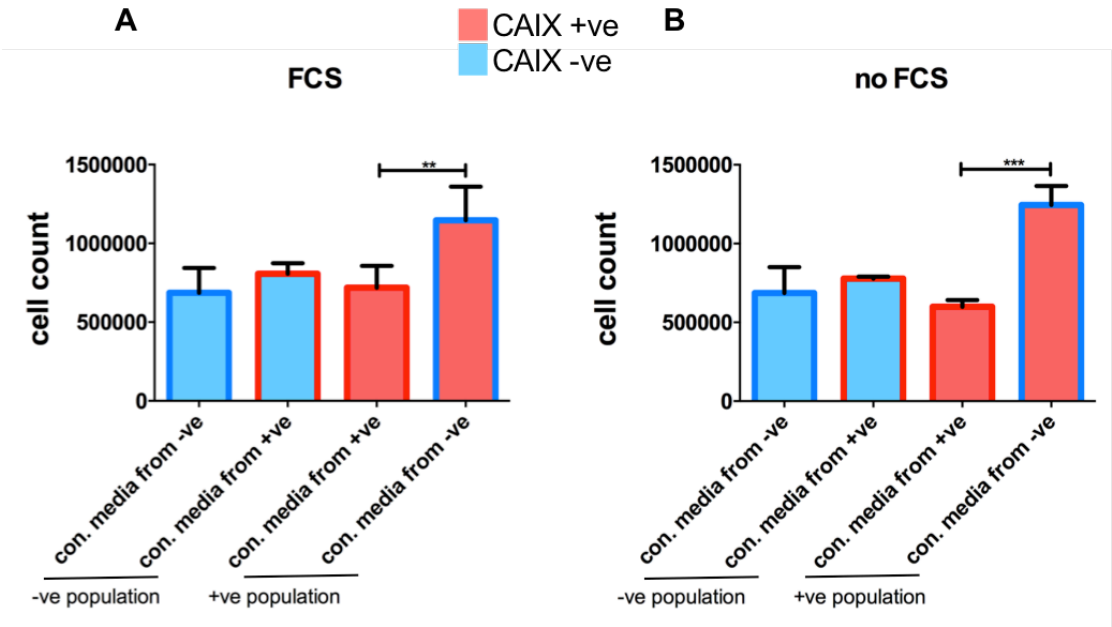


Figure 5.4 Media from MCF7 CAIX negative cells enhances cell number of the MCF7 CAIX positive population

500,000 cells of each population were seeded in a 10 cm dish in either 10% FCS (A) or no FCS (B), left to settle overnight and incubated in 0.1% hypoxia for 96 h. Conditioned media was then added to CAIX positive and negative cells in the combinations indicated and plates were incubated in 0.1% hypoxia for a further five days before final cell counting.

n=3, Graphs show mean ± SD, **p<0.01, ***<p0.001

The biological basis of the higher cell numbers observed in the cell counting experiments under hypoxic conditions was further elucidated. To this end cell apoptosis and cell cycle progression was assessed by flow cytometry. It was observed that the CAIX positive cells were significantly more viable when co-cultured with conditioned media from the CAIX negative population in comparison to conditioned media from the CAIX positive population. In contrast, no significant difference could be seen for the CAIX negative population co-cultured with conditioned media from either population (Figure 5.5 A). Moreover, a higher percentage of CAIX positive cells were found with PI binding, indicating the S- as well as G2/M phase when CAIX cells were incubated with media from CAIX negative cells.

Again, no significant differences were found for the CAIX negative population co-cultured with conditioned media from either population (Figure 5.5 B).

CAIX positive cells co-cultured with media from the CAIX negative population also showed a trend to form more colonies in a clonogenic assay, however, this was not statistically significant (Figure 5.5 C).

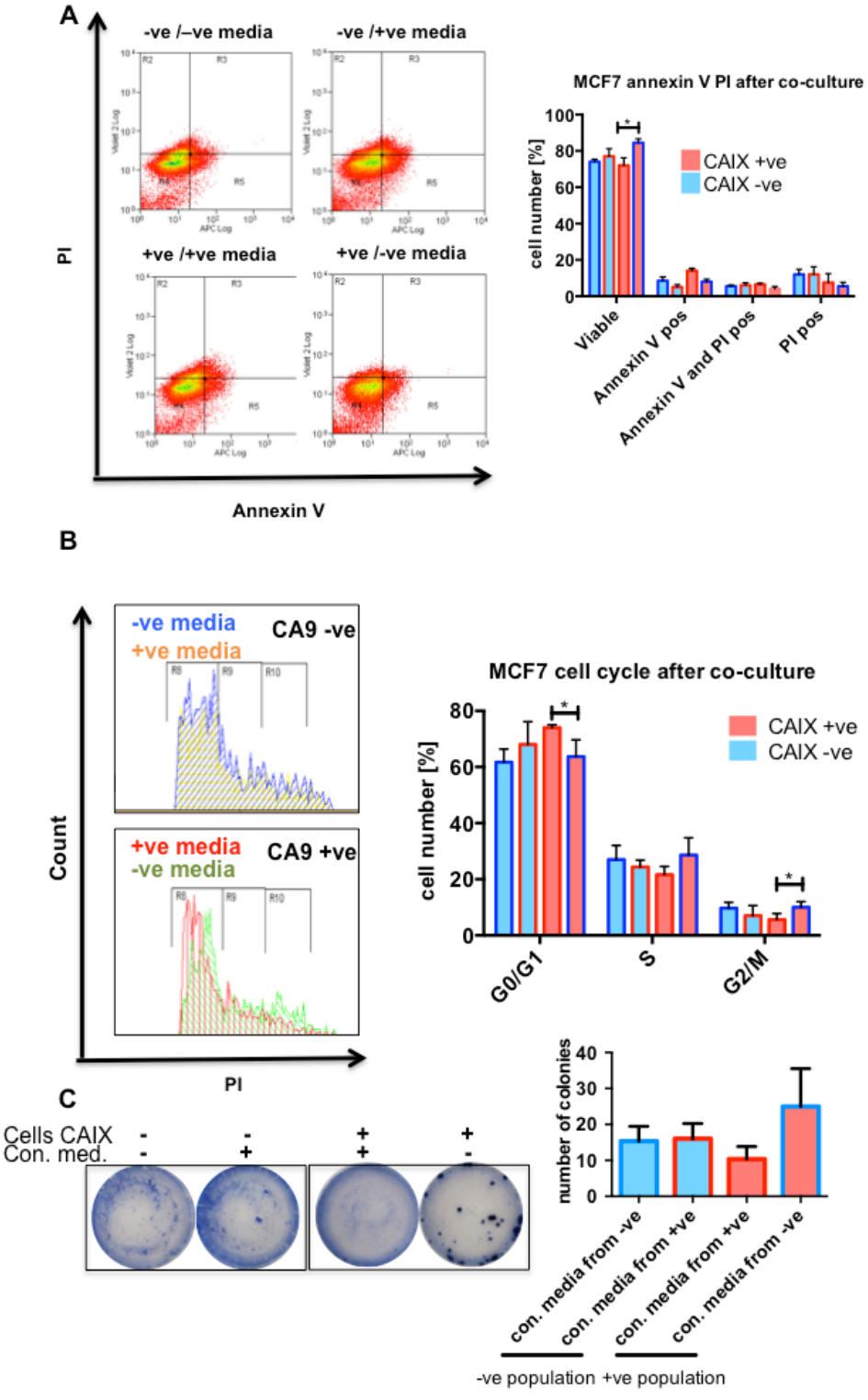


Figure 5.5 Effect of MCF7 CAIX positive and negative cells co-culture on cell viability and PI binding

Conditioned media from CAIX positive and negative cells was added to CAIX positive and negative cells in the combinations indicated and plates were incubated in 0.1% hypoxia for five days before cells were assessed for apoptosis using Annexin V as a marker (A), cell cycle stage using PI (B) and clonogenic ability (after an additional 12 days of growth) (C). n=3, Graphs show mean ± SD, *<p0.05, **p<0.01

5.2.4. Co-culture experiments are replicable using the HCT116 cell line

In order to obtain a more generalised idea of the co-culture effects seen with the MCF7 breast cancer cell line, co-culture experiments were repeated using the HCT116 colon cell line.

The same experimental setups – trans-well and conditioned media – were used to assess whether the CAIX negative population would support the growth of the CAIX positive population in the HCT116 cell line. Similar to the results found in the MCF7 cell line, there was a slight increase in cell number when cells of one population were cultured with cells / conditioned media from the other population in hypoxic conditions.

However, again this increase was only significant when the CAIX positive cells were exposed to CAIX negative cells (Figure 5.6 A) or their conditioned media (Figure 5.6 B). Moreover, in 3D culture, spheroids formed from CAIX positive cells only grew bigger than those comprised of CAIX negative cells only. However, mixed spheroids proliferated most (Figure 5.6 C).

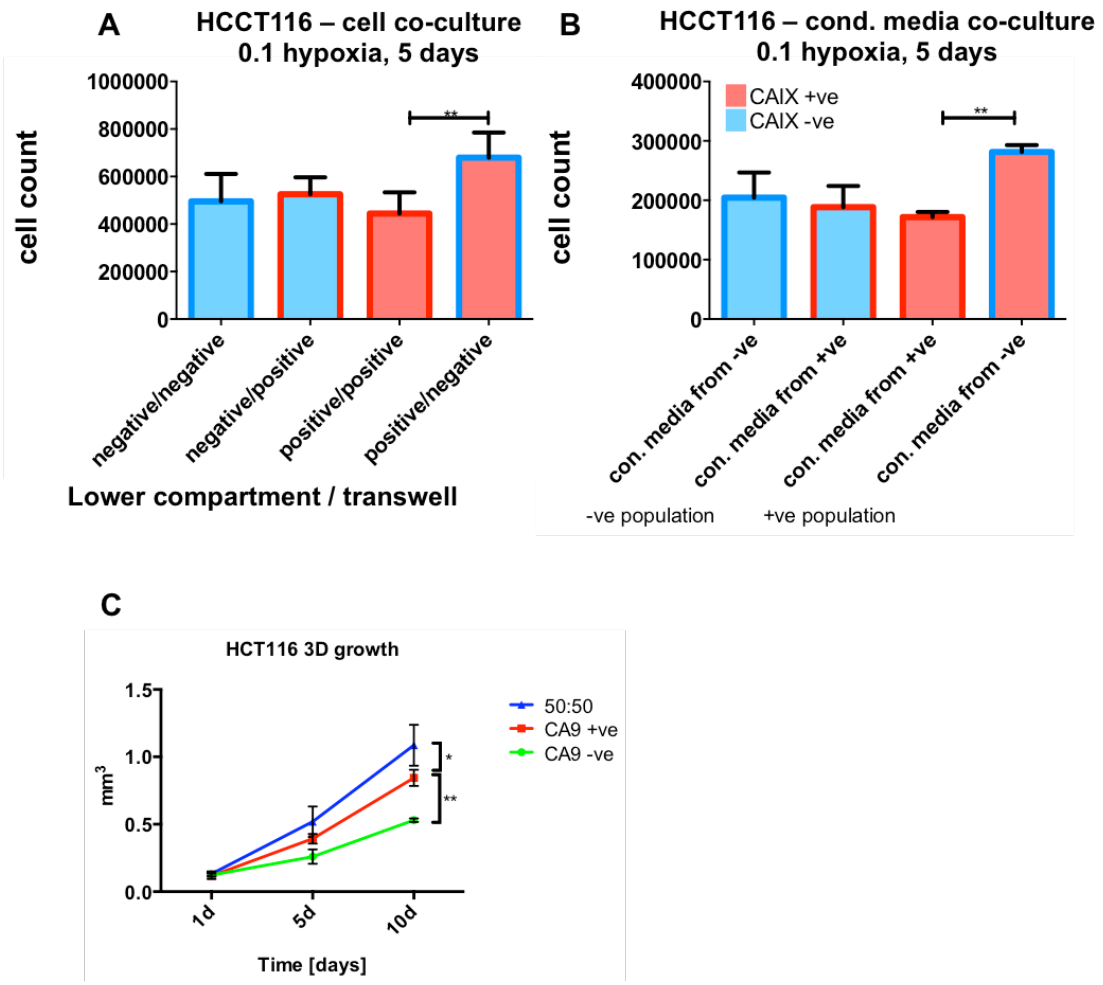


Figure 5.6 Co-culture experiments in HCT116 cells

(A) HCT116 CAIX positive and negative cells were co-cultured in a trans-well system as indicated and incubated in 0.1% hypoxia for five days before cells were counted. (B) HCT116 positive and negative populations were co-cultured with conditioned media of either the same or the other population as indicated for five days in hypoxia before cells were counted. (C) Spheroids were formed using 10,000 cells of either CAIX positive or negative cells or of a 1:1 ratio of both and spheroid growth was monitored over time.

n=3, Graphs show mean ± SD, *<p0.05, **p<0.01

5.2.5. Mechanisms underlying the co-culture effects

The co-culture advantage is conferred by a small molecule

Both the trans-well and the experiments using the conditioned media indicated that compounds in the media conferred the increase in the cell number of the CAIX positive cells. In order to narrow the possibilities, the co-culture experiments using the conditioned media were repeated in both cell models (Figure 5.7, A MCF7 cells, B HCT116 cells). However, this time two extra conditions where media was filtered either with a 30Kda or a 3Kda filter were included.

While overall cell numbers were lower when cells were grown with filtered conditioned media, the numbers of CAIX positive cells still were significantly higher with conditioned media from the CAIX negative cells when the cells were co-cultured. This indicated that the compound conferring the advantage is smaller than 3Kda (Figure 5.7).

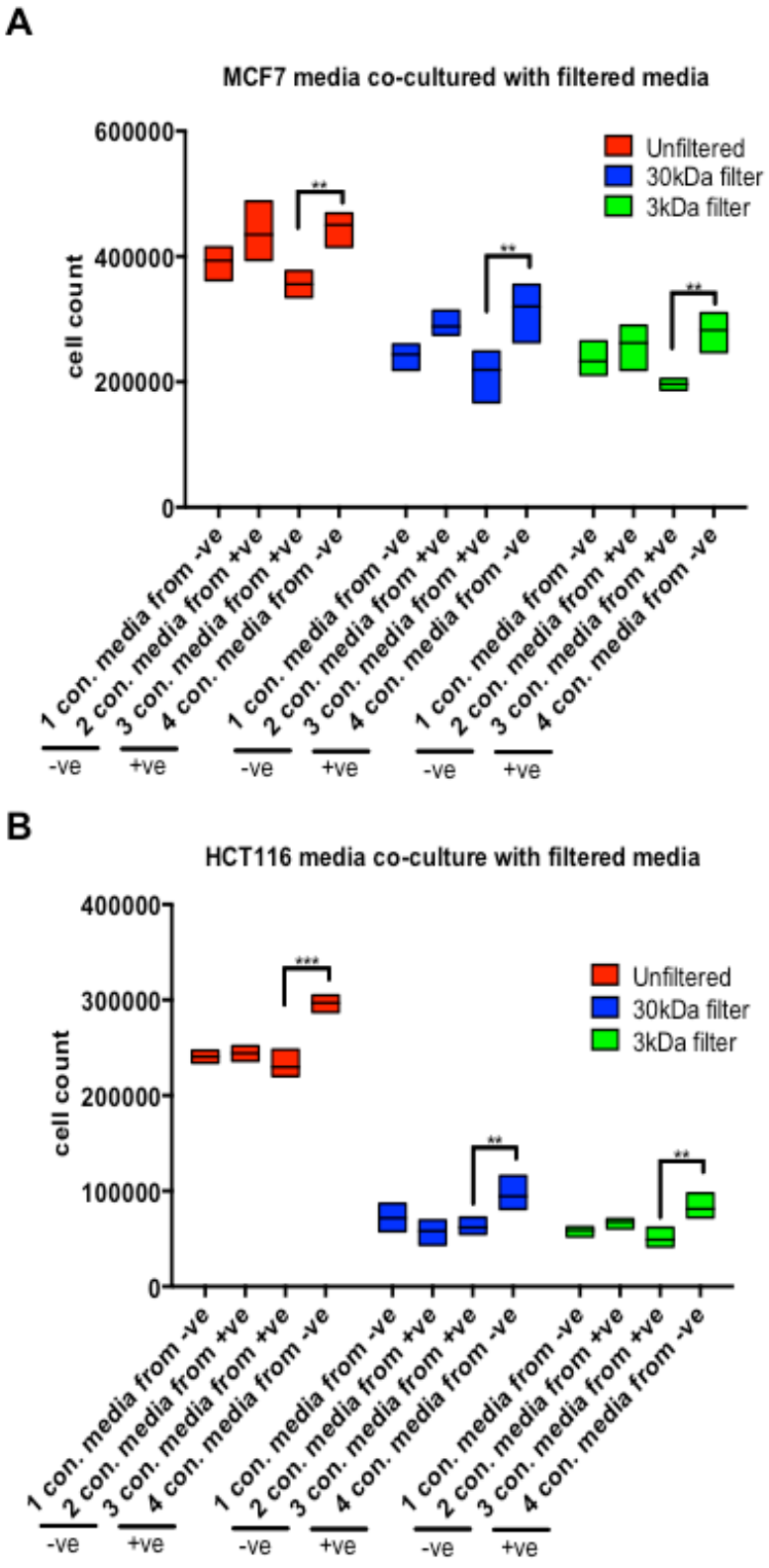


Figure 5.7 Filtered conditioned media still confers an advantage

MCF7 (A) or HCT116 (B) CAIX positive and negative cells were incubated with conditioned media from either the same or the other population for five days in

hypoxia before cells were counted. Additionally to unfiltered media, the effects of 30K and 3K filtered media was also assessed. n=3, Graphs show mean ± SD, **p<0.01, ***<p0.001

CAIX negative cells conditioned media enhances mitochondrial activity in the CAIX positive population

The data from the RNA microarray suggested an upregulation in pathways associated with oxidative phosphorylation in the CAIX positive population (Ledaki et al). Therefore, the oxygen consumption rate of both populations in different media was assessed using the MitoExpress system. The probe is added to the media and fluorescence measurements are correlated to the oxygen present.

Initial experiments using 5 mM glucose media showed that the slope of change was very flat, indicating that oxygen consumption was low. Therefore, cells were pre-incubated with 1 mM glucose or the pre-conditioned media for 6 h before the experiment.

Shown are typical time-course dependent measurements (Figure 5.8 A) as well as quantification of the slope of the curves (blue boxes), normalised to cell numbers (Figure 5.8 B).

Overall the CAIX positive population displayed a higher oxygen consumption rate in comparison to the CAIX negative population (Figure 5.8 B). Interestingly, the addition of CAIX negative conditioned media to the CAIX positive cells yielded a similar oxygen consumption / mitochondrial activity in comparison to normal media, whereas incubation with conditioned media from the CAIX positive cells decreased it. There also was a slight increase in oxygen consumption in the CAIX negative cells when incubated with conditioned media from the CAIX positive cells. However, similar to the counting experiments, this was not statistically significant (Figure 5.8 A and B).

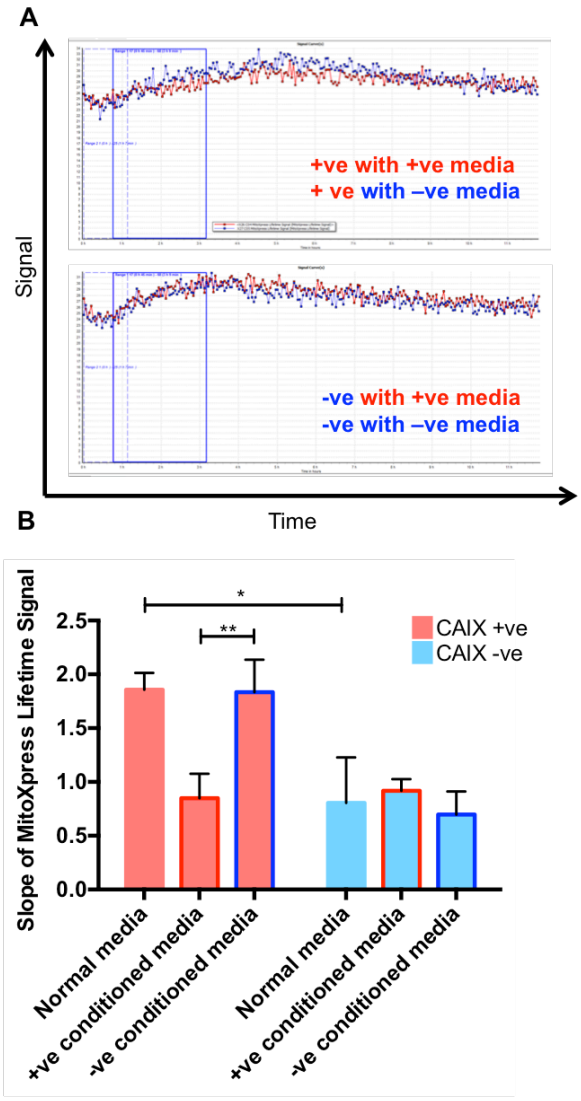


Figure 5.8 Oxygen consumption is higher in the MCF7 CAIX positive cells and is positively affected by co-culture with conditioned media from the CAIX negative cells

MCF7 CAIX positive (red bar graphs) and CAIX negative cells (blue bar graphs) were seeded in a 96-well plate and left to settle overnight. 6 h before the measurement, the media was changed to either conditioned media or 1mM glucose media (= normal). The fluorescent probe was added and O_2 concentration measured over time. (A) Representative curves of fluorescent measurements over time (B) Slope calculation of O_2 consumption relative to cell number. Graphs show mean ± SD, *<p0.05, **p<0.01

The role of lactate in co-culture conditions

Lactate is a relatively small molecule (≈ 0.1kDa) and is formed from pyruvate by the enzyme LDHA.

Previously it has been shown that lactate can be used to transfer energy between cells. It was reported that in the brain, astrocytes produce and excrete lactate, which in turn is taken up and used by neurons (Choi et al., 2012).

Several tools are available to measure metabolite levels and their effects. However, these methods often involve the need to convert a substrate and/or the destruction of the sample. Therefore, these methods interfere heavily with the cell culture system and limit the options of detecting real-life changes or cell-to-cell heterogeneity. To overcome these obstacles in the dynamic assessment of lactate levels within cells the FRET based laconic plasmid (San Martin et al., 2013) was used as described in section 4.2.5. Lactate levels of the CAIX positive and negative populations were assessed in DMEM medium under normoxic and hypoxic conditions.

A high variability of lactate levels in the cells was observed. Therefore, although most measurements fell in the region of the mean, cells with significantly higher or lower lactate levels could be observed, specifically under normoxic conditions (Figure 5.9 A data from 3 biological replicates, 10 cells counted/replicate/condition).

To obtain a clearer picture, the average of the three independent biological replicates was calculated (Figure 5.9 B). CAIX negative cells had a higher intracellular level of lactate and levels were increased in stress conditions (serum starvation). Hypoxic conditions led to a further increase in lactate levels in both populations, although this was more prominent in the CAIX negative cells (Figure 5.9 B and C).

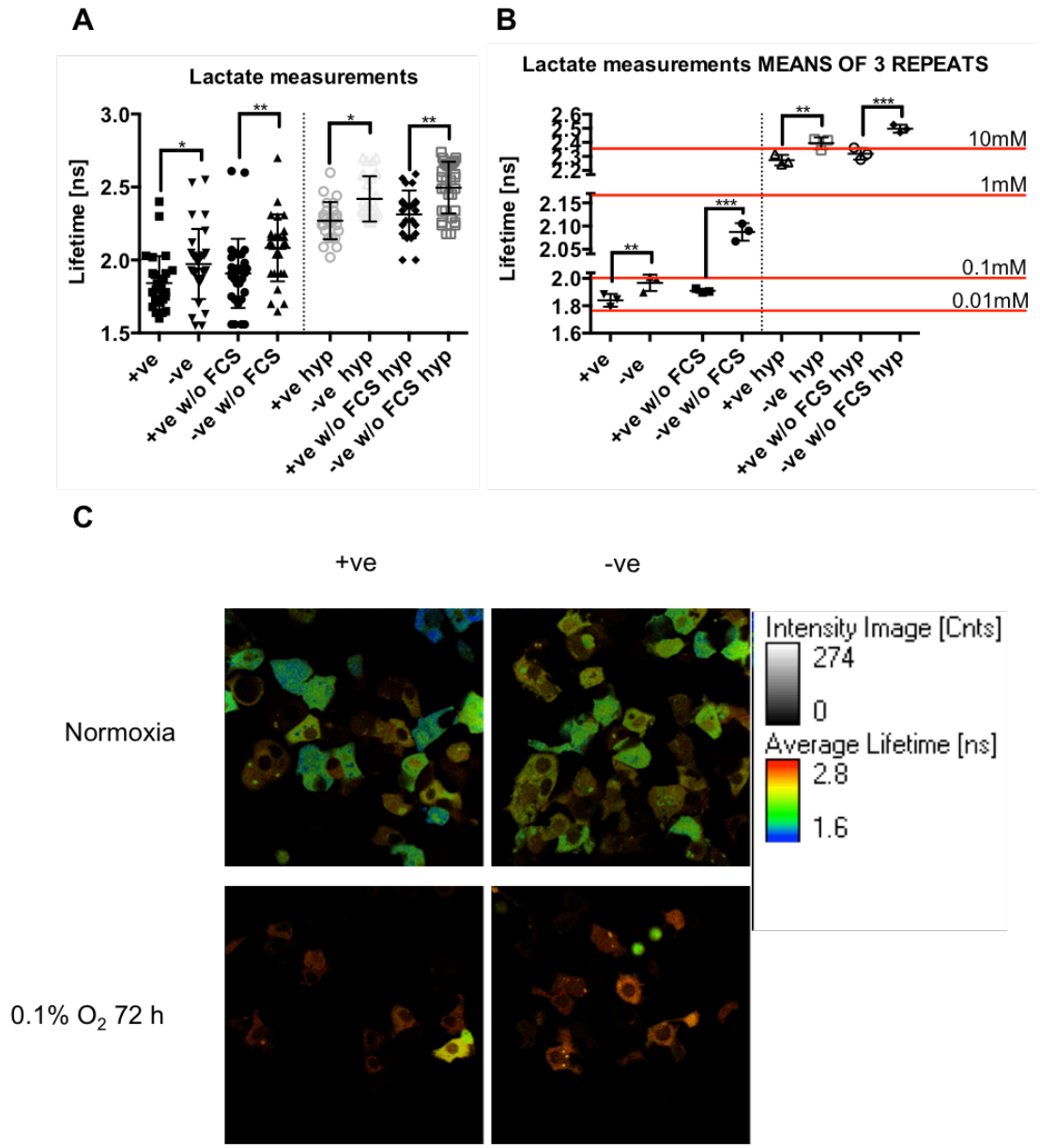


Figure 5.9 Lactate levels in MCF7 CAIX positive and negative populations

(A) MCF7 CAIX positive and negative cells were transfected with the laconic plasmid overnight and incubated in normoxia or 0.1% hypoxia for 72 h before intracellular lactate levels were assessed using a FRET microscope. 10 cells were assessed in each condition and the spread of measurements is shown in (A), whereas the averaged results of three experiments is shown in (B). Representative images are shown in (C).

n=3, Graphs show mean ± SD, *<p0.05, **p<0.01, ***p<0.001

Next, it was decided to assess lactate flux in time-lapse experiments. For this CAIX positive and negative cells were transiently transfected with the laconic plasmid, incubated in a glucose-free, pH stable, and glycolysis blocking buffer as described in the methods section. Basal lactate levels were imaged, before cells were spiked with 10mM lactate and images were taken every 2.5 min for the duration of 1 hour.

In the CAIX positive population there was an immediate response to the lactate, with the signal decreasing only slightly over time (Figure 5.10 A).

Interestingly, a heterogeneity in cell response to lactate spiking was observed, with cells in the field not showing any change (example in red circles).

In the CAIX negative population it could again be observed that basal lactate levels in this setup were slightly higher. Uptake of lactate after spiking the cells was not as dramatic and loss of signal (excretion of lactate) was observed more rapidly (Figure 5.10 A).

In line with the time-lapse experiments, which indicated that the CAIX positive population quickly took up lactate from the media, protein levels of MCT1 were higher in this population. MCT1 is transporter implicated in lactate import (Sonveaux et al., 2008). The level of MCT4, the transporter associated with lactate export (Pertega-Gomes and Baltazar, 2014), was similar in normoxic conditions, but was decreased in the CAIX positive population/higher in the CAIX negative population under hypoxic conditions (Figure 5.10 B).

Lactate levels were also assessed in the media of the MCF7 co-culture experiments (using the conditioned media). Lactate levels were significantly increased in the conditioned media taken from the CAIX negative population after the pre-culture. After the conditioned media had been transferred to the actual co-culture, lactate levels in the media of the CAIX negative continued to increase. In contrast, levels of lactate in the media of the CAIX positive population that was co-cultured with the media from the CAIX negative population actually decreased. This indicated that in

this condition the CAIX positive population could take up some of the lactate that had been excreted by the CAIX negative population in the pre-culture (Figure 5.10 C, comparing the first and the last bar).

Moreover, it was assessed whether lactate in the media could enhance cell numbers of either population. It was found that in normoxic conditions, lactate did not have much influence on cell numbers. In contrast, addition of 10mM lactate to the media yielded higher cell numbers of the CAIX positive population in hypoxic conditions. No significant changes could be seen for the CAIX negative population (Figure 5.10 D).

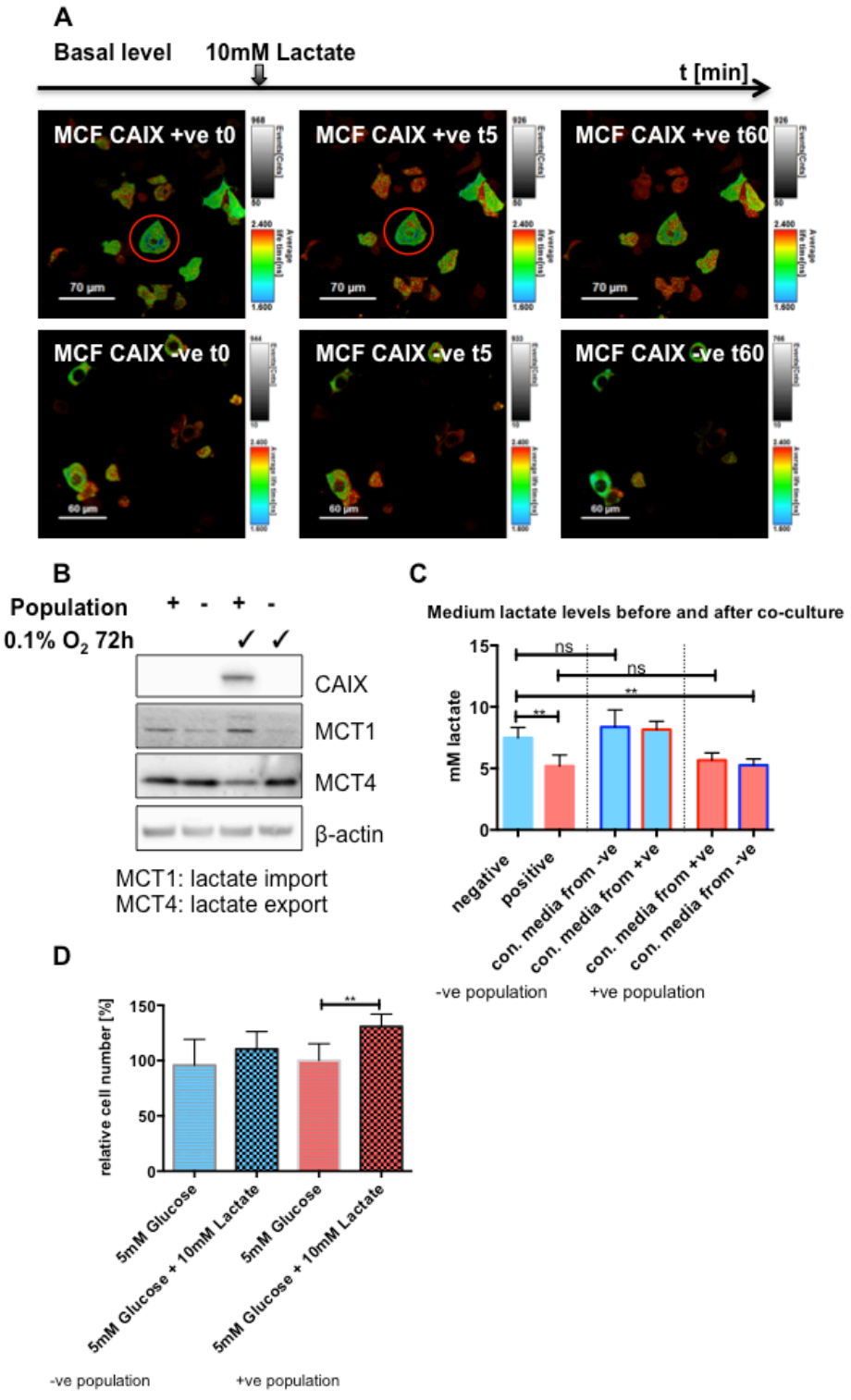


Figure 5.10 The MCF7 CAIX positive population can take up and use lactate

(A) MCF7 CAIX positive and negative cells were transfected with the laconic plasmid overnight. Cells were incubated with the glycolysis inhibitor iodoacetic acid for one

hour, before the media was changed to a glucose-free, potassium-rich buffer supplemented with the proton ionophore nigericine, and rotenone to inhibit mitochondrial metabolism. Cells were then spiked with the 10 mM lactate and the response of the plasmid was measured in a time-lapse experiment. (B) MCF7 CAIX positive and negative cells were incubated in normoxia or 0.1% of hypoxia for 72 h before cells were lysed and protein content analysed using Western blot. (C) Media lactate levels of MCF7 CAIX positive and negative cells after the pre-culture, or after the end of the co-culture were assessed by ELISA. (D) MCF7 CAIX positive and negative cells were cultured in media as indicated and cell number was assessed after five days of incubation in 0.1% hypoxia.

n=3, Graphs show mean ± SD, ns not significant, **p<0.01

Interfering with the lactate pathway

The process of glycolysis transforms glucose into pyruvate and ultimately into lactate. The proteins needed for this reversible conversion are LDHA and B.

Lactate is then transported across the cell membrane by monocarboxylate transporters (MCT) 1 and 4 (Figure 5.11 A). Therefore, the role of lactate in the described co-culture system was further investigated using a knockdown approach.

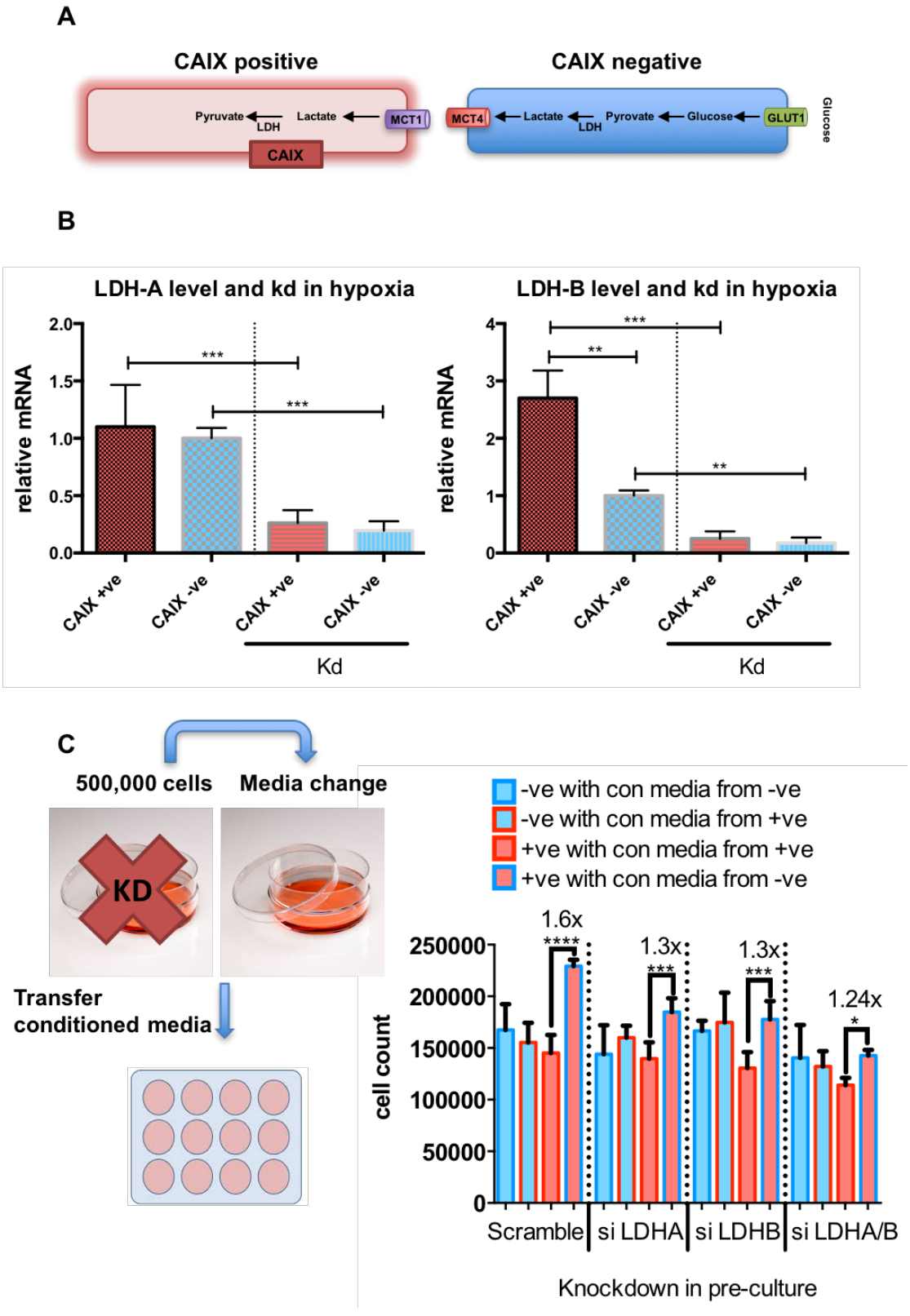
Co-culture experiments were repeated introducing either scramble control, LDHA, LDHB or double knockdown. Assessing mRNA levels indicated similar levels of LDHA in both populations, whereas LDHB was significantly increased in the CAIX positive population under hypoxic conditions (0.1% O2, 72h) (Figure 5.11 B).

Firstly, LDHA, LDHB or double knockdown was performed in the pre-culture (Figure 5.11 C left panel). In comparison to scramble, knockdown of LDHA and LDHB, and to greater effect LDHA/B, lowered the growth advantage conferred to the CAIX positive population by the conditioned media from the CAIX negative population (Figure 5.11 C right panel).

Likewise, when LDHA, LDHB or both proteins were knocked down in the cells receiving the conditioned media (Figure 5.11 D left panel), a decrease in the growth advantage was visible (Figure 5.11 D right panel).

Overall, cell numbers were decreased in the knockdown conditions in either experimental setup, indicating a general role for these proteins in cell proliferation/survival. However, the relative ratio of CAIX positive cells co-cultured with CAIX positive conditioned media vs CAIX negative conditioned media (i.e. the 3rd vs the 4th bar in each condition), decreased by trend in the knockdown conditions, suggesting a role of these proteins in the co-culture effect seen.

However, neither knockdown condition completely abolished the growth advantage, indicating the importance of additional mechanisms/pathways.


A
CAIX positive
CAIX negative
Pyruvate
LDH
Lactate
MCT1
CAIX
MCT4
Lactate
LDH
Pyrovate
Glucose
GLUT1
Glucose
B
LDH-A level and kd in hypoxia
LDH-B level and kd in hypoxia
relative mRNA
2.0
1.5
1.0
0.5
0.0
4
3
2
1
0
***
**
CAIX +ve
CAIX -ve
Kd
C
500,000 cells
Media change
KD
Transfer
conditioned media
-ve with con media from -ve
-ve with con media from +ve
+ve with con media from +ve
+ve with con media from -ve
cell count
250000
200000
150000
100000
50000
0
1.6x
****
1.3x
***
1.3x
***
1.24x
*
Scramble
si LDHA
si LDHB
si LDHA/B
Knockdown in pre-culture

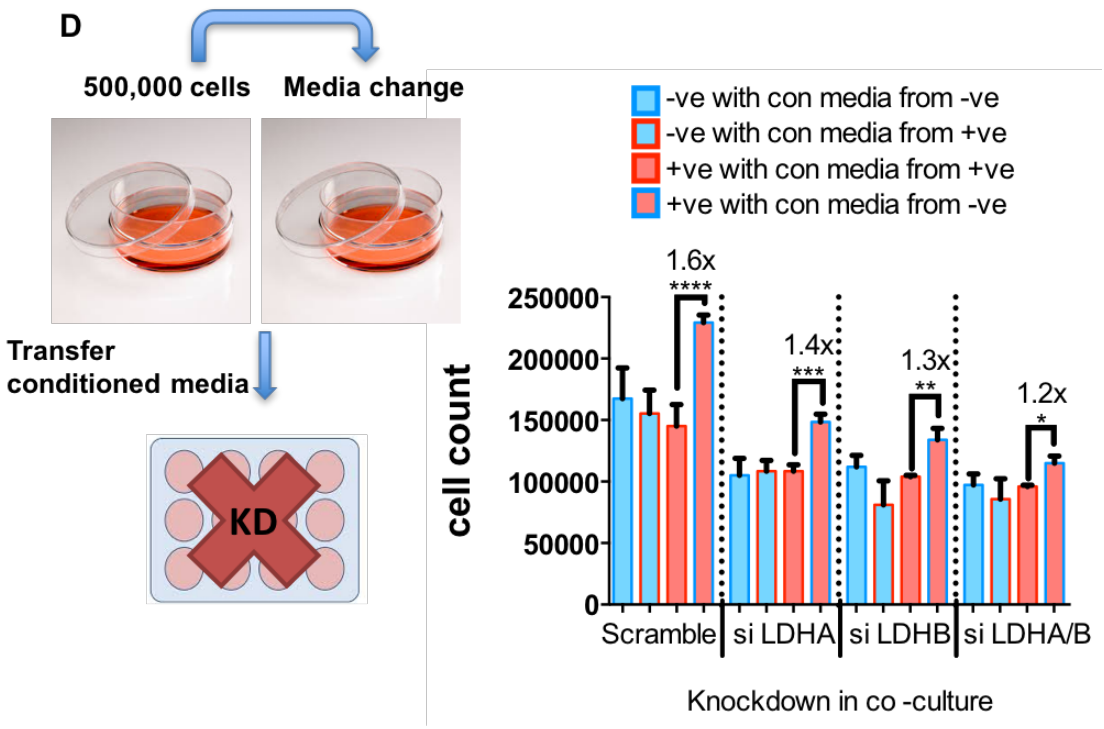


Figure 5.11 LDHA and LDHB knockdown affect growth benefit in MCF7 cells

(A) Schematic of pyruvate/lactate conversion and shuttling. (B) MCF7 CAIX positive and negative cells were transfected with either scramble or siLDHA/siLDHB/siLDHA and B and incubated in 0.1% hypoxia for 72 h before RNA extraction and qPCR analysis. Data is shown relative to mRNA levels in normoxic CAIX negative cells (normalised to actin). (C) Media from CAIX positive and negative cells transfected with scramble control or siLDHA/siLDHB/siLDHA and B was used for co-culture and cells counted after five days. (D) Conditioned media from CAIX positive and negative was transferred to cells that had been transfected with scramble control or siLDHA/siLDHB/siLDHA and B and cells were counted after five days.

n=3, Graphs show mean ± SD, *<p0.05, **p<0.01, ***<p0.001, ****p<0.0001

5.2.6. CAIX positive cells produce more lipid droplets under hypoxia

Apart from the lactate shuttle as a potential mechanism of collaboration between the CAIX positive and negative populations, another pathway involving small molecules was investigated: fatty acid uptake and lipid droplet formation. This was based on data from the initial RNA sequencing experiment indicating a relative increase of mRNAs associated with lipid droplet synthesis in the CAIX positive population (Ioanna Ledaki, unpublished). Moreover, Bensaad et al (2014) showed that, in MCF7 cells, lipid storage is enhanced under hypoxia in a HIF-1 dependent mechanism leading to fatty acid uptake (Bensaad et al., 2014).

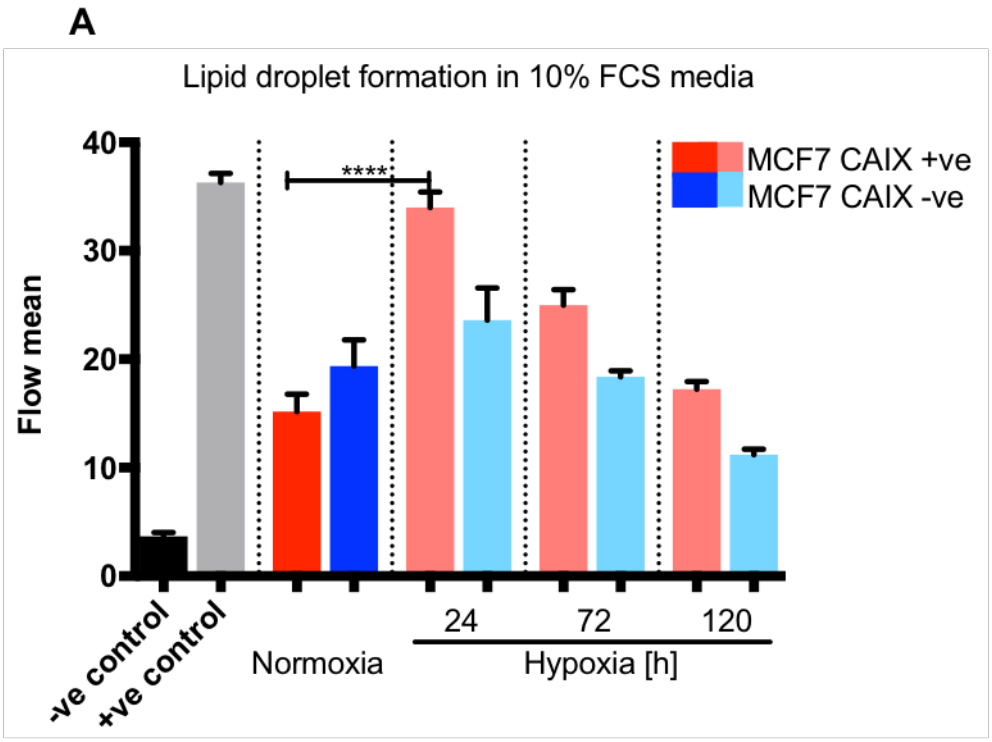
To assess the levels of lipid droplet formation in both populations, cells were incubated in normoxia or hypoxia over a time course as indicated in figure 5.12 A and analysed using flow cytometry. An unstained sample and cells that had been incubated overnight with 50mM oleic acid were used as negative and positive controls respectively.

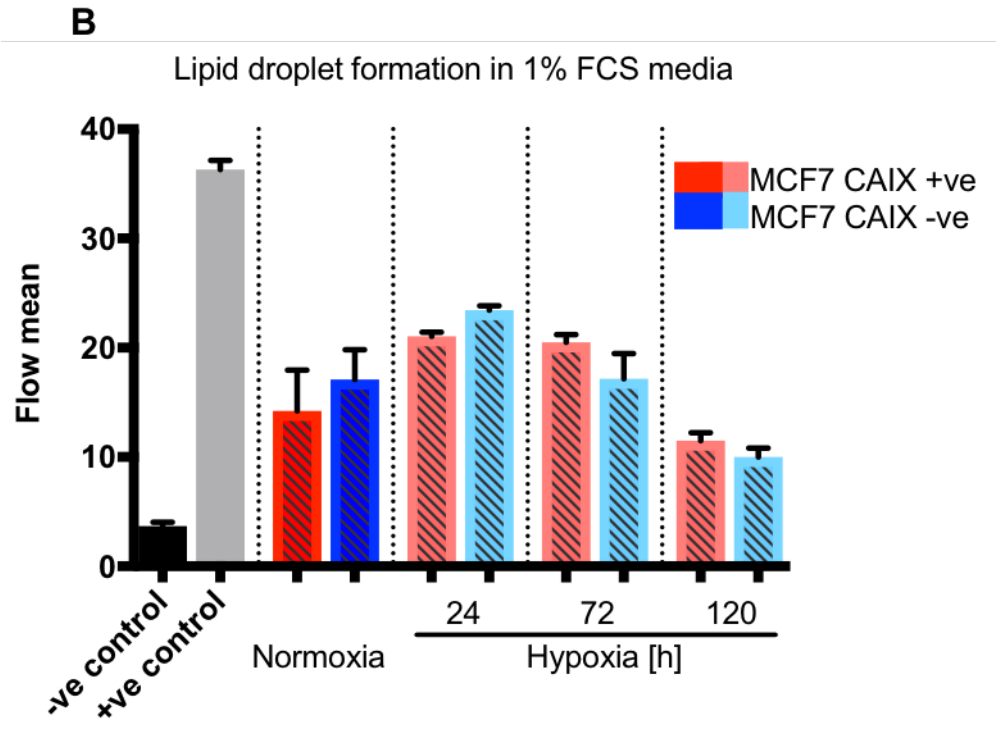
As shown in figure 5.12 A, lipid droplet formation in normoxic conditions was higher in the CAIX negative population. The onset of severe hypoxia (0.1% oxygen, time course) increased lipid droplet formation in both populations, especially at 24 h, after which the signal decreased over time. The increase of lipid droplets was bigger in the CAIX positive cells than in the negative population (19% increase in mean fluorescence at 24 h vs 5% increase).

The increase in lipid droplets during hypoxia was mainly due to fatty acid uptake from the media, since low FCS (1%, shaded bars, Figure 5.12 B) conditions had a lesser effect on lipid droplet formation in comparison to full medium (10% FCS, block colour bars) (Figure 5.12 A).

Lipid droplet formation was also imaged by immunofluorescence using a Zeiss fluorescence microscope. Similar to the flow cytometry results, more lipid droplets were found in the CAIX negative population incubated in normoxia, whereas CAIX positive cells formed considerably fewer.

However, in hypoxic conditions lipid droplet formation was upregulated in the CAIX positive population but was low in the CAIX negative population. Oleic acid was used as a positive control, showing that in the excess of fatty acid availability, both populations form lipid droplets; however, this was more marked in the CAIX positive population (Figure 5.12 C).


A
Lipid droplet formation in 10% FCS media
Flow mean
40
30
20
10
0
****
MCF7 CAIX +ve
MCF7 CAIX -ve
-ve control
+ve control
Normoxia
24
72
120
Hypoxia [h]


B
Lipid droplet formation in 1% FCS media
Flow mean
40
30
20
10
0
MCF7 CAIX +ve
MCF7 CAIX -ve
-ve control
+ve control
Normoxia
24
72
120
Hypoxia [h]

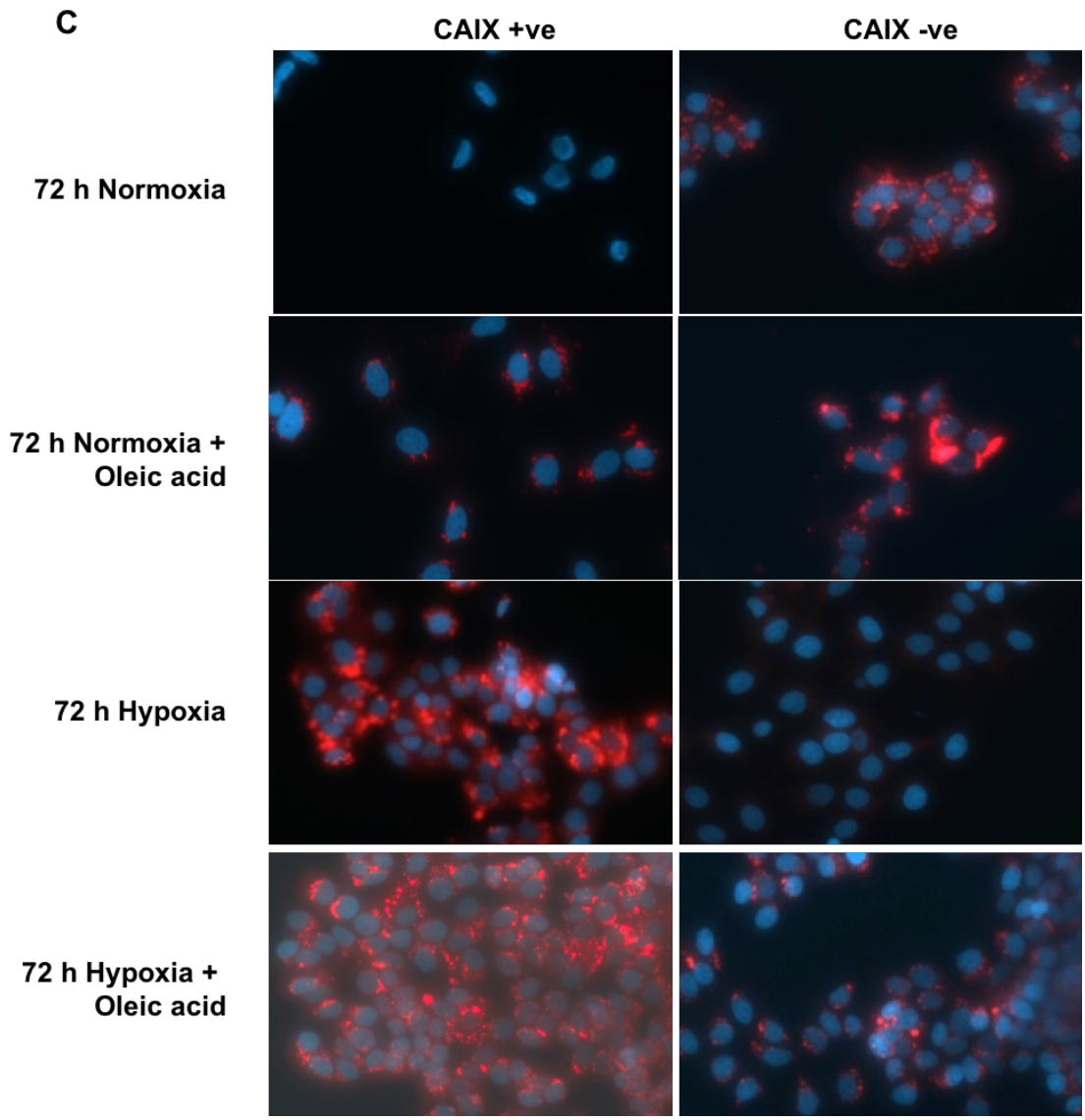


Figure 5.11 Fatty acid uptake is enhanced in the MCF7 CAIX positive cells

(A/B) MCF7 CAIX positive and negative populations were incubated in high (10%, A) or low (1%, B) FCS media in normoxia or 0.1% hypoxia for the indicated time points. Cells were then fixed, stained for lipid droplets and analysed by flow cytometry. No staining and overnight incubation with 50 mM oleic acid were used as negative and positive control respectively. Flow mean shows the percentage of positive cells. (C) MCF7 CAIX positive and negative populations were incubated in 10% FCS media in normoxia or 0.1% hypoxia for 72 h. Cells were then fixed, stained for lipid droplets and imaged using a fluorescence microscope. Overnight incubation with 50 mM oleic

acid was used as a positive control. 20x magnification images are shown. n=3, Graphs show mean +/- SD, ** $p<0.01$, *** $p<0.001$

Fatty acid uptake and transport as well as lipid droplet formation is dependent on the expression of transporter and lipid droplet membrane molecules. Therefore, a comparison of genes associated with these pathways was set up. Fatty acid transporter CD36 was upregulated in the CAIX positive after incubation in hypoxia (Figure 5.12 A). Family members of the FAB proteins were not significantly changed under hypoxia (Figure 5.12 B). Lastly, PLIN2 a protein needed for lipid droplet membrane formation was by trend higher under hypoxic conditions, confirming the upregulation of lipid droplet formation (Figure 5.12 C).

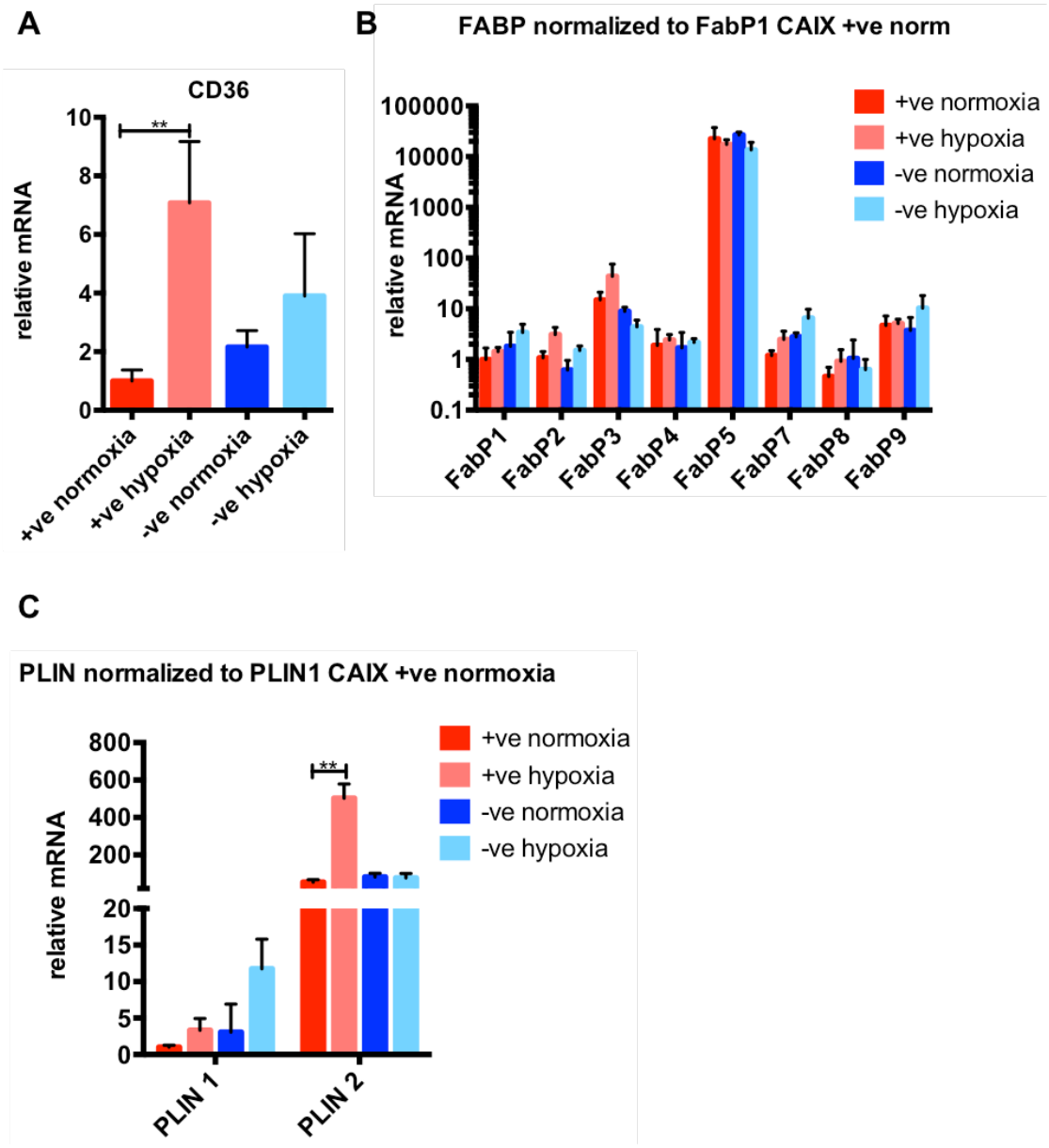


Figure 5.12 Comparison of genes associated with fatty acid transport and lipid droplet formation in MCF7 CAIX positive and negative cells

MCF7 CAIX positive and negative populations were incubated in normoxia or 0.1% hypoxia for 72 h before RNA extraction and qPCR analysis for levels of (A) CD36, (B) FAB protein family members, and (C) PLIN1 and PLIN2.

Values are normalised to actin and are shown relative to mRNA levels in normoxic CAIX positive cells (=1).

n=3, Graphs show mean ± SD, *<p0.05, **p<0.01

It has been previously proposed that increased lipid droplet formation during hypoxia leads to the increased proliferation of cells during re-oxygenation (Bensaad et al., 2014). In line with this, CAIX positive and negative cells were incubated in normoxia or hypoxia (0.1% oxygen, 24 h) before being placed in normoxia for the indicated times and cell numbers were counted. The 24 h time point was chosen for two reasons i) the increase in lipid droplet formation peaked at this time, ii) the difference in growth/cell number between the CAIX positive and negative population was negligible (Figure 5.14 A). In general, there was a non-significant trend that cells that had been incubated in normoxia grew better than cells exposed to hypoxia. However, there was no difference in cell numbers between the CAIX positive and the CAIX negative population (Figure 5.14 B dark red and dark blue lines). In contrast, when both populations had been incubated in hypoxia (0.1%) for 24 h the CAIX positive population yielded higher cell numbers upon re-oxygenation in comparison to the CAIX negative population (Figure 5.14 B light red and blue lines, Figure 5.14 E). Within the same experiment it was hypothesised that a potential effect would be related to an increased fatty acid uptake during the hypoxic phase of the experiment. Therefore, CAIX positive cells were transfected with a siRNA against CD36 (FAT). The knockdown of CD36 led to a 70-80% decrease in CD36 mRNA levels (Figure 5.14 C) and decreased lipid droplet formation during hypoxia (Figure 5.14 D). Upon re-oxygenation, cell numbers were decreased in the knockdown condition in comparison to the scramble control (Figure 5.14 E).

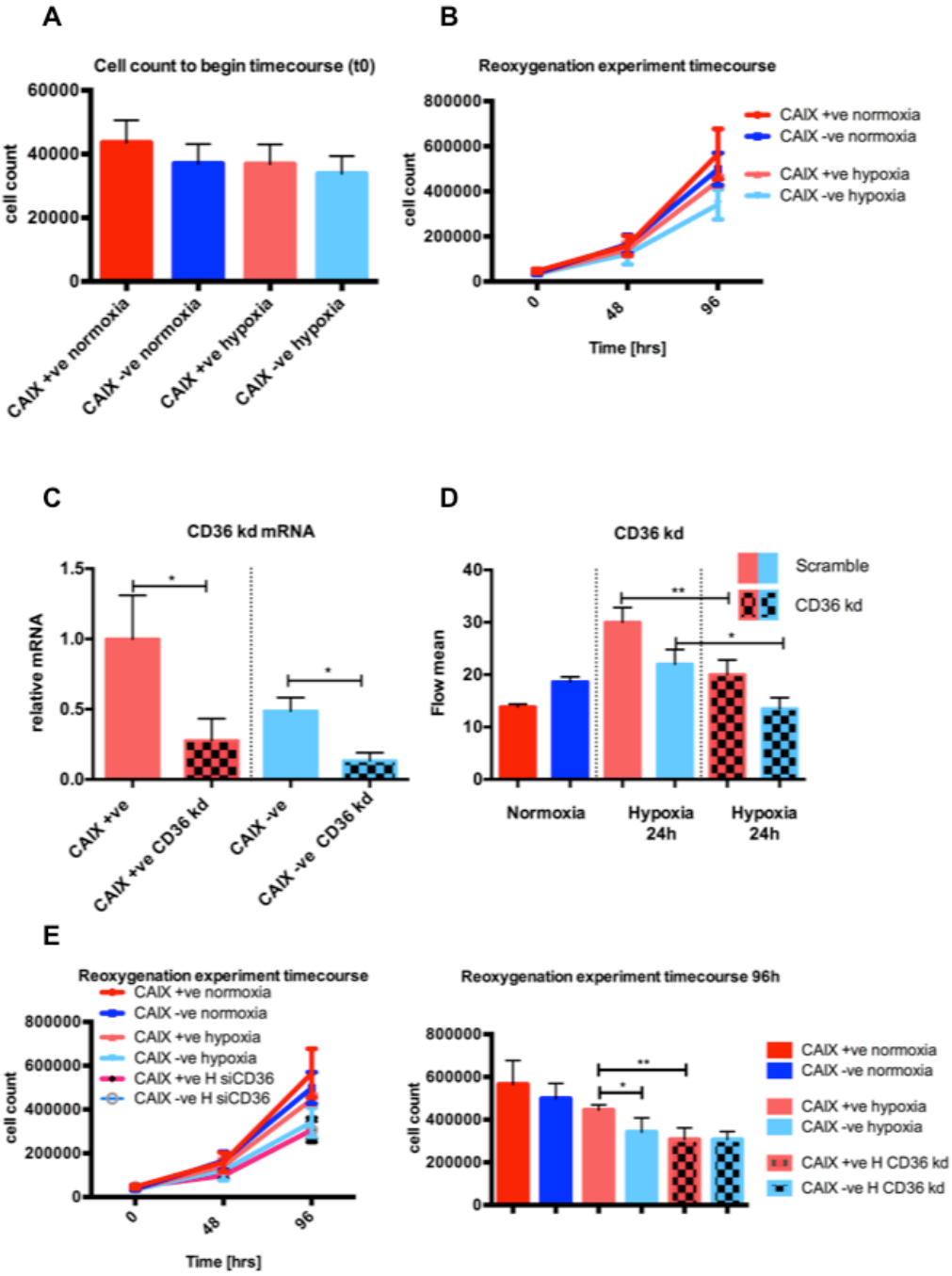


Figure 5.13 MCF7 CAIX positive cells grow better during re-oxygenation linked to fatty acid uptake during hypoxia

(A) MCF7 CAIX positive and negative populations were incubated in normoxia or 0.1% hypoxia for 24 h before re-oxygenation. (B) MCF7 CAIX positive and negative populations that had been subjected to normoxia or 24 h of 0.1% hypoxia were re-seeded to ensure equal numbers and incubated in normoxia. Cells were counted at the indicated time points. (C) Scramble control or siCD36 were transfected into CAIX

positive and negative cells and mRNA levels were assessed after 72 h. (D) CAIX positive and negative cells transfected with scramble control or siCD36 were incubated in 0.1% hypoxia for 72 h and lipid droplet formation was assessed by flow cytometry. (D) as (B) but also showing the siCD36 conditions.

n=3, Graphs show mean ± SD, *<p0.05, **p<0.01

Role of lipid droplets in co-culture condition

Since lipid droplet formation seemed to be different in the CAIX positive and negative populations during hypoxia, it was hypothesised that this could also contribute to the co-culture effect observed. Again, conditioned media of both populations cultured in hypoxia was used. At the end of the co-culture, CAIX negative cells co-cultured with either media showed very low levels of lipid droplets; therefore, the type of media (either from CAIX negative or positive cells) did not influence fatty acid uptake.

In contrast, CAIX positive cells co-cultured with CAIX negative media showed lipid droplet formation but not when co-cultured with CAIX positive media (Figure 5.15 A and B).

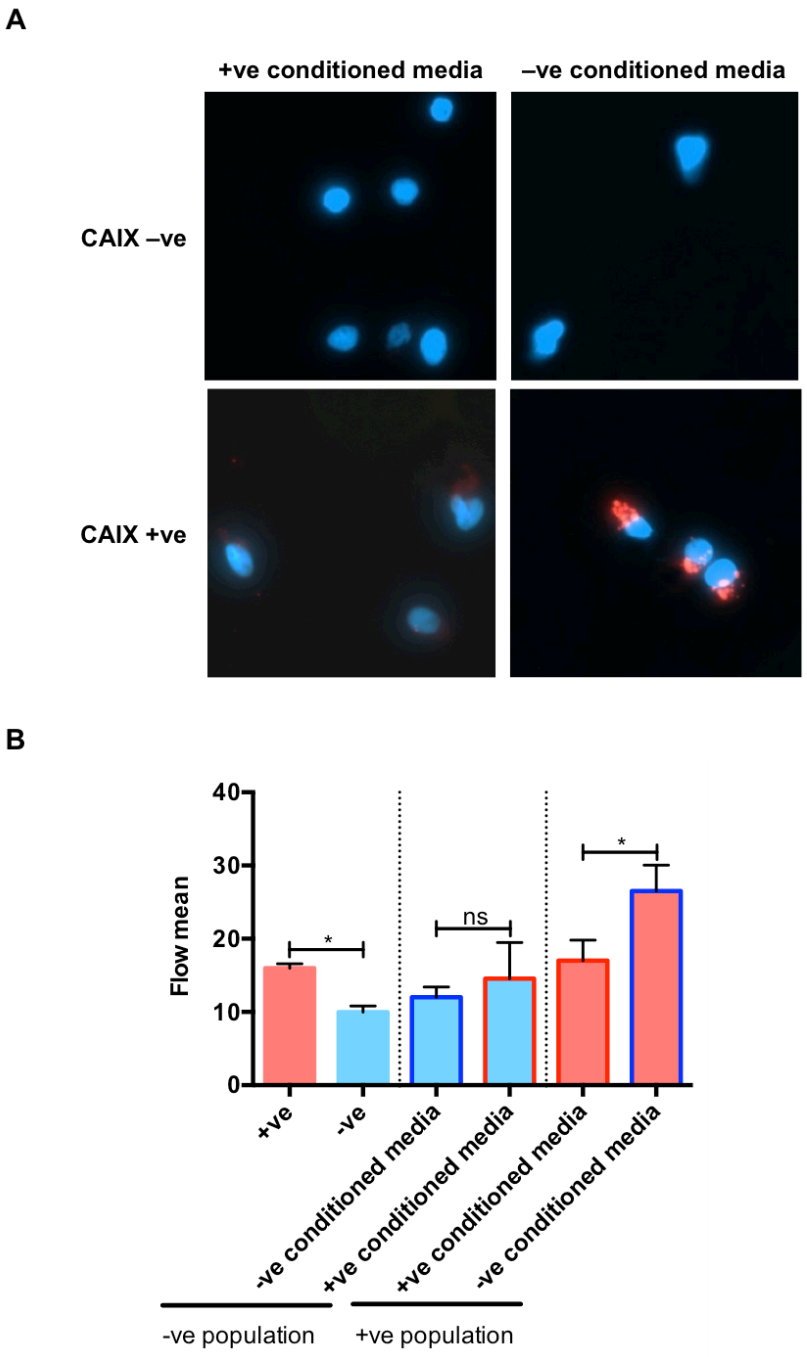


Figure 5.14 Lipid droplet formation in MCF7 CAIX positive cells is enhanced in co-culture with conditioned media from CAIX negative cells

MCF7 CAIX positive and negative cells were incubated with conditioned media from either the same or the other population for 72 h in 0.1% hypoxia. Cells were then fixed, stained for lipid droplet formation and assessed by (A) fluorescence microscopy (20x magnification) or (B) flow cytometry. n=3, Graphs show mean ± SD, *<p0.05, **p<0.01

The CAIX negative population displays a higher level of autophagy

To further investigate how the CAIX negative population might confer this advantage to the CAIX positive population, the former was more closely investigated. Data from the RNA-sequencing indicated higher levels of autophagy in the MCF7 CAIX negative population in hypoxic conditions. This was confirmed on mRNA levels, as there was an increased level of associated mRNAs such as LC3β, LAMP1.

It was further shown that the CAIX negative population had a higher protein level LC3β in hypoxic conditions, indicating a higher level of autophagy (Figure 5.16 A), which did not seem to be further enhanced by low FCS conditions. Autophagosomes were shown to merge later with vesicles with a lower pH to break down the enclosed compounds. In line with this, protein levels for LAMP1, a lysosome marker, were also increased in the CAIX negative population under hypoxic conditions. The relative amount of vesicles with low pH was further confirmed to be higher in the CAIX negative population using lysotracker blue and flow cytometry analysis (Figure 5.16 B).

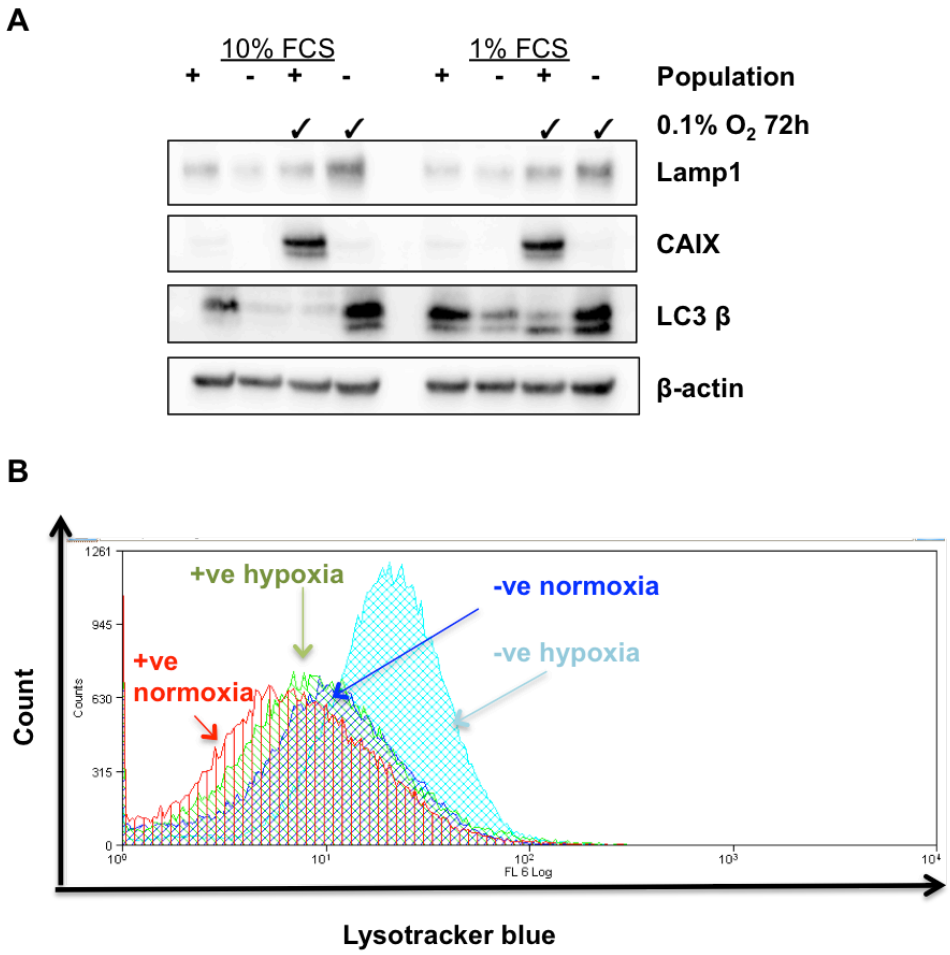


Figure 5.15 Autophagy is higher in the MCF7 CAIX negative population

(A) MCF7 CAIX positive and negative cells were incubated in normoxia or 0.1% hypoxia for 72 h in high or low FCS media before cells were lysed and protein levels were analysed by Western blot. (B) MCF7 CAIX positive and negative cells were incubated in normoxia or 0.1% hypoxia for 72 h before being stained with lysotracker blue and analysed using flow cytometry.

5.3. Discussion

A number of previous reports have described the interaction of different cell types and especially the interaction of tumour cells with the surrounding stroma.

Here we describe the interaction and metabolic collaboration between subpopulations of the same parental cell lines.

Specifically, the results imply that CAIX negative cells support the growth of CAIX positive cells. This has been shown in two cell lines, covering a breast as well as a colon cancer model, indicating that tumour cell collaboration is a wider mechanism across different tumour types.

In this model the CAIX negative population resembles some of the features that were previously shown in stromal fibroblasts. This includes the upregulation of autophagy and the production and release of lactate. It would be interesting to co-culture both populations, either individually or in combination with immortalised fibroblasts in order to assess further collaborative mechanisms and to see whether the behaviour of CAIX negative cells would change. This would especially be interesting in the outer regions of the tumour, where CAIX negative cells would interact with stromal cells.

Intercellular and subcellular lactate shuttles have been associated with normal metabolism in some tissues including brain (Hashimoto et al., 2008) and the myocardium (Gertz et al., 1988). Lactate produced by tumour cells has been associated with microenvironment acidification and tumour cell invasion. However, Sonveaux et al (2008) reported a symbiosis between lactate-producing and lactate-consuming cells. In their model, aerobic cells could take up lactate for energy metabolism. In contrast with the model presented here, MCT1 was only expressed in non-hypoxic regions, while hypoxic cells relied on glucose uptake (Sonveaux et al., 2008). However, in the current model all cells are incubated in hypoxia. The data suggests that, while glucose may be the preferred carbon source, lactate can also be

used as fuel to generate pyruvate for the TCA cycle. This is underlined by the result that LDHA/B knockdown in CAIX positive cells decreased the survival/proliferation advantage, indicating that lactate is indeed used for cell metabolism.

However, the uptake and release of lactate and other metabolites is likely to be continuous and may depend on various factors. Therefore, it may be hard to draw conclusions from time point data only. To put this in context, mathematical modelling of lactate flux in brain has been similarly confusing. A number of papers indicate a lactate flux from astrocytes to neurons, and this notion is also underlined by the respective expression patterns of transporters and LDH enzymes [reviewed in (Stobart and Anderson, 2013)]. Two mathematical models focusing on energy substrates, oxygen, and NADH concentrations within the neuronal and astrocyte energy compartments support the idea that lactate flows from astrocytes to neurons (Aubert et al., 2007, Cloutier et al., 2009). However, another model, which also considers transport from the blood-brain barrier, supports the notion that neurons may supply lactate to astrocytes (Mangia et al., 2009).

One way of addressing this in the current study was to use a FRET-based lactate sensor that could be imaged in live cells over time. Yet, to make matters even more complicated, this sensor revealed a heterogeneity in basal lactate levels as well as in the response to lactate spiking. This is not due to a technical limitation as the FLIM technique used is not dependent on the amount of plasmid present in the cells. Rather, the calculation depends on the assessment of the lifetime of the photons received. If a cell contains more plasmid, more photons will be received overall, although the lifetime remains constant. However, it was shown that CAIX positive cells take up lactate from the CAIX negative conditioned medium, which is in line with the time-lapse FRET experiments. Nevertheless, it would be interesting to concomitantly image glucose levels in the cells as well as other carbon sources such as glutamine to have a closer look at the flux of different carbon sources.

Previously, MCT1 and 4 have been associated with lactate transport. MCT1 is associated with lactate export (Bola et al., 2014) as well as import (Sonveaux et al., 2008, Fujiwara et al., 2015, Bola et al., 2014) and CAIX expression has been shown to augment MCT1 activity (Jamali et al., 2015). In line with this, MCT1 was more highly expressed in CAIX positive cells, potentially explaining the lactate uptake.

Conversely, MCT4 – the transporter associated with lactate export (Pertega-Gomes and Baltazar, 2014) – was more highly expressed in CAIX negative cells in hypoxia.

Lactate shuttling between MCT1-high tumour cells and MCT4-high stroma cells has been shown to play a role in prostate cancer progression (Sanita et al., 2014), and high respective expression was associated with poor prognosis (Pertega-Gomes et al., 2014).

Therefore, future work would include the assessment of MCT1 and 4 inhibitors on lactate uptake and release and also on cell viability of and the co-culture effect between CAIX positive and negative populations. Another two enzymes that are crucial for metabolite fate are PDH and PDK1. Inhibition of PDH or PDK1 (the latter with DCA) in the same setting would be expected to have a differential effect on the two populations which would be interesting to test.

It has previously been shown that knockdown of MCT1 and 4 in breast cancer led to decreased tumour aggressiveness and growth (Morais-Santos et al., 2015). MCT4 was upregulated in malignant cells of ascites and its silencing resulted in reduced tumour cell proliferation (Lee et al., 2016).

Pharmaceutical inhibition of MCT1 led to decreased tumour growth *in vitro* and *in vivo* (Sonveaux et al., 2008, Gurrapu et al., 2016, Takada et al., 2016, Hong et al., 2016, Zhao et al., 2014) and was additive to radiotherapy (Sonveaux et al., 2008, Bola et al., 2014), chemotherapy (Zhao et al., 2014, Amorim et al., 2015), and phenformin (Marchiq et al., 2015). Due to these results, a phase 1 clinical trial using a MCT1/2 inhibitor (AZD3965) in the setting of advanced cancers is currently ongoing/recruiting participants (NCT01791595) (ClinicalTrial.gov, 2016).

Another question would be how CAIX positive cells signal to CAIX negative cells. The increased level of oxidative phosphorylation and mitochondrial activity would lead to an increased level of ROS, which could be a signalling molecule.

In the brain it has been suggested that pH sensing could lead to an acute upregulation of cAMP levels and subsequent increase of glycolysis (Choi et al., 2012). Although pH sensing would be more associated with the CAIX positive population, it would be interesting to assess cAMP levels in both populations during single or co-culture. For example, an internal cAMP sensor (Klarenbeek et al., 2015) could be used in combination with staining for CAIX to assess cells by FACS or immunofluorescence after single or co-culture.

Metabolic symbiosis may not only mean that cells are being supplied with metabolites by other cells, but it could also be that different cells types have preferential uptake of different substrates from the media/blood and are therefore more efficient as a whole. Historically, the main focus in metabolism research has been on glucose, and there is still a debate about ideal culture conditions (i.e. high vs low glucose).

Nevertheless, it is now clear that glucose is not the only carbon source for cancer cell metabolism. HeLa cells are able to generate ATP almost entirely from glutamine and pyruvate (Rossignol et al., 2004). Prostate cancer on the other hand preferably uses fatty acids despite the presence of abundant glucose (Liu et al., 2010, Liu, 2006).

In the presented system the data also support the hypothesis of differential uptake of fatty acids and potentially other metabolites by the CAIX positive and negative populations. It seemed that CAIX positive cells formed more lipid droplets, specifically when incubated in hypoxia. Initial experiments showed that CAIX positive cells formed more and better colonies after sorting and incubation in hypoxia. This may be partly explained by findings by Bensaad et al. (2014), which suggested that lipid droplet generation under hypoxia had a protective effect during re-oxygenation (Bensaad et al., 2014). In line with this, a reduction of lipid droplet formation by knockdown of CD36 decreased the survival advantage.

In the same report the centre of U87 spheroids was shown to contain more lipid droplets. It would therefore be interesting to discover whether treatment of spheroids with etomoxir would affect lipid droplet formation and spheroid growth.

In summary this chapter describes the collaboration between subpopulations of the same parental cell type in two models. This model proposes two pathways – a lactate shuttle and differential use of fatty acids – that promote tumour cell survival and maintenance of energy production in the populations.

This underlines the importance of tumour heterogeneity for tumour growth and development, but also opens up new treatment options to inhibit this interaction.

Chapter Six

Final Discussion

6.1. CAIX expression and Hypoxic Heterogeneity

The fast growth of cancer cells during tumour development leads to poorly vascularised regions that are characterised by irregular blood flow and therefore a decreased abundance of nutrients as well as oxygen. These regions of hypoxia contribute to tumour heterogeneity by differential regulation of gene expression. This favours the outgrowth of the "fitter" cells, and leads to a more aggressive phenotype. In line with this, the onset and extent of hypoxic tumour regions is correlated with poor patient outcome and therapy resistance (Heddleston et al., 2010b).

Therefore, the accurate assessment and monitoring of areas of hypoxia in a given tumour is of clinical importance. Current biomarkers of hypoxia include pimonidazole staining, osteopontin, and ^{18}F-fluoromisonidazole, all of which have certain advantages and limitations. Additionally, markers of hypoxia that are under investigation include a tumour hypoxia gene signature, which can be determined from gene sequencing (Buffa et al., 2010).

The further identification of hypoxic biomarkers will also help in the exploration of the underlying molecular mechanisms driving these particularly aggressive tumour phenotypes. This knowledge enhances the development of targeted treatment options and patient stratification.

The transmembrane protein CAIX has been used as biomarker of hypoxia; due to its long half-life it is more stable and therefore is a more accurate measure of hypoxia then HIF-1α, which has a half-life of a few minutes. Moreover, CAIX expression itself has been associated with poor survival in multiple cancer types, including breast (Chia et al., 2001), non-small cell lung (Giatromanolaki et al., 2001) and head and neck cancer (Jonathan et al., 2006). CAIX is currently explored in several clinical trials as an imaging target, but also as a potential therapeutic target (Robertson et al., 2004).

Our laboratory previously showed that CAIX itself is heterogeneously expressed in hypoxia (Ledaki et al., 2015), with a CAIX positive and a CAIX negative population present in breast MCF7 cells. The populations were isolated and cultured separately. In the present work, it was confirmed that these populations are stable in their characteristics over a long period of time. Moreover, a second model – the colon cell line HCT116 – was established, where CAIX positive and negative cells were also isolated and shown to be stable over a period of time.

A panel of cell lines was tested and although no other cell line showed clear CAIX positive and negative populations, it was shown that CAIX high or low cells display similar characteristics to the sorted populations. Therefore, CAIX is highly regulated and does mark a particular subtype of cells, characterised by a higher clonogenic potential.

The basal-like/triple negative breast cancer cell lines induced CAIX to higher levels than other subtypes, which is in line with previous studies (Tan et al., 2009, Kajo et al., 2013, Neumeister et al., 2012).

The differential expression of CAIX in positive and negative populations was dependent on epigenetic regulation. In line with this, it has been previously suggested that hypoxia may induce chromatin alterations, including global deacetylation and an increase in H3K9me3/me2 (Johnson et al., 2008). The regulation of histone methylation is dependent on histone demethylases and histone methyltransferases. Hypoxia induces the expression of the Jumonji C (JmjC) domain-containing histone demethylases JMJD1A and JMJD2B (Wellmann et al., 2008, Pollard et al., 2008, Yang et al., 2009). Moreover, $CD133^{+}/CA9^{+}$ HCT166 cells express high levels of JMJD1A (Yang et al., 2009) suggesting that hypoxia can directly influence the expression of histone modifying enzymes. Thus, hypoxia may epigenetically regulate a number of genes, contributing to tumour heterogeneity. The

identification of these targets will provide a rationale for the development of novel drugs targeting hypoxia-induced methyltransferases or histone demethylases.

Another family of proteins involved in epigenetic regulation are bromodomain and extra-terminal (BET) proteins that act by selectively recognising acetylated lysine residues on chromatin. A recent study found that BET inhibitor JQ1 modulated 44% of hypoxia-induced genes including CA9, without altering HIF expression. The drug inhibited triple negative breast cancer growth *in vitro* and *in vivo* (da Motta et al., 2016). JQ-1 was further shown to be effective in gastric cancer cells derived from Brazilian patients but not from Asian ones, again indicating heterogeneity between tumours (Montenegro et al., 2016).

Overall the presented results confirm the presence of heterogeneity within tumours, indicated by presence/absence of the cell surface protein CAIX. This convenient localisation may help to use CAIX to easily classify those more aggressive subpopulations for better patient management.

6.2. Tumour cell reorganization and the hypoxic stem cell niche

A high-risk factor of malignant diseases is metastasis; once a tumour is spreading, the patient outcome prognosis worsens.

CAIX has been implicated with changes in cell adherence. It has been suggested that CAIX expression decreases E-cadherin association with the cytoskeleton (Svastova et al., 2003) and, in a separate study, CAIX high cells were found to have pathway enrichment for genes associated with cytoskeletal organisation (Shin et al., 2011). Both studies found that a high level of CAIX was correlated with reduced cell-cell adhesion. Moreover, the role of CAIX in tumour microenvironment acidification has been implicated in cell invasion mechanisms (Martinez-Zaguilan et al., 1996). Apart from the indication of hypoxia that is correlated with CAIX positivity, this increased

invasion/metastatic potential may also contribute to the poorer prognosis associated with CAIX expression.

In line with this, *in vivo* studies using sulphonamide/sulphamate based CAIX inhibitors have found a decreased metastatic burden in breast cancer models, even if the effects on the primary tumour were small (Pacchiano et al., 2011, Gieling et al., 2012).

In the present study, it was shown that CAIX positive cells have a higher migratory/invading potential and knockdown of CAIX by siRNA and inhibition with drug (sodium butyrate) diminished the spatial reorganisation seen in 3D models. CAIX positive cells had an increased level of MMP-14 in 2D models and CAIX expression partly overlapped with expression of MMP-14 in 3D models. This specific matrix metalloproteinase has been implicated as a mediator and cofactor of CAIX driven metastasis (Espi, 2015).

Therefore, the expression of MMP-14 and CAIX should be investigated in larger data sets to assess the prognostic/predictive value for patient outcome. This may lead to enhanced patient stratification. Moreover, MMP-14 inhibition may enhance CAIX inhibition in the reduction of metastatic burden.

The gene signature of the CAIX positive population is enriched for stem cell associated markers including Wnt and Nanog (Ledaki et al., 2015).

Apart from intrinsic pluripotency transcription factors, putative stem cells' maintenance and survival also depends on signalling from their microenvironment. Hypoxia has been implicated to act as a stem cell niche. The most direct evidence for this comes from research on haematopoietic stem cells, residing in the bone marrow. It has been shown previously that bone marrow aspirates were consistently found to be hypoxic (Harrison et al., 2002). Moreover, hypoxia has been shown to increase the cancer stem cell population in breast cancer models (Wicha et al., 2006, Conley et al., 2012) and multiple myeloma (Muz et al., 2014). Mechanistically, it was shown

that HIF-2 can upregulate pluripotency factor OCT-4 by direct binding in its promoter side (Covello et al., 2006).

This indicates that the hypoxic environment is favourable for cancer stem cells. Indeed, this has been demonstrated in various other tissues including the central nervous system (Studer et al., 2000), bone marrow (Ivanovic et al., 2000), and human embryonic stem cells (Ezashi et al., 2005).

Overall these results demonstrate an intrinsic mechanism for spatial reorganisation of tumour cells in a 3D environment. Considering that hypoxic regions can serve as a stem cell niche, we propose that this may also be a potential explanation for the spatial reorganisation seen in the presented 3D model. CAIX expression has been linked with stemness, as has migratory ability. Therefore, the core of a spheroid may serve as a protected niche for this population. CAIX expression in itself protects cells from the more acidic hypoxic microenvironment, providing a more physiological intracellular pH, which is needed for cell survival.

6.3. A symbiotic relationship between CAIX positive and CAIX negative cells

Cancer cells employ a number of mechanisms to promote a favorable tumour microenvironment; this includes the stimulation of angiogenesis, the evasion of detection by immune cells, and the utilisation of surrounding cells for the generation of high-energy metabolites.

In line with this, it has been shown that cancer cells can utilise various metabolic compounds besides glucose to cover their energy and catabolic needs.

HeLa cells use glutamine and pyruvate to generate ATP (Rossignol et al., 2004), whereas prostate cancers often depend on the beta-oxidation of fatty acids for the production of ATP (despite the presence of abundant glucose) (Liu et al., 2010, Liu, 2006). Hypoxia has been shown to increase lipid droplet formation in some cells in a HIF-dependent manner (Bensaad et al., 2014). Hypoxia / HIF-1 is also responsible for the upregulation of proteins involved in glycolysis and lactate production including LDH-A (Semenza et al., 1994) (Warburg effect). Interestingly, it has been shown that the “waste product” lactate can be used as a metabolite in several tissues including the brain (Hashimoto et al., 2008) and the myocardium (Gertz et al., 1988).

The reverse Warburg effect describes the metabolic symbiosis between cancer cells and stromal fibroblasts, where glycolysis and autophagy in stromal cells fuels anabolic metabolism processes in cancer cells (Martinez-Outschoorn et al., 2012b, Ertel et al., 2012, Martinez-Outschoorn et al., 2011a, Pecqueur et al., 2013)

Previously, the reverse Warburg effect between tumour and stroma cells has been associated with luminal breast cancer subtypes as assessed by IHC staining of patient samples for CAIX, MCT4, and various autophagy markers (Choi et al., 2013).

MCF7 is a luminal breast cancer cell line; however, in this report we propose a symbiotic interaction between subpopulations of tumour cells, as outlined in figure 6.1.

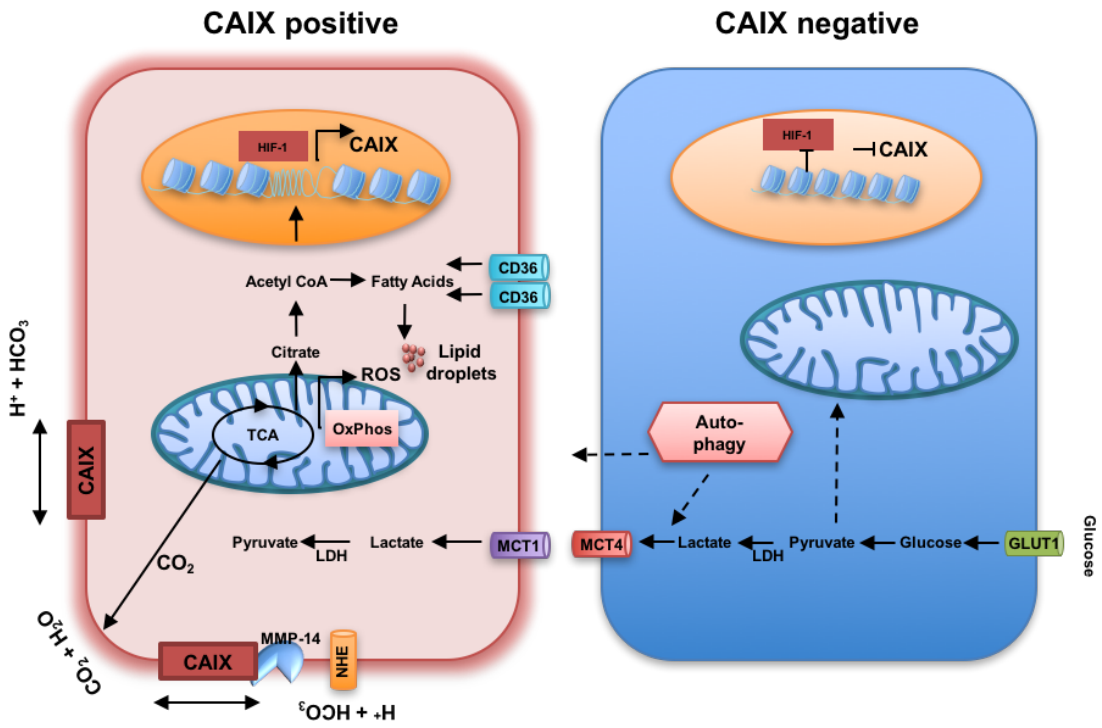


Figure 6.1 Proposed model of CAIX positive and CAIX negative cell interaction

In the CAIX positive cells, the genomic region encoding CA9 is more open to HIF-1 binding. The more stem cell-like CAIX positive cells show an upregulation of OxPhos and TCA cycle. The generated CO_2 from the mitochondria diffuses out of the cell. In the extracellular space CAIX can catalytically hydrate CO_2 to HCO_3^- and H^+. A fraction of HCO_3^- is recycled back into the cell by Na^+- HCO_3^- co-transporters (NBC) or Na^+- dependent Cl^- HCO_3^- exchange (NHE), thereby maintaining a diffusion gradient of CO_2. The high mitochondrial respiration enhances the production of mitochondrial ROS. Enhanced lipid droplet formation by increased fatty acid uptake from the media in the CAIX positive cells can protect from ROS; and ROS may act as a signaling molecule to CAIX negative cells. CAIX negative cells show an upregulation of autophagy and lactate production and secretion potentially via MCT4. Lactate may be taken up by the CAIX positive population through MCT1 transporters and can be converted to pyruvate by LDHB to fuel the TCA cycle and OxPhos. The more stem-like cells may favour the hypoxic niche and may actively reorganise with the help of the matrix metalloproteinase MMP-14.

The work in this thesis suggests that the more stem-like CAIX positive population benefits from the availability of high energy metabolites from the CAIX negative population as well as from differential uptake of fatty acids by the two populations.

Cancer stem cells have been shown to be able to utilise high-energy metabolites such as ketone bodies and lactate for their energy demands. Immunohistochemical staining of head and neck cancer specimens for proliferation marker Ki67 and markers for mitochondrial mass/function (TOMM20/Complex IV). The markers co-localise to the basal stem cell layer of human oral mucosal tissue. Moreover, staining for MCT1 was found in that region, suggesting the usage of lactate and ketone bodies for mitochondrial metabolism and stem cell proliferation (Curry et al., 2013). Considering the spatial reorganisation in 3D models, where putative stem cell like CAIX positive cells are located in the centre of the spheroid it is interesting that a previous study found an increased level of MCT1 staining from the spheroid periphery to the centre (Andersen et al., 2016). In line with this, cancer stem cells created by E-cadherin silencing preferentially use lactate and ketone bodies as mitochondrial fuels (Cuyas et al., 2014).

In addition lactate metabolism has been proposed to be sufficient for the increase in expression of genes normally associated with neuronal and haematopoietic stem cells (Martinez-Outschoorn et al., 2011b). Moreover, the transcriptional profile of MCF7 cells incubated with lactate or ketones predicted a poorer clinical outcome of ER-positive breast cancer patients (Martinez-Outschoorn et al., 2011b).

In agreement with these previous reports, a recent study examined the proteomic profile of MCF7 and T47D mammospheres. These showed an upregulation of mitochondrial proteins involved in mitochondrial biogenesis, as well as an increased level of proteins needed for lactate and ketone metabolism. Furthermore, they found an upregulation of beta-oxidation, indicating an involvement of fatty acids (Lamb et al., 2014). The CAIX positive population also showed an increased level of lipid

droplets, specifically under hypoxic conditions. Lipid droplet formation has previously been associated with colorectal cancer stem cells (Tirinato et al., 2015) and haematopoietic stem cells (Ito et al., 2012). Mechanistically, lipid droplets were shown to protect neuronal stem cells in periods of hypoxia and oxidative stress by limiting the levels of reactive oxygen species (ROS) in *Drosophila* (Bailey et al., 2015).

It is therefore proposed that CAIX negative cells support the maintenance and proliferation of stem cell CAIX positive cells in a hypoxic niche by the provision of lactate and the reduced uptake of fatty acids.

This highlights the importance of tumour heterogeneity for tumour progression as well as for treatment response and resistance. For example, metabolic symbiosis has been found to act as a resistance mechanism to anti-angiogenic therapy (Allen et al., 2016, Jimenez-Valerio et al., 2016), which was rescued by MCT4 knockdown (Pisarsky et al., 2016). Interestingly, this model proposed an increased lactate production in the more hypoxic cells with the lactate shuttle going towards the normoxic cells (Pisarsky et al., 2016). This shows that the exchange of metabolites may depend on various factors, including oxygen tension (i.e. which cells are hypoxic/normoxic) and cell state (stem cell vs more differentiated cell). Similarly, despite the general recognition of the existence of a lactate shuttle over 20 years ago, its direction between astrocytes and neurons is still under debate (see the discussion of the previous chapter, 5.3, page 171).

In light of these findings, treatments targeting metabolic symbiosis may be beneficial in combination with existing therapies. MCT1 inhibition has been shown to reduce breast cancer mammosphere formation (Lamb et al., 2014) and proliferation of glioblastoma stem cells (Takada et al., 2016).

A phase 1 clinical trial using a MCT1/2 inhibitor (AZD3965) in patients with advanced cancer is currently recruiting participants (NCT01791595) (ClinicalTrial.gov, 2016).

The metabolic symbiosis involved in anti-angiogenic resistance reported by Allen et al. (2016) was based on an underlying increase in mTOR signalling driven by lactate metabolism. Considering that our CAIX positive population also had an upregulated level of mTOR activation and was more sensitive to mTOR and HDAC inhibition than the CAIX negative population, combination therapy may have a beneficial effect. Important players in the fate of metabolites are PDH, PDK-1, and LDH A/B. PDK-1 regulates PDH, which in turn mediates conversion of pyruvate into acetyl-CoA. LDH A/B are involved in the reversible pyruvate to lactate conversion. Hence inhibition of these enzymes could also have a beneficial effect in treatment by blocking metabolite use, specifically in the CAIX positive population. In line with this, LDHA/B knockdown was shown to decrease the benefit for the CAIX positive cells from the CAIX negative conditioned media.

6.4. Concluding Remarks and Future Prospects

In summary, the data presented in this thesis confirm that hypoxia promotes tumour heterogeneity not only between well and less well-oxygenated regions of the tumour but also importantly within the hypoxic region. It links high CAIX expression with increased clonogenic potential and shows for the first time to our knowledge the self-driven reorganisation of tumour cell populations in a 3D *in vitro* model.

This may serve to support and maintain the more stem cell-like population in growth and survival in a hypoxic niche by a bulk of other cancer cells.

The regulation of CAIX expression in the CAIX positive and negative populations has been shown to be of an epigenetic nature, suggesting a differential expression of histone modifying enzymes during hypoxia. Further identification of

methylases/demethylases driving epigenetic changes during times of hypoxia, and also after re-oxygenation, may give a deeper insight on the mechanisms behind those changes and the resulting tumour cell heterogeneity.

Interestingly, there is a link between stemness, metabolism and epigenetics. It has been suggested that cell stemness is promoted by cancer metabolism via the utilisation of high-energy metabolites (Curry et al., 2013), fuelling high mitochondrial metabolism (Curry et al., 2013, Lamb et al., 2014) (Martinez-Outschoorn et al., 2011b).

The metabolism of these metabolites would increase the acetyl-CoA pools which has previously been shown to increase histone acetylation, which acts to enhance gene transcription (Galdieri and Vancura, 2012). Closing the circle, histone acetylation has been implicated in the regulation of the stemness in ES cells (Markowetz et al., 2010).

Given the above, together with the stem cell-like characteristics of the CAIX positive population and its uptake of lactate, it would be interesting to assess the general status of epigenetic markers (acetylation, methylation etc) in both populations and to investigate the link between cell metabolism and epigenetic control.

The CAIX positive cells have been shown to harbour a more aggressive cancer phenotype; therefore, it would be useful to image these cells for prognostic and predictive patient assessment. The utilisation of metabolites that are being taken up by these cells for the development of PET tracers or other imaging approaches in combination with a CAIX marker may give a better idea of tumour cell identity. For example, magnetic resonance spectroscopy (MRS) has been shown to be consistent in the measurements of several tumour metabolites including lactate and lipids (McLean et al., 2012).

Moreover, the development of inhibitors to block cell-cell metabolic symbiosis would be likely to have an additive effect if combined with current treatment options.

The findings of this thesis highlight the symbiotic nature of cancer, where a bulk of tumour cells supports the growth of a smaller, but more aggressive population. This may be further enhanced by stromal and other cells and signalling pathways in the tumour microenvironment. Therefore, this highlights the need for combinational therapies to target different cell populations and their symbiotic interactions.

6.5. Future Experimental Work

Expansion of cell lines and further assessment of hypoxia induced heterogeneity

Although a panel of breast cancer cell lines has been screened for CAIX expression after incubation in hypoxia, no other breast cancer cell line with a distinct CAIX positive and CAIX negative population was found. However, notably CAIX high and low cell populations displayed similar characteristics to positive and negative populations respectively.

Nevertheless, due to time constraints it was decided to proceed with two cell lines exhibiting clear CAIX positive and negative cells, encompassing a breast and a colon tumour model. However, more cell lines would be needed to investigate the general validity of the proposed model.

Furthermore, the investigation of differential expression of histone modifying enzymes such as the histone demethylases JMJD1A and JMJD2B would lead to insights into specific hypoxia-related epigenetic changes contributing to tumour heterogeneity.

Further assessment of the role of MMPs in conjunction with CAIX and pH in cell reorganisation

IHC staining of CAIX positive tissue micro arrays (TMAs) would be interesting, in order to assess the correlation of CAIX staining with staining for MMP-14 and its prognostic and predictive value for patient outcome. Furthermore, knockdown / pharmacological inhibition of MMP-14 would be needed to assess its role in tumour cell reorganisation seen in 3D models. Based on the report by Vallejo et al. work in this report focussed on MMP-14. However, it may be interesting to also assess the level of other family members.

Furthermore, tumour microenvironment acidification and associated metalloproteinase activity is causal for tumour cell invasion. Hence, work on pH

measurements inside spheroids has been looked at in collaboration with Thomas Tapmeier. This was facilitated by incubation of the spheroids with a **pH l**ow **i**nsertion **p**eptide (pHLIP) (Tapmeier et al., 2015). These peptides were shown to be soluble in aqueous solution at pH 7.4, binding to lipid bilayer surfaces at near neutral pH, and inserting as an alpha helix at low pH. (Reshetnyak et al., 2007) (Figure 6.2 A).

As CAIX is involved in pH regulation it was hypothesised that central localisation of CAIX positive cells is related to a more acidic environment. Initial results showed that there was an accumulation of pHLIP towards the centre of mixed spheroids, indicating a lower pH level (Figure 6.2 B).

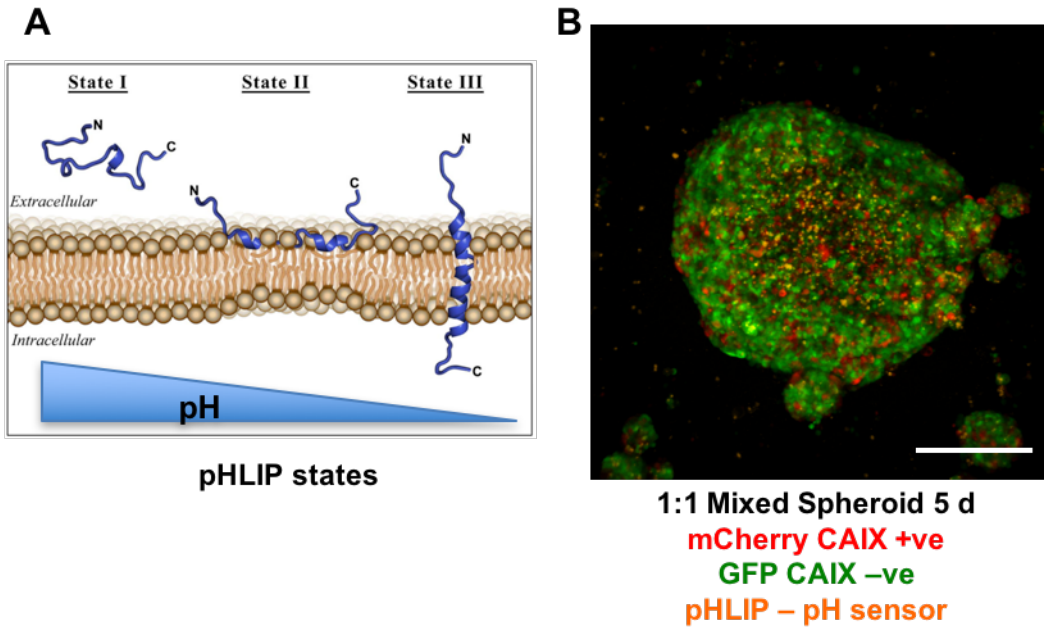


Figure 6.2 The centres of MCF7 spheroids are more acidic

(A) Potential states of the pHLIP peptide. Taken from Deacon et al, 2015 (Deacon et al., 2015), permission for reprint kindly granted.

(B) Spheroid generated from MCF7 mCherry CAIX positive and GFP CAIX negative cells incubated with the pHLIP peptide. This experiment was done by **Dr Thomas Tapmeier** as part of a collaboration. Scale bar: 250 μm

It would be interesting to further develop this experiment and to also assess pH levels in spheroids made from either population alone.

Furthermore, all experiments in this thesis have been done *in vitro*. Although 3D cultures gave an interesting insight into tumour cell organisation, an *in vivo* model would be needed to further investigate this. In line with this I would propose a zebrafish model, harnessing the advantages of the established stable colour labelling of the populations. Theses experiments are currently in the planning stage, but could unfortunately not be completed in time for the submission of the thesis.

Further exploration of metabolic pathways in CAIX positive and negative populations using carbon tracking and live imaging

To further explore the metabolic pathways in both populations, it would be crucial to assess rates of glycolysis under hypoxia. The laboratory owns a Seahorse reader, but under normoxia no differences in glycolysis were seen. Ideally, the same measurements should be taken under hypoxia; however, this was not possible with the current setup.

In this thesis, it could be shown that lactate and fatty acids play a role in the symbiotic nature of CAIX positive and negative populations. This was focussing on specific metabolites at specific time points or ranges (in the case of lactate).

Metabolites are highly interdependent on each other and there is a constant flux of compounds. To assess the level of all main metabolites in both populations a mass spectrometry experiment was done. However, it quickly became clear that the interpretation of the data was not very easy, since a low level of a compound could either mean that it was not produced or that it had been secreted or converted into the next compound in the chain.

Therefore, it would be useful to devise a similar experiment using 13C labelled carbon sources to track metabolic fluxes.

The opportunity to image lactate levels in live cells gave a good insight into the uptake and the release of this compound by both populations. However, it would be interesting to concomitantly image different carbon sources. Moreover, it would be valuable to be able to image these compounds in a 3D setting. It was attempted to optimise this by adjusting microscope settings, but it was hard to obtain high quality images. It was also tried to generate cell lines stably expressing the lactate sensing sequence by cloning it from the plasmid and inserting it into a viral vector. However, as several attempts failed it was decided not to continue this for the purpose of this thesis.

Exploration of the effects of metabolic inhibitors

It would be interesting to see whether inhibition of OxPhos and glycolysis in both populations has effects on CAIX expression. Furthermore, the inhibition of mTOR pathway components would be needed in order to study its influence on metabolic changes in CAIX positive cells, including during the co-culture and its effects on mitochondrial respiration and lipids synthesis.

Moreover, the inhibition of MCT1 and 4 would be interesting to elucidate lactate shuttling and its effect on the survival advantage during co-culture.

These inhibitors could also have an additive effect when used in combination with conventional treatment options.

Additionally, combination of these drugs with chemo- or radiotherapy may be interesting, since acidic pH has been linked to resistance to these treatment options.

Further investigation of the means of cell-cell interaction in tumours

In this thesis, a metabolic symbiosis of CAIX positive and negative cells is proposed. However, it is likely that other forms of interaction are present. For example, the initial RNA sequencing and microarray data indicated an upregulation of cytokines in the CAIX negative population including TGF-β, M-F and CXCL5. These cytokines could also act as paracrine signals, influencing the tumour microenvironment and the CAIX positive population. The actual secretion of these factors would need to be validated by ELISA. Moreover, inhibition of these factors may have an influence on cell-cell interaction and even organisation. In light of this, breast cancer stem cells have previously been shown to interact with cytokines in the tumour microenvironment (Korkaya et al., 2011).

Moreover, it would be interesting to investigate the co-culture of CAIX positive and CAIX negative populations with cancer-associated fibroblasts (CAFs) in order to study the interaction of each population with the stroma compartment and its effect on, for example, cancer stem cell behaviour and metabolite distribution.

Publications and Conference Abstracts

The following manuscripts were completed:

FELDINGER, K. & KONG, A. 2015. Profile of neratinib and its potential in the treatment of breast cancer. Breast Cancer (Dove Med Press), 7, 147-62.
(Feldinger and Kong, 2015)

Conference presentations

Heterogeneous hypoxia induced populations defined by CAIX expression display metabolic symbiosis
Poster presentation
Abcam Cancer and Metabolism Conference, 28th-30th September 2015

References

ABUMRAD, N. A., EL-MAGHRABI, M. R., AMRI, E. Z., LOPEZ, E. & GRIMALDI, P. A. 1993. Cloning of a rat adipocyte membrane protein implicated in binding or transport of long-chain fatty acids that is induced during preadipocyte differentiation. Homology with human CD36. *J Biol Chem,* 268**,** 17665-8.

AHLSKOG, J. K., DUMELIN, C. E., TRUSSEL, S., MARLIND, J. & NERI, D. 2009a. In vivo targeting of tumor-associated carbonic anhydrases using acetazolamide derivatives. *Bioorg Med Chem Lett,* 19**,** 4851-6.

AHLSKOG, J. K., SCHLIEMANN, C., MARLIND, J., QURESHI, U., AMMAR, A., PEDLEY, R. B. & NERI, D. 2009b. Human monoclonal antibodies targeting carbonic anhydrase IX for the molecular imaging of hypoxic regions in solid tumours. *British journal of cancer,* 101**,** 645-57.

AL-HAJJ, M. & CLARKE, M. F. 2004. Self-renewal and solid tumor stem cells. *Oncogene,* 23**,** 7274-82.

AL-HAJJ, M., WICHA, M. S., BENITO-HERNANDEZ, A., MORRISON, S. J. & CLARKE, M. F. 2003. Prospective identification of tumorigenic breast cancer cells. *Proc Natl Acad Sci U S A,* 100**,** 3983-8.

ALLEN, E., MIEVILLE, P., WARREN, C. M., SAGHAFINIA, S., LI, L., PENG, M. W. & HANAHAN, D. 2016. Metabolic Symbiosis Enables Adaptive Resistance to Anti-angiogenic Therapy that is dependent on mTOR signaling. *Cell Rep,* 15**,** 1144-60.

ALLRED, D. C. 2010. Ductal carcinoma in situ: terminology, classification, and natural history. *J Natl Cancer Inst Monogr,* 2010**,** 134-8.

ALPER, S. L. 2006. Molecular physiology of SLC4 anion exchangers. *Exp Physiol,* 91**,** 153-61.

ALTERIO, V., HILVO, M., DI FIORE, A., SUPURAN, C. T., PAN, P., PARKKILA, S., SCALONI, A., PASTOREK, J., PASTOREKOVA, S., PEDONE, C., SCOZZAFAVA, A., MONTI, S. M. & DE SIMONE, G. 2009. Crystal structure of the catalytic domain of the tumor-associated human carbonic anhydrase IX. *Proc Natl Acad Sci U S A,* 106**,** 16233-8.

AMORIM, R., PINHEIRO, C., MIRANDA-GONCALVES, V., PEREIRA, H., MOYER, M. P., PRETO, A. & BALTAZAR, F. 2015. Monocarboxylate transport inhibition potentiates the cytotoxic effect of 5-fluorouracil in colorectal cancer cells. *Cancer Lett,* 365**,** 68-78.

ANDERSEN, A. P., FLINCK, M., OERNBO, E. K., PEDERSEN, N. B., VIUFF, B. M. & PEDERSEN, S. F. 2016. Roles of acid-extruding ion transporters in regulation of breast cancer cell growth in a 3-dimensional microenvironment. *Mol Cancer,* 15**,** 45.

ANDERSON, K., LUTZ, C., VAN DELFT, F. W., BATEMAN, C. M., GUO, Y., COLMAN, S. M., KEMPSKI, H., MOORMAN, A. V., TITLEY, I., SWANSBURY, J., KEARNEY, L., ENVER, T. & GREAVES, M. 2011. Genetic variegation of clonal architecture and propagating cells in leukaemia. *Nature,* 469**,** 356-61.

ANDREEV, O. A., DUPUY, A. D., SEGALA, M., SANDUGU, S., SERRA, D. A., CHICHESTER, C. O., ENGELMAN, D. M. & RESHETNYAK, Y. K. 2007. Mechanism and uses of a membrane peptide that targets tumors and other acidic tissues in vivo. *Proc Natl Acad Sci U S A,* 104**,** 7893-8.

AUBELE, M., MATTIS, A., ZITZELSBERGER, H., WALCH, A., KREMER, M., HUTZLER, P., HOFLER, H. & WERNER, M. 1999. Intratumoral heterogeneity in breast carcinoma revealed by laser-microdissection and comparative genomic hybridization. *Cancer Genet Cytogenet,* 110**,** 94-102.

AUBERT, A., PELLERIN, L., MAGISTRETTI, P. J. & COSTALAT, R. 2007. A coherent neurobiological framework for functional neuroimaging provided by a model integrating compartmentalized energy metabolism. *Proc Natl Acad Sci U S A,* 104**,** 4188-93.

AVRIL, N., MENZEL, M., DOSE, J., SCHELLING, M., WEBER, W., JANICKE, F., NATHRATH, W. & SCHWAIGER, M. 2001. Glucose metabolism of breast cancer assessed by 18F-FDG PET: histologic and immunohistochemical tissue analysis. *J Nucl Med,* 42**,** 9-16.

BAILEY, A. P., KOSTER, G., GUILLERMIER, C., HIRST, E. M., MACRAE, J. I., LECHENE, C. P., POSTLE, A. D. & GOULD, A. P. 2015. Antioxidant Role for Lipid Droplets in a Stem Cell Niche of Drosophila. *Cell,* 163**,** 340-53.

BARSKI, A., CUDDAPAH, S., CUI, K., ROH, T. Y., SCHONES, D. E., WANG, Z., WEI, G., CHEPELEV, I. & ZHAO, K. 2007. High-resolution profiling of histone methylations in the human genome. *Cell,* 129**,** 823-37.

BASHANDY, M. S., ALSAID, M. S., ARAFA, R. K. & GHORAB, M. M. 2014. Design, synthesis and molecular docking of novel N,N-dimethylbenzenesulfonamide derivatives as potential antiproliferative agents. *J Enzyme Inhib Med Chem,* 29**,** 619-27.

BAUER, D. E., HATZIVASSILIOU, G., ZHAO, F., ANDREADIS, C. & THOMPSON, C. B. 2005. ATP citrate lyase is an important component of cell growth and transformation. *Oncogene,* 24**,** 6314-22.

BEASLEY, N. J., WYKOFF, C. C., WATSON, P. H., LEEK, R., TURLEY, H., GATTER, K., PASTOREK, J., COX, G. J., RATCLIFFE, P. & HARRIS, A. L. 2001. Carbonic anhydrase IX, an endogenous hypoxia marker, expression in head and neck squamous cell carcinoma and its relationship to hypoxia, necrosis, and microvessel density. *Cancer Res,* 61**,** 5262-7.

BENSAAD, K., FAVARO, E., LEWIS, C. A., PECK, B., LORD, S., COLLINS, J. M., PINNICK, K. E., WIGFIELD, S., BUFFA, F. M., LI, J. L., ZHANG, Q., WAKELAM, M. J., KARPE, F., SCHULZE, A. & HARRIS, A. L. 2014. Fatty acid uptake and lipid storage induced by HIF-1alpha contribute to cell growth and survival after hypoxia-reoxygenation. *Cell Rep,* 9**,** 349-65.

BENSAAD, K., TSURUTA, A., SELAK, M. A., VIDAL, M. N., NAKANO, K., BARTRONS, R., GOTTLIEB, E. & VOUSDEN, K. H. 2006. TIGAR, a p53-inducible regulator of glycolysis and apoptosis. *Cell,* 126**,** 107-20.

BERGER, S. L. 2007. The complex language of chromatin regulation during transcription. *Nature,* 447**,** 407-12.

BERNARDINO, J., ROUX, C., ALMEIDA, A., VOGT, N., GIBAUD, A., GERBAULT-SEUREAU, M., MAGDELENAT, H., BOURGEOIS, C. A., MALFOY, B. & DUTRILLAUX, B. 1997. DNA hypomethylation in breast cancer: an independent parameter of tumor progression? *Cancer Genet Cytogenet,* 97**,** 83-9.

BERWICK, D. C., HERS, I., HEESOM, K. J., MOULE, S. K. & TAVARE, J. M. 2002. The identification of ATP-citrate lyase as a protein kinase B (Akt) substrate in primary adipocytes. *J Biol Chem,* 277**,** 33895-900.

BINKER, M. G., BINKER-COSEN, A. A., RICHARDS, D., GAISANO, H. Y., DE COSEN, R. H. & COSEN-BINKER, L. I. 2010. Hypoxia-reoxygenation increase invasiveness of PANC-1 cells through Rac1/MMP-2. *Biochemical and Biophysical Research Communications,* 393**,** 371-376.

BOLA, B. M., CHADWICK, A. L., MICHOPOULOS, F., BLOUNT, K. G., TELFER, B. A., WILLIAMS, K. J., SMITH, P. D., CRITCHLOW, S. E. & STRATFORD, I. J. 2014. Inhibition of monocarboxylate transporter-1 (MCT1) by AZD3965 enhances radiosensitivity by reducing lactate transport. *Mol Cancer Ther,* 13**,** 2805-16.

BONUCCELLI, G., TSIRIGOS, A., WHITAKER-MENEZES, D., PAVLIDES, S., PESTELL, R. G., CHIAVARINA, B., FRANK, P. G., FLOMENBERG, N., HOWELL, A., MARTINEZ-OUTSCHOORN, U. E., SOTGIA, F. & LISANTI, M. P. 2010. Ketones and lactate "fuel" tumor growth and metastasis: Evidence that epithelial cancer cells use oxidative mitochondrial metabolism. *Cell Cycle,* 9**,** 3506-14.

BORON, W. F. 2004. Regulation of intracellular pH. *Adv Physiol Educ,* 28**,** 160-79.

BROWN, A. M., SICKMANN, H. M., FOSGERAU, K., LUND, T. M., SCHOUSBOE, A., WAAGEPETERSEN, H. S. & RANSOM, B. R. 2005. Astrocyte glycogen metabolism is required for neural activity during aglycemia or intense stimulation in mouse white matter. *J Neurosci Res,* 79**,** 74-80.

BUFFA, F. M., HARRIS, A. L., WEST, C. M. & MILLER, C. J. 2010. Large meta-analysis of multiple cancers reveals a common, compact and highly prognostic hypoxia metagene. *Br J Cancer,* 102**,** 428-35.

CAMPBELL, L. L. & POLYAK, K. 2007. Breast tumor heterogeneity: cancer stem cells or clonal evolution? *Cell Cycle,* 6**,** 2332-8.

CANCERRESEARCHUK. *Bowel cancer statistics* [Online]. Available: http://www.cancerresearchuk.org/health-professional/cancer-statistics/statistics-by-cancer-type/bowel-cancer - heading-One [Accessed July 2016].

CANCERRESEARCHUK. *Bowel Cancer TNM Staging* [Online]. Available: http://www.cancerresearchuk.org/about-cancer/type/bowel-cancer/treatment/tnm-and-number-stages-of-bowel-cancer [Accessed July 2015].

CANCERRESEARCHUK. 2014. *TNM breast cancer staging* [Online]. London: Cancer Research UK,. Available: http://www.cancerresearchuk.org/about-cancer/type/breast-cancer/treatment/tnm-breast-cancer-staging [Accessed September 24 2014].

CANCERRESEARCHUK. 2016. *Breast cancer statistics* [Online]. Available: http://www.cancerresearchuk.org/health-professional/cancer-statistics/statistics-by-cancer-type/breast-cancer - heading-Two [Accessed July 2016].

CANTOR, J. R. & SABATINI, D. M. 2012. Cancer cell metabolism: one hallmark, many faces. *Cancer Discov,* 2**,** 881-98.

CAPPARELLI, C., GUIDO, C., WHITAKER-MENEZES, D., BONUCCELLI, G., BALLIET, R., PESTELL, T. G., GOLDBERG, A. F., PESTELL, R. G., HOWELL, A., SNEDDON, S., BIRBE, R., TSIRIGOS, A., MARTINEZ-OUTSCHOORN, U., SOTGIA, F. & LISANTI, M. P. 2012a. Autophagy and senescence in cancer-associated fibroblasts metabolically supports tumor growth and metastasis via glycolysis and ketone production. *Cell Cycle,* 11**,** 2285-302.

CAPPARELLI, C., WHITAKER-MENEZES, D., GUIDO, C., BALLIET, R., PESTELL, T. G., HOWELL, A., SNEDDON, S., PESTELL, R. G., MARTINEZ-OUTSCHOORN, U., LISANTI, M. P. & SOTGIA, F. 2012b. CTGF drives autophagy, glycolysis and senescence in cancer-associated fibroblasts via HIF1 activation, metabolically promoting tumor growth. *Cell Cycle,* 11**,** 2272-84.

CARITO, V., BONUCCELLI, G., MARTINEZ-OUTSCHOORN, U. E., WHITAKER-MENEZES, D., CAROLEO, M. C., CIONE, E., HOWELL, A., PESTELL, R. G., LISANTI, M. P. & SOTGIA, F. 2012. Metabolic remodeling of the tumor microenvironment: migration stimulating factor (MSF) reprograms myofibroblasts toward lactate production, fueling anabolic tumor growth. *Cell Cycle,* 11**,** 3403-14.

CARRACEDO, A., CANTLEY, L. C. & PANDOLFI, P. P. 2013. Cancer metabolism: fatty acid oxidation in the limelight. *Nat Rev Cancer,* 13**,** 227-32.

CASTELLO-CROS, R., BONUCCELLI, G., MOLCHANSKY, A., CAPOZZA, F., WITKIEWICZ, A. K., BIRBE, R. C., HOWELL, A., PESTELL, R. G., WHITAKER-MENEZES, D., SOTGIA, F. & LISANTI, M. P. 2011. Matrix remodeling stimulates stromal autophagy, "fueling" cancer cell mitochondrial metabolism and metastasis. *Cell Cycle,* 10**,** 2021-34.

CATALDO, A. M. & BROADWELL, R. D. 1986. Cytochemical identification of cerebral glycogen and glucose-6-phosphatase activity under normal and experimental conditions. II. Choroid plexus and ependymal epithelia, endothelia and pericytes. *J Neurocytol,* 15**,** 511-24.

CHEN, C., PORE, N., BEHROOZ, A., ISMAIL-BEIGI, F. & MAITY, A. 2001. Regulation of glut1 mRNA by hypoxia-inducible factor-1. Interaction between H-ras and hypoxia. *J Biol Chem,* 276**,** 9519-25.

CHIA, S. K., WYKOFF, C. C., WATSON, P. H., HAN, C., LEEK, R. D., PASTOREK, J., GATTER, K. C., RATCLIFFE, P. & HARRIS, A. L. 2001. Prognostic significance of a novel hypoxia-regulated marker, carbonic anhydrase IX, in invasive breast carcinoma. *J Clin Oncol,* 19**,** 3660-8.

CHIANG, J. W., KARLAN, B. Y., CASS, L. & BALDWIN, R. L. 2006. BRCA1 promoter methylation predicts adverse ovarian cancer prognosis. *Gynecol Oncol,* 101**,** 403-10.

CHICHE, J., BRAHIMI-HORN, M. C. & POUYSSEGUR, J. 2010. Tumour hypoxia induces a metabolic shift causing acidosis: a common feature in cancer. *J Cell Mol Med,* 14**,** 771-94.

CHICHE, J., ILC, K., LAFERRIERE, J., TROTTIER, E., DAYAN, F., MAZURE, N. M., BRAHIMI-HORN, M. C. & POUYSSEGUR, J. 2009a. Hypoxia-inducible carbonic anhydrase IX and XII promote tumor cell growth by counteracting acidosis through the regulation of the intracellular pH. *Cancer research,* 69**,** 358-68.

CHICHE, J., ILC, K., LAFERRIERE, J., TROTTIER, E., DAYAN, F., MAZURE, N. M., BRAHIMI-HORN, M. C. & POUYSSEGUR, J. 2009b. Hypoxia-inducible carbonic anhydrase IX and XII promote tumor cell growth by counteracting acidosis through the regulation of the intracellular pH. *Cancer Res,* 69**,** 358-68.

CHOI, H. B., GORDON, G. R., ZHOU, N., TAI, C., RUNGTA, R. L., MARTINEZ, J., MILNER, T. A., RYU, J. K., MCLARNON, J. G., TRESGUERRES, M., LEVIN, L. R., BUCK, J. & MACVICAR, B. A. 2012. Metabolic communication between

astrocytes and neurons via bicarbonate-responsive soluble adenylyl cyclase. *Neuron,* 75**,** 1094-104.

CHOI, J., KIM DO, H., JUNG, W. H. & KOO, J. S. 2013. Metabolic interaction between cancer cells and stromal cells according to breast cancer molecular subtype. *Breast Cancer Res,* 15**,** R78.

CHRASTINA, A., PASTOREKOVA, S. & PASTOREK, J. 2003a. Immunotargeting of human cervical carcinoma xenograft expressing CA IX tumor-associated antigen by 125I-labeled M75 monoclonal antibody. *Neoplasma,* 50**,** 13-21.

CHRASTINA, A., ZAVADA, J., PARKKILA, S., KALUZ, S., KALUZOVA, M., RAJCANI, J., PASTOREK, J. & PASTOREKOVA, S. 2003b. Biodistribution and pharmacokinetics of 125I-labeled monoclonal antibody M75 specific for carbonic anhydrase IX, an intrinsic marker of hypoxia, in nude mice xenografted with human colorectal carcinoma. *Int J Cancer,* 105**,** 873-81.

CHRISTOFK, H. R., VANDER HEIDEN, M. G., HARRIS, M. H., RAMANATHAN, A., GERSZTEN, R. E., WEI, R., FLEMING, M. D., SCHREIBER, S. L. & CANTLEY, L. C. 2008. The M2 splice isoform of pyruvate kinase is important for cancer metabolism and tumour growth. *Nature,* 452**,** 230-3.

CIANCHI, F., VINCI, M. C., SUPURAN, C. T., PERUZZI, B., DE GIULI, P., FASOLIS, G., PERIGLI, G., PASTOREKOVA, S., PAPUCCI, L., PINI, A., MASINI, E. & PUCCETTI, L. 2010. Selective inhibition of carbonic anhydrase IX decreases cell proliferation and induces ceramide-mediated apoptosis in human cancer cells. *J Pharmacol Exp Ther,* 334**,** 710-9.

CLINICALTRIAL.GOV. 2016. *A Phase I Trial of AZD3965 in Patients With Advanced Cancer* [Online]. U.S. National Institutes of Health. Available: https://clinicaltrials.gov/show/NCT01791595. [Accessed June 13 2016].

CLOUTIER, M., BOLGER, F. B., LOWRY, J. P. & WELLSTEAD, P. 2009. An integrative dynamic model of brain energy metabolism using in vivo neurochemical measurements. *J Comput Neurosci,* 27**,** 391-414.

CLYNES, R. A., TOWERS, T. L., PRESTA, L. G. & RAVETCH, J. V. 2000. Inhibitory Fc receptors modulate in vivo cytotoxicity against tumor targets. *Nat Med,* 6**,** 443-6.

CONLEY, S. J., GHEORDUNESCU, E., KAKARALA, P., NEWMAN, B., KORKAYA, H., HEATH, A. N., CLOUTHIER, S. G. & WICHA, M. S. 2012. Antiangiogenic agents increase breast cancer stem cells via the generation of tumor hypoxia. *Proceedings of the National Academy of Sciences of the United States of America,* 109**,** 2784-9.

COSTELLO, J. F., FRUHWALD, M. C., SMIRAGLIA, D. J., RUSH, L. J., ROBERTSON, G. P., GAO, X., WRIGHT, F. A., FERAMISCO, J. D., PELTOMAKI, P., LANG, J. C., SCHULLER, D. E., YU, L., BLOOMFIELD, C. D., CALIGIURI, M. A., YATES, A., NISHIKAWA, R., SU HUANG, H., PETRELLI, N. J., ZHANG, X., O'DORISIO, M. S., HELD, W. A., CAVENEE, W. K. & PLASS, C. 2000. Aberrant CpG-island methylation has non-random and tumour-type-specific patterns. *Nat Genet,* 24**,** 132-8.

COVELLO, K. L., KEHLER, J., YU, H., GORDAN, J. D., ARSHAM, A. M., HU, C. J., LABOSKY, P. A., SIMON, M. C. & KEITH, B. 2006. HIF-2alpha regulates Oct-4: effects of hypoxia on stem cell function, embryonic development, and tumor growth. *Genes Dev,* 20**,** 557-70.

CULTER, S. J., BLACK, M. M. & GOLDENBERG, I. S. 1963. Prognostic Factors in Cancer of the Female Breast. I. An Investigation of Some Interrelations. *Cancer,* 16**,** 1589-97.

CURRY, J. M., TULUC, M., WHITAKER-MENEZES, D., AMES, J. A., ANANTHARAMAN, A., BUTERA, A., LEIBY, B., COGNETTI, D. M., SOTGIA, F., LISANTI, M. P. & MARTINEZ-OUTSCHOORN, U. E. 2013. Cancer metabolism, stemness and tumor recurrence: MCT1 and MCT4 are functional biomarkers of metabolic symbiosis in head and neck cancer. *Cell Cycle,* 12**,** 1371-84.

CURTIS, C., SHAH, S. P., CHIN, S. F., TURASHVILI, G., RUEDA, O. M., DUNNING, M. J., SPEED, D., LYNCH, A. G., SAMARAJIWA, S., YUAN, Y., GRAF, S., HA, G., HAFFARI, G., BASHASHATI, A., RUSSELL, R., MCKINNEY, S., GROUP, M., LANGEROD, A., GREEN, A., PROVENZANO, E., WISHART, G., PINDER, S., WATSON, P., MARKOWETZ, F., MURPHY, L., ELLIS, I., PURUSHOTHAM, A., BORRESEN-DALE, A. L., BRENTON, J. D., TAVARE, S., CALDAS, C. & APARICIO, S. 2012. The genomic and transcriptomic architecture of 2,000 breast tumours reveals novel subgroups. *Nature,* 486**,** 346-52.

CUYAS, E., COROMINAS-FAJA, B. & MENENDEZ, J. A. 2014. The nutritional phenome of EMT-induced cancer stem-like cells. *Oncotarget,* 5**,** 3970-82.

DA MOTTA, L. L., LEDAKI, I., PURSHOUSE, K., HAIDER, S., DE BASTIANI, M. A., BABAN, D., MOROTTI, M., STEERS, G., WIGFIELD, S., BRIDGES, E., LI, J. L., KNAPP, S., EBNER, D., KLAMT, F., HARRIS, A. L. & MCINTYRE, A. 2016. The BET inhibitor JQ1 selectively impairs tumour response to hypoxia and downregulates CA9 and angiogenesis in triple negative breast cancer. *Oncogene*.

DAI, X. Y., ZHUANG, L. H., WANG, D. D., ZHOU, T. Y., CHANG, L. L., GAI, R. H., ZHU, D. F., YANG, B., ZHU, H. & HE, Q. J. 2016. Nuclear translocation and activation of YAP by hypoxia contributes to the chemoresistance of SN38 in hepatocellular carcinoma cells. *Oncotarget*.

DANG, C. V. & SEMENZA, G. L. 1999. Oncogenic alterations of metabolism. *Trends Biochem Sci,* 24**,** 68-72.

DANG, L., WHITE, D. W., GROSS, S., BENNETT, B. D., BITTINGER, M. A., DRIGGERS, E. M., FANTIN, V. R., JANG, H. G., JIN, S., KEENAN, M. C., MARKS, K. M., PRINS, R. M., WARD, P. S., YEN, K. E., LIAU, L. M., RABINOWITZ, J. D., CANTLEY, L. C., THOMPSON, C. B., VANDER HEIDEN, M. G. & SU, S. M. 2009. Cancer-associated IDH1 mutations produce 2-hydroxyglutarate. *Nature,* 462**,** 739-44.

DAVIS, I. D., WISEMAN, G. A., LEE, F. T., GANSEN, D. N., HOPKINS, W., PAPENFUSS, A. T., LIU, Z., MOYNIHAN, T. J., CROGHAN, G. A., ADJEI, A. A., HOFFMAN, E. W., INGLE, J. N., OLD, L. J. & SCOTT, A. M. 2007. A phase I multiple dose, dose escalation study of cG250 monoclonal antibody in patients with advanced renal cell carcinoma. *Cancer Immun,* 7**,** 13.

DE SIMONE, G. & SUPURAN, C. T. 2010. Carbonic anhydrase IX: Biochemical and crystallographic characterization of a novel antitumor target. *Biochim Biophys Acta,* 1804**,** 404-9.

DEACON, J. C., ENGELMAN, D. M. & BARRERA, F. N. 2015. Targeting acidity in diseased tissues: mechanism and applications of the membrane-inserting peptide, pHLIP. *Arch Biochem Biophys,* 565**,** 40-8.

DEBERARDINIS, R. J., MANCUSO, A., DAIKHIN, E., NISSIM, I., YUDKOFF, M., WEHRLI, S. & THOMPSON, C. B. 2007. Beyond aerobic glycolysis: transformed cells can engage in glutamine metabolism that exceeds the requirement for protein and nucleotide synthesis. *Proceedings of the National Academy of Sciences of the United States of America,* 104**,** 19345-50.

DIAZ-CANO, S. J. 2012. Tumor heterogeneity: mechanisms and bases for a reliable application of molecular marker design. *Int J Mol Sci,* 13**,** 1951-2011.

DIRAT, B., BOCHET, L., DABEK, M., DAVIAUD, D., DAUVILLIER, S., MAJED, B., WANG, Y. Y., MEULLE, A., SALLES, B., LE GONIDEC, S., GARRIDO, I., ESCOURROU, G., VALET, P. & MULLER, C. 2011. Cancer-associated adipocytes exhibit an activated phenotype and contribute to breast cancer invasion. *Cancer Res,* 71**,** 2455-65.

DUBOIS, L., PEETERS, S., LIEUWES, N. G., GEUSENS, N., THIRY, A., WIGFIELD, S., CARTA, F., MCINTYRE, A., SCOZZAFAVA, A., DOGNE, J. M., SUPURAN, C. T., HARRIS, A. L., MASEREEL, B. & LAMBIN, P. 2011. Specific inhibition of carbonic anhydrase IX activity enhances the in vivo therapeutic effect of tumor irradiation. *Radiother Oncol,* 99**,** 424-31.

DUVEL, K., YECIES, J. L., MENON, S., RAMAN, P., LIPOVSKY, A. I., SOUZA, A. L., TRIANTAFELLOW, E., MA, Q., GORSKI, R., CLEAVER, S., VANDER HEIDEN, M. G., MACKEIGAN, J. P., FINAN, P. M., CLISH, C. B., MURPHY, L. O. & MANNING, B. D. 2010. Activation of a metabolic gene regulatory network downstream of mTOR complex 1. *Mol Cell,* 39**,** 171-83.

EHRLICH, M., JIANG, G., FIALA, E., DOME, J. S., YU, M. C., LONG, T. I., YOUN, B., SOHN, O. S., WIDSCHWENDTER, M., TOMLINSON, G. E., CHINTAGUMPALA, M., CHAMPAGNE, M., PARHAM, D., LIANG, G., MALIK, K. & LAIRD, P. W. 2002. Hypomethylation and hypermethylation of DNA in Wilms tumors. *Oncogene,* 21**,** 6694-702.

ELSTROM, R. L., BAUER, D. E., BUZZAI, M., KARNAUSKAS, R., HARRIS, M. H., PLAS, D. R., ZHUANG, H., CINALLI, R. M., ALAVI, A., RUDIN, C. M. & THOMPSON, C. B. 2004. Akt stimulates aerobic glycolysis in cancer cells. *Cancer Res,* 64**,** 3892-9.

ERTEL, A., TSIRIGOS, A., WHITAKER-MENEZES, D., BIRBE, R. C., PAVLIDES, S., MARTINEZ-OUTSCHOORN, U. E., PESTELL, R. G., HOWELL, A., SOTGIA, F. & LISANTI, M. P. 2012. Is cancer a metabolic rebellion against host aging? In the quest for immortality, tumor cells try to save themselves by boosting mitochondrial metabolism. *Cell Cycle,* 11**,** 253-63.

ESPI, M. 2015. *Characterization of the mechanisms by which Carbonic Anhydrase IX facilitates tumour growth and metastasis.* DPhil, University of British Columbia.

ESTELLER, M., CORN, P. G., BAYLIN, S. B. & HERMAN, J. G. 2001. A gene hypermethylation profile of human cancer. *Cancer Res,* 61**,** 3225-9.

ESTELLER, M., TOYOTA, M., SANCHEZ-CESPEDES, M., CAPELLA, G., PEINADO, M. A., WATKINS, D. N., ISSA, J. P., SIDRANSKY, D., BAYLIN, S. B. & HERMAN, J. G. 2000. Inactivation of the DNA repair gene O6-methylguanine-DNA methyltransferase by promoter hypermethylation is associated with G to A mutations in K-ras in colorectal tumorigenesis. *Cancer Res,* 60**,** 2368-71.

ESTRELLA, V., CHEN, T., LLOYD, M., WOJTKOWIAK, J., CORNNELL, H. H., IBRAHIM-HASHIM, A., BAILEY, K., BALAGURUNATHAN, Y., ROTHBERG, J.

M., SLOANE, B. F., JOHNSON, J., GATENBY, R. A. & GILLIES, R. J. 2013. Acidity generated by the tumor microenvironment drives local invasion. *Cancer Res,* 73**,** 1524-35.

EZASHI, T., DAS, P. & ROBERTS, R. M. 2005. Low O2 tensions and the prevention of differentiation of hES cells. *Proc Natl Acad Sci U S A,* 102**,** 4783-8.

FAVARO, E., LORD, S., HARRIS, A. L. & BUFFA, F. M. 2011. Gene expression and hypoxia in breast cancer. *Genome Med,* 3**,** 55.

FEINBERG, A. P. & VOGELSTEIN, B. 1983a. Hypomethylation distinguishes genes of some human cancers from their normal counterparts. *Nature,* 301**,** 89-92.

FEINBERG, A. P. & VOGELSTEIN, B. 1983b. Hypomethylation of ras oncogenes in primary human cancers. *Biochem Biophys Res Commun,* 111**,** 47-54.

FELDINGER, K. & KONG, A. 2015. Profile of neratinib and its potential in the treatment of breast cancer. *Breast Cancer (Dove Med Press),* 7**,** 147-62.

FIASCHI, T., MARINI, A., GIANNONI, E., TADDEI, M. L., GANDELLINI, P., DE DONATIS, A., LANCIOTTI, M., SERNI, S., CIRRI, P. & CHIARUGI, P. 2012. Reciprocal metabolic reprogramming through lactate shuttle coordinately influences tumor-stroma interplay. *Cancer Res,* 72**,** 5130-40.

FILION, G. J., VAN BEMMEL, J. G., BRAUNSCHWEIG, U., TALHOUT, W., KIND, J., WARD, L. D., BRUGMAN, W., DE CASTRO, I. J., KERKHOVEN, R. M., BUSSEMAKER, H. J. & VAN STEENSEL, B. 2010. Systematic protein location mapping reveals five principal chromatin types in Drosophila cells. *Cell,* 143**,** 212-24.

FÖRSTER, T. 1948. Intermolecular energy migration and fluorescence. *Annalen der Physik,* 437**,** 55-75.

FORSYTHE, J. A., JIANG, B. H., IYER, N. V., AGANI, F., LEUNG, S. W., KOOS, R. D. & SEMENZA, G. L. 1996. Activation of vascular endothelial growth factor gene transcription by hypoxia-inducible factor 1. *Mol Cell Biol,* 16**,** 4604-13.

FUJIWARA, S., WADA, N., KAWANO, Y., OKUNO, Y., KIKUKAWA, Y., ENDO, S., NISHIMURA, N., UENO, N., MITSUYA, H. & HATA, H. 2015. Lactate, a putative survival factor for myeloma cells, is incorporated by myeloma cells through monocarboxylate transporters 1. *Exp Hematol Oncol,* 4**,** 12.

GAGLIO, D., METALLO, C. M., GAMEIRO, P. A., HILLER, K., DANNA, L. S., BALESTRIERI, C., ALBERGHINA, L., STEPHANOPOULOS, G. & CHIARADONNA, F. 2011. Oncogenic K-Ras decouples glucose and glutamine metabolism to support cancer cell growth. *Mol Syst Biol,* 7**,** 523.

GALDIERI, L. & VANCURA, A. 2012. Acetyl-CoA carboxylase regulates global histone acetylation. *J Biol Chem,* 287**,** 23865-76.

GALLAGHER, F. A., SLADEN, H., KETTUNEN, M. I., SERRAO, E. M., RODRIGUES, T. B., WRIGHT, A., GILL, A. B., MCGUIRE, S., BOOTH, T. C., BOREN, J., MCINTYRE, A., MILLER, J. L., LEE, S. H., HONESS, D., DAY, S. E., HU, D. E., HOWAT, W. J., HARRIS, A. L. & BRINDLE, K. M. 2015. Carbonic Anhydrase Activity Monitored In Vivo by Hyperpolarized 13C-Magnetic Resonance Spectroscopy Demonstrates Its Importance for pH Regulation in Tumors. *Cancer Res,* 75**,** 4109-18.

GAMA-SOSA, M. A., SLAGEL, V. A., TREWYN, R. W., OXENHANDLER, R., KUO, K. C., GEHRKE, C. W. & EHRLICH, M. 1983. The 5-methylcytosine content of DNA from human tumors. *Nucleic Acids Res,* 11**,** 6883-94.

GATENBY, R. A. & GAWLINSKI, E. T. 1996. A reaction-diffusion model of cancer invasion. *Cancer Res,* 56**,** 5745-53.

GATENBY, R. A. & GILLIES, R. J. 2004. Why do cancers have high aerobic glycolysis? *Nat Rev Cancer,* 4**,** 891-9.

GENNARI, R., MENARD, S., FAGNONI, F., PONCHIO, L., SCELSI, M., TAGLIABUE, E., CASTIGLIONI, F., VILLANI, L., MAGALOTTI, C., GIBELLI, N., OLIVIERO, B., BALLARDINI, B., DA PRADA, G., ZAMBELLI, A. & COSTA, A. 2004. Pilot study of the mechanism of action of preoperative trastuzumab in patients with primary operable breast tumors overexpressing HER2. *Clin Cancer Res,* 10**,** 5650-5.

GERTZ, E. W., WISNESKI, J. A., STANLEY, W. C. & NEESE, R. A. 1988. Myocardial substrate utilization during exercise in humans. Dual carbon-labeled carbohydrate isotope experiments. *J Clin Invest,* 82**,** 2017-25.

GIATROMANOLAKI, A., KOUKOURAKIS, M. I., SIVRIDIS, E., PASTOREK, J., WYKOFF, C. C., GATTER, K. C. & HARRIS, A. L. 2001. Expression of hypoxia-inducible carbonic anhydrase-9 relates to angiogenic pathways and independently to poor outcome in non-small cell lung cancer. *Cancer Res,* 61**,** 7992-8.

GIELING, R. G., BABUR, M., MAMNANI, L., BURROWS, N., TELFER, B. A., CARTA, F., WINUM, J. Y., SCOZZAFAVA, A., SUPURAN, C. T. & WILLIAMS, K. J. 2012. Antimetastatic effect of sulfamate carbonic anhydrase IX inhibitors in breast carcinoma xenografts. *J Med Chem,* 55**,** 5591-600.

GILLIES, R. J., RAGHUNAND, N., GARCIA-MARTIN, M. L. & GATENBY, R. A. 2004. pH imaging. A review of pH measurement methods and applications in cancers. *IEEE Eng Med Biol Mag,* 23**,** 57-64.

GILLIES, R. J., RAGHUNAND, N., KARCZMAR, G. S. & BHUJWALLA, Z. M. 2002. MRI of the tumor microenvironment. *J Magn Reson Imaging,* 16**,** 430-50.

GIOIA, M., FASCIGLIONE, G. F., MONACO, S., IUNDUSI, R., SBARDELLA, D., MARINI, S., TARANTINO, U. & COLETTA, M. 2010. pH dependence of the enzymatic processing of collagen I by MMP-1 (fibroblast collagenase), MMP-2 (gelatinase A), and MMP-14 ectodomain. *J Biol Inorg Chem,* 15**,** 1219-32.

GORDAN, J. D., BERTOUT, J. A., HU, C. J., DIEHL, J. A. & SIMON, M. C. 2007. HIF-2alpha promotes hypoxic cell proliferation by enhancing c-myc transcriptional activity. *Cancer Cell,* 11**,** 335-47.

GOTTLIEB, E. & VOUSDEN, K. H. 2010. p53 regulation of metabolic pathways. *Cold Spring Harb Perspect Biol,* 2**,** a001040.

GRABMAIER, K., MC, A. D. W., VERHAEGH, G. W., SCHALKEN, J. A. & OOSTERWIJK, E. 2004. Strict regulation of CAIX(G250/MN) by HIF-1alpha in clear cell renal cell carcinoma. *Oncogene,* 23**,** 5624-31.

GRAEBER, T. G., OSMANIAN, C., JACKS, T., HOUSMAN, D. E., KOCH, C. J., LOWE, S. W. & GIACCIA, A. J. 1996. Hypoxia-mediated selection of cells with diminished apoptotic potential in solid tumours. *Nature,* 379**,** 88-91.

GRAWENDA, A. M. & O'NEILL, E. 2015. Clinical utility of RASSF1A methylation in human malignancies. *Br J Cancer,* 113**,** 372-81.

GURRAPU, S., JONNALAGADDA, S. K., ALAM, M. A., RONAYNE, C. T., NELSON, G. L., SOLANO, L. N., LUETH, E. A., DREWES, L. R. & MEREDDY, V. R. 2016. Coumarin carboxylic acids as monocarboxylate transporter 1 inhibitors: In vitro and in vivo studies as potential anticancer agents. *Bioorg Med Chem Lett,* 26**,** 3282-6.

HAINSWORTH, J. D., DAUGAARD, G., LESIMPLE, T., HUBNER, G., GRECO, F. A., STAHL, M. J., BUSCHENFELDE, C. M., ALLOUACHE, D., PENEL, N., KNOBLAUCH, P. & FIZAZI, K. S. 2015. Paclitaxel/carboplatin with or without belinostat as empiric first-line treatment for patients with carcinoma of unknown primary site: A randomized, phase 2 trial. *Cancer,* 121**,** 1654-61.

HAN, J. Y., LEE, S. H., LEE, G. K., YUN, T., LEE, Y. J., HWANG, K. H., KIM, J. Y. & KIM, H. T. 2015. Phase I/II study of gefitinib (Iressa((R))) and vorinostat (IVORI) in previously treated patients with advanced non-small cell lung cancer. *Cancer Chemother Pharmacol,* 75**,** 475-83.

HANAHAN, D. & WEINBERG, R. A. 2000. The hallmarks of cancer. *Cell,* 100**,** 57-70.

HANAHAN, D. & WEINBERG, R. A. 2011. Hallmarks of cancer: the next generation. *Cell,* 144**,** 646-74.

HARJES, U., KALUCKA, J. & CARMELIET, P. 2016. Targeting fatty acid metabolism in cancer and endothelial cells. *Crit Rev Oncol Hematol,* 97**,** 15-21.

HARRELL, J. C., PRAT, A., PARKER, J. S., FAN, C., HE, X., CAREY, L., ANDERS, C., EWEND, M. & PEROU, C. M. 2012. Genomic analysis identifies unique signatures predictive of brain, lung, and liver relapse. *Breast Cancer Res Treat,* 132**,** 523-35.

HARRIS, A. L. 2002. Hypoxia--a key regulatory factor in tumour growth. *Nat Rev Cancer,* 2**,** 38-47.

HARRIS, L., FRITSCHE, H., MENNEL, R., NORTON, L., RAVDIN, P., TAUBE, S., SOMERFIELD, M. R., HAYES, D. F., BAST, R. C., JR. & AMERICAN SOCIETY OF CLINICAL, O. 2007. American Society of Clinical Oncology 2007 update of recommendations for the use of tumor markers in breast cancer. *J Clin Oncol,* 25**,** 5287-312.

HARRISON, J. S., RAMESHWAR, P., CHANG, V. & BANDARI, P. 2002. Oxygen saturation in the bone marrow of healthy volunteers. *Blood,* 99**,** 394.

HASHIMOTO, T., HUSSIEN, R., CHO, H. S., KAUFER, D. & BROOKS, G. A. 2008. Evidence for the mitochondrial lactate oxidation complex in rat neurons: demonstration of an essential component of brain lactate shuttles. *PLoS One,* 3**,** e2915.

HATZIVASSILIOU, G., ZHAO, F., BAUER, D. E., ANDREADIS, C., SHAW, A. N., DHANAK, D., HINGORANI, S. R., TUVESON, D. A. & THOMPSON, C. B. 2005. ATP citrate lyase inhibition can suppress tumor cell growth. *Cancer Cell,* 8**,** 311-21.

HE, Y. F., LI, B. Z., LI, Z., LIU, P., WANG, Y., TANG, Q., DING, J., JIA, Y., CHEN, Z., LI, L., SUN, Y., LI, X., DAI, Q., SONG, C. X., ZHANG, K., HE, C. & XU, G. L. 2011. Tet-mediated formation of 5-carboxylcytosine and its excision by TDG in mammalian DNA. *Science,* 333**,** 1303-7.

HEDDLESTON, J. M., LI, Z., LATHIA, J. D., BAO, S., HJELMELAND, A. B. & RICH, J. N. 2010a. Hypoxia inducible factors in cancer stem cells. *British journal of cancer,* 102**,** 789-95.

HEDDLESTON, J. M., LI, Z., LATHIA, J. D., BAO, S., HJELMELAND, A. B. & RICH, J. N. 2010b. Hypoxia inducible factors in cancer stem cells. *Br J Cancer,* 102**,** 789-95.

HEGEDUS, C., TRUTA-FELES, K., ANTALFFY, G., VARADY, G., NEMET, K., OZVEGY-LACZKA, C., KERI, G., ORFI, L., SZAKACS, G., SETTLEMAN, J., VARADI, A. & SARKADI, B. 2012. Interaction of the EGFR inhibitors gefitinib, vandetanib,

pelitinib and neratinib with the ABCG2 multidrug transporter: implications for the emergence and reversal of cancer drug resistance. *Biochem Pharmacol,* 84**,** 260-7.

HEWITSON, K. S., MCNEILL, L. A., RIORDAN, M. V., TIAN, Y. M., BULLOCK, A. N., WELFORD, R. W., ELKINS, J. M., OLDHAM, N. J., BHATTACHARYA, S., GLEADLE, J. M., RATCLIFFE, P. J., PUGH, C. W. & SCHOFIELD, C. J. 2002. Hypoxia-inducible factor (HIF) asparagine hydroxylase is identical to factor inhibiting HIF (FIH) and is related to the cupin structural family. *J Biol Chem,* 277**,** 26351-5.

HILL, R. P. 2006. Identifying cancer stem cells in solid tumors: case not proven. *Cancer Res,* 66**,** 1891-5; discussion 1890.

HILL, S. A., PIGOTT, K. H., SAUNDERS, M. I., POWELL, M. E. B., ARNOLD, S., OBEID, A., WARD, G., LEAHY, M., HOSKIN, P. J. & CHAPLIN, D. J. 1996. Microregional blood flow in murine and human tumours assessed using laser Doppler microprobes. *British Journal of Cancer,* 74**,** S260-S263.

HILVO, M., BARANAUSKIENE, L., SALZANO, A. M., SCALONI, A., MATULIS, D., INNOCENTI, A., SCOZZAFAVA, A., MONTI, S. M., DI FIORE, A., DE SIMONE, G., LINDFORS, M., JANIS, J., VALJAKKA, J., PASTOREKOVA, S., PASTOREK, J., KULOMAA, M. S., NORDLUND, H. R., SUPURAN, C. T. & PARKKILA, S. 2008. Biochemical characterization of CA IX, one of the most active carbonic anhydrase isozymes. *J Biol Chem,* 283**,** 27799-809.

HINOUE, T., WEISENBERGER, D. J., LANGE, C. P., SHEN, H., BYUN, H. M., VAN DEN BERG, D., MALIK, S., PAN, F., NOUSHMEHR, H., VAN DIJK, C. M., TOLLENAAR, R. A. & LAIRD, P. W. 2012. Genome-scale analysis of aberrant DNA methylation in colorectal cancer. *Genome Res,* 22**,** 271-82.

HIRAGA, T., ITO, S. & NAKAMURA, H. 2011. Side population in MDA-MB-231 human breast cancer cells exhibits cancer stem cell-like properties without higher bone-metastatic potential. *Oncology Reports,* 25**,** 289-296.

HOCHEDLINGER, K. & PLATH, K. 2009. Epigenetic reprogramming and induced pluripotency. *Development,* 136**,** 509-23.

HONG, C. S., GRAHAM, N. A., GU, W., ESPINDOLA CAMACHO, C., MAH, V., MARESH, E. L., ALAVI, M., BAGRYANOVA, L., KROTEE, P. A., GARDNER, B. K., BEHBAHAN, I. S., HORVATH, S., CHIA, D., MELLINGHOFF, I. K., HURVITZ, S. A., DUBINETT, S. M., CRITCHLOW, S. E., KURDISTANI, S. K., GOODGLICK, L., BRAAS, D., GRAEBER, T. G. & CHRISTOFK, H. R. 2016. MCT1 Modulates Cancer Cell Pyruvate Export and Growth of Tumors that Co-express MCT1 and MCT4. *Cell Rep,* 14**,** 1590-601.

HULIKOVA, A., ZATOVICOVA, M., SVASTOVA, E., DITTE, P., BRASSEUR, R., KETTMANN, R., SUPURAN, C. T., KOPACEK, J., PASTOREK, J. & PASTOREKOVA, S. 2009. Intact intracellular tail is critical for proper functioning of the tumor-associated, hypoxia-regulated carbonic anhydrase IX. *Febs Letters,* 583**,** 3563-3568.

HUTCHINS, G., SOUTHWARD, K., HANDLEY, K., MAGILL, L., BEAUMONT, C., STAHLSCHMIDT, J., RICHMAN, S., CHAMBERS, P., SEYMOUR, M., KERR, D., GRAY, R. & QUIRKE, P. 2011. Value of mismatch repair, KRAS, and BRAF mutations in predicting recurrence and benefits from chemotherapy in colorectal cancer. *J Clin Oncol,* 29**,** 1261-70.

IAKOVLEV, V. V., PINTILIE, M., MORRISON, A., FYLES, A. W., HILL, R. P. & HEDLEY, D. W. 2007. Effect of distributional heterogeneity on the analysis of tumor hypoxia based on carbonic anhydrase IX. *Lab Invest,* 87**,** 1206-17.

ICHIM, C. V. & WELLS, R. A. 2006. First among equals: the cancer cell hierarchy. *Leuk Lymphoma,* 47**,** 2017-27.

IHNATKO, R., KUBES, M., TAKACOVA, M., SEDLAKOVA, O., SEDLAK, J., PASTOREK, J., KOPACEK, J. & PASTOREKOVA, S. 2006. Extracellular acidosis elevates carbonic anhydrase IX in human glioblastoma cells via transcriptional modulation that does not depend on hypoxia. *International journal of oncology,* 29**,** 1025-33.

ILIE, M., MAZURE, N. M., HOFMAN, V., AMMADI, R. E., ORTHOLAN, C., BONNETAUD, C., HAVET, K., VENISSAC, N., MOGRABI, B., MOUROUX, J., POUYSSEGUR, J. & HOFMAN, P. 2010. High levels of carbonic anhydrase IX in tumour tissue and plasma are biomarkers of poor prognostic in patients with non-small cell lung cancer. *British journal of cancer,* 102**,** 1627-35.

ILLINGWORTH, R. S., GRUENEWALD-SCHNEIDER, U., WEBB, S., KERR, A. R., JAMES, K. D., TURNER, D. J., SMITH, C., HARRISON, D. J., ANDREWS, R. & BIRD, A. P. 2010. Orphan CpG islands identify numerous conserved promoters in the mammalian genome. *PLoS Genet,* 6**,** e1001134.

INNOCENTI, A., PASTOREKOVA, S., PASTOREK, J., SCOZZAFAVA, A., DE SIMONE, G. & SUPURAN, C. T. 2009. The proteoglycan region of the tumor-associated carbonic anhydrase isoform IX acts as anintrinsic buffer optimizing CO2 hydration at acidic pH values characteristic of solid tumors. *Bioorganic & Medicinal Chemistry Letters,* 19**,** 5825-5828.

ITO, K., CARRACEDO, A., WEISS, D., ARAI, F., ALA, U., AVIGAN, D. E., SCHAFER, Z. T., EVANS, R. M., SUDA, T., LEE, C. H. & PANDOLFI, P. P. 2012. A PML-PPAR-delta pathway for fatty acid oxidation regulates hematopoietic stem cell maintenance. *Nat Med,* 18**,** 1350-8.

ITO, S., SHEN, L., DAI, Q., WU, S. C., COLLINS, L. B., SWENBERG, J. A., HE, C. & ZHANG, Y. 2011. Tet proteins can convert 5-methylcytosine to 5-formylcytosine and 5-carboxylcytosine. *Science,* 333**,** 1300-3.

IVANOVIC, Z., DELLO SBARBA, P., TRIMOREAU, F., FAUCHER, J. L. & PRALORAN, V. 2000. Primitive human HPCs are better maintained and expanded in vitro at 1 percent oxygen than at 20 percent. *Transfusion,* 40**,** 1482-8.

JAMALI, S., KLIER, M., AMES, S., BARROS, L. F., MCKENNA, R., DEITMER, J. W. & BECKER, H. M. 2015. Hypoxia-induced carbonic anhydrase IX facilitates lactate flux in human breast cancer cells by non-catalytic function. *Sci Rep,* 5**,** 13605.

JASS, J. R. 2007. Classification of colorectal cancer based on correlation of clinical, morphological and molecular features. *Histopathology,* 50**,** 113-30.

JETER, C. R., LIU, B., LIU, X., CHEN, X., LIU, C., CALHOUN-DAVIS, T., REPASS, J., ZAEHRES, H., SHEN, J. J. & TANG, D. G. 2011. NANOG promotes cancer stem cell characteristics and prostate cancer resistance to androgen deprivation. *Oncogene,* 30**,** 3833-45.

JIANG, B. H., RUE, E., WANG, G. L., ROE, R. & SEMENZA, G. L. 1996. Dimerization, DNA binding, and transactivation properties of hypoxia-inducible factor 1. *J Biol Chem,* 271**,** 17771-8.

JIMENEZ-VALERIO, G., MARTINEZ-LOZANO, M., BASSANI, N., VIDAL, A., OCHOA-DE-OLZA, M., SUAREZ, C., GARCIA-DEL-MURO, X., CARLES, J., VINALS, F., GRAUPERA, M., INDRACCOLO, S. & CASANOVAS, O. 2016. Resistance to Antiangiogenic Therapies by Metabolic Symbiosis in Renal Cell Carcinoma PDX Models and Patients. *Cell Rep,* 15**,** 1134-43.

JOENSUU, H., BONO, P., KATAJA, V., ALANKO, T., KOKKO, R., ASOLA, R., UTRIAINEN, T., TURPEENNIEMI-HUJANEN, T., JYRKKIO, S., MOYKKYNEN, K., HELLE, L., INGALSUO, S., PAJUNEN, M., HUUSKO, M., SALMINEN, T., AUVINEN, P., LEINONEN, H., LEINONEN, M., ISOLA, J. & KELLOKUMPU-LEHTINEN, P. L. 2009. Fluorouracil, epirubicin, and cyclophosphamide with either docetaxel or vinorelbine, with or without trastuzumab, as adjuvant treatments of breast cancer: final results of the FinHer Trial. *J Clin Oncol,* 27**,** 5685-92.

JOHNSON, A. B., DENKO, N. & BARTON, M. C. 2008. Hypoxia induces a novel signature of chromatin modifications and global repression of transcription. *Mutation research,* 640**,** 174-9.

JONATHAN, R. A., WIJFFELS, K. I., PEETERS, W., DE WILDE, P. C., MARRES, H. A., MERKX, M. A., OOSTERWIJK, E., VAN DER KOGEL, A. J. & KAANDERS, J. H. 2006. The prognostic value of endogenous hypoxia-related markers for head and neck squamous cell carcinomas treated with ARCON. *Radiother Oncol,* 79**,** 288-97.

KAJO, K., TURCAN, I., VALLOVA, M., LABOS, T., KAJO, M., MACHALEKOVA, K., S, G. & ZUBOR, P. 2013. [Expression of carbonic anhydrase IX in the breast carcinomas]. *Ceska Gynekol,* 78**,** 263-8.

KALUZ, S., KALUZOVA, M., CHRASTINA, A., OLIVE, P. L., PASTOREKOVA, S., PASTOREK, J., LERMAN, M. I. & STANBRIDGE, E. J. 2002. Lowered oxygen tension induces expression of the hypoxia marker MN/carbonic anhydrase IX in the absence of hypoxia-inducible factor 1 alpha stabilization: a role for phosphatidylinositol 3'-kinase. *Cancer research,* 62**,** 4469-77.

KALUZ, S., KALUZOVA, M., LIAO, S. Y., LERMAN, M. & STANBRIDGE, E. J. 2009. Transcriptional control of the tumor- and hypoxia-marker carbonic anhydrase 9: A one transcription factor (HIF-1) show? *Biochim Biophys Acta,* 1795**,** 162-72.

KALUZ, S., KALUZOVA, M., OPAVSKY, R., PASTOREKOVA, S., GIBADULINOVA, A., DEQUIEDT, F., KETTMANN, R. & PASTOREK, J. 1999. Transcriptional regulation of the MN/CA 9 gene coding for the tumor-associated carbonic anhydrase IX. Identification and characterization of a proximal silencer element. *J Biol Chem,* 274**,** 32588-95.

KALUZ, S., KALUZOVA, M. & STANBRIDGE, E. J. 2003. Expression of the hypoxia marker carbonic anhydrase IX is critically dependent on SP1 activity. Identification of a novel type of hypoxia-responsive enhancer. *Cancer Res,* 63**,** 917-22.

KALUZ, S., KALUZOVA, M. & STANBRIDGE, E. J. 2006. The role of extracellular signal-regulated protein kinase in transcriptional regulation of the hypoxia marker carbonic anhydrase IX. *J Cell Biochem,* 97**,** 207-16.

KALUZOVA, M., PASTOREKOVA, S., SVASTOVA, E., PASTOREK, J., STANBRIDGE, E. J. & KALUZ, S. 2001. Characterization of the MN/CA 9 promoter proximal

region: a role for specificity protein (SP) and activator protein 1 (AP1) factors. *Biochem J,* 359**,** 669-77.

KANG, G. H. 2011. Four molecular subtypes of colorectal cancer and their precursor lesions. *Arch Pathol Lab Med,* 135**,** 698-703.

KARHUMAA, P., KAUNISTO, K., PARKKILA, S., WAHEED, A., PASTOREKOVA, S., PASTOREK, J., SLY, W. S. & RAJANIEMI, H. 2001. Expression of the transmembrane carbonic anhydrases, CA IX and CA XII, in the human male excurrent ducts. *Mol Hum Reprod,* 7**,** 611-6.

KASISCHKE, K. A., VISHWASRAO, H. D., FISHER, P. J., ZIPFEL, W. R. & WEBB, W. W. 2004. Neural activity triggers neuronal oxidative metabolism followed by astrocytic glycolysis. *Science,* 305**,** 99-103.

KAYA, A. O., GUNEL, N., BENEKLI, M., AKYUREK, N., BUYUKBERBER, S., TATLI, H., COSKUN, U., YILDIZ, R., YAMAN, E. & OZTURK, B. 2012. Hypoxia inducible factor-1 alpha and carbonic anhydrase IX overexpression are associated with poor survival in breast cancer patients. *J BUON,* 17**,** 663-8.

KIM, C. F., JACKSON, E. L., WOOLFENDEN, A. E., LAWRENCE, S., BABAR, I., VOGEL, S., CROWLEY, D., BRONSON, R. T. & JACKS, T. 2005. Identification of bronchioalveolar stem cells in normal lung and lung cancer. *Cell,* 121**,** 823-35.

KIM, J. W., TCHERNYSHYOV, I., SEMENZA, G. L. & DANG, C. V. 2006. HIF-1-mediated expression of pyruvate dehydrogenase kinase: a metabolic switch required for cellular adaptation to hypoxia. *Cell Metab,* 3**,** 177-85.

KITAMURA, T., SUN, C., MARTIN, J., KITCH, L. J., SCHNITZER, M. J. & TONEGAWA, S. 2015. Entorhinal Cortical Ocean Cells Encode Specific Contexts and Drive Context-Specific Fear Memory. *Neuron,* 87**,** 1317-31.

KIVELA, A., PARKKILA, S., SAARNIO, J., KARTTUNEN, T. J., KIVELA, J., PARKKILA, A. K., WAHEED, A., SLY, W. S., GRUBB, J. H., SHAH, G., TURECI, O. & RAJANIEMI, H. 2000a. Expression of a novel transmembrane carbonic anhydrase isozyme XII in normal human gut and colorectal tumors. *Am J Pathol,* 156**,** 577-84.

KIVELA, A. J., PARKKILA, S., SAARNIO, J., KARTTUNEN, T. J., KIVELA, J., PARKKILA, A. K., PASTOREKOVA, S., PASTOREK, J., WAHEED, A., SLY, W. S. & RAJANIEMI, H. 2000b. Expression of transmembrane carbonic anhydrase isoenzymes IX and XII in normal human pancreas and pancreatic tumours. *Histochem Cell Biol,* 114**,** 197-204.

KLARENBEEK, J., GOEDHART, J., VAN BATENBURG, A., GROENEWALD, D. & JALINK, K. 2015. Fourth-generation epac-based FRET sensors for cAMP feature exceptional brightness, photostability and dynamic range: characterization of dedicated sensors for FLIM, for ratiometry and with high affinity. *PLoS One,* 10**,** e0122513.

KLEEBERGER, L. & ROTTINGER, E. M. 1993. Effect of pH and moderate hyperthermia on doxorubicin, epirubicin and aclacinomycin A cytotoxicity for Chinese hamster ovary cells. *Cancer Chemother Pharmacol,* 33**,** 144-8.

KOIVUNEN, P., HIRSILA, M., REMES, A. M., HASSINEN, I. E., KIVIRIKKO, K. I. & MYLLYHARJU, J. 2007. Inhibition of hypoxia-inducible factor (HIF) hydroxylases by citric acid cycle intermediates: possible links between cell metabolism and stabilization of HIF. *J Biol Chem,* 282**,** 4524-32.

KONDOH, H., LLEONART, M. E., GIL, J., WANG, J., DEGAN, P., PETERS, G., MARTINEZ, D., CARNERO, A. & BEACH, D. 2005. Glycolytic enzymes can modulate cellular life span. *Cancer Res,* 65**,** 177-85.

KOPACEK, J., BARATHOVA, M., DEQUIEDT, F., SEPELAKOVA, J., KETTMANN, R., PASTOREK, J. & PASTOREKOVA, S. 2005a. MAPK pathway contributes to density- and hypoxia-induced expression of the tumor-associated carbonic anhydrase IX. *Biochimica et biophysica acta,* 1729**,** 41-9.

KOPACEK, J., BARATHOVA, M., DEQUIEDT, F., SEPELAKOVA, J., KETTMANN, R., PASTOREK, J. & PASTOREKOVA, S. 2005b. MAPK pathway contributes to density- and hypoxia-induced expression of the tumor-associated carbonic anhydrase IX. *Biochim Biophys Acta,* 1729**,** 41-9.

KOPETZ, S., TABERNERO, J., ROSENBERG, R., JIANG, Z. Q., MORENO, V., BACHLEITNER-HOFMANN, T., LANZA, G., STORK-SLOOTS, L., MARU, D., SIMON, I., CAPELLA, G. & SALAZAR, R. 2015. Genomic classifier ColoPrint predicts recurrence in stage II colorectal cancer patients more accurately than clinical factors. *Oncologist,* 20**,** 127-33.

KORKAYA, H., LIU, S. & WICHA, M. S. 2011. Breast cancer stem cells, cytokine networks, and the tumor microenvironment. *J Clin Invest,* 121**,** 3804-9.

KOUKOURAKIS, M. I., GIATROMANOLAKI, A., SIVRIDIS, E., GATTER, K. C., HARRIS, A. L. & TUMOUR ANGIOGENESIS RESEARCH, G. 2006. Lactate dehydrogenase 5 expression in operable colorectal cancer: strong association with survival and activated vascular endothelial growth factor pathway--a report of the Tumour Angiogenesis Research Group. *J Clin Oncol,* 24**,** 4301-8.

KUBLI, D. A. & GUSTAFSSON, A. B. 2012. Mitochondria and mitophagy: the yin and yang of cell death control. *Circ Res,* 111**,** 1208-21.

KURDISTANI, S. K. 2007. Histone modifications as markers of cancer prognosis: a cellular view. *Br J Cancer,* 97**,** 1-5.

LADEROUTE, K. R. 2005. The interaction between HIF-1 and AP-1 transcription factors in response to low oxygen. *Seminars in Cell & Developmental Biology,* 16**,** 502-513.

LAMB, R., HARRISON, H., HULIT, J., SMITH, D. L., LISANTI, M. P. & SOTGIA, F. 2014. Mitochondria as new therapeutic targets for eradicating cancer stem cells: Quantitative proteomics and functional validation via MCT1/2 inhibition. *Oncotarget,* 5**,** 11029-37.

LANDES, T., EMORINE, L. J., COURILLEAU, D., ROJO, M., BELENGUER, P. & ARNAUNE-PELLOQUIN, L. 2010. The BH3-only Bnip3 binds to the dynamin Opa1 to promote mitochondrial fragmentation and apoptosis by distinct mechanisms. *EMBO Rep,* 11**,** 459-65.

LAPIDOT, T., SIRARD, C., VORMOOR, J., MURDOCH, B., HOANG, T., CACERES-CORTES, J., MINDEN, M., PATERSON, B., CALIGIURI, M. A. & DICK, J. E. 1994. A cell initiating human acute myeloid leukaemia after transplantation into SCID mice. *Nature,* 367**,** 645-8.

LEDAKI, I., MCINTYRE, A., WIGFIELD, S., BUFFA, F., MCGOWAN, S., BABAN, D., LI, J. L. & HARRIS, A. L. 2015. Carbonic anhydrase IX induction defines a heterogeneous cancer cell response to hypoxia and mediates stem cell-like properties and sensitivity to HDAC inhibition. *Oncotarget,* 6**,** 19413-27.

LEE, H. J., SEO, A. N., KIM, E. J., JANG, M. H., SUH, K. J., RYU, H. S., KIM, Y. J., KIM, J. H., IM, S. A., GONG, G., JUNG, K. H., PARK, I. A. & PARK, S. Y. 2014. HER2 heterogeneity affects trastuzumab responses and survival in patients with HER2-positive metastatic breast cancer. *Am J Clin Pathol,* 142**,** 755-66.

LEE, J. Y., LEE, I., CHANG, W. J., AHN, S. M., LIM, S. H., KIM, H. S., YOO, K. H., JUNG, K. S., SONG, H. N., CHO, J. H., KIM, S. Y., KIM, K. M., LEE, S., KIM, S. T., PARK, S. H., LEE, J., PARK, J. O., PARK, Y. S., LIM, H. Y. & KANG, W. K. 2016. MCT4 as a potential therapeutic target for metastatic gastric cancer with peritoneal carcinomatosis. *Oncotarget*.

LEE, S., SHIN, H. J., HAN, I. O., HONG, E. K., PARK, S. Y., ROH, J. W., SHIN, K. H., KIM, T. H. & KIM, J. Y. 2007. Tumor carbonic anhydrase 9 expression is associated with the presence of lymph node metastases in uterine cervical cancer. *Cancer Sci,* 98**,** 329-33.

LESTER, S. C., BOSE, S., CHEN, Y. Y., CONNOLLY, J. L., DE BACA, M. E., FITZGIBBONS, P. L., HAYES, D. F., KLEER, C., O'MALLEY, F. P., PAGE, D. L., SMITH, B. L., TAN, L. K., WEAVER, D. L., WINER, E. & MEMBERS OF THE CANCER COMMITTEE, C. O. A. P. 2009. Protocol for the examination of specimens from patients with invasive carcinoma of the breast. *Arch Pathol Lab Med,* 133**,** 1515-38.

LEVI, L., LOBO, G., DOUD, M. K., VON LINTIG, J., SEACHRIST, D., TOCHTROP, G. P. & NOY, N. 2013. Genetic ablation of the fatty acid-binding protein FABP5 suppresses HER2-induced mammary tumorigenesis. *Cancer Res,* 73**,** 4770-80.

LI, C. I., URIBE, D. J. & DALING, J. R. 2005a. Clinical characteristics of different histologic types of breast cancer. *Br J Cancer,* 93**,** 1046-52.

LI, F., WANG, Y., ZELLER, K. I., POTTER, J. J., WONSEY, D. R., O'DONNELL, K. A., KIM, J. W., YUSTEIN, J. T., LEE, L. A. & DANG, C. V. 2005b. Myc stimulates nuclearly encoded mitochondrial genes and mitochondrial biogenesis. *Mol Cell Biol,* 25**,** 6225-34.

LIAO, S. Y., AURELIO, O. N., JAN, K., ZAVADA, J. & STANBRIDGE, E. J. 1997. Identification of the MN/CA9 protein as a reliable diagnostic biomarker of clear cell carcinoma of the kidney. *Cancer Res,* 57**,** 2827-31.

LIAO, S. Y., BREWER, C., ZAVADA, J., PASTOREK, J., PASTOREKOVA, S., MANETTA, A., BERMAN, M. L., DISAIA, P. J. & STANBRIDGE, E. J. 1994. Identification of the MN antigen as a diagnostic biomarker of cervical intraepithelial squamous and glandular neoplasia and cervical carcinomas. *Am J Pathol,* 145**,** 598-609.

LIN, C. H., HSIEH, S. Y., SHEEN, I. S., LEE, W. C., CHEN, T. C., SHYU, W. C. & LIAW, Y. F. 2001. Genome-wide hypomethylation in hepatocellular carcinogenesis. *Cancer Res,* 61**,** 4238-43.

LIU, R. Z., GRAHAM, K., GLUBRECHT, D. D., GERMAIN, D. R., MACKEY, J. R. & GODBOUT, R. 2011. Association of FABP5 expression with poor survival in triple-negative breast cancer: implication for retinoic acid therapy. *Am J Pathol,* 178**,** 997-1008.

LIU, R. Z., GRAHAM, K., GLUBRECHT, D. D., LAI, R., MACKEY, J. R. & GODBOUT, R. 2012. A fatty acid-binding protein 7/RXRbeta pathway enhances survival and proliferation in triple-negative breast cancer. *J Pathol,* 228**,** 310-21.

LIU, Y. 2006. Fatty acid oxidation is a dominant bioenergetic pathway in prostate cancer. *Prostate Cancer Prostatic Dis,* 9**,** 230-4.

LIU, Y., ZUCKIER, L. S. & GHESANI, N. V. 2010. Dominant uptake of fatty acid over glucose by prostate cells: a potential new diagnostic and therapeutic approach. *Anticancer Research,* 30**,** 369-74.

LOCASALE, J. W., GRASSIAN, A. R., MELMAN, T., LYSSIOTIS, C. A., MATTAINI, K. R., BASS, A. J., HEFFRON, G., METALLO, C. M., MURANEN, T., SHARFI, H., SASAKI, A. T., ANASTASIOU, D., MULLARKY, E., VOKES, N. I., SASAKI, M., BEROUKHIM, R., STEPHANOPOULOS, G., LIGON, A. H., MEYERSON, M., RICHARDSON, A. L., CHIN, L., WAGNER, G., ASARA, J. M., BRUGGE, J. S., CANTLEY, L. C. & VANDER HEIDEN, M. G. 2011. Phosphoglycerate dehydrogenase diverts glycolytic flux and contributes to oncogenesis. *Nat Genet,* 43**,** 869-74.

LODILLINSKY, C., INFANTE, E., GUICHARD, A., CHALIGNE, R., FUHRMANN, L., CYRTA, J., IRONDELLE, M., LAGOUTTE, E., VACHER, S., BONSANG-KITZIS, H., GLUKHOVA, M., REYAL, F., BIECHE, I., VINCENT-SALOMON, A. & CHAVRIER, P. 2016. p63/MT1-MMP axis is required for in situ to invasive transition in basal-like breast cancer. *Oncogene,* 35**,** 344-57.

LOU, Y., MCDONALD, P. C., OLOUMI, A., CHIA, S., OSTLUND, C., AHMADI, A., KYLE, A., AUF DEM KELLER, U., LEUNG, S., HUNTSMAN, D., CLARKE, B., SUTHERLAND, B. W., WATERHOUSE, D., BALLY, M., ROSKELLEY, C., OVERALL, C. M., MINCHINTON, A., PACCHIANO, F., CARTA, F., SCOZZAFAVA, A., TOUISNI, N., WINUM, J. Y., SUPURAN, C. T. & DEDHAR, S. 2011a. Targeting tumor hypoxia: suppression of breast tumor growth and metastasis by novel carbonic anhydrase IX inhibitors. *Cancer Res,* 71**,** 3364-76.

LOU, Y., MCDONALD, P. C., OLOUMI, A., CHIA, S., OSTLUND, C., AHMADI, A., KYLE, A., AUF DEM KELLER, U., LEUNG, S., HUNTSMAN, D., CLARKE, B., SUTHERLAND, B. W., WATERHOUSE, D., BALLY, M., ROSKELLEY, C., OVERALL, C. M., MINCHINTON, A., PACCHIANO, F., CARTA, F., SCOZZAFAVA, A., TOUISNI, N., WINUM, J. Y., SUPURAN, C. T. & DEDHAR, S. 2011b. Targeting tumor hypoxia: suppression of breast tumor growth and metastasis by novel carbonic anhydrase IX inhibitors. *Cancer research,* 71**,** 3364-76.

LU, H., DALGARD, C. L., MOHYELDIN, A., MCFATE, T., TAIT, A. S. & VERMA, A. 2005. Reversible inactivation of HIF-1 prolyl hydroxylases allows cell metabolism to control basal HIF-1. *J Biol Chem,* 280**,** 41928-39.

LUMACHI, F., BRUNELLO, A., MARUZZO, M., BASSO, U. & BASSO, S. M. 2013. Treatment of estrogen receptor-positive breast cancer. *Curr Med Chem,* 20**,** 596-604.

LUO, W., HU, H., CHANG, R., ZHONG, J., KNABEL, M., O'MEALLY, R., COLE, R. N., PANDEY, A. & SEMENZA, G. L. 2011. Pyruvate kinase M2 is a PHD3-stimulated coactivator for hypoxia-inducible factor 1. *Cell,* 145**,** 732-44.

MA, B., CHEN, Y., CHEN, L., CHENG, H., MU, C., LI, J., GAO, R., ZHOU, C., CAO, L., LIU, J., ZHU, Y., CHEN, Q. & WU, S. 2015. Hypoxia regulates Hippo signalling through the SIAH2 ubiquitin E3 ligase. *Nat Cell Biol,* 17**,** 95-103.

MACHLER, P., WYSS, M. T., ELSAYED, M., STOBART, J., GUTIERREZ, R., VON FABER-CASTELL, A., KAELIN, V., ZUEND, M., SAN MARTIN, A., ROMERO-GOMEZ, I., BAEZA-LEHNERT, F., LENGACHER, S., SCHNEIDER, B. L., AEBISCHER, P., MAGISTRETTI, P. J., BARROS, L. F. & WEBER, B. 2016. In

Vivo Evidence for a Lactate Gradient from Astrocytes to Neurons. *Cell Metab,* 23**,** 94-102.

MAGALHAES, M. A., LARSON, D. R., MADER, C. C., BRAVO-CORDERO, J. J., GIL-HENN, H., OSER, M., CHEN, X., KOLESKE, A. J. & CONDEELIS, J. 2011. Cortactin phosphorylation regulates cell invasion through a pH-dependent pathway. *J Cell Biol,* 195**,** 903-20.

MAGISTRETTI, P. J. & PELLERIN, L. 1999. Cellular mechanisms of brain energy metabolism and their relevance to functional brain imaging. *Philos Trans R Soc Lond B Biol Sci,* 354**,** 1155-63.

MAGISTRETTI, P. J., PELLERIN, L., ROTHMAN, D. L. & SHULMAN, R. G. 1999. Energy on demand. *Science,* 283**,** 496-7.

MAKINO, Y., CAO, R., SVENSSON, K., BERTILSSON, G., ASMAN, M., TANAKA, H., CAO, Y., BERKENSTAM, A. & POELLINGER, L. 2001. Inhibitory PAS domain protein is a negative regulator of hypoxia-inducible gene expression. *Nature,* 414**,** 550-4.

MALHOTRA, G. K., ZHAO, X., BAND, H. & BAND, V. 2010. Histological, molecular and functional subtypes of breast cancers. *Cancer Biol Ther,* 10**,** 955-60.

MANABE, Y., TODA, S., MIYAZAKI, K. & SUGIHARA, H. 2003. Mature adipocytes, but not preadipocytes, promote the growth of breast carcinoma cells in collagen gel matrix culture through cancer-stromal cell interactions. *J Pathol,* 201**,** 221-8.

MANGIA, S., SIMPSON, I. A., VANNUCCI, S. J. & CARRUTHERS, A. 2009. The in vivo neuron-to-astrocyte lactate shuttle in human brain: evidence from modeling of measured lactate levels during visual stimulation. *J Neurochem,* 109 Suppl 1**,** 55-62.

MARCHIQ, I., LE FLOCH, R., ROUX, D., SIMON, M. P. & POUYSSEGUR, J. 2015. Genetic disruption of lactate/H+ symporters (MCTs) and their subunit CD147/BASIGIN sensitizes glycolytic tumor cells to phenformin. *Cancer Res,* 75**,** 171-80.

MARISA, L., DE REYNIES, A., DUVAL, A., SELVES, J., GAUB, M. P., VESCOVO, L., ETIENNE-GRIMALDI, M. C., SCHIAPPA, R., GUENOT, D., AYADI, M., KIRZIN, S., CHAZAL, M., FLEJOU, J. F., BENCHIMOL, D., BERGER, A., LAGARDE, A., PENCREACH, E., PIARD, F., ELIAS, D., PARC, Y., OLSCHWANG, S., MILANO, G., LAURENT-PUIG, P. & BOIGE, V. 2013. Gene expression classification of colon cancer into molecular subtypes: characterization, validation, and prognostic value. *PLoS Med,* 10**,** e1001453.

MARKOWETZ, F., MULDER, K. W., AIROLDI, E. M., LEMISCHKA, I. R. & TROYANSKAYA, O. G. 2010. Mapping dynamic histone acetylation patterns to gene expression in nanog-depleted murine embryonic stem cells. *PLoS Comput Biol,* 6**,** e1001034.

MARTINEZ-OUTSCHOORN, U. E., BALLIET, R., LIN, Z., WHITAKER-MENEZES, D., BIRBE, R. C., BOMBONATI, A., PAVLIDES, S., LAMB, R., SNEDDON, S., HOWELL, A., SOTGIA, F. & LISANTI, M. P. 2012a. BRCA1 mutations drive oxidative stress and glycolysis in the tumor microenvironment: implications for breast cancer prevention with antioxidant therapies. *Cell Cycle,* 11**,** 4402-13.

MARTINEZ-OUTSCHOORN, U. E., CURRY, J. M., KO, Y. H., LIN, Z., TULUC, M., COGNETTI, D., BIRBE, R. C., PRIBITKIN, E., BOMBONATI, A., PESTELL, R. G., HOWELL, A., SOTGIA, F. & LISANTI, M. P. 2013. Oncogenes and

inflammation rewire host energy metabolism in the tumor microenvironment: RAS and NFkappaB target stromal MCT4. *Cell Cycle,* 12**,** 2580-97.

MARTINEZ-OUTSCHOORN, U. E., PAVLIDES, S., HOWELL, A., PESTELL, R. G., TANOWITZ, H. B., SOTGIA, F. & LISANTI, M. P. 2011a. Stromal-epithelial metabolic coupling in cancer: integrating autophagy and metabolism in the tumor microenvironment. *The International Journal of Biochemistry & cell biology,* 43**,** 1045-51.

MARTINEZ-OUTSCHOORN, U. E., PRISCO, M., ERTEL, A., TSIRIGOS, A., LIN, Z., PAVLIDES, S., WANG, C., FLOMENBERG, N., KNUDSEN, E. S., HOWELL, A., PESTELL, R. G., SOTGIA, F. & LISANTI, M. P. 2011b. Ketones and lactate increase cancer cell "stemness," driving recurrence, metastasis, and poor clinical outcome in breast cancer: Achieving personalized medicine via Metabolo-Genomics. *Cell Cycle,* 10.

MARTINEZ-OUTSCHOORN, U. E., SOTGIA, F. & LISANTI, M. P. 2012b. Power surge: supporting cells "fuel" cancer cell mitochondria. *Cell Metab,* 15**,** 4-5.

MARTINEZ-OUTSCHOORN, U. E., TRIMMER, C., LIN, Z., WHITAKER-MENEZES, D., CHIAVARINA, B., ZHOU, J., WANG, C., PAVLIDES, S., MARTINEZ-CANTARIN, M. P., CAPOZZA, F., WITKIEWICZ, A. K., FLOMENBERG, N., HOWELL, A., PESTELL, R. G., CARO, J., LISANTI, M. P. & SOTGIA, F. 2010. Autophagy in cancer associated fibroblasts promotes tumor cell survival: Role of hypoxia, HIF1 induction and NFkappaB activation in the tumor stromal microenvironment. *Cell Cycle,* 9**,** 3515-33.

MARTINEZ-ZAGUILAN, R., LYNCH, R. M., MARTINEZ, G. M. & GILLIES, R. J. 1993. Vacuolar-type H(+)-ATPases are functionally expressed in plasma membranes of human tumor cells. *Am J Physiol,* 265**,** C1015-29.

MARTINEZ-ZAGUILAN, R., SEFTOR, E. A., SEFTOR, R. E., CHU, Y. W., GILLIES, R. J. & HENDRIX, M. J. 1996. Acidic pH enhances the invasive behavior of human melanoma cells. *Clin Exp Metastasis,* 14**,** 176-86.

MARUSYK, A., ALMENDRO, V. & POLYAK, K. 2012. Intra-tumour heterogeneity: a looking glass for cancer? *Nat Rev Cancer,* 12**,** 323-34.

MASHIMA, T., SEIMIYA, H. & TSURUO, T. 2009. De novo fatty-acid synthesis and related pathways as molecular targets for cancer therapy. *Br J Cancer,* 100**,** 1369-72.

MATHIEU, J., ZHANG, Z., ZHOU, W., WANG, A. J., HEDDLESTON, J. M., PINNA, C. M., HUBAUD, A., STADLER, B., CHOI, M., BAR, M., TEWARI, M., LIU, A., VESSELLA, R., ROSTOMILY, R., BORN, D., HORWITZ, M., WARE, C., BLAU, C. A., CLEARY, M. A., RICH, J. N. & RUOHOLA-BAKER, H. 2011. HIF induces human embryonic stem cell markers in cancer cells. *Cancer Research,* 71**,** 4640-52.

MATOBA, S., KANG, J. G., PATINO, W. D., WRAGG, A., BOEHM, M., GAVRILOVA, O., HURLEY, P. J., BUNZ, F. & HWANG, P. M. 2006. p53 regulates mitochondrial respiration. *Science,* 312**,** 1650-3.

MAXWELL, P. H., PUGH, C. W. & RATCLIFFE, P. J. 2001. Activation of the HIF pathway in cancer. *Curr Opin Genet Dev,* 11**,** 293-9.

MAXWELL, P. H., WIESENER, M. S., CHANG, G. W., CLIFFORD, S. C., VAUX, E. C., COCKMAN, M. E., WYKOFF, C. C., PUGH, C. W., MAHER, E. R. & RATCLIFFE, P. J. 1999. The tumour suppressor protein VHL targets hypoxia-inducible factors for oxygen-dependent proteolysis. *Nature,* 399**,** 271-5.

MAZUREK, S. 2011. Pyruvate kinase type M2: a key regulator of the metabolic budget system in tumor cells. *Int J Biochem Cell Biol,* 43**,** 969-80.

MCDONALD, P. C., WINUM, J. Y., SUPURAN, C. T. & DEDHAR, S. 2012. Recent developments in targeting carbonic anhydrase IX for cancer therapeutics. *Oncotarget,* 3**,** 84-97.

MCGILLEN, J. B., GAFFNEY, E. A., MARTIN, N. K. & MAINI, P. K. 2014. A general reaction-diffusion model of acidity in cancer invasion. *J Math Biol,* 68**,** 1199-224.

MCINTYRE, A., PATIAR, S., WIGFIELD, S., LI, J. L., LEDAKI, I., TURLEY, H., LEEK, R., SNELL, C., GATTER, K., SLY, W. S., VAUGHAN-JONES, R. D., SWIETACH, P. & HARRIS, A. L. 2012. Carbonic anhydrase IX promotes tumor growth and necrosis in vivo and inhibition enhances anti-VEGF therapy. *Clin Cancer Res,* 18**,** 3100-11.

MCLEAN, L. A., ROSCOE, J., JORGENSEN, N. K., GORIN, F. A. & CALA, P. M. 2000. Malignant gliomas display altered pH regulation by NHE1 compared with nontransformed astrocytes. *Am J Physiol Cell Physiol,* 278**,** C676-88.

MCLEAN, M. A., SUN, A., BRADSTREET, T. E., SCHAEFFER, A. K., LIU, H., IANNONE, R., HERMAN, G., RAILKAR, R. A., JOUBERT, I., GILLARD, J. H., PRICE, S. J. & GRIFFITHS, J. R. 2012. Repeatability of edited lactate and other metabolites in astrocytoma at 3T. *J Magn Reson Imaging,* 36**,** 468-75.

MERLO, L. M., PEPPER, J. W., REID, B. J. & MALEY, C. C. 2006. Cancer as an evolutionary and ecological process. *Nat Rev Cancer,* 6**,** 924-35.

MICHOR, F. & POLYAK, K. 2010. The origins and implications of intratumor heterogeneity. *Cancer Prev Res (Phila),* 3**,** 1361-4.

MIGNECO, G., WHITAKER-MENEZES, D., CHIAVARINA, B., CASTELLO-CROS, R., PAVLIDES, S., PESTELL, R. G., FATATIS, A., FLOMENBERG, N., TSIRIGOS, A., HOWELL, A., MARTINEZ-OUTSCHOORN, U. E., SOTGIA, F. & LISANTI, M. P. 2010. Glycolytic cancer associated fibroblasts promote breast cancer tumor growth, without a measurable increase in angiogenesis: evidence for stromal-epithelial metabolic coupling. *Cell Cycle,* 9**,** 2412-22.

MONTENEGRO, R. C., CLARK, P. G., HOWARTH, A., WAN, X., CERONI, A., SIEJKA, P., NUNEZ-ALONSO, G. A., MONTEIRO, O., ROGERS, C., GAMBLE, V., BURBANO, R., BRENNAN, P. E., TALLANT, C., EBNER, D., FEDOROV, O., O'NEILL, E., KNAPP, S., DIXON, D. & MULLER, S. 2016. BET inhibition as a new strategy for the treatment of gastric cancer. *Oncotarget*.

MORAIS-SANTOS, F., GRANJA, S., MIRANDA-GONCALVES, V., MOREIRA, A. H., QUEIROS, S., VILACA, J. L., SCHMITT, F. C., LONGATTO-FILHO, A., PAREDES, J., BALTAZAR, F. & PINHEIRO, C. 2015. Targeting lactate transport suppresses in vivo breast tumour growth. *Oncotarget,* 6**,** 19177-89.

MORGAN, P. E., PASTOREKOVA, S., STUART-TILLEY, A. K., ALPER, S. L. & CASEY, J. R. 2007. Interactions of transmembrane carbonic anhydrase, CAIX, with bicarbonate transporters. *Am J Physiol Cell Physiol,* 293**,** C738-48.

MORRIS, J. C., CHICHE, J., GRELLIER, C., LOPEZ, M., BORNAGHI, L. F., MARESCA, A., SUPURAN, C. T., POUYSSEGUR, J. & POULSEN, S. A. 2011. Targeting hypoxic tumor cell viability with carbohydrate-based carbonic anhydrase IX and XII inhibitors. *J Med Chem,* 54**,** 6905-18.

MORSY, S. M., BADAWI, A. M., CECCHI, A., SCOZZAFAVA, A. & SUPURAN, C. T. 2009. Carbonic anhydrase inhibitors. Biphenylsulfonamides with

inhibitory action towards the transmembrane, tumor-associated isozymes IX possess cytotoxic activity against human colon, lung and breast cancer cell lines. *J Enzyme Inhib Med Chem,* 24**,** 499-505.

MOTTAMAL, M., ZHENG, S., HUANG, T. L. & WANG, G. 2015. Histone deacetylase inhibitors in clinical studies as templates for new anticancer agents. *Molecules,* 20**,** 3898-941.

MUZ, B., DE LA PUENTE, P., AZAB, F., LUDERER, M. & AZAB, A. K. 2014. Hypoxia promotes stem cell-like phenotype in multiple myeloma cells. *Blood Cancer J,* 4**,** e262.

NEUMEISTER, V. M., SULLIVAN, C. A., LINDNER, R., LEZON-GEYDA, K., LI, J., ZAVADA, J., MARTEL, M., GLAZER, P. M., TUCK, D. P., RIMM, D. L. & HARRIS, L. 2012. Hypoxia-induced protein CAIX is associated with somatic loss of BRCA1 protein and pathway activity in triple negative breast cancer. *Breast Cancer Res Treat,* 136**,** 67-75.

NIEDERER, S. A., SWIETACH, P., WILSON, D. A., SMITH, N. P. & VAUGHAN-JONES, R. D. 2008. Measuring and modeling chloride-hydroxyl exchange in the Guinea-pig ventricular myocyte. *Biophys J,* 94**,** 2385-403.

NIELSEN, S. J., SCHNEIDER, R., BAUER, U. M., BANNISTER, A. J., MORRISON, A., O'CARROLL, D., FIRESTEIN, R., CLEARY, M., JENUWEIN, T., HERRERA, R. E. & KOUZARIDES, T. 2001. Rb targets histone H3 methylation and HP1 to promoters. *Nature,* 412**,** 561-5.

NIEMAN, K. M., KENNY, H. A., PENICKA, C. V., LADANYI, A., BUELL-GUTBROD, R., ZILLHARDT, M. R., ROMERO, I. L., CAREY, M. S., MILLS, G. B., HOTAMISLIGIL, G. S., YAMADA, S. D., PETER, M. E., GWIN, K. & LENGYEL, E. 2011. Adipocytes promote ovarian cancer metastasis and provide energy for rapid tumor growth. *Nat Med,* 17**,** 1498-503.

NOTTA, F., MULLIGHAN, C. G., WANG, J. C., POEPPL, A., DOULATOV, S., PHILLIPS, L. A., MA, J., MINDEN, M. D., DOWNING, J. R. & DICK, J. E. 2011. Evolution of human BCR-ABL1 lymphoblastic leukaemia-initiating cells. *Nature,* 469**,** 362-7.

NOWELL, P. C. 1976. The clonal evolution of tumor cell populations. *Science,* 194**,** 23-8.

O'CONNELL, M. J., LAVERY, I., YOTHERS, G., PAIK, S., CLARK-LANGONE, K. M., LOPATIN, M., WATSON, D., BAEHNER, F. L., SHAK, S., BAKER, J., COWENS, J. W. & WOLMARK, N. 2010. Relationship between tumor gene expression and recurrence in four independent studies of patients with stage II/III colon cancer treated with surgery alone or surgery plus adjuvant fluorouracil plus leucovorin. *J Clin Oncol,* 28**,** 3937-44.

ONG, C. T. & CORCES, V. G. 2009. Insulators as mediators of intra- and inter-chromosomal interactions: a common evolutionary theme. *J Biol,* 8**,** 73.

OPAVSKY, R., PASTOREKOVA, S., ZELNIK, V., GIBADULINOVA, A., STANBRIDGE, E. J., ZAVADA, J., KETTMANN, R. & PASTOREK, J. 1996. Human MN/CA9 gene, a novel member of the carbonic anhydrase family: structure and exon to protein domain relationships. *Genomics,* 33**,** 480-7.

ORUCEVIC, A., CHEN, J., MCLOUGHLIN, J. M., HEIDEL, R. E., PANELLA, T. & BELL, J. 2015. Is the TNM staging system for breast cancer still relevant in the era of biomarkers and emerging personalized medicine for breast cancer - an institution's 10-year experience. *Breast J,* 21**,** 147-54.

OXNARD, G. R. 2016. The cellular origins of drug resistance in cancer. *Nat Med,* 22**,** 232-4.

PACCHIANO, F., CARTA, F., MCDONALD, P. C., LOU, Y., VULLO, D., SCOZZAFAVA, A., DEDHAR, S. & SUPURAN, C. T. 2011. Ureido-substituted benzenesulfonamides potently inhibit carbonic anhydrase IX and show antimetastatic activity in a model of breast cancer metastasis. *J Med Chem,* 54**,** 1896-902.

PANDOLFI, P. P. 2001. Histone deacetylases and transcriptional therapy with their inhibitors. *Cancer Chemother Pharmacol,* 48 Suppl 1**,** S17-9.

PAO, W., MILLER, V., ZAKOWSKI, M., DOHERTY, J., POLITI, K., SARKARIA, I., SINGH, B., HEELAN, R., RUSCH, V., FULTON, L., MARDIS, E., KUPFER, D., WILSON, R., KRIS, M. & VARMUS, H. 2004. EGF receptor gene mutations are common in lung cancers from "never smokers" and are associated with sensitivity of tumors to gefitinib and erlotinib. *Proc Natl Acad Sci U S A,* 101**,** 13306-11.

PAPANDREOU, I., CAIRNS, R. A., FONTANA, L., LIM, A. L. & DENKO, N. C. 2006. HIF-1 mediates adaptation to hypoxia by actively downregulating mitochondrial oxygen consumption. *Cell Metab,* 3**,** 187-97.

PARANJAPE, A. N., MANDAL, T., MUKHERJEE, G., KUMAR, M. V., SENGUPTA, K. & RANGARAJAN, A. 2012. Introduction of SV40ER and hTERT into mammospheres generates breast cancer cells with stem cell properties. *Oncogene,* 31**,** 1896-909.

PARKER, J. S., MULLINS, M., CHEANG, M. C., LEUNG, S., VODUC, D., VICKERY, T., DAVIES, S., FAURON, C., HE, X., HU, Z., QUACKENBUSH, J. F., STIJLEMAN, I. J., PALAZZO, J., MARRON, J. S., NOBEL, A. B., MARDIS, E., NIELSEN, T. O., ELLIS, M. J., PEROU, C. M. & BERNARD, P. S. 2009. Supervised risk predictor of breast cancer based on intrinsic subtypes. *J Clin Oncol,* 27**,** 1160-7.

PARKS, S. K., CHICHE, J. & POUYSSEGUR, J. 2011. pH control mechanisms of tumor survival and growth. *J Cell Physiol,* 226**,** 299-308.

PASTOREK, J., PASTOREKOVA, S., CALLEBAUT, I., MORNON, J. P., ZELNIK, V., OPAVSKY, R., ZAT'OVICOVA, M., LIAO, S., PORTETELLE, D., STANBRIDGE, E. J. & ET AL. 1994. Cloning and characterization of MN, a human tumor-associated protein with a domain homologous to carbonic anhydrase and a putative helix-loop-helix DNA binding segment. *Oncogene,* 9**,** 2877-88.

PASTOREKOVA, S., PARKKILA, S., PARKKILA, A. K., OPAVSKY, R., ZELNIK, V., SAARNIO, J. & PASTOREK, J. 1997. Carbonic anhydrase IX, MN/CA IX: analysis of stomach complementary DNA sequence and expression in human and rat alimentary tracts. *Gastroenterology,* 112**,** 398-408.

PAVLIDES, S., VERA, I., GANDARA, R., SNEDDON, S., PESTELL, R. G., MERCIER, I., MARTINEZ-OUTSCHOORN, U. E., WHITAKER-MENEZES, D., HOWELL, A., SOTGIA, F. & LISANTI, M. P. 2012. Warburg meets autophagy: cancer-associated fibroblasts accelerate tumor growth and metastasis via oxidative stress, mitophagy, and aerobic glycolysis. *Antioxid Redox Signal,* 16**,** 1264-84.

PECQUEUR, C., OLIVER, L., OIZEL, K., LALIER, L. & VALLETTE, F. M. 2013. Targeting metabolism to induce cell death in cancer cells and cancer stem cells. *Int J Cell Biol,* 2013**,** 805975.

PEFANI, D. E. & O'NEILL, E. 2015. Safeguarding genome stability: RASSF1A tumor suppressor regulates BRCA2 at stalled forks. *Cell Cycle,* 14**,** 1624-30.

PELLERIN, L., PELLEGRI, G., BITTAR, P. G., CHARNAY, Y., BOURAS, C., MARTIN, J. L., STELLA, N. & MAGISTRETTI, P. J. 1998. Evidence supporting the existence of an activity-dependent astrocyte-neuron lactate shuttle. *Dev Neurosci,* 20**,** 291-9.

PENG, L., GU, L., ZHANG, H., HUANG, X., HERTZ, E. & HERTZ, L. 2007. Glutamine as an energy substrate in cultured neurons during glucose deprivation. *J Neurosci Res,* 85**,** 3480-6.

PENG, W., TOGAWA, C., ZHANG, K. & KURDISTANI, S. K. 2008. Regulators of cellular levels of histone acetylation in Saccharomyces cerevisiae. *Genetics,* 179**,** 277-89.

PEROU, C. M., SORLIE, T., EISEN, M. B., VAN DE RIJN, M., JEFFREY, S. S., REES, C. A., POLLACK, J. R., ROSS, D. T., JOHNSEN, H., AKSLEN, L. A., FLUGE, O., PERGAMENSCHIKOV, A., WILLIAMS, C., ZHU, S. X., LONNING, P. E., BORRESEN-DALE, A. L., BROWN, P. O. & BOTSTEIN, D. 2000. Molecular portraits of human breast tumours. *Nature,* 406**,** 747-52.

PERTEGA-GOMES, N. & BALTAZAR, F. 2014. Lactate transporters in the context of prostate cancer metabolism: what do we know? *Int J Mol Sci,* 15**,** 18333-48.

PERTEGA-GOMES, N., VIZCAINO, J. R., ATTIG, J., JURMEISTER, S., LOPES, C. & BALTAZAR, F. 2014. A lactate shuttle system between tumour and stromal cells is associated with poor prognosis in prostate cancer. *BMC Cancer,* 14**,** 352.

PETRUL, H. M., SCHATZ, C. A., KOPITZ, C. C., ADNANE, L., MCCABE, T. J., TRAIL, P., HA, S., CHANG, Y. S., VOZNESENSKY, A., RANGES, G. & TAMBURINI, P. P. 2012. Therapeutic mechanism and efficacy of the antibody-drug conjugate BAY 79-4620 targeting human carbonic anhydrase 9. *Mol Cancer Ther,* 11**,** 340-9.

PFAFFL, M. W. 2001. A new mathematical model for relative quantification in real-time RT-PCR. *Nucleic Acids Res,* 29**,** e45.

PHELPS, C. H. 1972. Barbiturate-induced glycogen accumulation in brain. An electron microscopic study. *Brain Res,* 39**,** 225-34.

PISARSKY, L., BILL, R., FAGIANI, E., DIMELOE, S., GOOSEN, R. W., HAGMANN, J., HESS, C. & CHRISTOFORI, G. 2016. Targeting Metabolic Symbiosis to Overcome Resistance to Anti-angiogenic Therapy. *Cell Rep,* 15**,** 1161-74.

POLLARD, P. J., LOENARZ, C., MOLE, D. R., MCDONOUGH, M. A., GLEADLE, J. M., SCHOFIELD, C. J. & RATCLIFFE, P. J. 2008. Regulation of Jumonji-domain-containing histone demethylases by hypoxia-inducible factor (HIF)-1alpha. *Biochem J,* 416**,** 387-94.

POPAT, S., HUBNER, R. & HOULSTON, R. S. 2005. Systematic review of microsatellite instability and colorectal cancer prognosis. *J Clin Oncol,* 23**,** 609-18.

PORTELA, A. & ESTELLER, M. 2010. Epigenetic modifications and human disease. *Nat Biotechnol,* 28**,** 1057-68.

POSSEMATO, R., MARKS, K. M., SHAUL, Y. D., PACOLD, M. E., KIM, D., BIRSOY, K., SETHUMADHAVAN, S., WOO, H. K., JANG, H. G., JHA, A. K., CHEN, W. W., BARRETT, F. G., STRANSKY, N., TSUN, Z. Y., COWLEY, G. S., BARRETINA, J., KALAANY, N. Y., HSU, P. P., OTTINA, K., CHAN, A. M., YUAN, B., GARRAWAY,

L. A., ROOT, D. E., MINO-KENUDSON, M., BRCAHTEL, E. F., DRIGGERS, E. M. & SABATINI, D. M. 2011. Functional genomics reveal that the serine synthesis pathway is essential in breast cancer. *Nature,* 476**,** 346-50.

POUYSSEGUR, J., SARDET, C., FRANCHI, A., L'ALLEMAIN, G. & PARIS, S. 1984. A specific mutation abolishing Na+/H+ antiport activity in hamster fibroblasts precludes growth at neutral and acidic pH. *Proc Natl Acad Sci U S A,* 81**,** 4833-7.

PROESCHOLDT, M. A., MAYER, C., KUBITZA, M., SCHUBERT, T., LIAO, S. Y., STANBRIDGE, E. J., IVANOV, S., OLDFIELD, E. H., BRAWANSKI, A. & MERRILL, M. J. 2005. Expression of hypoxia-inducible carbonic anhydrases in brain tumors. *Neuro Oncol,* 7**,** 465-75.

PUGH, C. W. & RATCLIFFE, P. J. 2003. Regulation of angiogenesis by hypoxia: role of the HIF system. *Nat Med,* 9**,** 677-84.

RAFAJOVA, M., ZATOVICOVA, M., KETTMANN, R., PASTOREK, J. & PASTOREKOVA, S. 2004. Induction by hypoxia combined with low glucose or low bicarbonate and high posttranslational stability upon reoxygenation contribute to carbonic anhydrase IX expression in cancer cells. *International journal of oncology,* 24**,** 995-1004.

RAGHUNAND, N. & GILLIES, R. J. 2001. pH and chemotherapy. *Novartis Found Symp,* 240**,** 199-211; discussion 265-8.

RAVI, R., MOOKERJEE, B., BHUJWALLA, Z. M., SUTTER, C. H., ARTEMOV, D., ZENG, Q., DILLEHAY, L. E., MADAN, A., SEMENZA, G. L. & BEDI, A. 2000. Regulation of tumor angiogenesis by p53-induced degradation of hypoxia-inducible factor 1alpha. *Genes Dev,* 14**,** 34-44.

REISEROVA, L., KALUZOVA, M., KALUZ, S., WILLIS, A. C., ZAVADA, J., ZAVODSKA, E., ZAVADOVA, Z., CIAMPOR, F., PASTOREK, J. & PASTOREKOVA, S. 1999. Identification of MaTu-MX agent as a new strain of lymphocytic choriomeningitis virus (LCMV) and serological indication of horizontal spread of LCMV in human population. *Virology,* 257**,** 73-83.

RESHETNYAK, Y. K., SEGALA, M., ANDREEV, O. A. & ENGELMAN, D. M. 2007. A monomeric membrane peptide that lives in three worlds: in solution, attached to, and inserted across lipid bilayers. *Biophys J,* 93**,** 2363-72.

RICCI-VITIANI, L., LOMBARDI, D. G., PILOZZI, E., BIFFONI, M., TODARO, M., PESCHLE, C. & DE MARIA, R. 2007. Identification and expansion of human colon-cancer-initiating cells. *Nature,* 445**,** 111-5.

RIKKA, S., QUINSAY, M. N., THOMAS, R. L., KUBLI, D. A., ZHANG, X., MURPHY, A. N. & GUSTAFSSON, A. B. 2011. Bnip3 impairs mitochondrial bioenergetics and stimulates mitochondrial turnover. *Cell Death Differ,* 18**,** 721-31.

RIVENBARK, A. G., O'CONNOR, S. M. & COLEMAN, W. B. 2013. Molecular and cellular heterogeneity in breast cancer: challenges for personalized medicine. *Am J Pathol,* 183**,** 1113-24.

ROBERTSON, N., POTTER, C. & HARRIS, A. L. 2004. Role of carbonic anhydrase IX in human tumor cell growth, survival, and invasion. *Cancer Res,* 64**,** 6160-5.

ROFSTAD, E. K., MATHIESEN, B., KINDEM, K. & GALAPPATHI, K. 2006. Acidic extracellular pH promotes experimental metastasis of human melanoma cells in athymic nude mice. *Cancer Res,* 66**,** 6699-707.

ROGEZ-FLORENT, T., MEIGNAN, S., FOULON, C., SIX, P., GROS, A., BAL-MAHIEU, C., SUPURAN, C. T., SCOZZAFAVA, A., FREDERICK, R., MASEREEL, B.,

DEPREUX, P., LANSIAUX, A., GOOSSENS, J. F., GLUSZOK, S. & GOOSSENS, L. 2013. New selective carbonic anhydrase IX inhibitors: synthesis and pharmacological evaluation of diarylpyrazole-benzenesulfonamides. *Bioorg Med Chem,* 21**,** 1451-64.

ROSSIGNOL, R., GILKERSON, R., AGGELER, R., YAMAGATA, K., REMINGTON, S. J. & CAPALDI, R. A. 2004. Energy substrate modulates mitochondrial structure and oxidative capacity in cancer cells. *Cancer Research,* 64**,** 985-93.

ROUSCHOP, K. M., VAN DEN BEUCKEN, T., DUBOIS, L., NIESSEN, H., BUSSINK, J., SAVELKOULS, K., KEULERS, T., MUJCIC, H., LANDUYT, W., VONCKEN, J. W., LAMBIN, P., VAN DER KOGEL, A. J., KORITZINSKY, M. & WOUTERS, B. G. 2010. The unfolded protein response protects human tumor cells during hypoxia through regulation of the autophagy genes MAP1LC3B and ATG5. *The Journal of clinical investigation,* 120**,** 127-41.

RYSMAN, E., BRUSSELMANS, K., SCHEYS, K., TIMMERMANS, L., DERUA, R., MUNCK, S., VAN VELDHOVEN, P. P., WALTREGNY, D., DANIELS, V. W., MACHIELS, J., VANDERHOYDONC, F., SMANS, K., WAELKENS, E., VERHOEVEN, G. & SWINNEN, J. V. 2010. De novo lipogenesis protects cancer cells from free radicals and chemotherapeutics by promoting membrane lipid saturation. *Cancer Res,* 70**,** 8117-26.

RZYMSKI, T. & HARRIS, A. L. 2007. The unfolded protein response and integrated stress response to anoxia. *Clin Cancer Res,* 13**,** 2537-40.

RZYMSKI, T., MILANI, M., PIKE, L., BUFFA, F., MELLOR, H. R., WINCHESTER, L., PIRES, I., HAMMOND, E., RAGOUSSIS, I. & HARRIS, A. L. 2010. Regulation of autophagy by ATF4 in response to severe hypoxia. *Oncogene,* 29**,** 4424-35.

SAARNIO, J., PARKKILA, S., PARKKILA, A. K., WAHEED, A., CASEY, M. C., ZHOU, X. Y., PASTOREKOVA, S., PASTOREK, J., KARTTUNEN, T., HAUKIPURO, K., KAIRALUOMA, M. I. & SLY, W. S. 1998. Immunohistochemistry of carbonic anhydrase isozyme IX (MN/CA IX) in human gut reveals polarized expression in the epithelial cells with the highest proliferative capacity. *J Histochem Cytochem,* 46**,** 497-504.

SALAZAR, R., ROEPMAN, P., CAPELLA, G., MORENO, V., SIMON, I., DREEZEN, C., LOPEZ-DORIGA, A., SANTOS, C., MARIJNEN, C., WESTERGA, J., BRUIN, S., KERR, D., KUPPEN, P., VAN DE VELDE, C., MORREAU, H., VAN VELTHUYSEN, L., GLAS, A. M., VAN'T VEER, L. J. & TOLLENAAR, R. 2011. Gene expression signature to improve prognosis prediction of stage II and III colorectal cancer. *J Clin Oncol,* 29**,** 17-24.

SALEM, A. F., WHITAKER-MENEZES, D., LIN, Z., MARTINEZ-OUTSCHOORN, U. E., TANOWITZ, H. B., AL-ZOUBI, M. S., HOWELL, A., PESTELL, R. G., SOTGIA, F. & LISANTI, M. P. 2012. Two-compartment tumor metabolism: autophagy in the tumor microenvironment and oxidative mitochondrial metabolism (OXPHOS) in cancer cells. *Cell Cycle,* 11**,** 2545-56.

SAN MARTIN, A., CEBALLO, S., RUMINOT, I., LERCHUNDI, R., FROMMER, W. B. & BARROS, L. F. 2013. A genetically encoded FRET lactate sensor and its use to detect the Warburg effect in single cancer cells. *PLoS One,* 8**,** e57712.

SANITA, P., CAPULLI, M., TETI, A., GALATIOTO, G. P., VICENTINI, C., CHIARUGI, P., BOLOGNA, M. & ANGELUCCI, A. 2014. Tumor-stroma metabolic relationship based on lactate shuttle can sustain prostate cancer progression. *BMC Cancer,* 14**,** 154.

SCAFFIDI, P. & MISTELI, T. 2011. In vitro generation of human cells with cancer stem cell properties. *Nat Cell Biol,* 13**,** 1051-61.

SCHUTZE, D., MILDE-LANGOSCH, K., WITZEL, I., RODY, A., KARN, T., SCHMIDT, M., CHOSCHZICK, M., JANICKE, F. & MULLER, V. 2013. Relevance of cellular and serum carbonic anhydrase IX in primary breast cancer. *J Cancer Res Clin Oncol,* 139**,** 747-54.

SEAGROVES, T. N., RYAN, H. E., LU, H., WOUTERS, B. G., KNAPP, M., THIBAULT, P., LADEROUTE, K. & JOHNSON, R. S. 2001. Transcription factor HIF-1 is a necessary mediator of the pasteur effect in mammalian cells. *Mol Cell Biol,* 21**,** 3436-44.

SEKAR, R. B. & PERIASAMY, A. 2003. Fluorescence resonance energy transfer (FRET) microscopy imaging of live cell protein localizations. *J Cell Biol,* 160**,** 629-33.

SEMENZA, G. L. 2003. Targeting HIF-1 for cancer therapy. *Nat Rev Cancer,* 3**,** 721-32.

SEMENZA, G. L., ROTH, P. H., FANG, H. M. & WANG, G. L. 1994. Transcriptional regulation of genes encoding glycolytic enzymes by hypoxia-inducible factor 1. *J Biol Chem,* 269**,** 23757-63.

SERMEUS, A., COSSE, J. P., CRESPIN, M., MAINFROID, V., DE LONGUEVILLE, F., NINANE, N., RAES, M., REMACLE, J. & MICHIELS, C. 2008. Hypoxia induces protection against etoposide-induced apoptosis: molecular profiling of changes in gene expression and transcription factor activity. *Mol Cancer,* 7**,** 27.

SETHI, K. K. & VERMA, S. M. 2013. A systematic quantitative approach to rational drug design and discovery of novel human carbonic anhydrase IX inhibitors. *J Enzyme Inhib Med Chem*.

SHAH, U. S., DHIR, R., GOLLIN, S. M., CHANDRAN, U. R., LEWIS, D., ACQUAFONDATA, M. & PFLUG, B. R. 2006. Fatty acid synthase gene overexpression and copy number gain in prostate adenocarcinoma. *Hum Pathol,* 37**,** 401-9.

SHANK, R. P. & APRISON, M. H. 1981. Present status and significance of the glutamine cycle in neural tissues. *Life Sci,* 28**,** 837-42.

SHANK, R. P., BENNETT, G. S., FREYTAG, S. O. & CAMPBELL, G. L. 1985. Pyruvate carboxylase: an astrocyte-specific enzyme implicated in the replenishment of amino acid neurotransmitter pools. *Brain Res,* 329**,** 364-7.

SHEN, L., TOYOTA, M., KONDO, Y., LIN, E., ZHANG, L., GUO, Y., HERNANDEZ, N. S., CHEN, X., AHMED, S., KONISHI, K., HAMILTON, S. R. & ISSA, J. P. 2007. Integrated genetic and epigenetic analysis identifies three different subclasses of colon cancer. *Proc Natl Acad Sci U S A,* 104**,** 18654-9.

SHETA, E. A., TROUT, H., GILDEA, J. J., HARDING, M. A. & THEODORESCU, D. 2001. Cell density mediated pericellular hypoxia leads to induction of HIF-1alpha via nitric oxide and Ras/MAP kinase mediated signaling pathways. *Oncogene,* 20**,** 7624-34.

SHI, Y. 2007. Histone lysine demethylases: emerging roles in development, physiology and disease. *Nat Rev Genet,* 8**,** 829-33.

SHIN, H. J., RHO, S. B., JUNG, D. C., HAN, I. O., OH, E. S. & KIM, J. Y. 2011. Carbonic anhydrase IX (CA9) modulates tumor-associated cell migration and invasion. *J Cell Sci,* 124**,** 1077-87.

SHOKATI, T., ZWINGMANN, C. & LEIBFRITZ, D. 2005. Contribution of extracellular glutamine as an anaplerotic substrate to neuronal metabolism: a re-evaluation by multinuclear NMR spectroscopy in primary cultured neurons. *Neurochem Res,* 30**,** 1269-81.

SIEBELS, M., ROHRMANN, K., OBERNEDER, R., STAHLER, M., HASEKE, N., BECK, J., HOFMANN, R., KINDLER, M., KLOEPFER, P. & STIEF, C. 2011. A clinical phase I/II trial with the monoclonal antibody cG250 (RENCAREX(R)) and interferon-alpha-2a in metastatic renal cell carcinoma patients. *World J Urol,* 29**,** 121-6.

SINGH, S. & SUPURAN, C. T. 2014. Chemometric modeling of breast cancer associated carbonic anhydrase IX inhibitors belonging to the ureido-substituted benzene sulfonamide class. *J Enzyme Inhib Med Chem,* 29**,** 877-83.

SINGH, S. K., CLARKE, I. D., TERASAKI, M., BONN, V. E., HAWKINS, C., SQUIRE, J. & DIRKS, P. B. 2003. Identification of a cancer stem cell in human brain tumors. *Cancer Res,* 63**,** 5821-8.

SMIRAGLIA, D. J., RUSH, L. J., FRUHWALD, M. C., DAI, Z., HELD, W. A., COSTELLO, J. F., LANG, J. C., ENG, C., LI, B., WRIGHT, F. A., CALIGIURI, M. A. & PLASS, C. 2001. Excessive CpG island hypermethylation in cancer cell lines versus primary human malignancies. *Hum Mol Genet,* 10**,** 1413-9.

SOARES, J., PINTO, A. E., CUNHA, C. V., ANDRE, S., BARAO, I., SOUSA, J. M. & CRAVO, M. 1999. Global DNA hypomethylation in breast carcinoma: correlation with prognostic factors and tumor progression. *Cancer,* 85**,** 112-8.

SONVEAUX, P., VEGRAN, F., SCHROEDER, T., WERGIN, M. C., VERRAX, J., RABBANI, Z. N., DE SAEDELEER, C. J., KENNEDY, K. M., DIEPART, C., JORDAN, B. F., KELLEY, M. J., GALLEZ, B., WAHL, M. L., FERON, O. & DEWHIRST, M. W. 2008. Targeting lactate-fueled respiration selectively kills hypoxic tumor cells in mice. *J Clin Invest,* 118**,** 3930-42.

SORLIE, T., PEROU, C. M., TIBSHIRANI, R., AAS, T., GEISLER, S., JOHNSEN, H., HASTIE, T., EISEN, M. B., VAN DE RIJN, M., JEFFREY, S. S., THORSEN, T., QUIST, H., MATESE, J. C., BROWN, P. O., BOTSTEIN, D., LONNING, P. E. & BORRESEN-DALE, A. L. 2001. Gene expression patterns of breast carcinomas distinguish tumor subclasses with clinical implications. *Proc Natl Acad Sci U S A,* 98**,** 10869-74.

SORLIE, T., TIBSHIRANI, R., PARKER, J., HASTIE, T., MARRON, J. S., NOBEL, A., DENG, S., JOHNSEN, H., PESICH, R., GEISLER, S., DEMETER, J., PEROU, C. M., LONNING, P. E., BROWN, P. O., BORRESEN-DALE, A. L. & BOTSTEIN, D. 2003. Repeated observation of breast tumor subtypes in independent gene expression data sets. *Proc Natl Acad Sci U S A,* 100**,** 8418-23.

SPANDL, J., WHITE, D. J., PEYCHL, J. & THIELE, C. 2009. Live cell multicolor imaging of lipid droplets with a new dye, LD540. *Traffic,* 10**,** 1579-84.

SPEDER, P. & BRAND, A. H. 2014. Gap junction proteins in the blood-brain barrier control nutrient-dependent reactivation of Drosophila neural stem cells. *Dev Cell,* 30**,** 309-21.

STINGL, J. & CALDAS, C. 2007. Molecular heterogeneity of breast carcinomas and the cancer stem cell hypothesis. *Nat Rev Cancer,* 7**,** 791-9.

STOBART, J. L. & ANDERSON, C. M. 2013. Multifunctional role of astrocytes as gatekeepers of neuronal energy supply. *Front Cell Neurosci,* 7**,** 38.

STRAHL, B. D., OHBA, R., COOK, R. G. & ALLIS, C. D. 1999. Methylation of histone H3 at lysine 4 is highly conserved and correlates with transcriptionally active nuclei in Tetrahymena. *Proc Natl Acad Sci U S A,* 96**,** 14967-72.

STRYER, L. 1995. Citric Acid Cycle. *Biochemistry.* 4th ed. New York: W.H. Freeman and Company.

STUDER, L., CSETE, M., LEE, S. H., KABBANI, N., WALIKONIS, J., WOLD, B. & MCKAY, R. 2000. Enhanced proliferation, survival, and dopaminergic differentiation of CNS precursors in lowered oxygen. *J Neurosci,* 20**,** 7377-83.

SUN, M., YANG, C., ZHENG, J., WANG, M., CHEN, M., LE, D. Q., KJEMS, J. & BUNGER, C. E. 2015. Enhanced efficacy of chemotherapy for breast cancer stem cells by simultaneous suppression of multidrug resistance and antiapoptotic cellular defense. *Acta Biomater*.

SUPURAN, C. T. 2008. Carbonic anhydrases: novel therapeutic applications for inhibitors and activators. *Nat Rev Drug Discov,* 7**,** 168-81.

SUPURAN, C. T. 2011. Carbonic anhydrase inhibitors and activators for novel therapeutic applications. *Future Med Chem,* 3**,** 1165-80.

SUPURAN, C. T., BRIGANTI, F., TILLI, S., CHEGWIDDEN, W. R. & SCOZZAFAVA, A. 2001. Carbonic anhydrase inhibitors: sulfonamides as antitumor agents? *Bioorg Med Chem,* 9**,** 703-14.

SUPURAN, C. T. & SCOZZAFAVA, A. 2000a. Carbonic anhydrase inhibitors--Part 94. 1,3,4-thiadiazole-2-sulfonamidederivatives as antitumor agents? *Eur J Med Chem,* 35**,** 867-74.

SUPURAN, C. T. & SCOZZAFAVA, A. 2000b. Carbonic anhydrase inhibitors: aromatic sulfonamides and disulfonamides act as efficient tumor growth inhibitors. *J Enzyme Inhib,* 15**,** 597-610.

SURFUS, J. E., HANK, J. A., OOSTERWIJK, E., WELT, S., LINDSTROM, M. J., ALBERTINI, M. R., SCHILLER, J. H. & SONDEL, P. M. 1996. Anti-renal-cell carcinoma chimeric antibody G250 facilitates antibody-dependent cellular cytotoxicity with in vitro and in vivo interleukin-2-activated effectors. *J Immunother Emphasis Tumor Immunol,* 19**,** 184-91.

SVASTOVA, E., HULIKOVA, A., RAFAJOVA, M., ZAT'OVICOVA, M., GIBADULINOVA, A., CASINI, A., CECCHI, A., SCOZZAFAVA, A., SUPURAN, C. T., PASTOREK, J. & PASTOREKOVA, S. 2004. Hypoxia activates the capacity of tumor-associated carbonic anhydrase IX to acidify extracellular pH. *FEBS Lett,* 577**,** 439-45.

SVASTOVA, E., ZILKA, N., ZAT'OVICOVA, M., GIBADULINOVA, A., CIAMPOR, F., PASTOREK, J. & PASTOREKOVA, S. 2003. Carbonic anhydrase IX reduces E-cadherin-mediated adhesion of MDCK cells via interaction with beta-catenin. *Exp Cell Res,* 290**,** 332-45.

SWIETACH, P., HULIKOVA, A., VAUGHAN-JONES, R. D. & HARRIS, A. L. 2010. New insights into the physiological role of carbonic anhydrase IX in tumour pH regulation. *Oncogene,* 29**,** 6509-21.

SWIETACH, P., PATIAR, S., SUPURAN, C. T., HARRIS, A. L. & VAUGHAN-JONES, R. D. 2009. The role of carbonic anhydrase 9 in regulating extracellular and intracellular ph in three-dimensional tumor cell growths. *J Biol Chem,* 284**,** 20299-310.

SZOLLOSI, J., BALAZS, M., FEUERSTEIN, B. G., BENZ, C. C. & WALDMAN, F. M. 1995. ERBB-2 (HER2/neu) gene copy number, p185HER-2

overexpression, and intratumor heterogeneity in human breast cancer. *Cancer Res,* 55**,** 5400-7.

TAHILIANI, M., KOH, K. P., SHEN, Y., PASTOR, W. A., BANDUKWALA, H., BRUDNO, Y., AGARWAL, S., IYER, L. M., LIU, D. R., ARAVIND, L. & RAO, A. 2009. Conversion of 5-methylcytosine to 5-hydroxymethylcytosine in mammalian DNA by MLL partner TET1. *Science,* 324**,** 930-5.

TAKADA, T., TAKATA, K. & ASHIHARA, E. 2016. Inhibition of monocarboxylate transporter 1 suppresses the proliferation of glioblastoma stem cells. *J Physiol Sci*.

TAN, E. Y., YAN, M., CAMPO, L., HAN, C., TAKANO, E., TURLEY, H., CANDILORO, I., PEZZELLA, F., GATTER, K. C., MILLAR, E. K., O'TOOLE, S. A., MCNEIL, C. M., CREA, P., SEGARA, D., SUTHERLAND, R. L., HARRIS, A. L. & FOX, S. B. 2009. The key hypoxia regulated gene CAIX is upregulated in basal-like breast tumours and is associated with resistance to chemotherapy. *British journal of cancer,* 100**,** 405-11.

TANG, D. G. 2012. Understanding cancer stem cell heterogeneity and plasticity. *Cell Res,* 22**,** 457-72.

TAPMEIER, T. T., MOSHNIKOVA, A., BEECH, J., ALLEN, D., KINCHESH, P., SMART, S., HARRIS, A., MCINTYRE, A., ENGELMAN, D. M., ANDREEV, O. A., RESHETNYAK, Y. K. & MUSCHEL, R. J. 2015. The pH low insertion peptide pHLIP Variant 3 as a novel marker of acidic malignant lesions. *Proc Natl Acad Sci U S A,* 112**,** 9710-5.

THOMAS, R. L., KUBLI, D. A. & GUSTAFSSON, A. B. 2011. Bnip3-mediated defects in oxidative phosphorylation promote mitophagy. *Autophagy,* 7**,** 775-7.

THOMLINSON, R. H. & GRAY, L. H. 1955. The histological structure of some human lung cancers and the possible implications for radiotherapy. *British journal of cancer,* 9**,** 539-49.

TIRINATO, L., LIBERALE, C., DI FRANCO, S., CANDELORO, P., BENFANTE, A., LA ROCCA, R., POTZE, L., MAROTTA, R., RUFFILLI, R., RAJAMANICKAM, V. P., MALERBA, M., DE ANGELIS, F., FALQUI, A., CARBONE, E., TODARO, M., MEDEMA, J. P., STASSI, G. & DI FABRIZIO, E. 2015. Lipid droplets: a new player in colorectal cancer stem cells unveiled by spectroscopic imaging. *Stem Cells,* 33**,** 35-44.

TOKUDA, Y., SATOH, Y., FUJIYAMA, C., TODA, S., SUGIHARA, H. & MASAKI, Z. 2003. Prostate cancer cell growth is modulated by adipocyte-cancer cell interaction. *BJU Int,* 91**,** 716-20.

TOUISNI, N., MARESCA, A., MCDONALD, P. C., LOU, Y., SCOZZAFAVA, A., DEDHAR, S., WINUM, J. Y. & SUPURAN, C. T. 2011. Glycosyl coumarin carbonic anhydrase IX and XII inhibitors strongly attenuate the growth of primary breast tumors. *J Med Chem,* 54**,** 8271-7.

TU, C., FOSTER, L., ALVARADO, A., MCKENNA, R., SILVERMAN, D. N. & FROST, S. C. 2012. Role of zinc in catalytic activity of carbonic anhydrase IX. *Arch Biochem Biophys,* 521**,** 90-4.

URICH, E., PATSCH, C., AIGNER, S., GRAF, M., IACONE, R. & FRESKGARD, P. O. 2013. Multicellular self-assembled spheroidal model of the blood brain barrier. *Sci Rep,* 3**,** 1500.

VADIVELU, R. K., OOI, C. H., YAO, R. Q., TELLO VELASQUEZ, J., PASTRANA, E., DIAZ-NIDO, J., LIM, F., EKBERG, J. A., NGUYEN, N. T. & ST JOHN, J. A. 2015.

Generation of three-dimensional multiple spheroid model of olfactory ensheathing cells using floating liquid marbles. *Sci Rep,* 5**,** 15083.

VALENCIA, T., KIM, J. Y., ABU-BAKER, S., MOSCAT-PARDOS, J., AHN, C. S., REINA-CAMPOS, M., DURAN, A., CASTILLA, E. A., METALLO, C. M., DIAZ-MECO, M. T. & MOSCAT, J. 2014. Metabolic reprogramming of stromal fibroblasts through p62-mTORC1 signaling promotes inflammation and tumorigenesis. *Cancer Cell,* 26**,** 121-35.

VAN KUIJK, S. J., YAROMINA, A., HOUBEN, R., NIEMANS, R., LAMBIN, P. & DUBOIS, L. J. 2016. Prognostic Significance of Carbonic Anhydrase IX Expression in Cancer Patients: A Meta-Analysis. *Front Oncol,* 6**,** 69.

VANDER HEIDEN, M. G., CANTLEY, L. C. & THOMPSON, C. B. 2009. Understanding the Warburg effect: the metabolic requirements of cell proliferation. *Science,* 324**,** 1029-33.

VAUPEL, P., KALLINOWSKI, F. & OKUNIEFF, P. 1989. Blood flow, oxygen and nutrient supply, and metabolic microenvironment of human tumors: a review. *Cancer Res,* 49**,** 6449-65.

VOET, D., VOET, J. G. & PRATT, C. W. 2006. *Fundamentals of Biochemistry*, John Wiley and Sons, Inc.

VORDERMARK, D., KAFFER, A., RIEDL, S., KATZER, A. & FLENTJE, M. 2005. Characterization of carbonic anhydrase IX (CA IX) as an endogenous marker of chronic hypoxia in live human tumor cells. *Int J Radiat Oncol Biol Phys,* 61**,** 1197-207.

WARBURG, O. 1956. On the origin of cancer cells. *Science,* 123**,** 309-14.

WARD, C., MEEHAN, J., MULLEN, P., SUPURAN, C., DIXON, J. M., THOMAS, J. S., WINUM, J. Y., LAMBIN, P., DUBOIS, L., PAVATHANENI, N. K., JARMAN, E. J., RENSHAW, L., UM, I. H., KAY, C., HARRISON, D. J., KUNKLER, I. H. & LANGDON, S. P. 2015. Evaluation of carbonic anhydrase IX as a therapeutic target for inhibition of breast cancer invasion and metastasis using a series of in vitro breast cancer models. *Oncotarget,* 6**,** 24856-70.

WARD, P. S. & THOMPSON, C. B. 2012. Metabolic reprogramming: a cancer hallmark even warburg did not anticipate. *Cancer Cell,* 21**,** 297-308.

WEINHOUSE, S. 1976. The Warburg hypothesis fifty years later. *Z Krebsforsch Klin Onkol Cancer Res Clin Oncol,* 87**,** 115-26.

WELLINGS, S. R. & JENSEN, H. M. 1973. On the origin and progression of ductal carcinoma in the human breast. *J Natl Cancer Inst,* 50**,** 1111-8.

WELLMANN, S., BETTKOBER, M., ZELMER, A., SEEGER, K., FAIGLE, M., ELTZSCHIG, H. K. & BUHRER, C. 2008. Hypoxia upregulates the histone demethylase JMJD1A via HIF-1. *Biochem Biophys Res Commun,* 372**,** 892-7.

WENDER, R., BROWN, A. M., FERN, R., SWANSON, R. A., FARRELL, K. & RANSOM, B. R. 2000. Astrocytic glycogen influences axon function and survival during glucose deprivation in central white matter. *J Neurosci,* 20**,** 6804-10.

WESTERTERP, M., SLOOF, G. W., HOEKSTRA, O. S., TEN KATE, F. J., MEIJER, G. A., REITSMA, J. B., BOELLAARD, R., VAN LANSCHOT, J. J. & MOLTHOFF, C. F. 2008. 18FDG uptake in oesophageal adenocarcinoma: linking biology and outcome. *J Cancer Res Clin Oncol,* 134**,** 227-36.

WICHA, M. S., LIU, S. & DONTU, G. 2006. Cancer stem cells: an old idea--a paradigm shift. *Cancer Res,* 66**,** 1883-90; discussion 1895-6.

WIESENER, M. S., JURGENSEN, J. S., ROSENBERGER, C., SCHOLZE, C. K., HORSTRUP, J. H., WARNECKE, C., MANDRIOTA, S., BECHMANN, I., FREI, U. A., PUGH, C. W., RATCLIFFE, P. J., BACHMANN, S., MAXWELL, P. H. & ECKARDT, K. U. 2003. Widespread hypoxia-inducible expression of HIF-2alpha in distinct cell populations of different organs. *FASEB J,* 17**,** 271-3.

WIGFIELD, S. M., WINTER, S. C., GIATROMANOLAKI, A., TAYLOR, J., KOUKOURAKIS, M. L. & HARRIS, A. L. 2008. PDK-1 regulates lactate production in hypoxia and is associated with poor prognosis in head and neck squamous cancer. *Br J Cancer,* 98**,** 1975-84.

WILSON, D. F., ERECINSKA, M., DROWN, C. & SILVER, I. A. 1977. Effect of oxygen tension on cellular energetics. *The American journal of physiology,* 233**,** C135-40.

WINUM, J. Y., CARTA, F., WARD, C., MULLEN, P., HARRISON, D., LANGDON, S. P., CECCHI, A., SCOZZAFAVA, A., KUNKLER, I. & SUPURAN, C. T. 2012. Ureido-substituted sulfamates show potent carbonic anhydrase IX inhibitory and antiproliferative activities against breast cancer cell lines. *Bioorg Med Chem Lett,* 22**,** 4681-5.

WISE, D. R., DEBERARDINIS, R. J., MANCUSO, A., SAYED, N., ZHANG, X. Y., PFEIFFER, H. K., NISSIM, I., DAIKHIN, E., YUDKOFF, M., MCMAHON, S. B. & THOMPSON, C. B. 2008. Myc regulates a transcriptional program that stimulates mitochondrial glutaminolysis and leads to glutamine addiction. *Proc Natl Acad Sci U S A,* 105**,** 18782-7.

WITTA, S. E., JOTTE, R. M., KONDURI, K., NEUBAUER, M. A., SPIRA, A. I., RUXER, R. L., VARELLA-GARCIA, M., BUNN, P. A., JR. & HIRSCH, F. R. 2012. Randomized phase II trial of erlotinib with and without entinostat in patients with advanced non-small-cell lung cancer who progressed on prior chemotherapy. *J Clin Oncol,* 30**,** 2248-55.

WOELBER, L., KRESS, K., KERSTEN, J. F., CHOSCHZICK, M., KILIC, E., HERWIG, U., LINDNER, C., SCHWARZ, J., JAENICKE, F., MAHNER, S., MILDE-LANGOSCH, K., MUELLER, V. & IHNEN, M. 2011. Carbonic anhydrase IX in tumor tissue and sera of patients with primary cervical cancer. *BMC Cancer,* 11**,** 12.

WOLFF, A. C., HAMMOND, M. E., HICKS, D. G., DOWSETT, M., MCSHANE, L. M., ALLISON, K. H., ALLRED, D. C., BARTLETT, J. M., BILOUS, M., FITZGIBBONS, P., HANNA, W., JENKINS, R. B., MANGU, P. B., PAIK, S., PEREZ, E. A., PRESS, M. F., SPEARS, P. A., VANCE, G. H., VIALE, G. & HAYES, D. F. 2013. Recommendations for Human Epidermal Growth Factor Receptor 2 Testing in Breast Cancer: American Society of Clinical Oncology/College of American Pathologists Clinical Practice Guideline Update. *J Clin Oncol*.

WOLFF, A. C., HAMMOND, M. E., HICKS, D. G., DOWSETT, M., MCSHANE, L. M., ALLISON, K. H., ALLRED, D. C., BARTLETT, J. M., BILOUS, M., FITZGIBBONS, P., HANNA, W., JENKINS, R. B., MANGU, P. B., PAIK, S., PEREZ, E. A., PRESS, M. F., SPEARS, P. A., VANCE, G. H., VIALE, G., HAYES, D. F., AMERICAN SOCIETY OF CLINICAL, O. & COLLEGE OF AMERICAN, P. 2014. Recommendations for human epidermal growth factor receptor 2 testing in breast cancer: American Society of Clinical Oncology/College of American Pathologists clinical practice guideline update. *Arch Pathol Lab Med,* 138**,** 241-56.

XIA, X., LEMIEUX, M. E., LI, W., CARROLL, J. S., BROWN, M., LIU, X. S. & KUNG, A. L. 2009. Integrative analysis of HIF binding and transactivation reveals its

role in maintaining histone methylation homeostasis. *Proc Natl Acad Sci U S A,* 106**,** 4260-5.

XU, W., YANG, H., LIU, Y., YANG, Y., WANG, P., KIM, S. H., ITO, S., YANG, C., WANG, P., XIAO, M. T., LIU, L. X., JIANG, W. Q., LIU, J., ZHANG, J. Y., WANG, B., FRYE, S., ZHANG, Y., XU, Y. H., LEI, Q. Y., GUAN, K. L., ZHAO, S. M. & XIONG, Y. 2011. Oncometabolite 2-hydroxyglutarate is a competitive inhibitor of alpha-ketoglutarate-dependent dioxygenases. *Cancer Cell,* 19**,** 17-30.

YAMADA, Y., NAKAMURA, K., AOKI, S., TOBIUME, M., ZENNAMI, K., KATO, Y., NISHIKAWA, G., YOSHIZAWA, T., ITOH, Y., NAKAOKA, A., YOSHIDA, E., UCHIYAMA, T. & HONDA, N. 2011. Lactate dehydrogenase, Gleason score and HER-2 overexpression are significant prognostic factors for M1b prostate cancer. *Oncol Rep,* 25**,** 937-44.

YAMANAKA, S. & BLAU, H. M. 2010. Nuclear reprogramming to a pluripotent state by three approaches. *Nature,* 465**,** 704-12.

YAMASHITA, K., DISCHER, D. J., HU, J., BISHOPRIC, N. H. & WEBSTER, K. A. 2001. Molecular regulation of the endothelin-1 gene by hypoxia. Contributions of hypoxia-inducible factor-1, activator protein-1, GATA-2, AND p300/CBP. *J Biol Chem,* 276**,** 12645-53.

YANG, J., LEDAKI, I., TURLEY, H., GATTER, K. C., MONTERO, J. C., LI, J. L. & HARRIS, A. L. 2009. Role of hypoxia-inducible factors in epigenetic regulation via histone demethylases. *Annals of the New York Academy of Sciences,* 1177**,** 185-97.

YANG, J., ZHANG, L., ERBEL, P. J., GARDNER, K. H., DING, K., GARCIA, J. A. & BRUICK, R. K. 2005. Functions of the Per/ARNT/Sim domains of the hypoxia-inducible factor. *J Biol Chem,* 280**,** 36047-54.

YANG, J. S., LIN, C. W., CHUANG, C. Y., SU, S. C., LIN, S. H. & YANG, S. F. 2015. Carbonic anhydrase IX overexpression regulates the migration and progression in oral squamous cell carcinoma. *Tumour Biol,* 36**,** 9517-24.

YANG, Z. & KLIONSKY, D. J. 2010. Eaten alive: a history of macroautophagy. *Nat Cell Biol,* 12**,** 814-22.

YAP, T. A., GERLINGER, M., FUTREAL, P. A., PUSZTAI, L. & SWANTON, C. 2012. Intratumor heterogeneity: seeing the wood for the trees. *Sci Transl Med,* 4**,** 127ps10.

YARDLEY, D. A., ISMAIL-KHAN, R. R., MELICHAR, B., LICHINITSER, M., MUNSTER, P. N., KLEIN, P. M., CRUICKSHANK, S., MILLER, K. D., LEE, M. J. & TREPEL, J. B. 2013. Randomized phase II, double-blind, placebo-controlled study of exemestane with or without entinostat in postmenopausal women with locally recurrent or metastatic estrogen receptor-positive breast cancer progressing on treatment with a nonsteroidal aromatase inhibitor. *J Clin Oncol,* 31**,** 2128-35.

YEE KOH, M., SPIVAK-KROIZMAN, T. R. & POWIS, G. 2008. HIF-1 regulation: not so easy come, easy go. *Trends Biochem Sci,* 33**,** 526-34.

YIN, X., DWYER, J., LANGLEY, S. R., MAYR, U., XING, Q., DROZDOV, I., NABEEBACCUS, A., SHAH, A. M., MADHU, B., GRIFFITHS, J., EDWARDS, L. M. & MAYR, M. 2013. Effects of perhexiline-induced fuel switch on the cardiac proteome and metabolome. *J Mol Cell Cardiol,* 55**,** 27-30.

YOU, Y. N., RUSTIN, R. B. & SULLIVAN, J. D. 2015. Oncotype DX((R)) colon cancer assay for prediction of recurrence risk in patients with stage II and III colon cancer: A review of the evidence. *Surg Oncol,* 24**,** 61-6.

YU, A. C., DREJER, J., HERTZ, L. & SCHOUSBOE, A. 1983. Pyruvate carboxylase activity in primary cultures of astrocytes and neurons. *J Neurochem,* 41**,** 1484-7.

YUN, C. H., MENGWASSER, K. E., TOMS, A. V., WOO, M. S., GREULICH, H., WONG, K. K., MEYERSON, M. & ECK, M. J. 2008. The T790M mutation in EGFR kinase causes drug resistance by increasing the affinity for ATP. *Proc Natl Acad Sci U S A,* 105**,** 2070-5.

ZATOVICOVA, M., JELENSKA, L., HULIKOVA, A., CSADEROVA, L., DITTE, Z., DITTE, P., GOLIASOVA, T., PASTOREK, J. & PASTOREKOVA, S. 2010. Carbonic anhydrase IX as an anticancer therapy target: preclinical evaluation of internalizing monoclonal antibody directed to catalytic domain. *Curr Pharm Des,* 16**,** 3255-63.

ZATOVICOVA, M., SEDLAKOVA, O., SVASTOVA, E., OHRADANOVA, A., CIAMPOR, F., ARRIBAS, J., PASTOREK, J. & PASTOREKOVA, S. 2005. Ectodomain shedding of the hypoxia-induced carbonic anhydrase IX is a metalloprotease-dependent process regulated by TACE/ADAM17. *British journal of cancer,* 93**,** 1267-76.

ZAVADA, J., ZAVADOVA, Z., PASTOREK, J., BIESOVA, Z., JEZEK, J. & VELEK, J. 2000. Human tumour-associated cell adhesion protein MN/CA IX: identification of M75 epitope and of the region mediating cell adhesion. *Br J Cancer,* 82**,** 1808-13.

ZAVADA, J., ZAVADOVA, Z., PASTOREKOVA, S., CIAMPOR, F., PASTOREK, J. & ZELNIK, V. 1993. Expression of MaTu-MN protein in human tumor cultures and in clinical specimens. *Int J Cancer,* 54**,** 268-74.

ZAVADA, J., ZAVADOVA, Z., ZAT'OVICOVA, M., HYRSL, L. & KAWACIUK, I. 2003. Soluble form of carbonic anhydrase IX (CA IX) in the serum and urine of renal carcinoma patients. *British journal of cancer,* 89**,** 1067-71.

ZHANG, H. S., GAVIN, M., DAHIYA, A., POSTIGO, A. A., MA, D., LUO, R. X., HARBOUR, J. W. & DEAN, D. C. 2000. Exit from G1 and S phase of the cell cycle is regulated by repressor complexes containing HDAC-Rb-hSWI/SNF and Rb-hSWI/SNF. *Cell,* 101**,** 79-89.

ZHANG, Y., YANG, C., WANG, W., LIU, J., LIU, Q., HUANG, F., CHU, L., GAO, H., LI, C., KONG, D., LIU, Q. & LIU, J. 2016. Co-delivery of doxorubicin and curcumin by pH-sensitive prodrug nanoparticle for combination therapy of cancer. *Sci Rep,* 6**,** 21225.

ZHAO, Z., WU, M. S., ZOU, C., TANG, Q., LU, J., LIU, D., WU, Y., YIN, J., XIE, X., SHEN, J., KANG, T. & WANG, J. 2014. Downregulation of MCT1 inhibits tumor growth, metastasis and enhances chemotherapeutic efficacy in osteosarcoma through regulation of the NF-kappaB pathway. *Cancer Lett,* 342**,** 150-8.

ZHONG, H., DE MARZO, A. M., LAUGHNER, E., LIM, M., HILTON, D. A., ZAGZAG, D., BUECHLER, P., ISAACS, W. B., SEMENZA, G. L. & SIMONS, J. W. 1999. Overexpression of hypoxia-inducible factor 1alpha in common human cancers and their metastases. *Cancer Research,* 59**,** 5830-5.

ZHOU, Q., DALGARD, C. L., WYNDER, C. & DOUGHTY, M. L. 2011. Histone deacetylase inhibitors SAHA and sodium butyrate block G1-to-S cell cycle progression in neurosphere formation by adult subventricular cells. *BMC Neurosci,* 12**,** 50.

ZHOU, S., SCHUETZ, J. D., BUNTING, K. D., COLAPIETRO, A. M., SAMPATH, J., MORRIS, J. J., LAGUTINA, I., GROSVELD, G. C., OSAWA, M., NAKAUCHI, H. & SORRENTINO, B. P. 2001. The ABC transporter Bcrp1/ABCG2 is expressed in a wide variety of stem cells and is a molecular determinant of the side-population phenotype. *Nat Med,* 7**,** 1028-34.

ZHULIN, I. B., TAYLOR, B. L. & DIXON, R. 1997. PAS domain S-boxes in Archaea, Bacteria and sensors for oxygen and redox. *Trends Biochem Sci,* 22**,** 331-3.

ZUNDEL, W., SCHINDLER, C., HAAS-KOGAN, D., KOONG, A., KAPER, F., CHEN, E., GOTTSCHALK, A. R., RYAN, H. E., JOHNSON, R. S., JEFFERSON, A. B., STOKOE, D. & GIACCIA, A. J. 2000. Loss of PTEN facilitates HIF-1-mediated gene expression. *Genes Dev,* 14**,** 391-6.

Appendix

Figure 1.1

ELSEVIER LICENSE
TERMS AND CONDITIONS

Sep 01, 2016

This Agreement between Katharina Feldinger ("You") and Elsevier ("Elsevier") consists of your license details and the terms and conditions provided by Elsevier and Copyright Clearance Center.

License Number	3940090988380
License date	Sep 01, 2016
Licensed Content Publisher	Elsevier
Licensed Content Publication	Cell
Licensed Content Title	Hallmarks of Cancer: The Next Generation
Licensed Content Author	Douglas Hanahan,Robert A. Weinberg
Licensed Content Date	4 March 2011
Licensed Content Volume Number	144
Licensed Content Issue Number	5
Licensed Content Pages	29
Start Page	646
End Page	674
Type of Use	reuse in a thesis/dissertation
Portion	figures/tables/illustrations
Number of figures/tables/illustrations	2
Format	both print and electronic
Are you the author of this Elsevier article?	No
Will you be translating?	No
Order reference number	Perm_Fig 1
Original figure numbers	Figures 1, 3
Title of your thesis/dissertation	Mechanisms and effects of the heterogenic response of CAIX to hypoxia
Expected completion date	Dec 2016
Estimated size (number of pages)	252
Elsevier VAT number	GB 494 6272 12
Requestor Location	Katharina Feldinger Flat 8 Saxon Court 2 Stephen Rd Oxford, OX3 9FA United Kingdom Attn: Katharina Feldinger
Total	0.00 GBP
Terms and Conditions	

INTRODUCTION

Figure1.4

NATURE PUBLISHING GROUP LICENSE TERMS AND CONDITIONS

Sep 01, 2016

This Agreement between Katharina Feldinger ("You") and Nature Publishing Group ("Nature Publishing Group") consists of your license details and the terms and conditions provided by Nature Publishing Group and Copyright Clearance Center.

License Number	3940100954157
License date	Sep 01, 2016
Licensed Content Publisher	Nature Publishing Group
Licensed Content Publication	Nature
Licensed Content Title	The genomic and transcriptomic architecture of 2,000 breast tumours reveals novel subgroups
Licensed Content Author	Christina Curtis, Sohrab P. Shah, Suet-Feung Chin, Gulisa Turashvili, Oscar M. Rueda, Mark J. Dunning
Licensed Content Date	Apr 18, 2012
Licensed Content Volume Number	486
Licensed Content Issue Number	7403
Type of Use	reuse in a dissertation / thesis
Requestor type	academic/educational
Format	print and electronic
Portion	figures/tables/illustrations
Number of figures/tables/illustrations	2
High-res required	no
Figures	Figure 4 The integrative subgroups have distinct copy number profiles. Figure 5 The integrative subgroups have distinct clinical outcomes.
Author of this NPG article	no
Your reference number	Fig 2
Title of your thesis / dissertation	Mechanisms and effects of the heterogenic response of CAIX to hypoxia
Expected completion date	Dec 2016
Estimated size (number of pages)	252
Requestor Location	Katharina Feldinger John Radcliffe Hospital Weatherall Institute of Molecular Medicine Oxford, OX3 9DS United Kingdom Attn: Katharina Feldinger
Billing Type	Invoice
Billing Address	Katharina Feldinger John Radcliffe Hospital Weatherall Institute of Molecular Medicine

Figure 1.5

00642841 RE: Request permission for reprint
"Jess RamosJr" <info@biomedcentral.com>
Gesendet: Donnerstag, 01. September 2016 10:31
An: Katharina Feldinger

SPRINGER NATURE

Dear Dr Feldinger,

Thank you for contacting BioMed Central.

Reproduction of figures or tables is permitted free of charge and without formal written permission from the publisher or the copyright holder, provided that the figure/table is original, BioMed Central is duly identified as the original publisher, and that proper attribution of authorship and the correct citation details are given as acknowledgement.

If you have any questions, please do not hesitate to contact me.

Best wishes,

Jess Ramos Jr.
Customer Services Executive
Open Research Group

Springer Nature
236 Gray's Inn Road, London WC1X 8HB, UK
T +44 (0)203 192 2009
F +44 (0)203 192 2010
Jess.RamosJr@springernature.com
www.springernature.com

Springer Nature is one of the world's leading global research, educational and professional publishers, created in 2015 through the combination of Nature Publishing Group, Palgrave Macmillan, Macmillan Education and Springer Science+Business Media.

Springer-Verlag London Ltd.
Registered Office: 236 Gray´s Inn Road / London WC1X 8HB / Registered in England No. 1738860 / VAT Registration No. GB 823826326

Figure 1.6

THE AMERICAN ASSOCIATION FOR THE ADVANCEMENT OF SCIENCE LICENSE TERMS AND CONDITIONS

Sep 01, 2016

This Agreement between Katharina Feldinger ("You") and The American Association for the Advancement of Science ("The American Association for the Advancement of Science") consists of your license details and the terms and conditions provided by The American Association for the Advancement of Science and Copyright Clearance Center.

License Number	3940110519444
License date	Sep 01, 2016
Licensed Content Publisher	The American Association for the Advancement of Science
Licensed Content Publication	Science
Licensed Content Title	Understanding the Warburg Effect: The Metabolic Requirements of Cell Proliferation
Licensed Content Author	Matthew G. Vander Heiden,Lewis C. Cantley,Craig B. Thompson
Licensed Content Date	May 22, 2009
Licensed Content Volume Number	324
Licensed Content Issue Number	5930
Volume number	324
Issue number	5930
Type of Use	Thesis / Dissertation
Requestor type	Scientist/individual at a research institution
Format	Print and electronic
Portion	Figure
Number of figures/tables	1
Order reference number	Metabolic pathways overview
Title of your thesis / dissertation	Mechanisms and effects of the heterogenic response of CAIX to hypoxia
Expected completion date	Dec 2016
Estimated size(pages)	252
Requestor Location	Katharina Feldinger John Radcliffe Hospital Weatherall Institute of Molecular Medicine Oxford, OX3 9DS United Kingdom Attn: Katharina Feldinger
Billing Type	Invoice
Billing Address	Katharina Feldinger John Radcliffe Hospital Weatherall Institute of Molecular Medicine Oxford, United Kingdom OX3 9DS Attn: Katharina Feldinger
Total	0.00 USD

Terms and Conditions

American Association for the Advancement of Science TERMS AND CONDITIONS

Figure 1.7

ELSEVIER LICENSE
TERMS AND CONDITIONS

Sep 01, 2016

This Agreement between Katharina Feldinger ("You") and Elsevier ("Elsevier") consists of your license details and the terms and conditions provided by Elsevier and Copyright Clearance Center.

License Number	3940110941596
License date	Sep 01, 2016
Licensed Content Publisher	Elsevier
Licensed Content Publication	Biochimica et Biophysica Acta (BBA) - Proteins and Proteomics
Licensed Content Title	Carbonic anhydrase IX: Biochemical and crystallographic characterization of a novel antitumor target
Licensed Content Author	Giuseppina De Simone,Claudiu T. Supuran
Licensed Content Date	February 2010
Licensed Content Volume Number	1804
Licensed Content Issue Number	2
Licensed Content Pages	6
Start Page	404
End Page	409
Type of Use	reuse in a thesis/dissertation
Intended publisher of new work	other
Portion	figures/tables/illustrations
Number of figures/tables/illustrations	1
Format	both print and electronic
Are you the author of this Elsevier article?	No
Will you be translating?	No
Order reference number	Intro 1.7
Original figure numbers	Figure 5 Proposed model showing the structural arrangement of the full-length CA IX dimer on the cellular membrane
Title of your thesis/dissertation	Mechanisms and effects of the heterogenic response of CAIX to hypoxia
Expected completion date	Dec 2016
Estimated size (number of pages)	252
Elsevier VAT number	GB 494 6272 12
Requestor Location	Katharina Feldinger John Radcliffe Hospital Weatherall Institute of Molecular Medicine Oxford, OX3 9DS United Kingdom Attn: Katharina Feldinger

Figure 6.2

ELSEVIER LICENSE
TERMS AND CONDITIONS

Sep 01, 2016

This Agreement between Katharina Feldinger ("You") and Elsevier ("Elsevier") consists of your license details and the terms and conditions provided by Elsevier and Copyright Clearance Center.

License Number	3940120249395
License date	Sep 01, 2016
Licensed Content Publisher	Elsevier
Licensed Content Publication	Archives of Biochemistry and Biophysics
Licensed Content Title	Targeting acidity in diseased tissues: Mechanism and applications of the membrane-inserting peptide, pHLIP
Licensed Content Author	John C. Deacon,Donald M. Engelman,Francisco N. Barrera
Licensed Content Date	1 January 2015
Licensed Content Volume Number	565
Licensed Content Issue Number	n/a
Licensed Content Pages	9
Start Page	40
End Page	48
Type of Use	reuse in a thesis/dissertation
Intended publisher of new work	other
Portion	figures/tables/illustrations
Number of figures/tables/illustrations	1
Format	both print and electronic
Are you the author of this Elsevier article?	No
Will you be translating?	No
Order reference number	Fig 6.2
Original figure numbers	Figure 1 - pHLIP states
Title of your thesis/dissertation	Mechanisms and effects of the heterogenic response of CAIX to hypoxia
Expected completion date	Dec 2016
Estimated size (number of pages)	252
Elsevier VAT number	GB 494 6272 12
Requestor Location	Katharina Feldinger John Radcliffe Hospital Weatherall Institute of Molecular Medicine Oxford, OX3 9DS United Kingdom Attn: Katharina Feldinger
Total	0.00 USD